UNIVERSITY OF SOUTHAMPTON

DYNAMICS OF LARGE FLEXIBLE MULTIBODY STRUCTURES IN SPACE

NIKOLAOS MANTIKAS

THESIS SUBMITTED FOR THE DEGREE OF

DOCTOR OF PHILOSOPHY

DEPARTMENT OF AERONAUTICS AND ASTRONAUTICS

FACULTY OF ENGINEERING AND APPLIED SCIENCE

MAY 2001

UNIVERSITY OF SOUTHAMPTON

ABSTRACT

Faculty of Engineering and Applied Science
Department of Aeronautics and Astronautics

Doctor of Philosophy

DYNAMICS OF LARGE FLEXIBLE MULTIBODY STRUCTURES IN SPACE

Nikolaos Mantikas

The scope of this work has been the development of an efficient method for the dynamics modelling of structural systems in category II missions in space. Specified by NASA, category II missions will employ large-scale articulated multibody structural systems of complex interconnected flexible and rigid components. Typical examples include space-science laboratories, earth-observation platforms and space-station configurations.

As opposed to the direct application of the finite element method for the dynamics modelling of an entire structure as a single entity, structural systems in this work have been modelled as collections of interacting components. It is required that the method should provide high accuracy, though low order, mathematical models, and amongst other critical advantages, should be computationally more efficient than the global finite element approach. A recursive Lagrangian formulation of generalised coordinates was considered the most efficient methodology for the modelling objectives specified. The recursive nature permits the formulation of kinematical expressions relative to the inboard component and results in a minimal set of differential equations of motion. Component linear elastic deformation is approximated using spatial discretisation techniques with a small number of component modes. Several component mode sets, combinations of dynamic and static modes, have been proposed or adapted from the area of component-mode synthesis. Truncation of the system order can be achieved at substructural level, by reducing the number of component modes, resulting in low order mathematical models.

A number of methods have been developed and thoroughly assessed on the suitability for the dynamics modelling of category II systems. The fittest of the methods, which directly utilises the finite element component matrices, has been shown to be computationally faster than the global finite element approach over a large number of case studies. A network of custom developed programs, based on this method, has been generated and interfaced to a commercial finite element code for modelling complex aerospace structures.

The network of programs has been used for both the verification of the theoretical integrity of the proposed method and as importantly for the assessment of the component mode sets employed in the analysis. For this purpose a wide range of eigenvalue and frequency response analyses have been undertaken. The results, which in all cases have been compared to those obtained by the direct finite element approach, demonstrate that for large flexible multibody structures in space the right selection of component modes is of foremost importance. Utilising appropriate combinations of component mode sets, excellent agreement of the method to the finite element approach can be achieved even with a low number of differential equations.

Table of Figures

Chapter II — **Content of Figures**

Chapter III — **Content of Figures**

Chapter V — **Content of Figures**

Chapter VI — **Content of Figures**

Chapter VII **Content of Figures**

Appendix A

Content of Figures

TABLE OF TABLES

Appendix-A Content of Tables

Appendix-B Content of Tables

List of Symbols

$\underset{\sim}{a}$ vector quantity.

$\dot{\underset{\sim}{a}}$ time derivative of the vector quantity $\underset{\sim}{a}$ relative to an inertial reference frame.

$\overset{+}{\underset{\sim}{a}}$ time derivative of the vector quantity $\underset{\sim}{a}$ relative to an local reference frame.

${}_{B}\underline{a}$ column matrix of the vector quantity $\underset{\sim}{a}$ expressed at reference frame B (projection).

A matrix quantity other than column matrix.

A^{T} transpose of A.

1 unity matrix.

0 null matrix.

$\left(\right)^{x}$ indicates a skew-symmetric matrix.

$\left(\right)_{J_i}$ the value of a quantity at a point J_i.

$\left\{ \right\}_{n}$ set (or subset) of size n.

Generic Notation for Tree-Configuration Multibody System

I inertial reference frame.

B_i floating reference frame (body reference frame) associated with component B_i.

J_i joint between component B_i and the inboard component B_{i-1}.

J_i^+ the interface point between component B_i and the inboard component B_{i-1}, within

component B_i.

$\bar{J}_i$ the interface point between component B_i and the inboard component B_{i-1}, within component B_{i-1}.

$\underset{\sim}{r}_i^{\,A}$ vector position of point A (arbitrary or specific) within component B_i measured from the origin of the inertial frame.

$\underset{\sim}{\rho}_i$ vector position of arbitrary point within component B_i measured from the origin of the floating reference frame B_i.

${}^{A}\underset{\sim}{v}_i^{\,B}$ linear velocity of point B (or reference frame positioned at point B) within component B_i relative to the reference frame A. If A the inertial reference frame, then the vector quantity is the absolute linear velocity of point B.

${}^{A}\underset{\sim}{\omega}_i^{\,B}$ angular velocity of a frame travelling with point B within component B_i relative to the reference frame A. If A the inertial reference frame, then the vector quantity is the absolute angular velocity of point B.

$\underset{\sim}{\omega}_i^{\,rel}$ angular velocity of the floating reference frame B_i of an articulating component, as observed from a reference frame attached at interface within the inboard component B_{i-1}.

$\underset{\sim}{u}_i$ the linear displacement vector of an arbitrary point within component B_i due to small linear elastic deformation.

$\underset{\sim}{\theta}_i$ the angular displacement vector of an arbitrary point within component B_i due to small linear elastic deformation.

n_f^i the number of flexible component modes retained in the analysis for approximating the small linear elastic deformation component B_i.

U_{fi} a $3\times n_f^i$ matrix containing the linear displacement vectors of an arbitrary point within component B_i for all the flexible component modes retained in the analysis.

Θ_{fi} a $3\times n_f^i$ matrix containing the angular displacement vectors of an arbitrary point within component B_i for all the flexible component modes retained in the analysis.

$\underset{-}{q}_{fi}$ generalised coordinates associated with the flexible component modes retained in the analysis.

C_i^{nom} rotation matrix specifying the nominal orientation of the component B_i relative to the inboard component B_{i-1}, i.e. at t=0.

C_i^{rot} time-varying rotation matrix specifying at any instant the orientation of the component B_i relative to its nominal position, $t \geq 0$.

$\underset{-}{f}^{c/d}$ symbolic function referring to the discrete (d) or continuous (c) domain.

E_i Euler angle matrix formed for a particular body sequence of principal rotations referring to the component B_i.

ϕ_p Euler angles (orientation or attitude angles), i.e. an angular displacement parametric set, for a particular sequence p=1,2,3.

$\underset{i}{\dot{\phi}}_i^A$ the rate of change of the orientation angles of the floating frame B_i positioned at point A, and expressed in the floating frame B_i.

K_i^{FEM} the stiffness matrix of component B_i derived by the finite element method.

M_i^{FEM} the consistent mass matrix of component B_i derived by the finite element method.

K_{Gi} the generalised stiffness matrix of component B_i.

K_G the global stiffness matrix of the multibody system.

M_G the global mass matrix of the multibody system.

$\underset{-}{q}$ the generalised coordinate set of component B_i.

T the kinetic energy of the multibody system.

V the elastic potential energy of the multibody system.

Notation for Cluster Formation Multibody System

Index for inboard body (i-1) substituted with index for main component (m).

Index for outboard component (i) substituted with index for appended component (j).

J is the joint point between the main component and an arbitrary appendage.

P is the point on the appendage where rigid payload is mounted.

$( )_j$ the value of a quantity at joint point J.

$( )_P$ the value of a quantity at point P, where a rigid payload is mounted on the appendage.

$\underset{D-}{\rho_d^*}$ the vector (column matrix) distance of the centre of mass of component d, from the origin of component's body reference frame D and expressed in the body frame D.

m_d the mass of component D.

C_j a direction cosine rotation matrix specifying the nominal orientation of appended component B_j, relative to the main platform carrier.

$I^{B_j/J}$ the rotary inertia of appended component B_j relative to joint point J.

$I^{P/P}$ the rotary inertia of a distributed mass rigid payload on an appended component relative to point P, where it mounts on the appendage.

$i(x)$ the rotary inertia per unit of length of a beam structure along its longitudinal axis.

$I^{M/O}$ the rotary inertia of the main component relative to the origin of its floating reference

frame.

$\left(\underset{\sim}{\rho}_j\right)_p$ the position of the mounting point of an arbitrary rigid payload within the appended component B_j , measured form the origin of the body reference frame B_i.

$\left(\underset{\sim}{r}_j^*\right)_p$ the vector distance of the centre of mass of a distributed mass rigid payload from the point where it mounts on the appended component B_j.

n_r^m the number of rigid-body modes of the platform carrier.

n_f^m the number of flexible component modes retained in the analysis for approximating the small linear elastic deformation of the platform carrier.

U_m a $3\times\left(n_r^m + n_f^m\right)$ matrix containing the linear displacement vectors of an arbitrary point within the main platform carrier for all rigid-body modes and the flexible component modes retained in the analysis

Θ_m a $3\times\left(n_r^m + n_f^m\right)$ matrix containing the angular displacement vectors of an arbitrary point within the main platform carrier for all rigid-body modes and the flexible component modes retained in the analysis

n_t^m the total number of nodes of the main carrier platform

Φ_m a $\left(6\times n_t^m\right)\times\left(n_r^m + n_f^m\right)$ matrix containing the linear and angular displacement vectors of all nodal points of the carrier platform for all rigid-body modes and the flexible component modes retained in the analysis

I Introduction

I-1. Prologue

I-1-1. Background

A number of future space missions will use large flexible structures in low-earth and geostationary orbits. Possible structures include antenna concepts, space-science laboratories, earth-observation systems and space-station configurations. Such multibody systems typically consist of complex tubular-frame platforms with appended components such as booms, solar arrays, reflector antennas, robotic manipulators, and their dimensions may range from meters to hundreds of meters. These structures, due to their particular design, large dimensions, lightweight construction for launching purposes, and the large number of components, exhibit high modal density and local deformation at the component interfaces and actuator locations. These characteristics distinguish such structures to the more conventional satellite systems and demand more elaborated treatment for design and simulation purposes.

Studies related to the dynamical behaviour of structures in space may include, amongst others, manoeuvring and deployment/reconfiguration dynamics, active vibration suppression, accurate payload pointing, platform attitude control and sequential or integrated control–structure optimisation. The mathematical modelling requirements, for treating the system dynamics, depend on the actual mission objectives, which define the particular performance envelope of the multibody structure. In this sense the mathematical models for flexible structures in space have been divided by NASA / DoD into various broad categories[1].

The category I missions in space will employ structural systems with non-articulating components. Typical examples are large antenna concepts, such as the hoop-

column and wrap-rib antennas. The mission objectives are restricted to fine pointing of the structure and vibration suppression for improving performance. In category II, the interest is concentrated in developing mathematical models for systems where the components are connected in single-point holonomic interfaces and form in general open-loop articulated multibody systems. Typical examples are space-science laboratories, earth-observation systems and space-station configurations. The mission requirements may include precision attitude control of the main platform, stringent pointing of the articulated payloads and vibration suppression. The mathematical models for the dynamics modelling of structural systems employed in category I, II missions are linear, since the rotational manoeuvring of the main structure is maintained sufficiently small and the relative rotational motion of the components is restricted either completely or in the linear range.

Categories III, IV are the nonlinear counterparts of categories I, II respectively. Missions that belong in Category III will require large angle precision rotational manoeuvring of the entire structure for retargeting or tracking purposes, and subsequently or simultaneously suppression of any induced vibration. Moreover, category IV may require large angle manoeuvring of the main platform, while simultaneously and independently deploying, pointing or driving with accuracy, through large angle rotations, various articulating components and perhaps suppressing the induced vibration at the same time. Typical examples include solar panel deployment, reflector-antennas reorientation, robotic manipulator operations or general reconfiguration of the structure in space. Nonlinear mathematical models are essential for the description of the dynamical behaviour of these systems.

I-1-2. Scope and Approach

The scope of this work has been the development of a method suited to the particular dynamics modelling requirements of structural systems in category II missions in space. The method should be able to model open-loop multibody structural systems with single-point articulated flexible or rigid components. It is of critical importance that the method would provide low order mathematical models which at the same time would approximate the dynamics of complex structural configurations with high accuracy.

As opposed to the direct finite element method that considers the entire structural system as a single entity, structural systems in this work have been considered as collections of distinct interacting components. The individual components are treated separately to each other, process akin to substructuring methodologies. A substructuring approach has a number of benefits over the more conventional direct application of the finite element method. Most important attributes include the lower computational cost and memory requirements for dynamics analysis.

Using the finite element method, a complex structural system is modelled as a single structural entity. For reducing the computational cost, large order systems undergo a transformation to modal generalised coordinates prior to any dynamic analysis. The transformation involves an eigenvalue analysis of the entire structural system, and since computer time increases at about the square or cube with an increase in the number of degrees of freedom, the dynamic analysis of a large structure can be computationally expensive.

In the case of a substructuring approach the eigenvalue analysis of the complete structure is substituted by a series of eigenvalue analyses of the individual components. The small number of derived normal modes, complemented by static modes, can be used to describe the linear elastic deformation of each component. Importing the component modes into a generic mathematical model that can couple the overall motion of the components, low order differential equations of a particular structural system can be produced. The resulting low order system is very economical for obtaining the eigenvalues and eigenvectors of the global system or for any further dynamic analysis. In general, the total computational time spent for the derivation of component modes, coupling process and analysis of the resulting low order system is lower to the time spend for the direct finite element analysis of the entire structure.

In fact, the computational time saved relative to the global finite element method increases as the number of degrees of freedom of the structural system increase. Moreover, memory requirement is reduced since mathematical manipulations at component level involve lower order matrices. A substructuring approach is therefore particularly suitable for large-scale system modelling, like those treated in this work.

Further time benefits can be realised since structural systems in space contain a large number of repeated components.

Despite this work is not concerned with proposing or implementing control strategies, a substructuring approach would facilitate control application. This is attributed to the independent modelling of each individual articulated component with a low number of component modes which allows the design of decentralised control algorithms. Additional advantages are introduced since designing control systems for articulated structures requires analysis over a large number of structural configurations. Component reorientation studies are efficiently performed using a substructuring approach since only a small part of the overall dynamic analysis has to be executed at each iteration.

Although there is a number of reasons that support the use of substructuring, the success of such an approach is ultimately linked to the component modes implemented in the analysis. It proves that the kind of component mode sets utilised is of vital importance for the modelling accuracy of large flexible structures in space. The reasons are linked to inherent characteristics of these systems such as high modal density and local deformation at component interfaces. Inappropriate component mode sets not only negate the computer time benefits of a substructuring approach due to convergence issues but may also result in inaccurate dynamics modelling. The latter can prove detrimental since unmodelled dynamics, due to control-structure interaction, can result in catastrophic destabilisation. The right selection of component modes is therefore central to the implementation of a substructuring approach. In this work several component mode sets have been employed and include redundant constraint, constraint, loaded-interface, fixed-interface and free-interface sets.

I-1-3. Proposed Methodology

Within the framework of substructuring one is confronted with a number of methodology strategies. The particular methodology followed has been decided upon the particular modelling requirements of structural systems in category II missions in space. From a critical review of the area of multibody dynamics and component-

mode synthesis, it has been decided that the most efficient methodology, for meeting the modelling objectives set, would be a nonlinear recursive Lagrangian formulation of generalised coordinates.

In nonlinear kinematics the overall motion of each component can be perceived as a rigid body motion relative to which elastic deformation can be observed. In this sense, one can assign to each component a suitably positioned floating reference frame that moves with the rigid part of the motion and relative to which linear elastic deformation can be measured. Therefore, the overall motion of each component can be described in terms of the motion of a floating reference frame, and the deformation measured relative to it.

For modelling the linear elastic deformation, a simple geometry component can be spatially discretised using the continuous version of the assumed-modes method, whereas for a complex geometry component spatial discretisation can be accomplished using the finite element method. The finite element model of the component is subsequently reduced using the discrete version of the assumed-modes method. For the description of small linear elastic deformation, in both cases the transformation involves a finite set of generating modes, referred to as component mode set, which may be a combination of a number of dynamic modes complemented by static modes. By truncating the number of the dynamic modes, the system order is reduced at the component level, which is particularly beneficial for large-scale systems modelling.

In recursive formulations, the orientation of the floating reference frame of a component is specified relative to a local reference frame positioned within the preceding component and located at the interface attachment between the adjacent components. To ensure that the various components act as part of the whole structure, a suitable kinematical procedure has been proposed to accommodate the interface conditions between each component and the preceding one. The component absolute kinematical expressions are formed relative to the suitably positioned reference frame within the preceding component. The exact expressions of the outboard component kinematics are subject to the constraints at the interface with the inboard component. The interface kinematics in this work allow any of the three articulation axes to be completely free or locked. For articulating structural

systems, one is particularly interested in relative kinematical formulations, since relative component orientation, velocity and acceleration are directly measured for controller feedback purposes, therefore a recursive formulation proves an added advantage. Utilising the kinematical relationship, established for any two adjacent bodies, repeatedly for all components in the structure, the absolute kinematical expressions characterising the motion of any component can be expressed in terms of the independent generalised coordinates of all preceding components in the same multibody chain.

The kinematical procedure followed in this wok is only feasible for multibody systems where no closed-loops and multi-point interfaces are formed between the articulated components. Structures in space are typical examples of such configurations. The formulation of the interface kinematics proposed is general enough to employ any component mode set without violating the geometric interface conditions between adjacent components. This is accomplished by the introduction of 'correction terms' into the interface kinematical expressions.

I-1-4. Methods of Mathematical Modelling

The nonlinear recursive kinematical expressions have been linearised in order to obtain expressions for the formulation of the linear system dynamics. Transition from the nonlinear to linear expressions has been performed using symbolic manipulations. Distinct linear kinematical expressions have been accomplished and formulated using either hybrid or generalised coordinate sets. Utilising these, three linear methods for the dynamics modelling of structures in category II missions have been produced.

The first of the methods uses a hybrid set of coordinates where for each component the rigid-body part of the motion is described by physical displacement coordinates and the linear elastic deformation by generalised coordinates. In the second method, the hybrid set has been substituted by a generalised coordinate set, since the rigid-body motion of each component has been described using rigid-body modes, modelling allowed only with the assumption of small rotational displacement. In both methods the structural subdomains can be spatially discretised using the continuous

version of the assumed modes method or the finite element approach. In the third method all components have been spatially discretised using the finite element method. The consistent mass matrices of each component in the structure appears explicitly in the equations of motion of the multibody system. The third method also utilises a generalised coordinate set.

All methods proposed can treat open-loop tree-configuration multibody structural systems with single-point articulated rigid or flexible components. For assessment and comparison, the methods have been utilised to develop mathematical models of peripheral multibody structures of varying modelling complexity. Such systems consist of an arbitrary number of components attached to a main carrier platform without forming any closed-loops. Peripheral formation multibody mathematical models are easier to present analytically than generic tree-configuration models, which are best generated computationally. The configuration limitation of the mathematical models does not in any extend restrict the conclusions drawn form this work since it is of quantitative and not qualitative nature.

I-2. Summary of Chapters

I-2-1. Chapter I : Introduction

The remaining of this chapter looks into various areas of research that are closely related to the modelling requirements in this work. The modelling of the linear elastic domain was first examined. Clear understanding of this area is critical for comprehending more complex subjects such as the coupling of the elastic deformation to the nonlinear component kinematics, modelling of interface kinematics between adjacent components and component mode representations. The limitations and advantages of the exact and approximate modelling have been discussed. Amongst others, Rayleigh-Ritz type approximate methods, such as the continuous version of the assumed-modes method and the finite element method, have been presented.

Subsequently the discussion turned to the examination of global modelling practices as opposed to the substructuring approach. A number of advantages of

substructuring over the more conventional global finite element approach have been detailed. This part of the review is important for justifying the primary modelling step of this work.

Within the framework of substructuring a number of methodologies have been presented. The scope was to determine the particular methodology that can meet the modelling requirements of this work in the most efficient way. A thorough discussion on minimal versus augmented modelling, non-recursive versus recursive formulations and Lagrangian versus Netwon-Euler methods has been given. A brief review of the area of component-mode synthesis follows.

I-2-2. Chapter II : Component Mode Sets.

Component modes have been proposed or adapted from the area of component-mode synthesis. This field of geometrically linear dynamics is concerned with large-scale structures where the substructures are in general connected to each other in multi-point interfaces. The physical coordinate constraint sets of the component have been defined so that the component characterisation is generalised to include the statically indeterminate, determinate and underdeterminate cases. The component mode sets used are combinations of dynamic and static modes. Variations of component mode sets found in the literature have also been proposed. Component modes utilised include redundant constraint, constraint, loaded-interface, fixed-interface and free-interface sets. Mathematical proofs for determining the size of the physical coordinate constraint sets in order to define the various static modes are also provided where necessary. Preliminary advantages and disadvantages of the various component mode sets are discussed, previous to their implementation and assessment for simulating the system dynamics.

I-2-3. Chapter III : Nonlinear Recursive Component Kinematics

This chapter is concerned with the kinematics modelling of open-loop multibody flexible structures in space. The nonlinear kinematical expressions of a single flexible component are first derived. In Appendix-A the kinematics of an arbitrary component joint to the preceding one via a non-translating single-point interface have been developed. This part of the nonlinear kinematical analysis is recursive. Suitable

kinematical component expressions have been developed in order to accommodate the component interface conditions with the inboard component. The resulting mathematical expressions are general enough to employ any component mode set without violating the interface conditions. This is accomplished with the introduction of 'correction terms' in the component interface kinematical expressions. The final expressions of the component kinematics connected to the preceding component for arbitrary interface constraints have been presented. Utilising the kinematical relationship, established for any two adjacent bodies, repeatedly for all components in the structure, the absolute kinematical expressions characterising the motion of any arbitrary component can be expressed in terms of all the independent generalised coordinates that specify the time-varying configuration of the components preceding and including the arbitrary component in the same multibody chain.

I-2-4. Chapter IV : Methods of Multibody Dynamics Modelling

Having obtained the nonlinear recursive kinematical expressions for an arbitrary component in a multibody chain, the aim of this chapter is to linearise them in order to obtain expressions for the formulation of the linear system dynamics. For this purpose the theoretical background of the large arbitrary angular displacement and nonlinear rotational kinematics has been reviewed in Appendix-B and the distinct mechanisms that introduce geometrical nonlinearity into the multibody system dynamics have been thoroughly examined. Returning to chapter IV, transition from the nonlinear to linear kinematical expressions for a component as part of a multibody chain has been performed using symbolic formulations. Dinstinct linear kinematical expressions are accomplished and formulated using either hybrid or generalised coordinate sets. Utilising these kinematical expressions, three linear methods for the dynamics modelling of category II missions in space have been proposed.

The kinetic energy of each component can be expressed in terms of all the independent generalised coordinates that describe, at any instance, the configuration of the preceding multibody chain of components. The elastic potential energy can readily be derived using the expressions approximating the linear elastic deformation of the component. These approximate expressions of the component's deformation

field are independent of the exact position of the component in the multibody system. Dissipation energy can be included as structural damping at substructural level and also as viscous damping.

Using a unified coordinate set formulation, the energy functions for all methods and for discrete or continuous flexible components have been derived. An initial assessment of the methods and discussion on their differences on theoretical and numerical implementation level has been presented.

I-2-5. Chapter V : Mathematical Models of Peripheral Multibody Structures

For assessment and comparison, the methods developed have been utilised to derive mathematical models of peripheral formation multibody structures. Four distinct mathematical models have been developed. Based on these mathematical models, the three methods have been assessed and compared on a large variety of criteria on their suitability for modelling the dynamics of Category II missions in space. The comparison clearly demonstrated the most efficient method. The resulting model uses explicitly the consistent mass matrix of the individual components and a generalised coordinate set. This model provides an excellent tool for research, analysis and design of large-scale flexible structures in space.

This chapter concludes with the derivation of the generalised force expressions for a multibody structure and the mathematical steps for performing a direct or modal frequency response analysis using the reduced order mathematical model of the multibody system. Structural and localised viscous damping has been included at substructural level.

I-2-6. Chapter VI : Computational Implementation

A network of programs has been developed for the computational implementation of the most efficient of the methods. The final deliverables of the network are the eigenvalues of the multibody system and the eigenvectors in modal or physical space. Additionally, physical displacement, velocity and acceleration of any point on the structure can be derived as a function of the forcing frequency using either direct

or modal frequency response analysis.

Since structures in space are composed of complex components, within the framework of this network each component has been spatially discretised using the finite element method. For this purpose, the network has been interfaced with the commercial finite element package ANSYS. Redundant constraint, constraint, loaded-interface, fixed-interface and free-interface component mode sets have been employed. Within the network of programs the redundant constraint and constraint modes, that complement the dynamic modes to form a component mode set, are calculated using specifically developed algorithms.

The capabilities and the structure of the network are presented in the first part of chapter IV. The remaining of the chapter is dedicated to computational cost analysis studies of the proposed method relative to the direct finite element approach. A number of studies have been undertaken and demonstrate that in general the proposed method can be considerably faster over the more conventional global finite element approach. A number of conclusions on the efficiency of the method and its potential limitations have been reached.

I-2-7. Chapter VII : Results

Using the network of programs, the natural frequencies of peripheral structural configurations have been derived by incorporating several kinds of component mode sets, and the results have been compared to those obtained by modelling the entire structure using the finite element method. Similarly several frequency response analyses have been undertaken to further examine the integrity of the method and the accuracy of the component modes used. Employing the finite element method as a benchmark has long been established both for the verification of the theoretical integrity and the accuracy of results obtained from linear mathematical models.

Conclusions on the efficiency of the component mode sets have been firmly established. The right selection of component mode sets is challenging for large-scale flexible multibody structures in space, since these structures exhibit high modal density and local deformation at the component interfaces. Moreover, the inherently large differential problem would increase further if the component modes employed

cannot efficiently model the linear elastic deformation of the components. A qualitative criterion has been established that predicts the possibility of local deformation being low or high. The criterion can be used to guide the analyst on the number and type of component modes best utilised.

Finally the theoretical integrity of the proposed maethod has been demonstrated, since it can provide results with excellent accuracy relative to the finite element method, even with a low number of degrees of freedom, subject to the kind of component modes used.

I - 3. Elastic Domain Modelling

I-3-1. Exact and Approximate Modelling

Of foremost importance within the framework of flexible multibody dynamics is the modelling of the distributed elastic domain. Small linear elastic deformation has been assumed throughout this work. A linear elastic structure can be either modelled as an infinite parameter system or discretised to a finite one. Structural systems are in reality distributed parameter systems, therefore their description requires an infinite number of degrees of freedom. Although distributed parameter modelling is desirable for the exact solution of the structural dynamics problem, this is only feasible for systems with fairly simple geometry or systems idealised as such[2]. Moreover, not all distributed parameter mathematical models have closed-form solution[34]. Numerical solutions, although difficult, are possible to produce, but render the 'exact' character of the modelling approximate. Since distributed parameter modelling posses the aforementioned difficulties, alternative methodologies have been established where the infinite number parameter system is approximated by a finite dimensional model. Such a procedure, called generally discretisation, may be considered any approximation process that aims in reducing the infinite number of degrees of freedom representation of a real system to a finite number. Discretisation may either involve lumping mass and stiffness characteristics or expanding the linear deformation of a system in a finite series of functions, procedure referred to as spatial discretisation. Lumped parameter models are more intuitive, arbitrary in character and the analyst has little control over the error involved in the discretisation

process.

I-3-2. Rayleigh-Ritz Type Spatial Discretisation Methods

I-3-2-1. Continuous Version of the Assumed-Modes Method

Whereas the Rayleigh-Ritz method is a methodology for solving the differential eigenvalue problem, the continuous version of the assumed-modes method is a Rayleigh-Ritz type spatial discretisation of a distributed parameter system prior to the derivation of the equations of motion[25]. Therefore, there is no longer need to establish the partial differential equations describing the dynamics of the distributed system. As in the Rayleigh-Ritz method, the deformation is approximated in the form of finite series of space-dependant admissible functions, with the difference that the coefficients are not constant but time dependant and form the generalised coordinates of the system. The series can be substituted in the kinetic and potential energy expressions, thus rendering them to discrete form, and the equations of motion can be derived by means of a variational method such as the Lagrange equations. The assumed-modes method can therefore be also used in deriving the response of a system to external forces and initial excitation. Utilising the continuous form of the assumed-modes method, a continuous media, described normally by partial differential equations, can be modelled by a reduced order finite set of ordinary differential equations. More interestingly the assumed-modes method yields the same eigenvalue problem as the Rayleigh-Ritz method, i.e. the Galerkin equations[22]. The assumed-modes method will be considered here, in agreement with the literature, as a method suited for spatial discretisation of a complete structural system or a large subdomain of a system[31]. This implies that the admissible functions used are 'global' functions capable of describing large parts of the system. This makes the method difficult to deal with complex, geometrically irregular structures. It is indeed a very difficult task, and most of the cases impossible, to select admissible functions capable of describing complex systems with accuracy. An answer to complex geometries is provided by the finite element method.

I-3-2-2. The Finite Element Method

The finite element method is recognised as another Rayleigh-Ritz type discretisation,

which like the assumed-modes method is not designed for solving differential eigenvalue problems, but for modelling a distributed parameter system with finite degrees of freedom. Like the assumed-modes method, the finite element method is seeking admissible functions for approximating the system dynamics, but as opposed to the assumed-modes method these trial functions are defined for much smaller structure subdomains, the elements. Therefore, the trial functions are not considered 'global' functions but 'local'. Although this difference seems to be of quantitative nature, a particular methodology facilitated by the use of 'local' functions results to a distinct mathematical model. In other words, although the finite element method qualifies as a Rayleigh-Ritz type spatial discretisation technique, the associated (discrete parameter) algebraic eigenvalue problem does not result to the Galerkin equations. Defining admissible functions for only small subdomains is one of the features of the finite element method that makes it so versatile for modelling complex structures. Indeed for most of the cases one needs to use only simple admissible functions, known as interpolation functions, in order to approximate the linear deformation within an element. At the elemental level the distributed deformation, approximated by a finite series of local functions, is finally expressed in terms of the unknown nodal displacements[7]. It is this mathematical manipulation that really distinguishes, on mathematical level, the finite element method to the assumed-modes method and gives it extreme power as an engineering tool. The nodal displacements play the role of generalised coordinates in the element entity. The local functions are very attractive computationally, as integrals for the derivation of Lagrangian expressions at the elemental domain, involve functions that can be evaluated in closed-form, thus eliminating numerical integration errors. Displacement compatibility between elements can directly be enforced in an assembling process. Assembling the energy functions of the system from the elemental energy expressions is straightforward. By applying the Lagrange equations, the linear differential equations of motion are readily obtained. The system degrees of freedom are the nodal physical displacement coordinates of the structure.

I-3-3. Discrete Version of the Assumed-Modes Method

It has been discussed that the continuous version of the assumed-modes method and the finite element method are Rayleigh-Ritz type spatial discretisation techniques. Their purpose is not to approximate the solution of partial differential

equations, but to create in their place a set of ordinary differential equations. This is particularly convenient, since partial differential equations can only be derived for a small family of systems. Moreover, the solution of the ordinary differential problem is much simpler than the solution of the partial differential problem. Other than spatial discretisation techniques, lumped parameter modelling also concludes to a set of ordinary differential equations. In general, however, both the lumping and particularly the finite element method result in high order differential systems. In any case, the analyst may wish to reduce the order of the resulting system, and this may be accomplished, amongst other techniques, by the application of the discrete version of the assumed-modes method[6]. This method can be considered as a linear transformation of a discretised system from one finite dimensional space to another. The discrete version, although in mathematical formalism is similar to the continuous version, it is not considered a spatial discretisation technique, but just a transformation of a high order discretised model to a lower one. It can be shown that the discrete version of the assumed-modes method satisfies the Rayleigh's quotient for discrete parameter systems. Thus a finite set of time-varying coordinates describing a particular discretised system can be approximated by a series of admissible vectors multiplied by a set of time-varying generalised coordinates[3]. The discrete version of the assumed-modes method is therefore an extremely useful tool for truncation purposes of high order spatially discretised systems.

I - 4. Global Modelling versus Substructuring

In the literature there is a plethora of methodologies for modelling the geometrically nonlinear and linear dynamics of large-scale flexible systems. Linear structural systems can be composed of any number of substructures connected together in multi-point or single-point interfaces, forming open-loop or closed-loop configurations and allowing any possible small displacement between the substructures. In the content of this work, substructure is considered any distinct component or more generally any idealised finite subdomain of a structure much larger than a finite element. The most general separation of methodologies regarding the formulation of the dynamics of multibody structures is to either model the entire system as a single entity - global modelling - or consider the structure as a collection of a number of substructures and treat each one individually - substructuring approach.

I-4.1. Global Modelling

Traditionally, the linear dynamical behaviour of large-scale complex structures has been modelled, in engineering practice, by the direct use of the finite element method. As analysed earlier, distributed parameter formulations (exact modelling) or the continuous version of the assumed-modes method may not be feasible for modelling complex systems. Lumping methods are more applicable, but control over the modelling error is generally restricted. On the other hand, using the direct finite element method, the structural system can be treated as a single entity and the dynamics of the structure are represented by a high-order coupled ordinary linear differential equations. The global modes (eigenvectors) of the system and natural frequencies can be straightforwardly obtained by solving the associated algebraic eigenvalue problem. For a forced problem the solution of the nonhomogeneous differential equations is facilitated by the modal analysis method. This is accomplished by appropriately introducing a small number of modal vectors (number usually decided on the forcing frequency of interest) into the high-order differential equations. The coupled high-order differential set not only reduces to a smaller one but also the homogeneous part acquires an uncoupled form, due to the orthogonality property of the modal vectors. The high number of coupled differential equations are reduced to a small number of uncoupled equations.

Although treating the structural system as a single entity by the use of finite element method is a straightforward and very accurate process, and has been successfully used for numerous structural and control applications[35], there are inherent disadvantages with such an approach. The primary concern is linked to computing time considerations. The resulting eigenvalue problem, of a high order coupled algebraic equations, needs to be solved prior to proceeding with the order reduction of the differential system. The computing time involved in solving the eigenvalue problem is about proportionate to the square or cube of the degrees of freedom of the system. In the case that numerical solution is possible by solving only part of the eigenvalue problem, i.e. extract only a small number of eigenvalues and eigenvectors, the computing time is significantly reduced, but still depends highly on the order of the problem. At the same time large-scale problems need advanced computer hardware and software to be able to store and solve the eigenvalue problem.

Moreover, the design of control algorithms and their implementation to real-time systems is not possible using high order mathematical models. For control applications, a series of global level truncation techniques[32,71,65] have long now been established to reduce the size of linear mathematical models taking into account the control strategies to be implemented. The global order reduction techniques estimate which of the modes of the global system do not contribute to the control-structure interaction and eliminate those from the modal set. The reduced size linear mathematical models can subsequently be used for control algorithm design and real-time (on-board) implementation. Nevertheless, solution of a large part of the high order formulated linear problem is still necessary prior to the application of truncation techniques, increasing the computational cost significantly.

I-4-2. The Substructuring Approach

The alternative to global modelling of large-scale systems is provided with treating each substructure individually. Most of the methodologies established, utilising the substructuring concept, can alleviate all the above mentioned difficulties. Moreover, other benefits are to be gained.

Most importantly, system order reduction can be performed at the substructure level, resulting directly in low order linear differential equations. This is accomplished by approximating the linear elastic deformation of each substructure using spatial discretisation techniques. As discussed previously, for complex geometry substructures the finite element method can be applied. The finite element model of the component is subsequently reduced using the discrete version of the assumed-modes method. For the description of the small linear elastic deformation, the transformation involves a finite set of generating modes (vectors), referred to as component mode set, which may be a combination of a number of dynamic modes (vectors) complemented by a number of static modes (vectors)[30]. For deriving the dynamic modes of each substructure an algebraic eigenvalue should be solved. This eigenvalue problem is of much smaller dimension to the eigenvalue problem of the entire structure. Since computer time in vibration analysis increases at about the square or cube with an increase in the number of degrees of freedom, it is beneficial if the eigenvalue analysis of the complete system is substituted by the eigenvalue

analysis of its individual substructures. By truncating the number of the dynamic modes of each substructure, the reduced size component mode sets can subsequently be imported in any generic mathematical model that can couple the overall motion of the substructures, and the low order linear differential equations of a particular structural system can be produced. Similar comments apply if the substructures are of simple geometry and spatial discretisation can be achieved by the continuous version of the assumed-modes method.

An additional computing time advantage is obtained due to the inherent nature of large-scale systems. Such systems are composed of a large number of identical components, and in the case of structures in space these may include solar panels, radiation booms, antennas, spacetruss boxes etc. Therefore, utilising a substructuring approach, modelling and analysis of common components has to be performed only once. Therefore, not only the solution of the dynamical problem is accelerated, but at the same time low order systems do not need advanced computer hardware and software capabilities for storing and solving the formulated problem.

Moreover, structural systems may include articulated components, allowing the change in orientation of these components for facilitating various operations. It is therefore always a demand for the dynamic analysis of the structure in different configurations. Modelling and solving the complete system over a large domain of different configurations of interest can prove an extremely time consuming process. However, modelling the structure as a collection of substructures this problem can be overcome easily, just by allowing different orientations to the articulated substructures and solving only part of the substructuring analysis. Similarly, in the design process, even the location of some members may be altered, hence the substructuring approach will definitely facilitate efficient repositioning operations. In optimisation problems computational time is greatly reduced if a small number of substructures are to be optimised.

Since complete structural systems have become very complex, major components are often designed, produced and tested by different organisations. Therefore, not only it is often difficult to assemble an entire finite element model in a timely manner, but experimental data for individual components has sometimes to be incorporated

into the analysis of the entire system[9]. Such implementation would not be possible using the finite element model of the entire structure.

The control community is also interested in modelling the structural systems as collections of components. Additionally to the benefits obtained concerning the structural dynamics part, truncation techniques can be further implemented at component level, considering the particular control strategy to be utilised. This particular approach is preferential for control applications, especially so, for the complex structures with articulated components[19,20]. If necessary, further order truncation can be performed at the global level. Moreover, decentralised control algorithms can be implemented.

I-4-3. Multibody Dynamics and Component-Mode Synthesis

Both the areas of multibody dynamics and component-mode synthesis employ the concept of substructuring. As the term implies, the multibody dynamics field considers a structural system as a collection of interacting bodies. The genesis of this field is traced to the need for the description of the dynamical behaviour of systems composed of interconnected rigid components undergoing large rotational displacements. Gradually, due to new demands in applications, the rigid body assumption was relaxed and rigid bodies were replaced with flexible ones. The contribution of this area lies mainly in the formulation of nonlinear mathematical models for structural systems composed of interconnected flexible and rigid components. Multibody dynamics, unlike most of the nonlinear finite element formulations, inherently utilises the concept of substructuring, and the nonlinear mathematical models obtained are of low order. By linearising the large angular displacement, some of the approaches in the area of multibody dynamics lead to efficient low order linear mathematical modes.

Component-mode synthesis is an area of geometrically linear structural dynamics that is concerned with the modelling of large-scale complex structures. The area was mainly initiated for overcoming difficulties associated with the modelling of the entire structure using the finite element method, such a computing time and storing problems. In the component-mode synthesis, the large-scale structural system is decomposed to substructures, which, in general, are connected to each other in

multi-point interfaces. Initially the synthesis processes for deriving the linear differential equation of motion for the global system, using the component modes of each substructure, were very much dependant on the kind component modes utilised. Subsequently, it was shown that the most efficient way to derive mathematical models, regardless of the component modes used, is by a Lagrangian formulation using the Jacobian partitions of the constraint equations[15]. In this sense, component-mode synthesis can be considered a linear multibody dynamics method, particularly effective for handing large number of substructures connected generally in multi-point interfaces.

Component-mode synthesis area has vastly contributed in providing component mode sets for accurately capturing the linear deformation of components. Component mode sets, and mainly those that include static modes, have been recently used extensively in the nonlinear multibody dynamics area, for structural dynamics and control applications[19,20]. In fact, the kind of component modes imported in a mathematical model is of foremost importance for the accurate modelling of the dynamics of large flexible multibody structures.

The current state of the art methodologies for treating large-scale flexible nonlinear or linear systems are multibody dynamics methods for establishing generic mathematical models, and incorporate component mode sets, from the component-mode synthesis area. The formulations can model exactly the geometrically nonlinear or linear rigid-body motion and with high accuracy the linear elastic deformation of the components with a low number of differential equations[61].

I - 5. Selection of Modelling Methodology

I-5-1. Background

The intention in this work has been the development a method suitable for the linear dynamics modelling of large multibody structures that belong in the category II missions in space. The method should result in a low order linear mathematical model that at the same time would approximate accurately the dynamics of large complex flexible structures.

A methodology framework has been fully established and can deliver geometrically nonlinear and linear methods. The study in this section has been compiled for justifying that the methodology framework developed in this work is capable of producing linear and nonlinear methods for multibody dynamics modelling for all categories of missions in space. The modelling objectives of the methodology are the following:

Exact modelling of the large geometrically nonlinear motion.

Single-point holonomic constraints.

Open-loop topology.

Linear elastic deformation modelling.

Multi-point articulation, non-holonomic constraints, closed-loop topology and nonlinear elastic deformation are outside the modelling objectives. The restrictions of the methodology are limited and are not often encountered in the dynamics modelling of structures in space. In general, structural systems in space are typical examples of open-loop multibody systems with operational components connected at single-point interfaces. Setting the above objectives, the methodology should be able to generate nonlinear and linear mathematical models for most of the current and near future applications involved in all categories of missions in space.

More specifically, the subject of this review is to establish the characteristics of the methodology followed in this work in such a way as to demonstrate that it is mostly efficient for satisfying all modelling objectives set. With such broad objectives, one is confronted with a series of decisions on methodology strategies. These may be prioritised in the following way:

Augmented versus minimal formulations.

Non-recursive versus recursive formulations.

Lagrangian versus Netwon-Euler formulations.

I-5-2. Augmented versus Minimal Formulation

In the augmented formulation, the kinematic constraint equations are adjoint to the system of dynamic differential equations using the technique of Lagrange multipliers. If N the number of interdependent generalised coordinates of the multibody system

and N_c the number of independent kinematic constraints, then the multibody system in the augmented approach is described by a set of N number of differential equations coupled to the set of N_c kinematic constraint equations. The coupled system of equations has to be solved simultaneously. It is obvious that the independent generalised coordinates (degrees of freedom) of the system are $N-N_c$. Therefore, the augmented formulation does not result in the minimum number of equations.

Using an augmented Lagrangian approach both holonomic and non-holonomic constraints can be modelled. Moreover, the constraint forces and torques (Lagrange multipliers) of the multibody system are directly furnished by solving the augmented set of equations. In addition, the coupled set of the nonlinear differential equations and the constraint equations can be derived in a systematic way facilitating computational implementation. Nevertheless, the solution phase of the augmented formulation is numerically complex and, in some applications, complications with integration schemes can be encountered[67]. An additional penalty is that the computational cost is very high compared to the minimal formulations.

For the case of non-holonomic constraints and using a Lagrangian approach the non-minimal formulation is unavoidable. The complications of this sophisticated numerical formulation, of having to solve a higher than needed set of coupled nonlinear differential equations along with generally nonlinear algebraic equations, can be avoided for holonomic systems. For multibody systems with holonomic constraints (scleronomic or rheonomic) there is always possible to express the interdependent generalised coordinates of the system as functions of the independent ones. This is accomplished by the use of partitions of the Jacobian matrix of the constraint equations. In the case of a non-holonomic system this procedure is not possible since the constraint equations cannot be integrated. It can be proved, by the use of the Lagrange form of D'Alembert's principle, that in the case of holonomic constraints the resulting set of differential equations can always acquire a minimal size $(N-N_c)$[43]. Therefore, the Lagrangian formulation with multiplies can be substituted by a Lagrangian formulation with Jacobian matrix partitions. For holonomic systems the benefit of such an approach over the augmented method is reduced computational cost and less complex numerical treatment that this methodology requires. Nevertheless, it is not always straightforward to select the

right partitions, i.e. to decide which of the coordinates should be dependent and which independent, in order to result to nonsingular partitioned matrices. Computational techniques such as Gaussian elimination[67] and singular value decomposition have been used to account for matrices ill-conditioning. Moreover, the constraint forces eliminated from the analysis by the use of the Jacobian matrix partitions need systematic treatment in order to be recovered. An example of the use of Lagrangian formulation with Jacobian matrix partitions, can be found in the literature of component-mode synthesis techniques[30]. It has been demonstrated that for the case of multi-point holonomic interfaces between substructures, the most efficient way to synthesise the component modes of the various substructures, in order to derive the linear equation of motion of the system, is by the use of the Jacobian matrix partitions. The proof considered the general case of Lagrange multipliers formulation and reduced that to a minimal set of linear differential equations.

Other than Lagrangian formulations, Kane's method of generalised speed[52] can also treat non-holonomic constraints. Unlike the Lagrange multipliers formulation, the resulting differential equations are of minimal dimensions. At the same time, Kane's method is computationally efficient since it combines the advantages of both Netwon-Euler approach and the recursive Lagrangian formulation - the non-working constraint forces and torques do not appear in the equations and the large number of differentiation of the kinetic energy expressions are avoided[43]. Considering the minimal character of Kane's formulation and the computational advantages mentioned, it may seem inexplicable that the method is not that popular for all-purpose multibody coding. Perhaps the answer is dual. Firstly there is not an easy and systematic way to derive the constraint forces and torques of the system, and secondly the mathematical treatment needed for resulting to the computational implementation is very complex and elaborate[23].

Conclusively, the use of the augmented Lagrangian formulation for all-purpose multibody codes is justified, since it is computationally straightforward to apply, can solve both holonomic and non-holonomic systems and furnishes directly the constraint forces and torques of the multibody system. Nerertheless, indiscriminate use of the method for any application has been encountered in the literature. With less generic modelling objectives, such as those involving holonomic constraints, the

augmented method cannot be considered the most efficient methodology, because of the high computational cost involved. Straightforward mathematical modelling for computational implementation can also be accomplished by the Lagrangian formulation of the Jacobian partitions, which is faster to produce results. In fact the higher the number of the interconnected bodies and holonomic constraints, the more costly the Lagrangian augmented formulation can be relative to the minimum Lagrangian formulation. Accounting for all parameters, and considering the mathematical complexity of formulating mathematical models using Kane's minimum approach, the Lagrangian formulation of the Jacobian partitions seems to be the preferential one for holonomic system modelling between all three methodologies examined.

However, since computational difficulties are also encountered on separating the independent to the dependent generalised coordinates in the minimal Lagrangian approach of Jacobian partitions, one is motivated to seek for an alternative minimum formulations for solving holonomic multibody systems. An additional reason for seeking for alternative minimum formulations is that, in the case of the Lagrangian formulation with Jacobian partitions, the constraint equations and more significantly the component kinematics are derived relative to an absolute frame of reference (the same applies for the Lagrangian augmented approach). This means that the history of the orientation, position and their rates for each component, obtained from the solution of the differential equations, are given relative to an inertial observer. Ideally, one is interested, especially so in spatially nonlinear dynamics, in the relative orientation and position between adjacent bodies. The implication that the component kinematics are formed relative to an absolute reference frame is that the relative joint coordinates and their derivatives are not explicitly available, and this limits at some extend the implementation of control strategies, since it usually much easier to measure relative joint displacements, velocities and accelerations. In order to acquire relative kinematical expression one needs to transform at each time step the absolute expressions to relative ones, adding to the computational cost. The answer to the computational difficulties and the drawback of the absolute reference frame kinematical expressions, encountered in the minimum Lagrangian formulation of Jacobian partitions, can be provided by the recursive formulations.

I-5-3. Recursive versus Non-Recursive Formulations

In the recursive methods, the component absolute kinematical expressions are written directly relative to a suitably positioned reference frame within the preceding component. The exact expressions of the outboard component kinematics are subject to the constraints at the interface with the inboard component. The absolute kinematical expressions of the outboard component involve the absolute kinematical expressions of the local reference frame positioned in the inboard component and relative kinematical expressions of the outboard component (relative) to the local reference frame. These relative kinematical expressions are only functions of the independent generalised coordinates of the outboard component. In a systematic manner, the absolute kinematical expressions characterising the motion of any component in a system can be expressed in terms of all the independent generalised coordinates of the components that precede it in the multibody chain.

Recursive methods are more elaborate in deriving the absolute kinematical expressions of components, since they account for the motion of the preceding component and at the same time the interface constraints. The procedure may be complex in terms of kinematical descriptions, but on the other hand does not involve intensive mathematical treatment. In actual fact, this complex analytical process gives an excellent insight in the kinematics of the component, unlike the case of non-recursive methods. Moreover, the resulting differential equations are of minimal size, since the kinematical expressions of each component are only functions of independent generalised coordinates. The solution of the differential equations furnishes directly the orientation and position (and their time derivatives) of any component relative to the preceding one, with the aforementioned advantages. Since the Jacobian matrices do not need to be formulated and the mathematical treatment is not that involving, recursive methods can be computationally and mathematically less complicated to the other minimal approaches.

The main drawbacks of recursive methods are that the description of rheonomic constraints may be difficult and the constraint forces and torques need systematic treatment in order to be derived, since, as anticipated, they are not furnished directly by the solution of the minimal of differential equations. Moreover, in the author's knowledge, treatment for multi-point interfaces has not yet been established in the

literature using minimal recursive methods. In any case, multi-point interfaces have been set outside of the modelling objectives since such cases are rarely treated in the dynamics modelling of structures in space.

I-5-4. Lagrangian versus Netwon-Euler Recursive Formulations

Recursive methods can be obtained using either a Lagrangian approach, a Newton-Euler formulation or hybrid Netwon-Lagrange methods. The Netwon-Euler equations have the main disadvantage that the non-working constraint forces and torques need to be eliminated from the system equations. On the other hand the recursive Lagrange formulation needs a large number of differentiations for obtaining the nonlinear differential equations of motion. The hybrid methods have essentially the disadvantages encountered in the Netwon-Euler approach.

In a Netwon-Euler formulation there are systematic ways to eliminate the non-working forces using amongst others graph theory or projection matrices[66], but in general these techniques are more elaborate than differentiating systematically the kinetic energy of the system. Moreover, the recursive derivation of the acceleration expressions from one component to the next, in order to obtain the absolute acceleration of the terminal body, is a much more involving process than dealing with the velocity expressions of the components, especially so for flexible components. The recursive Lagrangian approach seems less demanding than the Netwon-Euler for resulting to the set of the nonlinear differential equations. For geometrically linear system, the amount and form of the expressions to be differentiated is simplified in such an extend that the linear differential equations can be readily obtained form the scalar energy functions in a single step.

Conclusively, the most efficient methodology for modelling holonomic open-loop multibody systems is a recursive Lagrangian formulation of generalised coordinates. It results to a minimum set of differential equations, uses relative reference frame component kinematical expressions, offers a better physical insight into the components kinematics, and does not implicate complex computational algorithms. The structural dynamics methodology is shown in Table I-1.

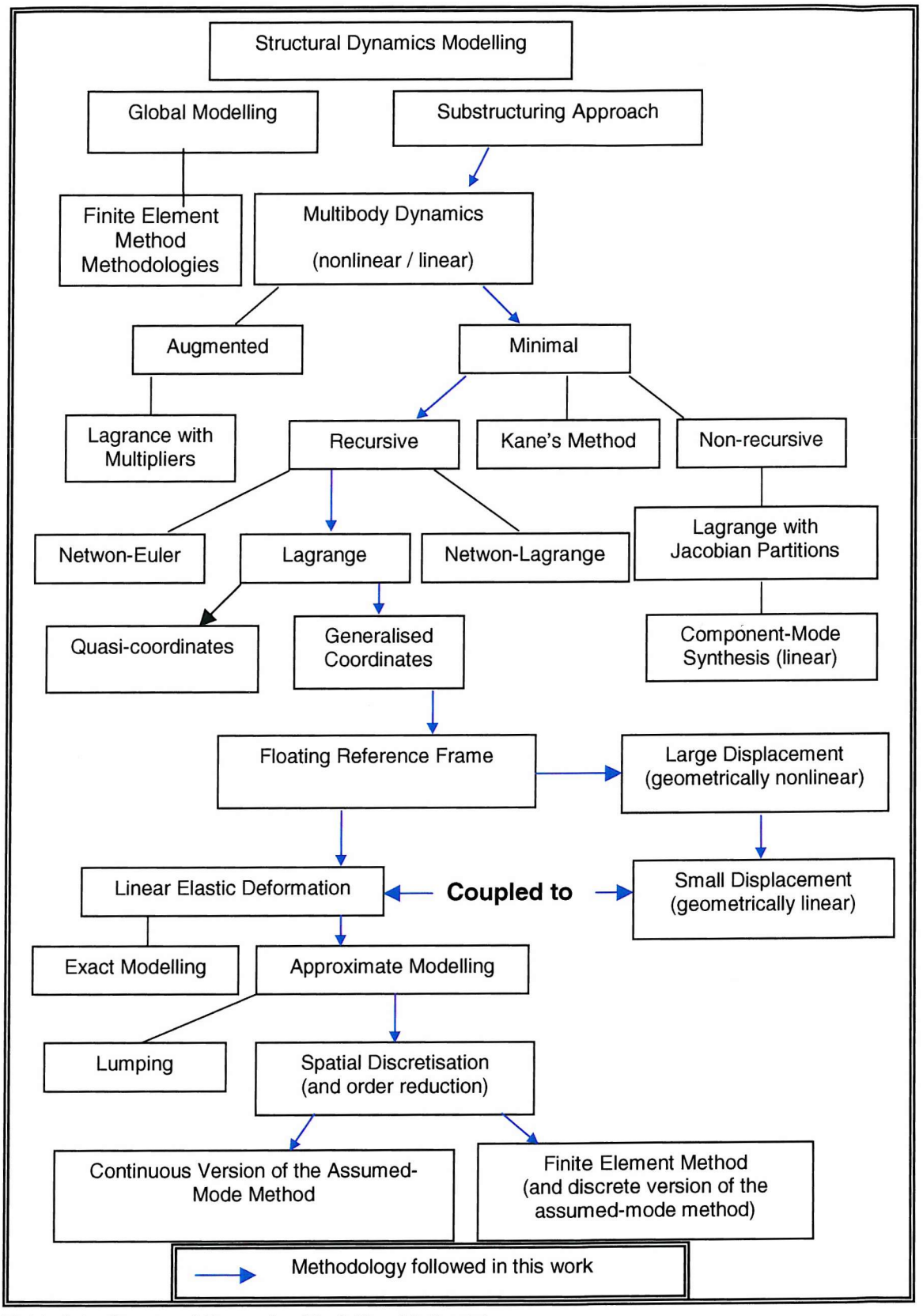

Table I-1 Structural Dynamics Modelling Methodology

I - 6. Component - Mode Synthesis

The research in the area of component-mode synthesis has been focused in two main areas. Most importantly in identifying component mode sets that would accurately and efficiently capture the actual deformation of the substructures, once they are reassembled to form the structural system. Secondarily the interest is focused on effectively synthesising the component modes to form the linear differential equations of the structural system.

In most component-mode synthesis methods, the synthesis techniques, for assembling the substructures component modes to form the differential equations of the global system, are coupled to the actual description of the component modes utilised. As pointed out in the 'Critical Selection of Modelling Methodolody', it has been proved that all the separate techniques of synthesis (in the time domain) can be substituted by a Lagrangian formulation of Jacobian partitions. This approach can allow any component mode sets to be directly employed in the equations, and therefore the tailored synthesis techniques are not essential. In this respect, component mode synthesis methods can be considered as a subset of the multibody dynamics modelling for geometrically linear systems where components are connected in general in multi-point interfaces. In fact the Lagrangian formulation of Jacobian partitions is the most efficient way of formulating the linear differential equations of motion when multi-point interfaces are considered.

On the other hand, the most important contribution of the area is the development of efficient component mode sets for the approximation of the linear deformation of the substructures. In this respect the research involved in component mode synthesis can be used in multibody dynamics of flexible systems. The first component-mode synthesis method[11] that appeared in the literature uses fixed-interface normal modes complemented with a number of redundant contraint modes. The fixed-interface normal modes are the eigenmodes of the component with all internal (interface) and external (boundary) constraints fixed. Redundant interface constraint modes are defined by applying successive unit displacements to all redundant constraints in the system while the rest of the constraints (interface and boundary) remain fixed. Therefore, the number of the static modes equals the number of the redundant

constraints of the component, whereas the number of dynamic modes can be truncated to reduce the size of the formulated problem.

Following this pioneering work, a lot of interest was generated for deriving alternative component mode sets. A significant modification to the original redundant constraint method was proposed[68] where all the interface constraints of the system are treated alike. Seperation to redundant and nonredundant constraints is avoided. This is particular beneficial since it is not always an easy task to separate the interface constraints. In the constraint mode method, the fixed-interface normal modes are defined exactly as in the redundant constraint method and the number of constraint modes equals the number of the total interface constraints of the system. A variation on constraint interface component mode sets is proposed in this work to allow for application in determinate and underdeterminate interfaces.

Another component mode set with excellent convergence properties is the inertia-relief attachment mode set[13,8], which is complemented to free-interface normal modes. The inertia-relief attachment modes can be defined by applying successive unit equilibrated force at the interface constraints. This equilibrated force consists of an external applied force equilibrated by a rigid-body inertia force. These modes are then modified to be orthogonal to the rigid body modes[9,15]. To make these modes linearly independent to the kept free-interface normal modes, residual inertia relief attachment modes are defined by modifying the inertia relief attachment modes to be linear independent to kept free-interface normal modes[14].

The residual inertia-relief attachment mode set, along with any existing rigid-body modes of the component, have been proved to be a statically complete mode set[12]. That is, the superposition of the modes in this set is sufficient to determine exactly the 'static' response of the component subject to the interface forces. Since this static mode set is statically complete, can be complemented with either free-interface or fixed-interface normal modes.

A component mode set that does not use any static modes is the loaded-interface normal mode set. The substructure is loaded with the equivalent mass and stiffness contributions from the remaining components and the loaded-interface normal modes are obtained by the solution of the loaded component eigenvalue problem[14]. Unlike

the previous sets, the loaded-interface component mode set is not appropriate for independent modelling, since the data needed for its derivation depends on data obtained form the other components in the structure. For this reason its application may become very involving for the modelling requirements of large chains of components. A variation of the loaded interface component mode set has been proposed and implemented in this work.

Several other component modes have been proposed in the literature of component-modes synthesis[64,18,21] for improving convergence, but it is mainly the components mode sets referred previously that have been employed with success in the multibody dynamics area.[16,17,20,36,54,55]

It is interesting to note that the component modes are also used in the controls community[19,20] for component order reduction, as a first step, prior to reducing the order of the component further considering the control strategy.[65]

II Component Mode Sets

II-1. Prologue

II-1-1. Background

The information regarding the component modes has been drawn from the area of component-mode synthesis. This field of geometrically linear dynamics is concerned with large-scale structures where the substructures are in general connected to each other in multi-point interfaces. Therefore, the substructures in the area of component-mode synthesis are in general statically indeterminate. On the other hand, in the area of articulated multibody dynamics the components are in general connected in single-point interfaces and may perform large spatial rotational displacement via gimbal joints. In other cases particular articuration axes may be locked and the component may be undergoing large planar angular motion relative to the adjacent components. Other examples may involve small, geometrically linear spatial or planar motion of the components, excited by the control system for either readjusting the components to a line of sight or suppressing induced vibration. In most of its operational time, the component may be completely locked relative to the adjacent components. The components in the articulated multibody dynamics can be statically indeterminate, determinate or underdeteterminate.

In this work, the physical coordinate constraint sets of the component (interface and external) are redefined so that the component characterisation is generalised to include the statically determinate and underdeterminate cases. Additional constraints that belong to the set of internal physical coordinates are proposed for defining static modes in the cases of statically determinate and underdeterminate components. These additional constraints are imaginary since they do not correspond to any physical interface constraints of the components. Several component mode sets are defined and may be combinations of dynamic and static modes or dynamic modes alone. The dynamic modes used in this work are normal modes of vibration. Mathematical proofs to determine the size of the physical coordinate constraint sets

in order to define the various static modes has also been provided where necessary. The only assumption made in this part of the work is that adjacent components are connected in single-point interfaces. This assumption, however, does not restrict the generality of definitions of the physical coordinate constraint sets or the component characterisation.

II-1-2. Physical Coordinate Sets

Several groups of physical coordinates, illustrated in Figure II-1, have been redefined in order to generalise the definitions found in the component-mode synthesis literature.

{B}: Set with b number of boundary constrains
{β} : Set with β number of nonredundant boundary constraints
{I}: Set with i number of internal physical coordinates
{S}: Set with s number of nonredundant interface constraints
{R}: Set with r number of redundant interface constraints
{C}: Set of the total number c of interface constraints
{H}: Set with h number of imaginary constraints
{T}: Set of the total number t of physical coordinates

More specifically, we can define

i. Boundary constraint set {B} contains the externally constrained physical coordinates, i.e. constraints fixed in the inertial space. Nonredundant boundary constraint set {β} contains the minimum number β of boundary constraints that can restrict the rigid-body motion of a component.

ii. Constraint set {C} contains the total of interface constraints that a component shares with the adjacent components.

iii. Nonredundant constraint set {S} contains the minimum number s of interface constraints that can 'remove' any rigid-body degrees of freedom from a component, and is a subset of {C}. The maximum number of interface nonredundant constraints is 6.

iv. Redundant constraint set {R} is the complement of {S} in {C}, i.e. {R}+{S}={C}.

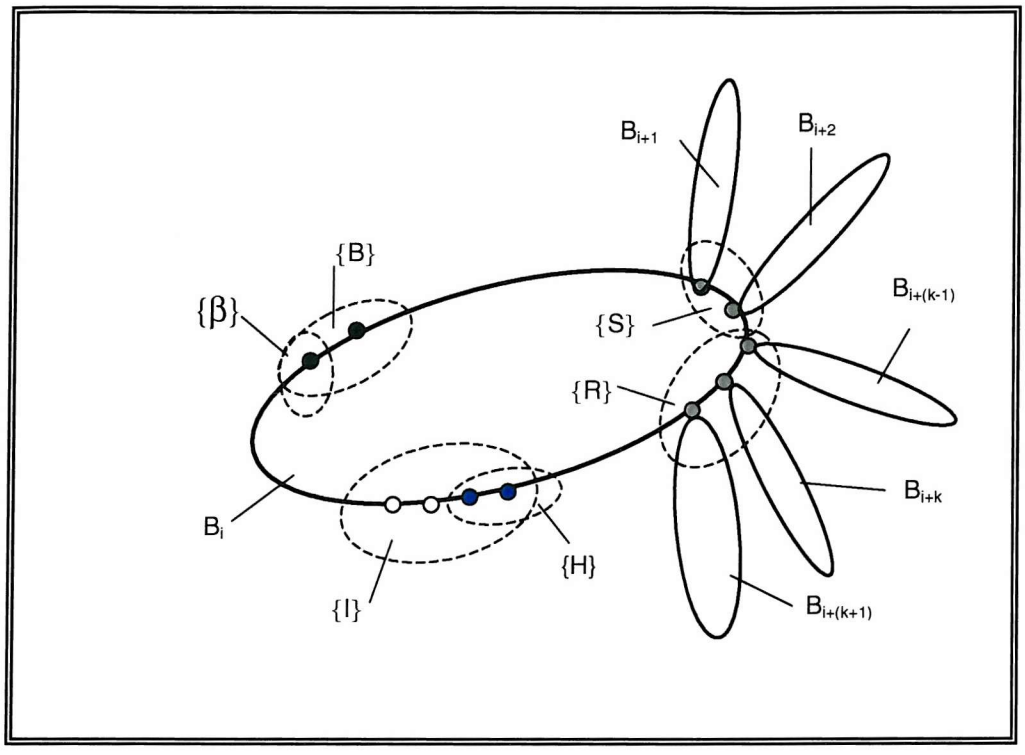

Figure II-1 Inboard component B_i and appended components B_{i+k} attached at single-point interfaces / illustration of the physical coordinate sets

v. Imaginary constraint set {H} contains h number of constraints. Imaginary constraints are a subset of the internal physical coordinates of the component. {H} is not a subset of interface constraints {C} , thus these constraints are imaginary.

vi. The set {T} contains the total number of physical coordinates t of the component, {T}={B}+{I}+{C}.

The nonredundant constraints {S} are a subset of interface constraints of the component and do not reduce the rigid-body degrees of freedom of a component in actual terms. These can only be reduced by the nonredundant boundary constraints

{β}, i.e. the external to the component nonredundant constraints that are fixed in the inertial space. This is the reason the word 'remove' in the definition of the nonredundant internal constraints is in quotation marks. One 'removes' the rigid-body degrees of freedom for the purpose of defining a statics problem that may furnish static modes. For example, a component free of external constraints has 6 rigid-body degrees of freedom, but by being connected to other bodies it may have 6 nonredundant interface constraints and therefore 'no rigid-body degrees of freedom'.

As discussed, in the same sense that the term 'nonredundant' can be used to describe internal constraints, it can also be used for external constraints, i.e. constraints fixed in the inertial space. The difference is that external nonredundant constraints remove the actual degrees of freedom. The number of rigid-body degrees of freedom n_r of a body in space is given by

$$n_r = 6 - \beta$$

where β the number of nonredundant external boundary constraints imposed on the body. The rest of the physical coordinate constraints in {B}, b-β, are considered redundant, because they cannot restrict the actual rigid-body motion of the component any further.

II-1-3. Component Characterisation

The component characterisation depends on the size of particular constraint sets (interface and boundary), and will prove useful for defining and deriving dynamic and static modes. The following component characterisations can be defined:

i. If s=nr and r≥1 then the component is considered statically indeterminate.

This means that there are enough nonredundant interface constraints to 'remove' the rigid-body degrees of freedom of the component, and the rest of the interface constraints, since they cannot 'remove' any further rigid-body degrees of freedom are considered redundant. The definition $s=n_r$, r≥1 is valid for any value of s in [0,6].

ii. If s=nr and r=0 then the component is considered statically determinate.

There are just enough interface constraints to 'remove' the rigid-body degrees of freedom of the component. Therefore, {S}≡{C} and {R} is an empty set. The definition $s=n_r$, $r=0$ is valid for any values of s in [1,6].

ii. If s<nr, regardless of the value of r, then the component is considered statically underdeterminate.

There are not enough nonredundant interface constraints to 'remove' the rigid-body degrees of freedom, but there may still be a number of redundant interface constraints, which are not capable of 'removing' any more rigid-body degrees of freedom, and therefore are considered redundant.

The three cases have been demonstrated with suitable examples. Figures II-2, II-3, II-4 have been used to illustrate examples of statically determinate, indeterminate and underdeterminate components respectively. In all cases the rigid-body degrees of freedom n_r are equal to 6, since no external boundaries are applied (b=0). The axes of rotational constraints at the joints are illustrated where is needed. A collective Table II-1 is presented to account for all cases. The calculation of the number s of the nonredundant constraints has been performed by inspection.

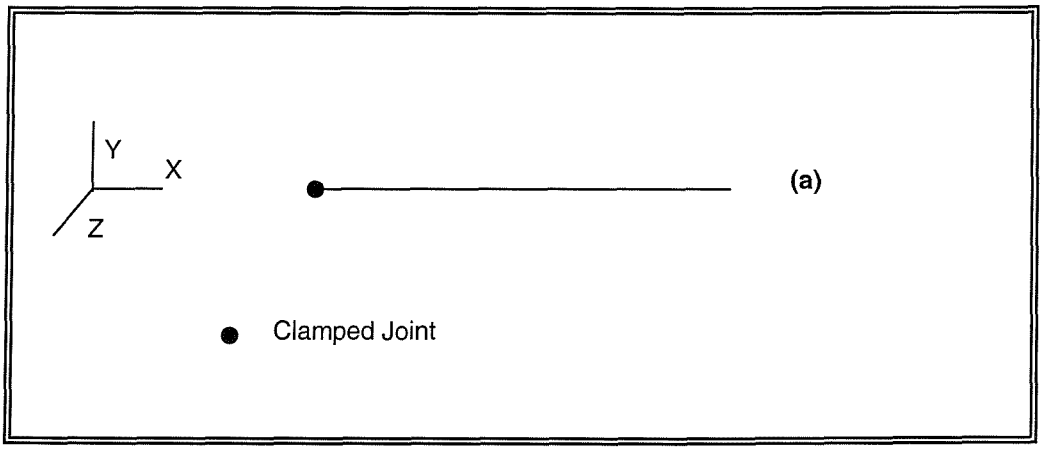

Figure II-2 Statically determinate component

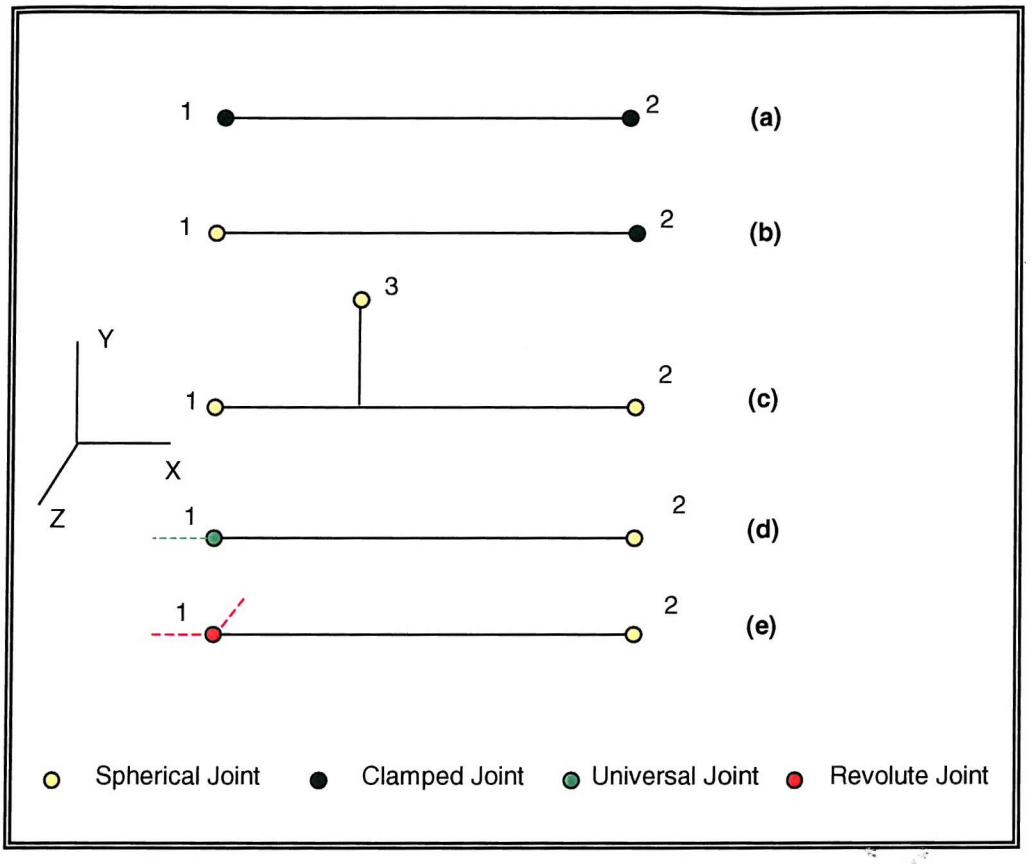

Figure II-3 Statically indeterminate components

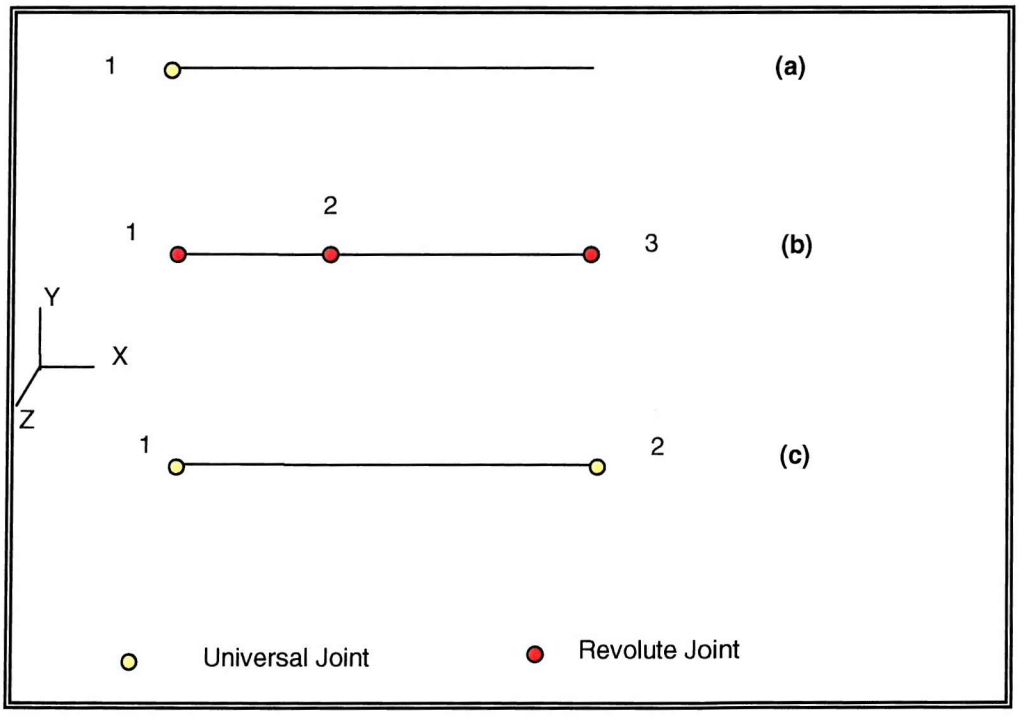

Figure II-4 Statically underdeterminate component

Example Case	Nonredundant Interface Constraints* {S}	Total Interface Constraints {C} ($C=\sum c_d$)	Redundant Interface Constraints {R} (r=s-c)	Component Characterisation
III-2(a)	s=6	$c=1xc_1=6$	r=0	Statically determinate
III-3(a)	s=6	$c=2xc_1=12$	r=6	Statically indeterminate
III-3(b)	s=6	$c=c_1+c_4=9$	r=3	Statically indeterminate
III-3(c)	s=6	$c=3xc_4=9$	r=3	Statically indeterminate
III-3(d)	s=6	$c=c_4+c_3=7$	r=1	Statically indeterminate
III-3(e)	s=6	$c=c_2+c_4=8$	r=2	Statically indeterminate
III-4(a)	s=3	$c=1xc_4=3$	r=0	Statically underdeterminate
III-4(b)	s=5	$c=3xc_2=15$	r=10	Statically underdeterminate
III-4(c)	s=5	$c=2xc_4=6$	r=1	Statically underdeterminate
Clamped joint: number of constraints $c_1=6$ Revolute joint: number of constraints $c_2=5$ Universal joint: number of constraints $c_3=4$ Spherical joint: number of constraints $c_4=3$				

Table II-1 Collective table for the component characterisation examples of Figure II-2, II-3, II-4

*External constraints {B}={0} for all cases $\Rightarrow n_r=6$

II - 2. Dynamic Mode Sets

Three sets of dynamic modes have been used in this work, namely the free-interface normal mode set, fixed-interface normal mode set and loaded-interface normal mode set.

A free-interface normal mode set can be obtained from an eigenvalue analysis of the component with the total of the interface constraints of the component free, i.e. $\{C\}$ is null in this analysis. If $\beta<6$, the body has a number of rigid body modes, $n_r=6-\beta$, and these should be removed from the analysis.

Fixed-interface normal mode set can be obtained from an eigenvalue analysis with the total of the interface and external constraints of the component fixed. If the system is statically underdeterminate, i.e. there are not enough nonredundant interface constraints to 'remove' the rigid-body degrees of freedom from the eigenvalue analysis (s<nr), then n_r-s 'rigid-body modes' should be removed from the analysis (equation (II-3)).

As for a free-interface mode set, the loaded-interface normal mode set proposed in this work can be obtained from an eigenvalue analysis with all internal constraints of the component B_i free, $\{C\}=0$ for the analysis. The same remarks apply in this case for the removal of 'rigid-body modes' as in the case of free-interface modes. In this work, the loaded-interface normal modes are defined for a cluster formation structure but can easily be generalised for a tree-configuration. Each interface node of a component B_i is loaded with the generalised inertia of the adjacent component. The modelling assumption that components attach to each other at single-point interfaces has been utilised. The rigid mass matrices, i.e. the generalised inertias, of the appended components B_{i+k}, k=1,2,... are superimposed on the consistent mass matrix of the component B_i at the interface nodes. The rigid body mass matrix of the appended component B_{i+k}, where k is the k^{th} appended component on component B_i is given by

$$M_{i+k}^{rigid} = \left(\begin{array}{c|c} M & m \left(\rho_{i+k}^{*} \right)^{x} \\ \hline sym & {}_{Bi}I^{Bi+k/Ji+k}_{Bi} \end{array} \right) \qquad \text{(II-4)}$$

where m is the mass of the appended component B_{i+k}

M is a diagonal matrix with $m_{ii} = m$

$\left({}_{Bi}\rho^{*}_{i+k} \right)^{x}$ is the skew-symmetric distance matrix of the interface node to the centre of mass of the appended component B_{i+k}, expressed in the body frame of the component B_I

${}_{Bi}I^{Bi+k\,/\,Ji+k}$ is the inertia of the appended component B_{i+k} relative to the interface node J_{i+k}, and expressed in the body frame of component B_i.

If the nodal interface constraints are less than 6, i.e. the interface node allows articulation, one needs to appropriately truncate the full form of the appended component rigid mass matrix to allow for the rotational degrees of freedom.

II-3. Static Mode Sets

In the content of this work two sets of static modes have been defined, the redundant constraint mode set and the constraint mode set. Either of these static mode sets can be calculated in a single step using the multiple algebraic equation

$$K_{Bi}^{FEM}\Phi_{Bi} - R_{Bi} = 0 \qquad \text{(II-5)}$$

where

K_{Bi}^{FEM} is the txt finite element stiffness matrix of the component B_i.

Φ_{Bi} is the txn static mode matrix containing either the redundant constraint modes

or constraint modes. n is the number of static modes derived in each set.

R_{Bi} is the txn reaction force matrix on component B_i resulting from the application of the redundant constraint displacements or constraint displacements. n is the number of static modes derived in each set.

II-3-1. Redundant Constraint Mode Set

A redundant constraint mode set is always well defined for statically indeterminate components, i.e. $s=n_r$ and $r\geq 1$. By definition redundant constraint modes cannot be obtained for statically determinate components, since {R}={0}. Later in this section, it will be shown that they cannot be derived for the case of underdeterminate components, even if {R} is not an empty set. The following definition applies in the case of a statically indeterminate component[11].

A redundant constraint mode set is obtained by applying a unit displacement to each redundant interface constraint in the set {R} set in turn, while the rest of the interface constraints in {C} remain fixed in space. Using the multiple equation expression (II-5), the matrix of the redundant constraint modes is defined by

$$\left(\begin{array}{c|c|c|c} K_{ii} & K_{ir} & K_{is} & K_{ib} \\ \hline K_{ri} & K_{rr} & K_{rs} & K_{rb} \\ \hline K_{si} & K_{sr} & K_{ss} & K_{sb} \\ \hline K_{bi} & K_{br} & K_{bs} & K_{bb} \end{array}\right)_{Bi} \left(\begin{array}{c} X_{ir} \\ \hline I_{rr} \\ \hline 0_{sr} \\ \hline 0_{br} \end{array}\right)_{Bi} = \left(\begin{array}{c} 0_{ir} \\ \hline R_{rr} \\ \hline R_{sr} \\ \hline R_{br} \end{array}\right)_{Bi} \qquad \text{(II-6)}$$

where

X_{ir} is the ixr matrix containing the displacements of the physical coordinates in {I} for each redundant constraint mode.

I_{rr} is the rxr unit matrix corresponding the unit displacement imposed on each redundant constraint in {R} in turn and the zero displacements imposed on the remaining redundant constraints.

0_{sr} is the sxr null matrix formed for the restriction that the nonredundant constraints have zero displacement values imposed for each unit displacement applied on the redundant constraints in turn.

0_{br} is the bxr null matrix corresponding to the values of displacement at the external boundary constraints.

0_{ir} is the ixr null matrix representing the reactions on the internal degrees of freedom {I} due to application of unit displacement imposed at each redundant constraint in turn.

R_{rr} is the rxr matrix containing the reactions on the redundant constraints {R} due to application of unit displacement imposed at each redundant constraint in turn.

R_{sr} is the sxr matrix containing the reactions on the nonredundant constraints {S} due to application of unit displacement imposed at each redundant constraint in turn.

R_{br} is the bxr matrix containing the reactions on the boundary constraints {B} due to application of unit displacement imposed at each redundant constraint in turn.

The matrix equation (II-6) has been partitioned into the different sets of coordinates participating to define the redundant constraint mode matrix. The coordinate sets have been repositioned in a suitable form to facilitate the mathematical operations. The solution of the multiple algebraic equation (II-6) gives the r number of redundant constraint modes in the form

$$\Phi_{Bi}^{rc} = \begin{pmatrix} -K_{ii}^{-1}K_{ir} \\ \hline I_{rr} \\ \hline 0_{sr} \\ \hline 0_{br} \end{pmatrix}_{Bi} \qquad \text{(II-7)}$$

where

Φ_{Bi}^{rc} is the txr redundant constraint matrix containing r number of redundant constraint modes of the component B_i.

K_{ii} matrix represents the stiffness matrix of the component with all interface constraints {C} and the total external constraints {B} fixed.

If s+β=6, then for any indeterminate case possible, K_{ii} matrix represents the stiffness matrix of a component with no 'rigid-body degrees of freedom', $n_r' = 0$ (equation (II-3)). A structural component with no rigid degrees of freedom has a positive definite potential energy, therefore the stiffness matrix of the component is positive definite. If the $K_{ii} > 0$ then the matrix is non-singular and the inverse always exists, so does the solution of (II-6).

For the proof to be complete it has to be shown that in the case of a statically indeterminate system the sum of the nonredundant internal constraints and the nonredundant boundary constraints is always equal to 6, i.e. β+s=6. It is

$$n_r = 6 - \beta \Leftrightarrow s + \beta = 6 + (s - n_r) \qquad \text{(II-8)}$$

By definition n_r=s for a statically indeterminate system, therefore from (II-8) s+β=6 for any acceptable values of s, β.

In the case of a statically underdeterminate component the matrix K_{ii} is always singular for any value of r, since always β+s<6. Using equation (II-8) and the definition of the statically underdeterminate component, s<n_r for any value of r, it can readily be proved that β+s<6 in all cases. The stiffness matrix is singular, cannot be inverted, so no redundant constraint modes can be derived, even in the case that redundant interface constraints exist, i.e. {R}≠{0}.

II-3-2. Constraint Mode Set

Constraint mode sets can generally be well defined for statically indeterminate components, but there are exceptions as will be demonstrated in this section. For statically determinate components constraint mode sets can be defined, but are not flexible modes since they reduce to rigid-body modes, and therefore are not useful for the purposes of this analysis. In the case of statically underdeterminate components, constraint mode sets cannot be derived. By introducing additional constraints, the imaginary constraints, it will be shown that constraint modes can be redefined for any possible component characterisation.

A constraint mode set is obtained by applying a unit displacement to each interface constraint in the set {C} in turn while the rest of the internal constraints in {C} remain fixed in space[14]. Using the multiple equation expression (II-5), the matrix of the constraint modes is defined as

$$\left(\begin{array}{c|c|c} K_{ii} & K_{ic} & K_{ib} \\ \hline K_{ci} & K_{cc} & K_{cb} \\ \hline K_{bi} & K_{bc} & K_{bb} \end{array}\right)_{Bi} \left(\begin{array}{c} X_{ic} \\ \hline I_{cc} \\ \hline 0_{bc} \end{array}\right)_{Bi} = \left(\begin{array}{c} O_{ic} \\ \hline R_{cc} \\ \hline R_{bc} \end{array}\right)_{Bi} \qquad \text{(II-9)}$$

where

X_{ic} is the ixc matrix containing the displacements of the physical coordinates in {I} in each constraint mode derived.

I_{cc} is the cxc unit matrix corresponding the unit displacement imposed on each interface constraint in {C} in turn and the zero displacements imposed on the remaining constraints.

0_{bc} is the bxc null matrix corresponding to the values of the displacements at the external boundary constraints in each constaint mode.

0_{ic} is the ixc null matrix representing the reactions at the internal degrees of freedom {I} due to application of unit displacement imposed at each interface constraint in turn.

R_{cc} is the cxc matrix containing the reactions at the interface constraints {C} due to application of unit displacement imposed at each interface constraint in turn.

R_{bc} is the bxc matrix containing the reactions on the boundary constraints {B} due to application of unit displacement imposed at each interface constraint in turn.

The matrix equation (II-9) has been partitioned into the different sets of coordinates participating to define the constraint mode matrix. The solution of the multiple algebraic equation (II-9) gives the c number of constraint modes in the form

$$\Phi_{Bi}^{c} = \begin{pmatrix} -K_{ii}^{-1}K_{ic} \\ \hline I_{cc} \\ \hline 0_{bc} \end{pmatrix}_{Bi} \qquad \text{(II-10)}$$

where

Φ_{Bi}^{c} is the txc constraint mode matrix containing c number of constraint modes for the component B_i.

K_{ii} represents the stiffness matrix of the component with all external and internal interface constraints fixed

It was proven before that for the case of statically indeterminate components β+s=6 holds. Similarly for the constraint modes, K_{ii} is non-singular, so the solution of (II-9) exists. Although, for statically indeterminate systems it has been proven that the inverse of K_{ii} always exists, since the system has no 'rigid-body degrees of freedom', thus a solution of (II-9) also exist, it may come as an unexpected fact that rigid-body modes may be furnished in the solution (II-9) in particular cases.

To demonstrate this, it is helpful to return to examples of Figure II-3 and Table II-1. It can be shown by inspection, and also proved mathematically, without solving equation (II-9), that cases 3(b), 3(d), 3(e) which correspond to statically

indeterminate components will furnish one single rigid-body mode, along with the c-1 constraint modes. More specifically, in case 3(b) a unit displacement of the nonredundant interface constraint θ_x at node 2 will cause a rigid-body rotation around axis X. Similarly, in case 3(d), 3(e) a unit displacement of the nonredundant interface constraint θ_x at node1 will cause a rigid-body rotation around axis X. It is obvious that in order to proceed with the approximation of the linear deformation of the component using the constraint mode set obtained, the rigid-body modes should be removed from the analysis. However, a possibly useful constraint mode cannot be derived.

Another interesting case emerges if the number of total constraints in {C} equals the number of the nonredundant constraints in {S}, i.e. there are no redundant interface constraints, {R}={0}, so the component is statically determinate. The multiple solution equation (II-9) will furnish only rigid-body modes. Rigid-body modes are not of interest since the aim is to obtain a number of constraint modes, in order to approximate the deformation field of the component. Therefore constraint modes cannot be obtained for a statically determinate component.

Furthermore, in the case of redundant constraint modes, constraint modes cannot be derived in the case of a statically underdeterminate component.

In summary, constraint modes cannot be derived in the cases of statically determinate and underdeterminate components. Also there are cases in the derivation of the constraint mode set for a statically indeterminate component that there may be 1 rotational rigid-body mode furnished along with the c-1 constraint modes. In an attempt to define constraint modes for any component characterisation, an additional set of constrains {H}, subset of the internal physical coordinates, is introduced in the system. In other words, the imaginary constraints are not a subset of the inteface constraint set {C}.

One may redefine the constraint mode set by imposing a unit displacement at each internal constraint in {C} in turn, while keeping the rest of the interface constraints in {C} and the imaginary constraints in {H} zero. The multiple algebraic equation can be written as

$$\left(\begin{array}{c|c|c|c} K_{ii} & K_{ic} & K_{ih} & K_{ib} \\ \hline K_{ci} & K_{cc} & K_{ch} & K_{cb} \\ \hline K_{hi} & K_{hc} & K_{hh} & K_{hb} \\ \hline K_{bi} & K_{bc} & K_{bh} & K_{bb} \end{array}\right)_{Bi} \left(\begin{array}{c} X_{ic} \\ \hline I_{cc} \\ \hline 0_{hc} \\ \hline 0_{bc} \end{array}\right)_{Bi} = \left(\begin{array}{c} 0_{ic} \\ \hline R_{cc} \\ \hline R_{hc} \\ \hline R_{bc} \end{array}\right)_{Bi} \qquad \text{(II-11)}$$

where

X_{ic} is the ixc matrix containing the displacements of the physical coordinates in {I} for each constraint mode.

I_{cc} is the cxc unit matrix corresponding the unit displacement imposed on each interface constraint in {C} in turn and the zero displacements imposed on the remaining interface constraints.

0_{hc} is the hxc null matrix formed with the restriction that the imaginary constraints have zero displacement values imposed for each unit displacement applied on the interface constraints {C} in turn.

0_{bc} is the bxc null matrix corresponding to the values of displacement at the external boundary constraints.

0_{ic} is the ixc null matrix representing the reactions on the internal degrees of freedom {I} due to application of unit displacement imposed at each interface constraint in turn.

R_{cc} is the cxc matrix containing the reactions on the interface constraints {C} due to application of unit displacement imposed at each interface constraint in turn.

R_{hc} is the hxc matrix containing the reactions on the imaginary constraints {H} due to application of unit displacement imposed at each interface constraint in turn.

R_{bc} is the bxc matrix containing the reactions on the boundary constraints {B} due to application of unit displacement imposed at each interface constraint in turn.

The imaginary constraints need to contain at least a nonredundant constraint set in order for $h+\beta \geq 6$ to hold *and* the component to have no 'rigid-body degrees of freedom' (n_r'). It can be proved that if the aforementioned hold, then for any component statically indeterminate, determinate or underdeterminate there will be a solution of equation (II-11) and also no rigid-body modes will be furnished in the analysis. In practice though it is difficult to determine for every component the value or position of the {H} set in order for {H} to contain a nonredundant imaginary constraint set. For this reason one may define the imaginary constraint set for all cases as an imaginary fixed point within the component. It is important to note that the size of the {H} set does not affect the size of the constraint mode set, which is fixed to c, i.e. equal to the number of the interface constraints.

By repositioning the partitions, the solution of equation (II-11) is given by

$$\Phi_{Bi}^{hc} = \begin{pmatrix} -K_{ii}^{-1}K_{ic} \\ \hline I_{cc} \\ \hline 0_{hc} \\ \hline 0_{bc} \end{pmatrix}_{Bi} \tag{II-12}$$

A collective Table II-2 is presented with the component characterisation and the solution of the dynamics and statics problem for defining the various dynamic and static mode sets.

Component Characterisation	Free-Interface or Loaded-Interface Mode Set	Fixed-Interface Mode Set	Redundant Constraint Mode Set	Constraint Mode Set + Imaginary Constraints
	Eigenvalue Analysis	Eigenvalue Analysis	Multiple Algebraic Solution	Multiple Algebraic Solution
Statically Indeterminate	N_K normal modes + $n_r' = 6-\beta$ rigid-body modes	N_K normal modes + $n_r' = 0$ rigid-body modes	r static modes	c static modes
Statically Determinate	N_K normal modes + $n_r' = 6-\beta$ rigid-body modes	N_K normal modes + $n_r' = 0$ rigid-body modes	No Definition {R}=0	c (=s) static modes
Statically Underdeterminate	N_K normal modes + $n_r' = 6-\beta$ rigid-body modes	N_K normal modes + $n_r' = 6-\beta-s$ rigid-body modes	No Solution K_{ii} singular	c static modes

Table II-2. Component characterisation and size of formulated dynamic and static mode sets.

II-4. Component Mode Sets

A component mode set, may be a combination of a finite number of dynamic modes complemented by a number of static modes or can be a dynamic mode set alone. Various component mode sets are derived using the dynamic and static modes defined, and are presented in Table II-3.

Component Mode Set	Dynamic Modes	Static Modes
Free-Interface Component Mode Set	n_k free-interface normal modes	—
Fixed-Interface Component Mode Set	n_k fixed-interface normal modes	—
Loaded-Interface Component Mode Set	n_k loaded-interface normal modes	—
Redundant Constraint Component Mode Set	n_k fixed-interface normal modes	r redundant constraint modes
Constraint Component Mode Set	n_k fixed-interface normal modes	c constraint modes

Table II-3 Definition of component mode sets

It is clear that the redundant constraint component mode sets cannot be defined or furnished for statically determinate or underdeterminate components. Constraint component mode sets can always be defined with the addition of imaginary constraints. For all component mode sets the rigid-body modes have been removed from the eigenvalue solution. Details have been presented in Table II-2.

II - 5. Conclusions

i. The loaded-interface component mode set has the following disadvantages:

- Component dependence: The loaded-interface component mode set defined for one component is dependent from the data of the appended components.
- It may be laborious to be applied to a chain of components.
- It is not suitable for geometrically nonlinear dynamics, since for large rotation analysis the rotary inertia of the appended component constantly changes relative to the inboard component. Its application would mean derivation of loaded-interface mode sets at each time step of the analysis. This would surely increase the cost of the analysis by a considerable amount.
- Even in the linear cases of appendage reorientation exercises the analyst would have to derive the loaded-interface mode set at each configuration of interest.

ii. The redundant component mode set has the following disadvantages:

- Separation between the nonredundant and the redundant constraints is essential and this may prove an involving procedure for a large multibody structure.
- Static modes are not obtained for the whole internal constraint set {C}, which may be fine for a highly redundant interface, but for a component with a small set of internal constraints may prove inappropriate. Even if an interface has a moderate number of constraints the decision on which redundant constraints static modes need to be defined for, is difficult to be decided a priori.
- The redundant constraint component mode set reduces to the fixed-interface component mode set for a statically determinate and underdeterminate component, since redundant constraint modes cannot be obtained in either case.

iii. Using constraint component mode sets most of the disadvantages of the redundant constraint component mode sets are circumvented. Separation of the internal constraints to nonredundant and redundant is avoided and all constraints are treated alike. Static modes can be defined for the whole interface. By appropriately selecting a set of imaginary constraints, the constraint component mode set can be defined for statically determinate and underdeterminate components. At the same time no 'rigid-body modes' are furnished in particular cases of statically indeterminate components. If imaginary constraints are defined as an imaginary fixed point within the component, all applications are treated alike and no special consideration is needed for the selection of imaginary constraints.. For well defined statically indeterminate components imaginary constraints need not to be used. But even if they are used, the number of constraint modes does not increase, thus computational cost is not affected.

III Nonlinear Recursive Component Kinematics

III - 1. Prologue

In nonlinear kinematics the overall motion of each component can be perceived as a rigid body motion relative to which elastic deformation can be observed. In this sense, one can assign to each component a suitably positioned floating reference frame that moves with the rigid part of the motion and relative to which the linear elastic deformation can be measured. Therefore, the overall motion of each component can be described in terms of the motion of the floating reference frame, and the deformation relative to it.

A floating reference frame is an orthogonal set of axes assigned to each component and follows the imaginary rigid-body part of the motion of the component. It is positioned at a point and orientation of preference within the imaginary rigid-body and therefore the position and the orientation of the rigid-body relative to an inertial or an arbitrary reference frame can be specified. At the same time an observer travelling with the floating reference frame can perceive the motion of the flexible component just as a time-varying deformation. In this sense, deformation can be measured and described relative to the floating frame in exactly the same fashion as a time-varying deformation of a component restrained in the inertial space would have been measured and described by an inertial observer.

The small linear elastic deformation of the components can be approximated using spatial discretisation techniques. The recursive Lagrangian formulation acquires a simple form, and includes in the set of (independent) coordinates the subset of the finite number of generalised coordinates associated with the elastic deformation of each component. As discussed in detail in the section 'Elastic Domain Modelling' within the introduction, if a component is of simple geometry, it can be spatially discretised using the continuous version of the assumed-modes method. For

complex geometry, the component can be spatially discretised using the finite element method. The finite element model of the component is subsequently reduced using the discrete version of the assumed-modes method. The transformation involves a finite set of generating modes (functions for the continuous version, vectors for the discrete version), referred to as component mode sets, which may be a combination of a number of dynamic modes (functions or vectors) complemented by static modes (functions or vectors).

In the recursive formulation, the time-varying configuration of each component is specified by the use of the floating reference frame where the rigid-part of the motion is described by the position and orientation of the floating frame relative to a reference frame within the inboard component, and the linear deformation using component modes measured relative to the floating frame. By truncating the number of dynamic modes, system order reduction can be performed at the component level.

With the use of the floating reference frame the nonlinear kinematical expressions for a single component have been derived. As discussed, in recursive formulations the orientation of the floating reference frame of a component is specified relative to a local reference frame positioned within the preceding component and located at the interface attachment between the adjacent components. To ensure that the various components act as part of the whole structure, a suitable kinematical procedure, common in all methods, has been proposed to accommodate the interface conditions between each component and the preceding one. The component absolute kinematical expressions are written directly relative to the suitably positioned reference frame within the preceding component. The exact expressions of the outboard component kinematics are subject to the constraints at the interface with the inboard component.

More specifically, in Appendix-A the kinematics of an arbitrary component connected to the preceding component via a non-translating single-point interface have been developed. The particular kinematical procedure followed in this work is only possible for multibody systems where no closed-loops and multi-joint interfaces are formed between the articulated components. Structures in space are typical examples of open-loop multibody systems with operational components joint at single-point interfaces. Initially the interface constraints between the two adjacent components

are considered as either rotationally free (spatially articulating component) or fixed (locked component). The resulting mathematical expressions are general enough to employ any component mode set without violating the interface conditions. This is accomplished with the introduction of 'correction terms' into the component recursive kinematical expressions. The physical significance of these terms has been analysed by the use of rotating observers positioned appropriately in the adjacent components. From this nonlinear analysis a great deal of insight is profited into the kinematics of the components in a multibody system, and suitable geometric interface conditions between adjacent bodies have been defined. Since any interface constraints can be considered a combination of locked (fixed) and articulating (free) axes, the component interface kinematics can be generalised for any possible joint configuration. The final expressions for the kinematics of a component connected to the inboard one have been presented for arbitrary interface constraints.

The absolute kinematical expressions of the outboard component involve the absolute kinematical expressions of the local reference frame positioned at the interface within the inboard component and relative kinematical expressions of the outboard component (relative) to the local inboard reference frame. These relative kinematical expressions are functions of the independent kinematical parameters of the outboard component. Utilising the kinematical relationship, established for any two adjacent bodies, repeatedly for all components in a multibody chain, the absolute kinematical expressions characterising the motion of any component B_i can be expressed in terms of the independent kinematical parameters of all components preceding and including B_i in the chain.

Figure III-1 demonstrates an open-loop tree-configuration multibody system and the notation of joints used in this chapter.

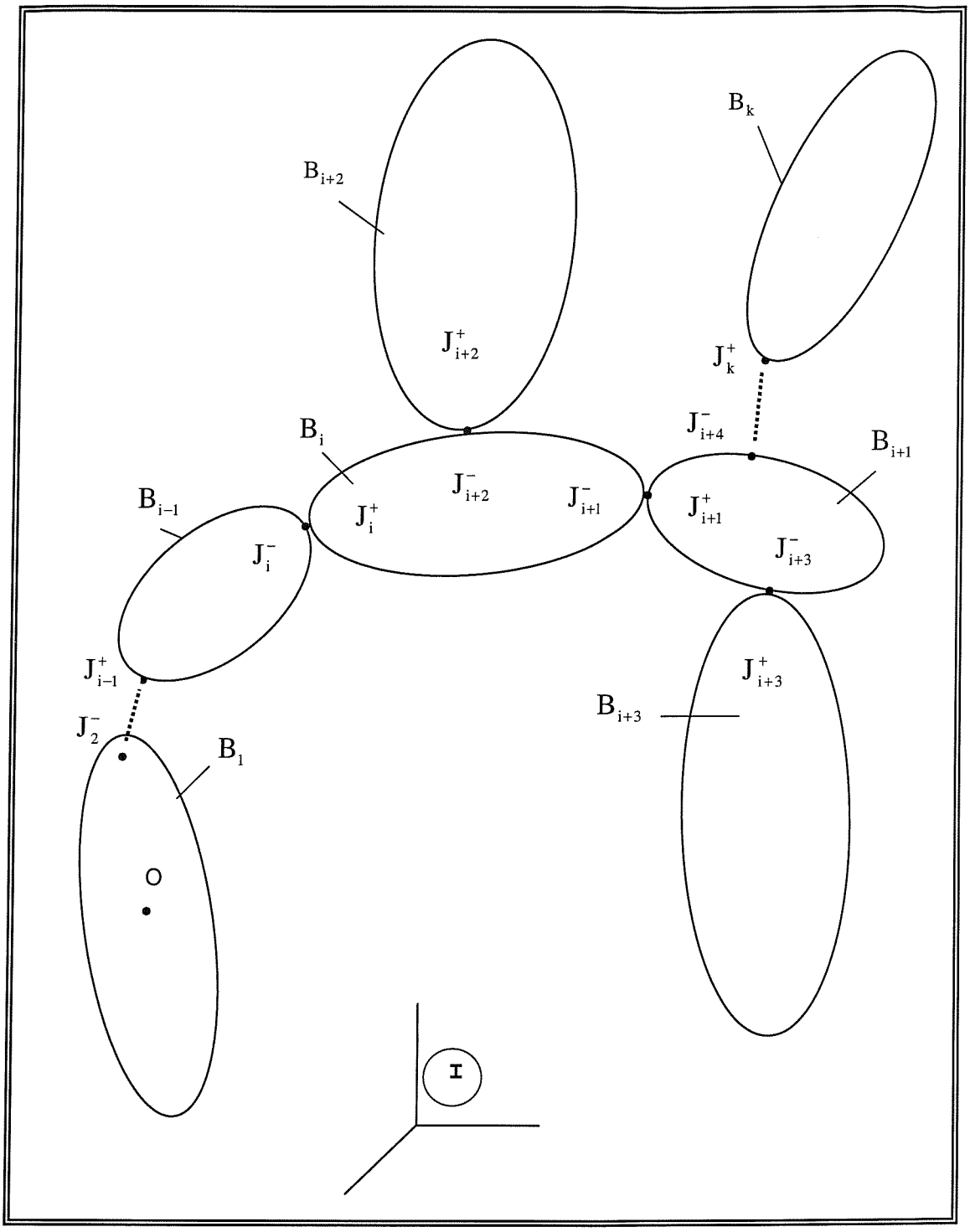

Figure III-1 Open-loop tree-configuration multibody system and joint notation

III-2. Nonlinear Component Kinematics

III-2-1. Floating Reference Frame

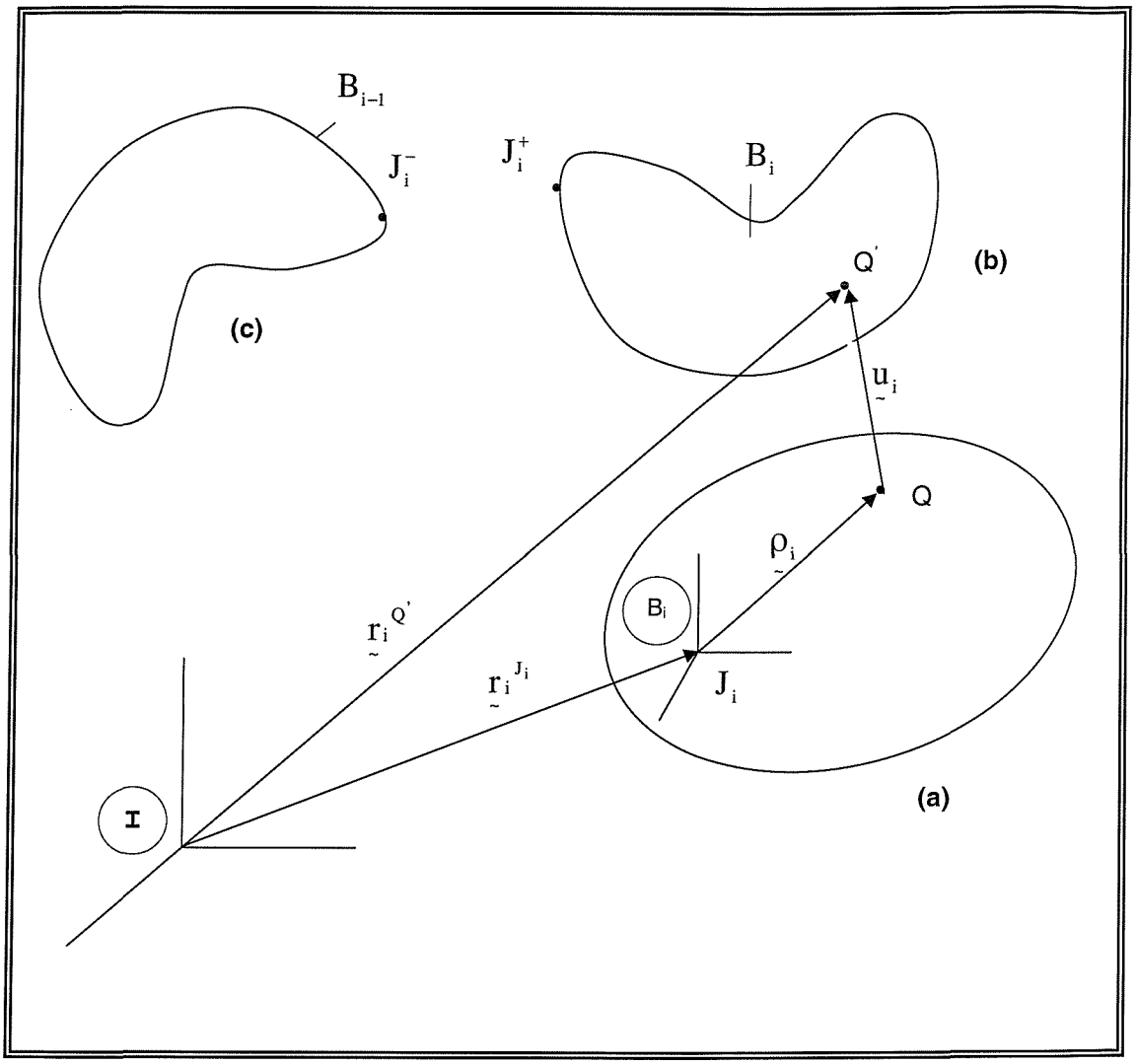

Figure III-2. General displacement component kinematics

(a) Rigid-body motion of component B_i

(b) Combined rigid-body motion and deformation of component B_i

(c) Component B_{i-1} arbitrarily displaced and deformed

Figure III-2 is used for explaining and illustrating the kinematics of a general displacement of an arbitrary point Q' within an arbitrarily moving (rotating and translating) linear elastic body B_i. Figure III-2(a) shows the body after rigid-body displacement and the attached body-frame B_i (floating reference frame) at the point of origin J_i. Figure III-2(b) shows the final position of the body in the rigidly displaced and linearly deformed state. The arbitrary point Q has undergone a vector displacement u due to the deformation and is depicted as Q'. A local observer positioned at the rotating and translating floating reference frame B_i can comprehend the final position of the body only as the deformed state of the body. Figure III-2(c) shows the preceding (inboard) body B_{i-1} at its final position. Bodies B_i and B_{i-1} at their final positions are joint together at the points J_i^+ and J_i^-, where J_i^+ is the position of J_i within component B_i after the deformation. It is obvious that the intermediate position 2(a) of the body B_i is fictitious and its purpose is to view the body's motion, at any instant, as a rigid-body motion relative to which an elastic domain deformation can be measured. The rigid-body part of the motion can be perceived as an instantaneous equilibrium position about which the elastic domain vibrates.

III-2-2. Nonlinear Kinematics of a Single Flexible Component

Assigning an inertial frame I (global frame), the absolute velocity of the point Q' can be written as

$$\underset{\sim}{v}_i^{Q'} = \dot{\underset{\sim}{r}}_i^{Q'} = \dot{\underset{\sim}{r}}_i^{Ji} + \dot{\underset{\sim}{\rho}}_i + \dot{\underset{\sim}{u}}_i \qquad \text{(III-1)}$$

where the symbols are obvious from Figure III-2 and the overdot implies differentiation relative to the inertial frame. The rate of change of the position of point Q, moving with the rigid-body, relative to an absolute (inertial) observer can be expressed[23] as

$$\dot{\underset{\sim}{\rho}}_i = \dot{\underset{\sim}{\rho}}_i^{+} + \underset{\sim}{\omega}_i^{Bi} \times \underset{\sim}{\rho}_i \qquad \text{(III- 2)}$$

where the overcross refers to time differentiation relative to the body frame B_i , i.e. the rate of change of the vector position of Q as observed from the local frame B_i. It is apparent that, since Q is a point of the rigid-body configuration,

$$\overset{+}{\underset{\sim}{\rho}}_i = 0 \tag{III-3}$$

Similarly, one can express the absolute rate of change of the vector deformation u as

$$\dot{\underset{\sim}{u}}_i = \overset{+}{\underset{\sim}{u}}_i + {}^{I}\underset{\sim}{\omega}_i^{Bi} \times \underset{\sim}{u}_i \tag{III- 4}$$

where ${}^{I}\underset{\sim}{\omega}_i^{Bi}$ is the angular velocity of body frame B_i (floating reference frame) relative to the inertial frame.

Symbolising the absolute velocity of the origin J_i of the local frame as ${}^{I}\underset{\sim}{v}_i^{Ji}$ it is

$${}^{I}\underset{\sim}{v}_i^{Ji} = \dot{\underset{\sim}{r}}_i^{Ji} \tag{III-5}$$

Substituting (III-2), (III-3), (III-4), (III-5) into (III-1) the absolute velocity of Q' can be written as

$${}^{I}\underset{\sim}{v}_i^{Q'} = {}^{I}\underset{\sim}{v}_i^{Ji} + {}^{I}\underset{\sim}{\omega}_i^{Bi} \times \underset{\sim}{\rho}_i + \overset{+}{\underset{\sim}{u}}_i + {}^{I}\underset{\sim}{\omega}_i^{Bi} \times \underset{\sim}{u}_i \tag{III-6}$$

The vector equation (III-6) expresses the absolute linear velocity of an arbitrary point in a moving flexible component, in terms of the absolute angular and linear velocity of the origin of the component body reference frame B_i (Figure III-2).

The vector equation (III-6) can also be derived in the following alternative way

$${}^{I}\underset{\sim}{v}_i^{Q'} = {}^{I}\underset{\sim}{v}_i^{Q} + {}^{I}\underset{\sim}{v}_i^{Q/Q'} \tag{III-7}$$

where the last term in (III-7) is the velocity of point Q' relative to Q, due to the deformation, as observed by an inertial observer. It can be directly verified that

$$\underset{\sim}{{}^{I}v_i^{Q}} = \underset{\sim}{{}^{I}v_i^{Ji}} + \underset{\sim}{{}^{I}\omega_i^{Bi}} \times \underset{\sim}{\rho_i} \qquad \text{(III-8)}$$

$$\underset{\sim}{{}^{I}v_i^{Q/Q'}} = \underset{\sim}{\overset{+}{u}_i} + \underset{\sim}{{}^{I}\omega_i^{Bi}} \times \underset{\sim}{u_i} \qquad \text{(III-9)}$$

By substitution of (III-8),(III-9) into (III-7) equation (III-6) can be furnished.

Utilising the addition theorem for angular velocities[27], the absolute angular velocity of frame travelling with the point Q' can be immediately recognised as

$$\underset{\sim}{{}^{I}\omega_i^{Q'}} = \underset{\sim}{{}^{I}\omega_i^{Bi}} + \underset{\sim}{{}^{Bi}\omega_i^{Q'}} \overset{def}{=} \underset{\sim}{{}^{I}\omega_i^{Bi}} + \underset{\sim}{\overset{+}{\theta}_i} \qquad \text{(III-10)}$$

where

$\underset{\sim}{\overset{+}{\theta}_i}$ is rate of change of the angular displacement due to component deformation at an arbitrary point Q', measured at the floating reference frame of component B_i.

The vector equation (III-10) expresses the absolute angular velocity of a frame travelling with an arbitrary point in a disjoint and arbitrarily moving flexible component, in terms of the absolute angular velocity of the origin of the component body reference frame B_i (Figure III- 2).

The kinematical equations (III-6), (III-10) depend explicitly on the motion of the preceding (inboard) body and the interface conditions. Equations (III-6), (III-10) are the most general nonlinear vector kinematical expressions for a single flexible component. In other mathematical formalisms[24] equations (III-6), (III-10) may have different, but equivalent, expressions.

With the intention of keeping only zeroth-order nonlinear terms, one may reduce the kinematical expressions by placing

$$ {}^{I}\underset{\sim}{\omega}_i \, {}^{Bi}\times \underset{\sim}{u}_i \cong 0 \qquad \text{(III-11)} $$

Substituting (III-11) into (III-6) the absolute velocity of $Q^{'}$ is given by the following vector equation

$$ {}^{I}\underset{\sim}{v}_i^{\,Q^{'}} = {}^{I}\underset{\sim}{v}_i^{\,Ji} + {}^{I}\underset{\sim}{\omega}_i^{\,Bi} \times \underset{\sim}{\rho}_i + \overset{+}{\underset{\sim}{u}}_i \qquad \text{(III-12)} $$

The vector equation (III-12) expresses the absolute linear velocity of an arbitrary point in a disjoint and arbitrarily moving non-spinning flexible component, in terms of the absolute angular and linear velocity of the origin of the component body reference frame B_i.

III-2-3. Nonlinear Kinematics of a Flexible Component in a Multibody Chain

For the purposes of this research, where no closed loops and multi-joint interfaces are intended in the analysis, a suitable kinematical procedure can be derived to accommodate the interface conditions and the kinematics of the preceding body explicitly into equations (III-10), (III-12). In this way, the influence of the motion of the inboard body B_{i-1} can be directly accounted for in the motion of the current body B_i in the analysis.

Using equations (III-10), (III-12), the derivation of the joint component kinematics is performed in Appendix-A, and is given by equations (A-24) and (A-25), repeated in this chapter as (III-14) and (III-13) respectively.

$$ {}^{I}\underset{\sim}{v}_i^{Q'} = {}^{I}\underset{\sim}{v}_{i-1}^{Ji^-} + {}^{I}\underset{\sim}{\omega}_{i-1}^{Ji^-} \times \underset{\sim}{\rho}_i + \underset{\sim}{\omega}_i^{rel} \times \underset{\sim}{\rho}_i + \overset{+}{\underset{\sim}{u}}_i - \left(\left(\overset{+}{\underset{\sim}{u}}_i \right)_{Ji} + \left(\overset{+}{\underset{\sim}{\theta}}_i \right)_{Ji} \times \underset{\sim}{\rho}_i \right) \qquad \text{(III-13)} $$

$$ {}^{I}\underset{\sim}{\omega}_i^{Q'} = {}^{I}\underset{\sim}{\omega}_{i-1}^{Ji^-} + \underset{\sim}{\omega}_i^{rel} + \overset{+}{\underset{\sim}{\theta}}_i - \left(\overset{+}{\underset{\sim}{\theta}}_i \right)_{Ji} \qquad \text{(III-14)} $$

where

${}^{I}\underset{\sim}{v}_{i-1}^{Ji^-}$ is the absolute linear velocity at the interface point J_i^- within the inboard component B_{i-1}.

${}^{I}\underset{\sim}{\omega}_{i-1}^{Ji^-}$ is the absolute angular velocity of a frame travelling with the interface point J_i^- within the inboard component B_{i-1}.

$\underset{\sim}{\omega}_i^{rel}$ is the angular velocity of the body reference frame of an articulating component B_i, as observed from the reference frame J_i^-, travelling with the interface point J_i^-, within the inboard component B_{i-1}.

$\left(\overset{+}{\underset{\sim}{\theta}}_i \right)_{Ji}$ is the rate of the angular displacement due to component deformation at the interface point J_i^+ of the component B_i, as measured by an observer travelling with the body reference frame of the component B_i.

$\left(\overset{+}{\underset{\sim}{u}}_i \right)_{Ji}$ is the rate of the linear displacement due to deformation at the interface point J_i^+ of the component B_i, as measured by an observer travelling with the body reference frame of the component B_i.

Equations (III-13), (III-14) give the absolute linear and angular velocity of a frame travelling with an arbitrary point Q' for a flexible component B_i part of a multibody chain, in terms of the absolute linear and angular velocity at the interface within the inboard component B_{i-1} for any possible non-translating joint configuration. In other words, the kinematics of a flexible component B_i joint to the preceding one, can be described with the equations (III-13), (III-14) for any joint configuration that does not allow relative translation of the adjacent components at their interface. Such an non-translating interface may represent a spherical, universal, revolute, fixed or torsionally elastic joint.

The formulation of the interface kinematics allows the incorporation into the equations (III-13), (III-14) of any possible component mode set without violating the interface compatibility between adjacent components. This is achieved by the introduction of the 'correction terms' $\left(\overset{+}{\underset{\sim}{\theta}}_i\right)_{Ji}$, $\left(\overset{+}{\underset{\sim}{u}}_i\right)_{Ji}$ in the equations (III-13), (III-14). Details of the derivation of the equations (III-13), (III-14) and the physical significance of the 'correction terms' is provided in appendix A.

Expressing the vector equations (III-13), (III-14) in appropriately selected reference frames, the following matrix equations (III-15), (III-16) are furnished respectively

$$ {}^{I}_{Bi-}v_i^{Q'} = C_i \, {}^{I}_{Bi-1-}v_{i-1}^{Ji-} - {}^{\times}_{Bi-}\rho_i \, C_i \, {}^{I}_{Bi-1-}\omega_{i-1}^{Ji-} - {}^{\times}_{Bi-}\rho_i \, {}^{rel}_{Bi-}\omega_i + {}_{Bi-}\dot{u}_i - \left(\left({}_{Bi-}\dot{u}_i \right)_{Ji} + {}^{\times}_{Bi-}\rho_i \left({}_{Bi-}\dot{\theta}_i \right)_{Ji} \right) \qquad \text{(III-15)} $$

$$ {}^{I}_{Bi-}\omega_i^{Q'} = C_i \, {}^{I}_{Bi-1-}\omega_{i-1}^{Ji-} + {}^{rel}_{Bi-}\omega_i + {}_{Bi-}\dot{\theta}_i - \left({}_{Bi-}\dot{\theta}_i \right)_{Ji} \qquad \text{(III-16)} $$

The left subscript on the above symbols indicates the reference frame where the associated vector quantities have been expressed.

The C_i matrix is in general a time-varying rotation matrix, which, with the assumption that the deformation of the component is linear, specifies at any instant the orientation of the body reference frame of the outboard component B_i relative to the body reference frame of the inboard component B_{i-1}. The rotation matrix C_i can generally be written as

$$C_i = C_i^{nom} \; C_i^{rot}(t)$$

where

C_i^{nom} is a rotation matrix specifying the nominal orientation of the component B_i relative to the inboard component B_{i-1}, i.e. at t=0.

$C_i^{rot}(t)$ is a time-varying rotation matrix specifying at any instant the orientation of the body reference frame B_i relative to its nominal position, for $t \geq 0$.

Details for parametric descriptions of a time-varying matrix are provided in Appendix-B.

The linear and angular rate of displacement of a frame travelling with point Q', due to the linear deformation of the component B_i , and as measured by a observer travelling with the body reference frame B_i , can be expressed in the body reference frame B_i as

$$\underset{Bi}{\underline{\dot{u}}}_i = U_{fi} \underline{\dot{q}}_{fi} \qquad \text{(III-17)}$$

$$\underset{Bi}{\underline{\dot{\theta}}}_i = \Theta_{fi} \underline{\dot{q}}_{fi} \qquad \text{(III-18)}$$

where

U_{fi} is a $3x\,n_i^f$ matrix containing the linear displacement of an arbitrary point Q'

due to small linear elastic deformation of the component B_i and n_i^f the number of flexible component modes retained in the analysis for approximating the linear deformation of the component B_i.

Θ_{fi} is a $3x\,n_i^f$ matrix containing the angular displacement of a frame travelling with an arbitrary point Q' due to small linear elastic deformation of the component B_i.

$\dot{\underline{q}}_{fi}$ $n_i^f \times 1$ vector containing the rates of the generalised coordinates associated to the flexible component modes.

The forms (III-17), (III-18) are presented in matrix form, for both discrete and continuous component modelling, since it is convenient for computational implementation.

By applying equations (III-15) and (III-16), along with (III-17), (III-18), repeatedly for all components in a multibody chain, the absolute angular and linear velocities of an arbitrary point on any component B_i can be expressed in terms of the independent kinematical parameters that specify the motion of the components preceding and including B_i in the chain. In this way the motion of any flexible articulated component in an open-loop multibody system can be coupled to the motion of all other components in the system.

Kinematical equations (III-15), (III-16), along with expressions (III-17), (III-18), regarding the linear deformation of a component B_i, can be used in order to develop various methods for describing the dynamical behaviour of multibody structures in space. Although this work is aimed in the development of linear methods, the kinematical descriptions up to this point in the analysis are general enough to accommodate geometrical nonlinearities and can treat any open-loop articulated multibody structure in space. Simplification of the kinematical equations for linear system dynamics modelling will be introduced as needed latter in the analysis.

IV Methods of Multibody Dynamics Modelling

IV-1. Prologue

The vast capabilities and the limited restrictions of the recursive Lagrangian methodology allow the modelling of a large number of structural systems in space, involving either geometrically nonlinear or linear dynamical analysis. In this chapter, the nonlinear analysis has to be adapted for developing methods suitable for the linear dynamics modelling for the Category II missions in space.

More specifically, having obtained nonlinear kinematical expressions for a component as part of a multibody system, the aim of this chapter is to linearise them in order to obtain expressions for the formulation of linear system dynamics. For this purpose, in Appendix-B, the theoretical background of the large arbitrary angular displacement and nonlinear rotational kinematics has been reviewed and the distinct mechanisms that introduce geometrical nonlinearity into the multibody system dynamics have been thoroughly examined. In this chapter transition from the nonlinear to linear kinematical expressions for a component as part of a multibody chain has been performed using symbolic formulations. The nonlinear kinematical expressions of a component B_i have been written as symbolic functions of all the independent kinematical parameters, in quasicoordinate form, that describe the motion of all components preceding and including the component B_i in a multibody chain. Subsequently, the nonlinear kinematical expressions of the component can be written as symbolic functions of independent generalised coordinates (in the Lagrangian content). This is accomplished by importing in the nonlinear kinematical expressions of quasicoordinate form the mathematical expressions of the mechanisms that introduce the geometrical nonlinearity in the multibody system. These mathematical expressions are nonlinear functions of the angular displacement parametric set. By eliminating the mathematical nonlinearities, the linear kinematical expressions of the component B_i can be formed as symbolic functions of all the independent generalised coordinates. Dinstinct linear kinematical expressions have

been accomplished and formulated using either hybrid or generalised coordinate sets.

At this stage the linear methods can be readily obtained. All three methods developed can treat the linear dynamics of any open-loop tree-configuration multibody structure in space with single-point articulated rigid or flexible components. The first method uses a hybrid set of coordinates where for each component the rigid-body part of the motion is described by physical displacement coordinates and the linear elastic deformation by generalised coordinates. This method is akin to nonlinear dynamics modelling. In the second method, the hybrid set is substituted by a generalised coordinate set, since the rigid-body motion of each component has been described using rigid-body modes, modelling allowed only with the assumption of small rotational displacement. In both methods the structural system can be composed of either continuous or discrete components. In the third method all components are necessarily considered discrete. The consistent mass matrix of each component in the structure appears explicitly in the equations of motion of the multibody system. The third method also utilises a generalised coordinate set.

The kinetic energy of each component is expressed in terms of all the independent generalised coordinates that describe, at any instance, the configuration of the preceding multibody chain of components. The elastic potential energy expression can readily be derived using the expressions approximating the linear elastic deformation of the component. Dissipation energy can be included at substructural level.

A unified coordinate set formalism has been defined to account for both the hybrid and generalised coordinate sets. Using the unified coordinate set, the multibody system kinetic, potential and dissipative energy expressions can be presented in a uniform form for all methods as well as for discrete or continuous components.

In the context of this chapter and for reasons of brevity, a discrete component (or elastic domain) will be considered any component (or elastic domain) that has been spatially discretised using the finite element method. On the other hand, a continuous component (or elastic domain) has been spatially discretised using the continuous version of the assumed-modes method.

IV-2. Transition from Nonlinear to Linear Kinematical Expressions

The kinematical expressions derived in chapter III and appendix-A are considered nonlinear, since no assumption of small angular displacement has been employed. For the purpose of presenting methods for linear system dynamics, in this section the transition from nonlinear kinematical expressions to linear expressions has been formulated symbolically, and the coordinate sets utilised in each method have been defined.

IV-2-1. Symbolic Nonlinear Parametric Velocity Expressions for a Component Joint in a Multibody Chain

The absolute linear and angular velocity of a frame travelling with an arbitrary point on a component B_i in a chain of components can be written as a symbolic function of all the kinematical parameters that define the motion of all components in the chain, preceding and including B_i. For facilitating the symbolic presentation, the vector velocity of the component B_i is expressed at an inertial reference frame, unlike in the equations (III-15), (III-16) where it has been expressed in the components' body reference frame.

For an open-loop single-point interface multibody system with non-translating joints, the following expressions can be obtained

$$ {}^{I}_{I-}v_i^{Q'} = \underset{-}{f}^{c/d}\left(\left\{ C_1^{rot}\ ,\ {}^{I}_{1-}v_1^{O}\ ,\ {}^{I}_{1-}\omega_1^{O}\ ,\ \underset{-}{\dot{q}}_{f1} \right\}_1 ,\ \left\{ C_{i-k}^{rot}\ ,\ {}^{rel}_{i-k\ -}\omega_{i-k}\ ,\ \underset{-}{\dot{q}}_{f(i-k)} \right\}_{i-1} \right), $$

$$ i \ni [2,m] \text{ and } k \ni [0,i-2] \qquad \text{(IV-1)} $$

$$ {}^{I}_{I-}\omega_i^{Q'} = \underset{-}{g}^{c/d}\left(\left\{ C_1^{rot}\ ,\ {}^{I}_{1-}\omega_1^{O}\ ,\ \underset{-}{\dot{q}}_{f1} \right\}_1 ,\ \left\{ C_{i-k}^{rot}\ ,\ {}^{rel}_{i-k\ -}\omega_{i-k}\ ,\ \underset{-}{\dot{q}}_{f(i-k)} \right\}_{i-1} \right), $$

$$ i \ni [2,m] \text{ and } k \ni [0,i-2] \qquad \text{(IV-2)} $$

where

$\underline{f}^{c/d}$, $\underline{g}^{c/d}$ are symbolic functions in the discrete (d) or continuous (c) domain.

$\{\ \}_n$ symbolises a set of n subsets of kinematical parameters.

${}^{I}_{I-}v_1^{O}$ is the absolute linear velocity of the reference frame at point O, which is the origin of the body reference frame of the carrier component B_1, and is expressed at the inertial frame.

${}^{I}_{I-}\omega_1^{O}$ is the absolute angular velocity of the reference frame at point O, and is expressed at the inertial frame.

$\underline{\dot{q}}_{f1}$ is the vector $n_f^1 \times 1$ of the rates of the generalised coordinates, associated with the n_f^1 number of the component modes retained in the analysis for the carrier component B_1.

C_1^{rot} is a generic time-varying rotation matrix, that specifies at any instant the orientation of the carrier platform relative to its nominal orientation for t≥0.

${}_{i-k}\underline{\omega}_{i-k}^{rel}$ is the angular velocity of the reference body frame of an articulating component B_{i-k} relative to the interface reference frame of the inboard component B_{i-k-1} and is expressed at the local reference frame B_{i-k}.

$\underline{\dot{q}}_{f(i-k)}$ is the vector $n_f^{(i-k)} \times 1$ of the generalised coordinate rates, associated with the $n_f^{(i-k)}$ number of the component modes retained in the analysis for the component B_{i-k}.

C_{i-k}^{rot} is a generic time-varying rotation matrix, that specifies at any instant the orientation of the component B_{i-k} body reference frame relative to its nominal orientation for t≥0.

m is the total number of components in the multibody chain, with the first being the carrier platform, which in general is the natural choice.

The symbolic expressions (IV-1), (IV-2) relate the absolute linear and angular velocity of a frame travelling with an arbitrary point Q' in a flexible component B_i, where B_i can be any component in a chain of m number of components, to the kinematical parameters that can describe the motion of all components in the chain preceding and including component B_i. For each component, the associated kinematical parametric set can be considered the generalised coordinate set of the component, in the general Lagrangian sense. In fact, because of the explicit appearance of angular velocity expressions in (IV-1), (IV-2) the parametric set of each component is a quasicoordinate set. Angular velocity as such is not, in general, a quantity that can be directly integrated for obtaining angular displacements expressions, since angular displacements are not vector quantities.

The rotation matrices that appear in the expressions (IV-1), (IV-2) are time-varying quantities since they are functions of the parametric description of the angular displacements, and therefore are included in the symbolic parametric expressions. The purpose of the rotation matrices is to express vector or dyadic quantities from one reference frame to another.

It is obvious that if a particular component B_m is not articulating to the preceding one in any direction, the kinematical parameters in the subset m will be truncated accordingly. It can be also be observed from equation (IV-1) that it is only the parameter set corresponding to the carrier platform that contains linear velocity parameters. This is so since it has been assumed that the components are connected to each other via non-translating joints. If the platform carrier is assumed docked in a much larger orbiting structure, then the rigid-body motion parameters should be truncated from (IV-1), (IV-2) accordingly.

The symbolic expressions (IV-1) and (IV-2) are nonlinear in the angular displacement / orientation parametric sets that implicitly enter the (IV-1), (IV-2). As analysed in Appendix-B, for large arbitrary rotation, the angular velocity and the time-varying rotation matrices are in general nonlinear in the angular displacement parametric set. More specifically, the following expression is obtained for the angular

velocity using the Euler angle parametric set (which is a minimal parametric set and can be used along with the general methodology of this work)

$$\underset{i-k}{\underset{-}{\omega}}_{i-k}^{rel} = E_{i-k}\left(\phi_1, \phi_2, \phi_3\right) \underset{i-k}{\underset{-}{\dot{\phi}}}_{i-k} \qquad \text{(IV-3)}$$

where

E_{i-k} is an Euler angle matrix, formed for a particular body sequence of principal rotations for the component B_{i-k}.

ϕ_p the orientation angles, i.e. the angular parametric set, for each sequence, p=1,2,3

$\underset{i-k}{\underset{-}{\dot{\phi}}}_{i-k}$ the rate of change of the orientation angles for component B_{i-k}

The time-varying Euler angle rotation matrix is given by

$$C_{i-k}^{rot} = \left(C_r(\phi_1)\, C_s(\phi_2)\, C_z(\phi_3) \right)_{i-k} \qquad \text{(IV-4)}$$

which is valid for any sequence r,s,z=1,2,3 as long as $r \neq s$, $s \neq z$, i.e. for independent principal axis sequential description. The matrices in the parentheses are time-varying direction cosine matrices corresponding to each principal rotation in the sequence pattern selected.

Substituting symbolically the angular velocity expression (IV-3) and the orientation angles rotation matrix expression (IV-4) into (IV-1) and (IV-2), the following forms are obtained

$$\underset{I-}{{}^{I}v_i^{Q'}} = \underset{-}{f}^{c/d}\left(\left\{ C_1^{rot}\left(\underset{-}{\phi}\right), \underset{1-}{{}^{I}v_1^{O}}, E_1\left(\underset{-}{\phi}\right), \underset{1-}{\dot{\phi}_1^{O}}, \underset{-}{\dot{q}_{f1}} \right\}_1, \left\{ C_{i-k}^{rot}\left(\underset{-}{\phi}\right), E_{i-k}\left(\underset{-}{\phi}\right), \underset{i-k-}{\dot{\phi}_{i-k}^{rel}}, \underset{-}{\dot{q}_{f(i-k)}} \right\}_{i-1} \right)$$

$$i \in [2,m] \text{ and } k \in [0,i-2] \qquad \text{(IV-5)}$$

$$ {}^{I}\underset{I}{\omega}_{i}^{Q'} = \underset{}{g}^{c/d} \left(\left\{ C_1^{rot}\left(\underset{}{\phi}\right), E_1\left(\underset{}{\phi}\right), \dot{\phi}_1^{O}, \dot{\underset{}{q}}_{f1} \right\}_1, \left\{ C_{i-k}^{rot}\left(\underset{}{\phi}\right), E_{i-k}\left(\underset{}{\phi}\right), \dot{\phi}_{i-k}^{rel}, \dot{\underset{}{q}}_{f(i-k)} \right\}_{i-1} \right) $$

$$ i \ni [2,m] \text{ and } k \ni [0,i-2] \quad \text{(IV-6)} $$

Expressions (IV-5),(IV-6) seem to be different from (IV-1),(IV-2) only in the explicit appearance of the Euler angle matrices E(ϕ), and in the substitution of the generic rotation matrices to the specific Euler angle rotation matrices C(ϕ). In fact, by expressing the angular velocity as a nonlinear function of the Euler angle parametric set ϕ , the symbolic forms (IV-5),(IV-6) are expressed in terms of the independent generalised coordinates of the system. The sequencing of rotations, which is directly employed in the Euler angle matrix form (IV-3), offers enough information regarding the relationship of the angular velocity and the angular displacement parametric set ϕ. The parametric set ϕ and the rate of ϕ can be considered generalised coordinates of the system. Therefore, from the quasicoordinate form of symbolic expressions (IV-1),(IV-2), transition to generalised coordinate form of (IV-5), (IV-6) has been accomplished. More specifically, the generalised coordinate set ϕ and its rates is considered a physical coordinate set, since it is related to particular reference frames positioned at specific points on the component. In this way the angular displacement parametric set ϕ is separated in description from the generalised coordinate sets, which in the context of this work are associated to the rigid-body and component modes.

Both the Euler angle matrix and the time-varying Euler angle rotation matrix (IV-3), (IV-4) are in general nonlinear in the orientation angles parameter set. It is obvious that in order to obtain linear expressions in (IV-5), (IV-6) the nonlinear dependence of these matrices to the parametric sets should be eliminated. For a chain of

components the only possible way to derive linear expressions is under the assumption of small angular displacement. In that case both the Euler angle matrix and Euler rotation matrices become unity matrices (Appendix-B, Table B-1).

IV-2-2. Symbolic Linear Parametric Velocity Expressions for a Component Part of a Multibody Chain

IV-2-2-1. Method I

With the assumption of small angular displacement, the Euler angle and Euler angle rotation matrices become unity matrices for all components in the system, and the expressions (IV-5) and (IV-6) result in the following linear form

$$ {}^{I}_{I}\underline{v}_i^{Q'} = \underline{f}^{c/d}\left(\left\{ {}^{I}_{1}\underline{\dot{r}}_1^{O}, {}^{I}_{1}\underline{\dot{\phi}}_1^{O}, \underline{\dot{q}}_{f1}\right\}_1, \left\{ \underline{\dot{\phi}}^{rel}_{i-k}, \underline{\dot{q}}_{f(i-k)}\right\}_{i-1}\right), $$

$$ i \ni [2,m] \text{ and } k \ni [0,i-2] \qquad \text{(IV-7)} $$

$$ {}^{I}_{I}\underline{\omega}_i^{Q'} = \underline{g}^{c/d}\left(\left\{ {}^{I}_{1}\underline{\dot{\phi}}_1^{O}, \underline{\dot{q}}_{f1}\right\}_1, \left\{ \underline{\dot{\phi}}^{rel}_{i-k}, \underline{\dot{q}}_{f(i-k)}\right\}_{i-1}\right), $$

$$ i \ni [2,m] \text{ and } k \ni [0,i-2] \qquad \text{(IV-8)} $$

It is obvious from (IV-7) and (IV-8) that the coordinate set for the method I is a hybrid coordinate set, consisting of the physical coordinate set and the generalised coordinate set for each component preceding and including component B_i.

It has to be mentioned, that in the case of small rotational displacement, the sequencing is irrelevant to the orientation of the body. In this respect the attitude

angle rates $\underline{\phi}$ do not have to be assigned with a particular sequencing and their interpretation is simplified.

IV-2-2-2. Methods II, III

In methods II, III the linearisation of equations (IV-5),(IV-6) is implemented in two steps. The first step has already been described and essentially is that of method I. Moreover, for methods II, III the physical coordinate set of each component is transformed to an equal size generalised coordinate set multiplied by the rigid-body modes of each component. Rigid-body modes are vector quantities in the sense that the cumulative rule of addition is valid in their case. Therefore, rigid-body modes description of rigid body motion is only permitted for small angular displacements.

Equations (IV-7) and (IV-8) obtain the following forms with the use of rigid-body modes

$$ {}^{I}_{I}\underline{v}_i^{Q'} = \underline{f}^{c/d}\left(\left\{ \dot{\underline{q}}_{r1}, \dot{\underline{q}}_{f1} \right\}_1 , \left\{ \dot{\underline{q}}_{r(i-k)}, \dot{\underline{q}}_{f(i-k)} \right\}_{i-1} \right) $$

$$ i \ni [2,m] \text{ and } k \ni [0,i-2] \qquad \text{(IV-9)} $$

$$ {}^{I}_{I}\underline{\omega}_i^{Q'} = \underline{g}^{c/d}\left(\left\{ \dot{\underline{q}}_{r1}, \dot{\underline{q}}_{f1} \right\}_1 , \left\{ \dot{\underline{q}}_{r(i-k)}, \dot{\underline{q}}_{f(i-k)} \right\}_{i-1} \right) $$

$$ i \ni [2,m] \text{ and } k \ni [0,i-2] \qquad \text{(IV-10)} $$

where the additional symbols represent

$\dot{\underline{q}}_{r1}$ is a $n_r^1 \times 1$ vector containing the generalised coordinate rates associated with the n_r^1 rigid-body modes of the main component, the carrier platform.

$\dot{\underline{q}}_{r(i-k)}$ is a $n_r^{i-k} \times 1$ vector containing the generalised coordinate rates associated with the n_r^{i-k} rigid-body modes of the component B_{i-k}.

Method III is only possible in the discrete elastic domain, therefore the symbolic function $\underline{f}^{c/d}$ has only meaning as $\underline{f}^{d}$.

IV-3. Unified Coordinate Set Formalism

As detailed previously, method I utilises a hybrid coordinate set and methods II, III a generalised coordinate set. For facilitating the expressions of energy functions the coordinate set of a component B_i can be written for all methods in the following unified form

$$\underline{q}_i = \begin{pmatrix} \underline{x}_{ri} \\ \hline \underline{q}_{fi} \end{pmatrix} \qquad \text{(IV-11)}$$

where

$\underline{x}_{ri}$ is a $n_r^i \times 1$ column matrix containing the coordinates associated with the rigid-body motion of the component B_i, and n_r^i equals the number of rigid-body degrees of freedom of the component.

$\underline{q}_{fi}$ is a $n_f^i \times 1$ column matrix containing the generalised coordinates associated with the linear elastic deformation of the component B_i, and n_f^i equals the number of component modes retained in the analysis of component B_i.

In method I, $\underline{x}_{ri}$ is a physical displacement (rotational and translational) coordinate set and is related to the particular point on each component where the origin of the body reference frame (floating reference frame) is positioned. In methods II and III,

$\underline{x}_{ri}$ is the generalised coordinate set $\underline{q}_{ri}$, since the rigid-body motion is described with the use of rigid-body modes. For components other than the platform carrier, the $\underline{x}_{ri}$ has a maximum of three coordinates, since the multibody system consists of components that are connected with non-translational joints.

The different coordinate sets used in method I and II is the only difference between these methods. Although this seems a minor point it will prove to have a huge effect on the presentation of the global mass matrix for a multibody structure. Methods II and III use a generalised coordinate set and this is the main common feature between these methods.

In method I,II the multibody structure can be composed of either continuous or discrete components. In method III the components are necessarily discrete. The absolute angular and linear velocity of a point Q' on the component B_i, for all methods can be written symbolically as functions of the coordinate set of each component.

IV-4. Elastic Potential Energy Expressions for a Multibody System

IV-4-1. Elastic Potential Energy for Continuous components;

The elastic potential energy of a multibody system composed of a number of continuous linear elastic components is given by

$$V = \frac{1}{2} \sum_{i=1}^{k} \int_{Bi} \left(\underline{\sigma}_i \right)^T \underline{\varepsilon}_i \, dV_i \qquad \text{(IV-12)}$$

where

k is the total number of components in the system.

$\underline{\sigma}_i$ is the stress vector (6x1) at an arbitrary point in the component B_i.

$\underline{\varepsilon}_i$ is the stain vector (6x1) at an arbitrary point in the component B_i.

dV_i is the infinitesimal volume within the component B_i.

For linear material properties the stress is related to the strain as follows,

$$\underline{\sigma}_i = D_i \ \underline{\varepsilon}_i \tag{IV-13}$$

where D_i is the material stiffness matrix of the component B_i.

The strain is related to the deformation at the arbitrary point as follows,

$$\underline{\varepsilon}_i = \Lambda_i \ \underline{u}_i \tag{IV-14}$$

where Λ_i is a partial differential operator matrix.

Substituting (IV-13) and (IV-14) into (IV-12) and using the integrated form of (17), the elastic potential energy of a continuous multibody system is given by

$$V = \frac{1}{2} \sum_{i=1}^{k} \left(\underline{q}_{fi} \right)^T K_{fi} \ \underline{q}_{fi} \tag{IV-15}$$

where

$$K_{fi} = \int_{Bi} U_{fi}^T \ \Lambda_i^T \ D_i \ \Lambda_i \ U_{fi} \ dV_i \tag{IV-16}$$

and the additional symbolism

U_{fi} is a $3 \times n_f^i$ matrix containing the deformation at an arbitrary point in the continuous component B_i, and n_f^i the number of component modes

(functions) retained in the analysis of the component B_i .

$\underline{q}_{fi}$ is a n_f^i X1 vector containing the generalised coordinates associated with the component modes.

The component has been spatially discretised using the assumed-modes method, in order to approximate the distibuted parameter (infinite) elastic domain with a finite dimensional one. The finite number of component modes, which are space-dependent functions, are in general trial functions (in the Rayleigh-Ritz sense), but they may also be exact solutions of a differential eigenvalue problem, if closed-form solution can be obtained.

IV-4-2. Elastic Potential Energy for Discrete Components;

Potential energy expressions in the form of (IV-15), (IV-16) are possible to derive for components with fairly regular geometry. For complex geometry components, exact modelling of a component is usually infeasible, and if not so the closed-form solutions are even more unlikely. Moreover, even trial functions may be difficult to obtain for describing the deformation with an acceptable accuracy. For irregular geometry, the structural components can be spatially disretised using the finite element method. The resulting high order discrete parameter elastic domain is truncated with the use of the discrete version of the assumed-modes method.

For a multibody structure, modelled with the use of the finite element method, the elastic potential energy of the system is given by

$$V = \frac{1}{2}\sum_{i=1}^{k}\left(\underline{x}_i\right)^T K_i^{FEM}\ \underline{x}_i \qquad \text{(IV-17)}$$

where

K_i^{FEM} is the stiffness matrix of the component B_i derived using the finite element method.

$\underline{x}_i$ is the nodal displacement vector, $n_t^i \times 1$, where n_t^i is the number of nodal degrees of freedom of the component.

The high order discrete elastic domain description can be truncated using the discrete version of the assumed-modes method, hence

$$\underline{x}_i = \Phi_{fi} \; \underline{q}_{fi} \tag{IV-18}$$

where

Φ_{fi} is a $n_t^i \times n_f^i$ matrix containing n_f^i component modes (vectors) retained in the analysis of the component B_i.

Even in the case that the component is discretised using the finite element method, and the solution of the eigenvalue problem is numerically convenient, the component modes are not necessarily only the eigenvectors of the algebraic eigenvalue problem, but can be complemented by other trial vectors such as static modes, for improving convergence and local deformation modelling.

Substituting (IV-18) into (IV-17), the elastic potential energy of the multibody system can be written as

$$V = \frac{1}{2} \sum_{i=1}^{k} \left(\underline{q}_{fi} \right)^T K_{fi} \; \underline{q}_{fi} \tag{IV-19}$$

where

$$K_{fi} = \left(\Phi_{fi}\right)^T \; K_i^{FEM} \; \Phi_{fi} \tag{IV-20}$$

IV-4-3. Unified Expression of the Elastic Potential Energy of a Multibody Structure

For continuous or discrete components, the potential energy of the system can be expressed in exactly the same form as appears in equations (IV-15), (IV-19). The potential energy of the multibody structure can be written as

$$V = \tfrac{1}{2}\, \underline{q}^{T}\ K_G\ \underline{q} \qquad \text{(IV-21)}$$

K_G is the global stiffness matrix of the multibody structure and has the form

$$K_G = \begin{pmatrix} K_{G_1} & & & & \\ & K_{G_2} & & & \\ & & \ddots & & \\ & & & K_{Gi} & \\ & & & & \ddots \end{pmatrix} \qquad \text{(IV-22)}$$

where all other entries not designated are zero and component B_i generalised stiffness matrix is given by

$$K_{Gi} = \left(\begin{array}{c|c} 0 & \\ \hline & K_{fi} \end{array}\right) \qquad \text{(IV-23)}$$

where

0 is a $n_r^i \times n_r^i$ null matrix and n_r^i are the rigid-body degrees of freedom of the component B_i.

K_{fi} is given by (IV-16) for a continuous component B_i and by (IV-20) for a discrete component.

The coordinate set of the multibody structure is

$$\underline{q}^T = \left(\left(\underline{q}_1 \right)^T \left(\underline{q}_2 \right)^T \cdots \left(\underline{q}_i \right)^T \cdots \right) \qquad \text{(IV-24)}$$

and

$\underline{q}_i$ is a hybrid or generalised coordinate set for each discrete or continuous component B_I corresponding to either method I or methods II,III respectively.

IV-5. Dissipative Energy Expressions for a Muitibody System

There are a lot of distinct damping mechanisms that cause energy dissipation in structures. In this work two dissipation mechanisms are addressed at substructural level, namely structural and localised viscous damping. Structural damping will be included directly in the frequency domain equations of motion.

IV-5-1. Localised Viscous Damping Modelling

Viscous dampers can be modelled as acting within the component's structural domain. The viscous damping dissipative energy expression is essentially similar to the elastic potential energy expressions derived for discrete components.

$$D_v = \tfrac{1}{2} \sum_{i=1}^{k} \left(\dot{\underline{x}}_i \right)^T B_{vi} \, \dot{\underline{x}}_i \qquad \text{(IV-25)}$$

where

B_{vi} is the viscous damping matrix of the component B_i

$\dot{\underline{x}}_i$ is the nodal rate of displacement vector, $n_t^i \times 1$, where n_t^i is the number of nodal degrees of freedom of the component.

Transforming (IV-25) from the physical coordinate space to a reduced generalised one with the use of (IV-18), the following dissipative energy expression is readily available.

$$D_v = \frac{1}{2} \sum_{i=1}^{k} \left(\dot{\underline{q}}_{fi} \right)^T B_{Gi} \dot{\underline{q}}_{fi} \qquad \text{(IV-26)}$$

where

$$B_{Gi} = \left(\Phi_{fi}\right)^T B_{vi} \Phi_{fi} \qquad \text{(IV-27)}$$

The viscous damping dissipative energy expression (IV-26) can readily written using the unified coordinate set formalism as

$$D_v = \frac{1}{2} \dot{\underline{q}}^T B_G \dot{\underline{q}} \qquad \text{(IV-28)}$$

B_G is the global viscous matrix of the multibody structure and has the form

$$B_G = \begin{pmatrix} B_{G_1} & & & & \\ & B_{G_2} & & & \\ & & \ddots & & \\ & & & B_{Gi} & \\ & & & & \ddots \end{pmatrix} \qquad \text{(IV-29)}$$

where all other entries not designated are zero and component B_i

IV-6. Kinetic Energy Expression for a Multibody System

IV-6-1. Kinetic Energy Expression; Methods I, II

IV-6-1-1. Continuous Component

For a multibody structure with continuous components the kinetic energy of the system is given by

$$T = \frac{1}{2} \sum_{i=1}^{k} \int_{Bi} \left({}^{I}_{I-}\mathbf{v}_i^{Q'} \right)^T {}^{I}_{I-}\mathbf{v}_i^{Q'} \, dm_i \qquad \text{(IV-30)}$$

where

k is the number of continuous components in the multibody structure.

${}^{I}_{I-}\mathbf{v}_i^{Q'}$ is the absolute linear velocity of an arbitrary point Q' in the component B_i

dm_i is the infinitesimal mass associated with the point Q' .

For method I, the ${}^{I}_{I-}\mathbf{v}_i^{Q'}$ is given symbolically by expression (IV-7) and for method II by (IV-10). For a continuous component the symbolic function $\underline{f}^{c/d}$ in (IV-7) and (IV-10) have only meaning as $\underline{f}^{c}$, referring to continuous modelling.

IV-6-1-2. Discrete Component

For a multibody system composed of discrete components the kinetic energy expression is given by

$$T = \frac{1}{2} \sum_{i=1}^{k} \sum_{n=1}^{n_i^i} \left({}^{I}_{I-}\mathbf{v}_i^{Q_n'} \right)^T {}^{I}_{I-}\mathbf{v}_i^{Q_n'} \, \delta m_i \qquad \text{(IV-31)}$$

where

k the total number of discrete components in the multibody sytem.

n_t^i the total number of nodes of the component B_i .

${}^{I}_{I-}v_i^{Q'_n}$ is the absolute linear velocity of Q' associated to the nodal point N.

δm_i is the finite mass concentrated at the nodal point.

For method I, the ${}^{I}_{I-}v_i^{Q'}$ is given symbolically by expression (IV-7) and for method II by (IV-10). For a discrete component the symbolic function $\underline{f}^{c/d}$ in (IV-7) and (IV-10) have only meaning as $\underline{f}^{d}$, referring to discrete modelling.

IV-6-1-3. Comparison of Continuous and Discrete Forms of the Kinetic Energy Expressions

Comparing the continuous expression (IV-30) to the discrete expression (IV-31), the main difference is noticed at the integration scheme in the former, which has been substituted with a summation scheme in the later. It is obvious that in the case of the continuous modelling the integration scheme may be treated as summation scheme for the purpose of numerical integration. Therefore for numerical implementation both continuous and discrete kinetic energy expressions will have the form of (IV-31). This, nevertheless, does not imply that the methods are numerically equivalent. In the case of the continuous modelling, the analyst can select the number of integration points, whereas in the case of discrete modelling the number of summation points is dictated by the finite element model mesh of the component. More importantly, in the case of continuous modelling, the analyst is also able to choose a numerical integration scheme of preference. On the contrary, in the case of discrete modelling the summation scheme is predetermined by the lumped mass model of the discretised component. For example, integrating numerically the velocity expressions of a dicretised beam structure, the summation scheme is

necessarily that of the trapezoid integration. In more complex structures the summation scheme is arbitrary and determined by the mass concentrated at the nodal point, obtained from the lumped mass matrix of the finite element model. The continuous modelling accuracy depends on the number of integration points and the integration scheme utilised, which both can be manipulated independently of the structural model. Continuous modelling can therefore be more accurate than discrete modelling, which relies only on the number of nodes and the mass distribution predetermined by the finite element model.

It has to be mentioned, that in the case of the discrete method the vectors (component modes) are typically obtained from a consistent finite element model for better accuracy, whereas the distribution of mass from a lumped mass model. In computational terms, using discrete modelling means the extraction of both consistent and inconsistent mass matrices, with obvious disadvantages.

IV-6-2. Kinetic Energy Expression; Method III

Method III is subject only to discrete modelling and it circumvents the problems associated to numerical accuracy of the discrete versions of methods I, II. Method III does not involve summation schemes and does not rely on the lumped mass matrix. It utilises directly the consistent mass matrices of the components to obtain the kinetic energy expression of the multibody structure.

The kinetic energy of the multibody system can be written as

$$T = \frac{1}{2} \sum_{i=1}^{k} \left({}_{I}\dot{\underline{X}}_{i} \right)^{T} M_{i}^{FEM} \, {}_{I}\dot{\underline{X}}_{i} \qquad \text{(IV-32)}$$

where

k is the number of discrete components in the multibody system.

M_i^{FEM} is the consistent mass matrix of component B_i.

${}_{I}\dot{\underline{X}}_{i}$ is the $n_t^i \times 1$ vector, where n_t^i the nodal degrees of freedom of the

component, and contains the nodal absolute linear and angular velocity vectors for component B_i.

The absolute linear and angular nodal velocities for method III are given by the symbolic expressions (IV-9) and (IV-10) respectively. For a discrete component the symbolic functions $\underline{f}^{c/d}$ in (IV-9) and $\underline{g}^{c/d}$ in (IV-10) have only meaning as $\underline{f}^{d}$ and $\underline{g}^{d}$, referring to discrete modelling.

IV-6-3. Unified Expression for the Kinetic Energy of a Multibody System

The kinetic energy expressions for all methods and regardless the discrete or continuous modelling assumptions can be written in the following form

$$T = \frac{1}{2}\ \underline{\dot{q}}^{T}\ M_G\ \underline{\dot{q}} \qquad \text{(IV-33)}$$

where

M_G is the global mass matrix of the multibody system.

$\underline{\dot{q}}$ the rate of the coordinate set of the multibody system given by the first derivative of (IV-24).

For method I the coordinate set is hybrid and for methods II, III a generalised coordinate set. Unlike the global stiffness matrix, the global mass matrix of a multibody structure is highly coupled, since the linear and angular velocities of an arbitrary point in a component B_i are not only functions of the coordinate set of the component B_i , but also functions of all the coordinate sets of the preceding components in the chain.

V Mathematical Models of Peripheral Multibody Structures

V-1. Prologue

For comparison and assessment, the methods derived in chapter IV have been utilised to derive mathematical models for generic peripheral multibody structures in space. Such systems consist of an arbitrary number of components attached to a main carrier platform without forming closed-loops. A peripheral or else cluster formation multibody structure is shown in Figure V-1. Cluster formation multibody mathematical models are easier to present analytically than generic tree-configuration models, which are best generated computationally. In this respect a better understanding of the component interaction dynamics is accomplished with the cluster formation multibody models. Moreover, the different methods are better compared on their efficiency employing the analytical expressions of the mathematical models. In reality, cluster configuration covers a large number of the structural systems in space for the present and near future applications. In addition, by appropriate assumptions almost any tree-configuration multibody structure can be modelled as a cluster formation for the purposes of linear dynamics modelling. The configuration limitation of the mathematical models does not in any extent restrict the conclusions drawn form this work since it is of quantitative and not qualitative nature.

For the purpose of comprehensive assessment of the methods, 4 mathematical models of varying complexity have been developed. Mathematical model A, B are formulated using methods I, II respectively, and refer to a flexible cluster formation structure where the appendages can only carry concentrated mass rigid payloads. Mathematical models C, D are obtained from methods II, III respectively, and refer to a cluster formation structure where appended components can also carry distributed mass rigid payloads. Moreover, explicit expressions of the torsional deformation of beam modelled appendages appear in mathematical model C, along with terms that allow the kinematical description of Timoshenko beam theory. In mathematical model D these terms are included implicitly in the consistent mass and

stiffness matrices of the components. Detailed assessment and comments on each individual mathematical model follow the mathematical derivation. The methods and mathematical models generated have been illustrated for reference purposes in Table V-1.

The three methods have been compared on their suitability for modelling the dynamics of Category II missions in space. For comparison purposes, a particular pairing has been chosen. Method I is compared to method II using the mathematical models A,B respectively. Mathematical model A, B have exactly the same modelling capabilities. In both cases, the appended components can carry concentrated mass, but not distributed mass. Neither of the models includes beam-modelled appendages. Beam-modelled appendages need detailed mathematical treatment and are included only in the more complex mathematical models. The second pair of comparisons is between methods II and III, using mathematical models C, D. Mathematical model C is a very comprehensive model, and utilising it, any cluster formation structure can be modelled. The same applies for mathematical model D. Conclusions, on which method is the most efficient for developing mathematical models for the category II missions in space, have been presented at the end of the chapter.

The general criteria for the comparison have been established out of the experience gained in developing and programming the methods for obtaining efficient and accurate mathematical models of flexible multibody systems. Criteria include mathematical model development effort and complexity, physical insight capability, programming effort, potential numerical accuracy, potential computing time for application completion, programming validation effort, analyst interference with the data input and ease for modelling a generic tree-configuration multibody system.

In chapter IV the global stiffness and damping matrices of a generic multibody structure have been explicitly developed utilising a unified coordinate set for discrete or continuous components and for all methods involved. Unlike the global stiffness and damping matrices, the global mass matrix is highly coupled, since the velocity terms of a point within a component are functions of the generalised coordinates preceding the component in the multibody chain.

The chapter concludes with the derivation of the generalised force expressions for a multibody structure and the mathematical steps for performing a direct or modal

frequency response analysis using the reduced order mathematical model of a multibody system. Structural and localised viscous damping has been included at substructural level.

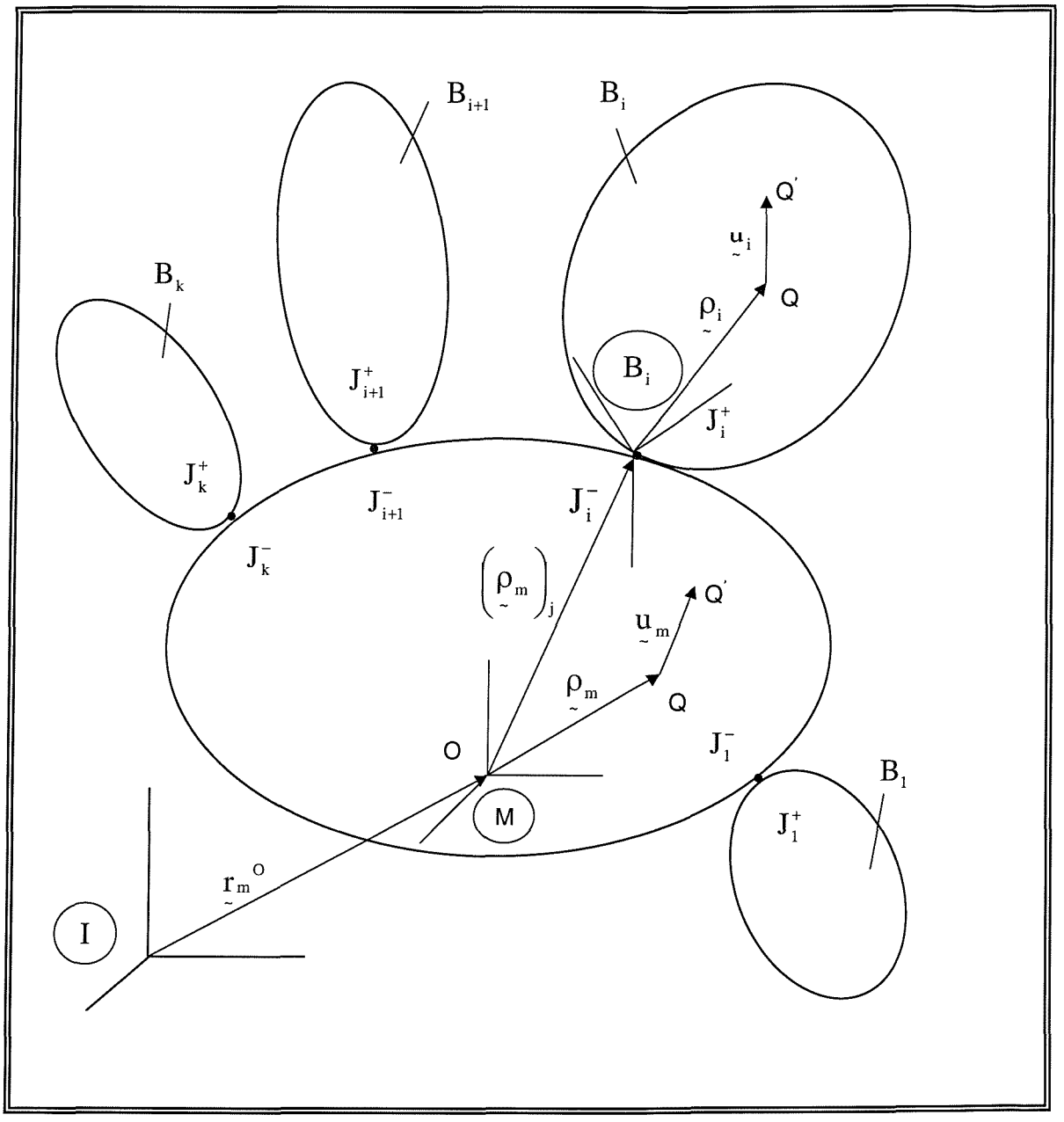

Figure V-1 Peripheral multibody structural system

Cluster Formation Structure	**Mathematical Model A**	**Mathematical Model B**	**Mathematical Model C**	**Mathematical Model D**
Method	I	II	II	III
Continuous Components	Yes	Yes	Yes	No
Discrete Components	Yes	Yes	Yes	Yes
Coordinate Set	Hybrid	Generalised	Generalised	Generalised
Concentrated Mass Payload on Appendages	Yes	Yes	Yes	Yes
Distributed Mass Payload on Appendages	No	No	Yes	Yes
Beam-modelled Component Terms	No	No	Yes	Yes

Table V-1 Reference table for the methods and mathematical models developed

V-2. Mathematical Model A

V-2-1. Global Mass Matrix Derivation

Using method I, the global mass matrix of a cluster formation structure in space, which can carry arbitrary number of concentrated masses on the appended components, has been developed. In method I the components can be modelled as either continuous or discrete.

The kinetic energy of the system having k number of appendages is given by

$$T = \frac{1}{2}\int_{M}\left({}^{I}_{M-}v_m{}^{Q'} \right)^{T}\left({}^{I}_{M-}v_m{}^{Q'} \right) dm + \frac{1}{2}\sum_{j=1}^{k}\int_{Bj}\left({}^{I}_{Bj-}v_j{}^{Q'} \right)^{T}\left({}^{I}_{Bj-}v_j{}^{Q'} \right) dm \quad \text{(V-1)}$$

The kinetic energy expression has been presented in (IV-1) for a continuous multibody system. For discrete modelling the integration schemes should be substituted by summations over the nodal points of each component.

Kinetic Energy of Main Platform

Using (III-15),(III-16),(III-17),(III-18), and the specific notation for cluster formation structures, the absolute angular and linear velocity for an arbitrary point on the flexible carrier platform can be expressed as

$${}^{I}_{M-}v_m{}^{Q'} = {}^{I}_{I-}v_m{}^{O} - \left({}^{}_{M-}\rho_m \right)^{x} {}^{I}_{I-}\omega_m{}^{M} + U_{fm}\dot{q}_{fm} \quad \text{(IV-2)}$$

$$ {}^{I}_{M-}\omega_m{}^{Q'} = {}^{I}_{I-}\omega_m{}^{M} + \Theta_{fm}\dot{q}_{fm} \qquad \text{(IV-3)} $$

where the rotation matrix has been placed to unity, with the assumption of small angular displacement. Since the main platform carrier is the inboard component of the structure, the correction terms appearing in (III-15),(III-16) have not been included in (IV-2),(IV-3).

With the assumption of small angular displacement the Euler angle matrix becomes a unity matrix and the absolute angular velocity of the body reference frame of the main platform can be expressed as

$$ {}^{I}_{I-}\omega_m{}^{M} = E\left(\phi_m{}^{O}, t\right)\dot{\phi}_m{}^{O} = \dot{\phi}_m{}^{O} \qquad \text{(IV-4)} $$

Substituting (IV-4) into the equations (IV-2),(IV-3) the absolute linear and angular velocity expressions at any point on the main platform can be expressed as

$$ {}^{I}_{M-}v_m{}^{Q'} = \dot{r}_m{}^{O} - \left(\rho_m\right)^{\times}_{M-}\dot{\phi}_m{}^{O} + U_{fm}\dot{q}_{fm} \qquad \text{(IV-5)} $$

$$ {}^{I}_{M-}\omega_m{}^{Q'} = \dot{\phi}_m{}^{O} + \Theta_{fm}\dot{q}_{fm} \qquad \text{(IV-6)} $$

where

$$ {}^{I}_{I-}v_m{}^{O} = \dot{r}_m{}^{O} \qquad \text{(IV-7)} $$

has been utilised.

Kinetic Energy of Appended Component B_j

From equations (IV-5),(IV-6) and for $Q' \equiv J$, the linear and angular velocity of the junction point J can be readily obtained. Substituting (IV-5),(IV-6) for $Q' \equiv J$ into (III-15), and using (III-17), the absolute linear velocity at an arbitrary point in an appended component B_j, with the assumption of small angular displacement, can be expressed as

$$
{}^{I}_{Bj}\underline{v}_j^{Q'} = C_j\left({}^{I}\dot{\underline{r}}_m^{O} - \left({}^{M}\underline{\rho}_m \right)_j^{x} {}^{I}\dot{\underline{\phi}}_m^{O} + \left(U_{fm}\right)_j \dot{\underline{q}}_{fm} \right) - \left({}^{Bj}\underline{\rho}_j \right)^{\times} C_j \left({}^{I}\dot{\underline{\phi}}_m^{O} + \left(\Theta_{fm}\right)_j \dot{\underline{q}}_{fm} \right)
$$

$$
- \left({}^{Bj}\underline{\rho}_j \right)^{\times} {}^{Bj}\dot{\underline{\phi}}^{rel}_j + V_{fj}\dot{\underline{q}}_{fj} \qquad \text{(IV-8)}
$$

where

$$
V_{fj} = \left(U_{fj} - \left(U_{fj} \right)_j + \left({}^{Bj}\underline{\rho}_j \right)^{x} \left(\Theta_{fj} \right)_j \right) \qquad \text{(IV-9)}
$$

Substituting (IV-5),(IV-6) into (IV-1), the global mass matrix of the cluster formation multibody structure can be readily derived

$$
M_G = \begin{pmatrix}
M_{rr} & M_{r\phi} & M_{rm} & M_{r\omega_1} & M_{rb_1} & \cdots & M_{r\omega_j} & M_{rb_j} \\
 & M_{\phi\phi} & M_{\phi m} & M_{\phi\omega_1} & M_{\phi b_1} & \cdots & M_{\phi\omega_j} & M_{\phi b_j} \\
 & & M_{mm} & M_{m\omega_1} & M_{mb_1} & \cdots & M_{m\omega_j} & M_{mb_j} \\
 & & & M_{\omega_1\omega_1} & M_{\omega_1 b_1} & \cdots & 0 & 0 \\
 & & & & M_{b_1 b_1} & \cdots & 0 & 0 \\
 & \textbf{SYM} & & & & \ddots & \vdots & \vdots \\
 & & & & & & M_{\omega_j\omega_j} & M_{\omega_j b_j} \\
 & & & & & & & M_{b_j b_j}
\end{pmatrix} \qquad \text{(IV-10)}
$$

where the hybrid coordinate set of the multibody structure is

$$\left(\underset{\sim}{q}\right)^T = \left(\left({}_{I}\underset{\sim}{r}_m^{\,O} \right)^T \left({}_{I}\underset{\sim}{\phi}_m^{\,O} \right)^T \left(\underset{\sim}{q}_{fm} \right)^T \left({}_{B_1}\underset{\sim}{\phi}_1^{rel} \right)^T \left(\underset{\sim}{q}_{f1} \right)^T \cdots \left({}_{B_j}\underset{\sim}{\phi}_j^{rel} \right)^T \left(\underset{\sim}{q}_{fj} \right)^T \right) \tag{V-11}$$

The matrices appearing in the global mass matrix (IV-10) of the multibody structure have the following forms

$$M_{rr} = \left(m_m + \sum_{j=1}^{k} m_j \right) 1 \tag{IV-12}$$

$$M_{r\phi} = \left(\underset{\sim}{\rho}_m^{*} \right)^x m_m + \sum_{j=1}^{k} \left(-\left(\underset{\sim}{\rho}_m \right)_j^x m_j - C_j^T \left(\underset{\sim}{\rho}_j^{*} \right)^x m_j C_j \right) \tag{IV-13}$$

$$M_{rm} = \int_M U_{fm} dm + \sum_{j=1}^{k} \left(\left(U_{fm} \right)_j m_j - C_j^T \left(\underset{\sim}{\rho}_j^{*} \right)^x m_j C_j \left(\Theta_{fm} \right)_j \right) \tag{IV-14}$$

$$M_{r\omega j} = C_j^T \left(\underset{\sim}{\rho}_j^{*} \right)^x m_j \tag{IV-15}$$

$$M_{rbj} = C_j^T \int_{Bj} V_{fj} dm \tag{IV-16}$$

$$M_{\phi\phi} = I^{M/O} + \sum_{j=1}^{k} \left(-\left(\underset{\sim}{\rho}_m \right)_j^x \left(\underset{\sim}{\rho}_m \right)_j^x m_j - \left(\underset{\sim}{\rho}_m \right)_j^x C_j^T \left(\underset{\sim}{\rho}_j^{*} \right)^x m_j C_j - C_j^T \left(\underset{\sim}{\rho}_j^{*} \right)^x m_j C_j \left(\underset{\sim}{\rho}_m \right)_j^x \right)$$

$$+ \sum_{j=1}^{k} \left(C_j^T \; {}^{Bj/Jj}I \; C_j \right) \tag{IV-17}$$

$$M_{\phi m}=\int_M \left(\underset{\sim}{\rho}_m\right)^x U_{fm}\,dm+\sum_{j=1}^{k}\left(\left(\underset{\sim}{\rho}_m\right)_j^x\left(U_{fm}\right)_j m_j-\left(\underset{\sim}{\rho}_m\right)_j^x C_j^T\left(\underset{\sim}{\rho}_j^*\right)^x m_j\left(\Theta_{fm}\right)_j\right)$$

$$+\sum_{j=1}^{k}\left(C_j^T\left(\underset{\sim}{\rho}_j^*\right)^x m_j C_j\left(U_{fm}\right)_j-C_j^T\ I^{Bj/J}\ C_j\left(\Theta_{fm}\right)_j\right) \qquad \text{(IV-18)}$$

$$M_{\phi\omega j}=\left(\underset{\sim}{\rho}_m\right)_j^x C_j^T\left(\underset{\sim}{\rho}_j^*\right)^x m_j+C_j^T\ I^{Bj/J} \qquad \text{(IV-19)}$$

$$M_{\phi bj}=\left(\underset{\sim}{\rho}_m\right)_j^x C_j^T\int_{Bj} V_{fj}\,dm+C_j^T\int_{Bj}\left(\underset{\sim}{\rho}_j\right)^x V_{fj}\,dm \qquad \text{(IV-20)}$$

$$M_{mm}=\int_M U_{fm}U_{fm}\,dm+\sum_{j=1}^{k}\left(\left(U_{fm}\right)_j^T\left(U_{fm}\right)_j m_j-\left(\Theta_{fm}\right)_j^T C_j^T\ I^{Bj/J}\ C_j\left(\Theta_{fm}\right)_j\right)$$

$$+\sum_{j=1}^{k}\left(-\left(U_{fm}\right)_j^T C_j^T\left(\underset{\sim}{\rho}_j^*\right)^x m_j C_j\left(\Theta_{fm}\right)_j+\left(\Theta_{fm}\right)_j^T C_j^T\left(\underset{\sim}{\rho}_j^*\right)^x m_j C_j\left(U_{fm}\right)_j\right) \qquad \text{(IV-21)}$$

$$M_{m\omega_j}=-m_j\left(U_{fm}\right)_j^T\ C_j^T\left(\underset{\sim}{\rho}_j^*\right)^x+\left(\Theta_{fm}\right)_j^T\ C_j^T\ I^{Bj/J} \qquad \text{(IV-22)}$$

$$M_{mb_j}=\left(U_{fm}\right)_j^T C_j^T\int_{B_j} V_{fj}\ dm+\left(\Theta_{fm}\right)_j^T C_j^T\int_{B_j}\left(\underset{\sim}{\rho}_j\right)^x V_{fj}\ dm \qquad \text{(IV-23)}$$

$$M_{\omega j\ \omega j}=I^{Bj/J} \tag{IV-24}$$

$$M_{\omega j\ bj}=\int_{Bj}\left(\underset{\sim}{\rho}_j\right)^{x} V_{f\,j}\,dm \tag{IV-25}$$

$$M_{bj\ bj}=\int_{Bj}\left(V_{f\,j}\right)^{T} V_{f\,j}\,dm \tag{IV-26}$$

V-2-2. Comments and Assessment of Method I Based on Mathematical Model A

Method I is akin to nonlinear dynamics modelling. The hybrid set of coordinates is necessary for accommodating large angular displacements. The resulting expressions are fairly complex for a linear articulated peripheral multibody structure, even for this case that the appended components do not carry any distributed mass payload. The development effort for the formulation of mathematical model A, is not high as such, but caution should be exercised for the correct interpretation of resulting integrals from the mathematical manipulations.

It may be useful to examine three different partitions of the global mass matrix in order to gain insight into the physics of the system. These are

$$\begin{pmatrix} M_{rr} & M_{r\phi} & M_{rm} \\ & M_{\phi\phi} & M_{\phi m} \\ \text{Sym} & & M_{mm} \end{pmatrix} \tag{IV-27}$$

$$\begin{pmatrix} M_{r\omega_j} & M_{rb_j} \\ M_{\phi\omega_j} & M_{\phi b_j} \\ M_{m\omega_j} & M_{mb_j} \end{pmatrix} \qquad \text{(IV-28)}$$

$$\begin{pmatrix} M_{\omega_j\omega_j} & M_{b_j\omega_j} \\ Sym & M_{b_jb_j} \end{pmatrix} \qquad \text{(IV-29)}$$

The partition matrix (IV-27) would give the kinetic energy of the multibody system if the appendages were rigid and rigidly attached at the interfaces, i.e. all articulation axes locked. This is not a very obvious observation, since by examining the individual terms, the particular form of the terms obscures physical interpretation. If the main platform is restrained externally, so that it possesses no rigid-body degrees of freedom, the first two columns and rows of global mass matrix should be removed, along with terms in the first two columns and rows of the global stiffness matrix.

The partition matrix (IV-28) contains the interaction of the rigid-body motion and the deformation of the main platform with the rigid-body motion (due to articulation) and the deformation of the appended component B_j, columns 1 and 2 respectively.

The partition matrix (IV-29) would be the kinetic energy of the appendage B_j, if the interface constraints were external boundary constraints of the appendage. The contribution of the articulation and the flexibility appear explicitly and the interaction term exists only if the component modes used are not the normal modes of the boundary eigenvalue problem.

By examining individual terms, it is difficult, in a lot of cases, to decide on their physical significance, and the interpretation of the mathematical expressions is not readily obvious. Interpretation of the significance of particular terms is only feasible by examining those as part of the global mass matrix.

In the computational part, the large number of integration schemes for each component, the arbitrary number of appended components and the 'correction' terms appearing in most of the expressions complicate the programming part of the model. In addition to this, if specific terms should not be included for an application, particular attention should be exercised for their elimination. Moreover, the validation of parts of the program can become very tedious. The potential accuracy of the results is subject to the large number of integration schemes appearing in the terms. Verification of the final results can only be possible with comparison to results obtained from commercial packages.

V-3. Mathematical Model B

V-3-1. Global Mass Matrix Derivation

Using method II, the mathematical model B has been developed for modelling exactly the same structure as mathematical model A; that is, a cluster formation multibody structure where the appended components can carry concentrated, but not distributed, mass payloads. The difference of method II to I, is mainly that the second utilises a generalised coordinate set instead of a hybrid one. This is only possible under the assumption of small angular displacement, hence the rigid-body motion of the components can be described with the use of rigid-body modes.

The kinetic energy for a multibody structure with k number of appended components is expressed as

$$T = \frac{1}{2}\int_{M}\left({}^{I}_{M}v_{m}^{Q'} \right)^{T}\left({}^{I}_{M}v_{m}^{Q'} \right) dm + \frac{1}{2}\sum_{j=1}^{k}\int_{Bj}\left({}^{I}_{Bj}v_{j}^{Q'} \right)^{T}\left({}^{I}_{Bj}v_{j}^{Q'} \right) dm \quad \text{(IV-30)}$$

The kinetic energy expression has been presented in (IV-30) for a continuous multibody system. For discrete modelling the integration schemes should be substituted by summations over the nodal points of each component.

Kinetic Energy of the Main Platform

In the second method, simplification is accomplished by describing the rigid-body motion using rigid-body modes. The absolute linear and angular velocity at any point in the main flexible platform can readily be expressed as

$$\underset{M}{{}^{I}v_{m}}{}^{Q'} = U_{m}\dot{\underset{}{q}}_{m} \tag{V-31}$$

$$\underset{M}{{}^{I}\omega_{m}}{}^{Q'} = \Theta_{m}\dot{\underset{}{q}}_{m} \tag{V-32}$$

Kinetic Energy of Appended Component B_j

Similarly the angular velocity of the reference body frame of an articulating appended component B_j relative to the interface reference frame of the main platform can be expressed as

$$\underset{Bj}{{}^{}\omega_{j}}{}^{rel} = \left(\Theta_{rj}\right)_{j}\dot{\underset{}{q}}_{rj} \tag{V-33}$$

From equations (V-31),(V-32) for $Q' \equiv J$, the linear and angular velocity of a frame travelling with the junction point J can be readily obtained. Substituting the (V-31),(V-32) for $Q' \equiv J$ and (V-33) into (III-15), and using (III-17), the absolute linear velocity at an arbitrary point in an appended component B_j, with the assumption of small angular displacement, can be expressed as

$$\underset{Bj}{{}^{I}v_{j}}{}^{Q'} = \left(C_{j}\left(U_{m}\right)_{j} - \left(\underset{Bj}{\rho_{j}}\right)^{x} C_{j}\left(\Theta_{m}\right)_{j}\right)\dot{\underset{}{q}}_{m} - V_{j}\dot{\underset{}{q}}_{j} \tag{V-34}$$

where

$$V_j = \left(U_{rj} \vdots U_{fj} - \left(U_{fj} \right)_j + \left(\underset{-}{\rho}_j \right)^x \left(\Theta_{fj} \right)_j \right) \tag{V-35}$$

Substituting (V-31) and (V-34) into the kinetic energy expression (IV-30), the global mass matrix for a cluster configuration multibody structure can be readily obtained in the following form

$$M_G = \begin{pmatrix} M_{mm} & M_{mb_1} & \cdots & M_{mb_j} \\ & M_{b_1b_1} & 0 & 0 \\ & & \ddots & 0 \\ SYM & & & M_{b_jb_j} \end{pmatrix} \tag{V-36}$$

where generalised coordinate set of the multibody structure is given by

$$\left(\underset{-}{q} \right)^T = \left(\left(\underset{-}{q}_m \right)^T \left(\underset{-}{q}_1 \right)^T \cdots \left(\underset{-}{q}_j \right)^T \right) \tag{V-37}$$

and j=1,..,k , where k is the total number of appended components on the main platform.

The submatrices in the global mass matrix of the structure have the following expressions

$$M_{mm} = \int_M \left(U_m \right)^T U_m dm + \sum_{j=1}^{k} \left\{ \left(\Theta_m \right)_j^T \; C_j^T \; I^{Bj/J} \; C_j \left(\Theta_m \right)_j + m_j \left(\left(U_m \right)_j^T \left(U_m \right)_j \right) \right\}$$

$$+ \sum_{j=1}^{k} \left\{ m_j \left(- \left(U_m \right)_j^T C_j^T \left(\underset{-}{\rho}_j^* \right)^x C_j \left(\Theta_m \right)_j + \left(\Theta_m \right)_j^T C_j^T \left(\underset{-}{\rho}_j^* \right)^x C_j \left(U_m \right)_j \right) \right\} \tag{V-38}$$

$$M_{mbj}=\left(U_m\right)_j^T C_j^T \int_{Bj} V_j dm+\left(\Theta_m\right)_j^T C_j^T \int_{Bj}\left(\underset{\sim}{\rho}_j\right)^x V_j dm \qquad \text{(V-39)}$$

$$M_{bj\ bj}=\int_{Bj}\left(V_j\right)^T V_j dm \qquad \text{(V-40)}$$

V-3-2. Comments and Assessment of Method II Based on Mathematical Model B

The use of generalised coordinates, for the description of the rigid-body motion for a geometrical linear system, simplifies the form of the resulting equations. Moreover, the physical interpretation of the terms is obvious, and possible even without examining the terms as part of the global mass matrix.

Expression (V-38) would give the kinetic energy of the system if all appendages were rigid and fixed on the main platform. This term cannot recognise that the appended component may be articulating. If in actual fact the appendages were rigid and articulating, (V-38) alone would not be able to give the correct kinetic energy of the system. Contribution of the other terms would be essential for the differential system to recognise the articulation of the appended components.

Expression (V-40) would represent the kinetic energy of component B_j, if the interface conditions were the external boundary constraints of the component, i.e. the component isolated and restrained relatively to the inertial space. The kinetic energy of the component, not interacting to the platform, is a contribution from the rigid-body motion, due to articulation, and the deformation of the component due to flexibility. The term (V-40) exists if either of the two contributions exist.

Expression (V-39) represents the interaction of the rigid-body motion and deformation of the main platform with the angular motion and deformation of an appended component B_j. If one assumes that the appended component is not

articulating relatively to the main platform, then the term would only give the interaction of the platform motion (flexible and rigid) with the deformation of the component. If the appended component were rigid and non-articulating, then this term would disappear, along with (V-40), and the kinetic energy of the system would be represented by (V-38) alone.

The programming, validation and verification of results has been simplified compared to mathematical model A. Furthermore, the lower number of integration schemes will potentially give more accurate results, than those obtained form model A.

V-4. Mathematical Model C

V-4-1. Global Mass Matrix Derivation

Using method II, the mathematical model of a cluster formation structure has been derived for the case the appended flexible components can carry distributed mass rigid payloads. In the same mathematical model explicit expressions of the torsional deformation of beam-modelled appendages, along with terms that allow the kinematical description of the Timoshenko beam theory, have been included.

The kinetic energy of the multibody system can be written as

$$T = \frac{1}{2}\int_{M}\left({}^{I}_{M-}v_{m}^{Q'} \right)^{T}\left({}^{I}_{M-}v_{m}^{Q'} \right) dm$$

$$+\frac{1}{2}\sum_{j=1}^{k}\left\{\int_{Bj}\left({}^{I}_{Bj-}v_{j}^{M'} \right)^{T}\left({}^{I}_{Bj-}v_{j}^{M'} \right)dm+\sum_{p=1}^{s}\left\{\int_{Bjp}\left({}^{I}_{Bj-}v_{jp}^{M'} \right)^{T}\left({}^{I}_{Bj-}v_{jp}^{M'} \right)dm\right\}\right\} \qquad \text{(V-41)}$$

where

k is the total number of appended components

s is the total number of distributed mass rigid payloads on each appended

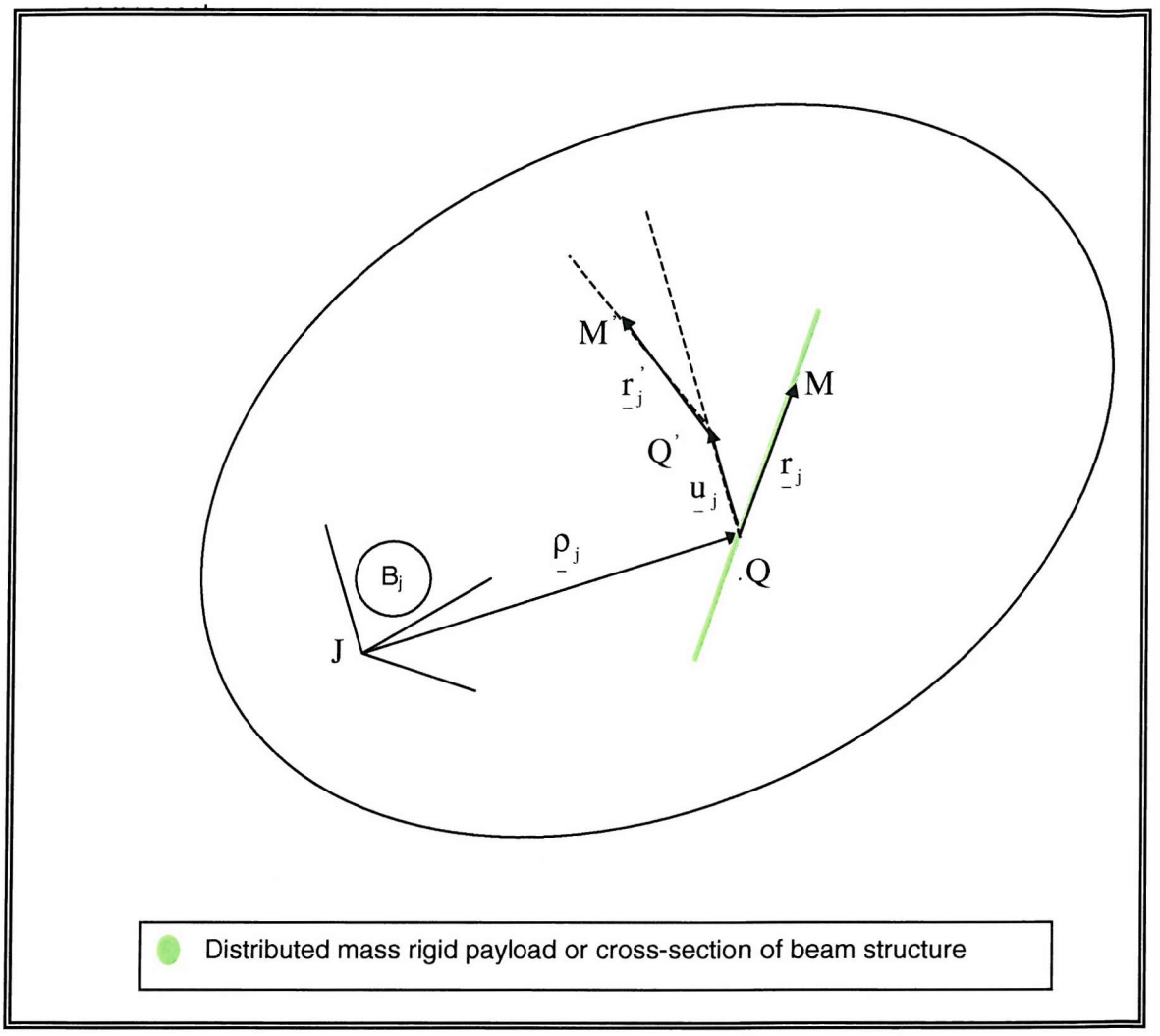

Figure V-2 Component B_j and distributed mass rigid payload or beam cross-section.

In Figure V-2, the vector quantity $\underline{r}_j$ locates the position a point M which is part of the rigid body configuration of the component B_j , i.e. before the deformation of the component. The point M can be the position of an integration point on a cross-

section of a beam structure and/or the location at an integration point on a distributed mass rigid payload before the deformation of component B_j. In both accounts, the position of the $\underline{r}_j$ after the deformation of the component B_j will be designated by vector $\underline{r}_j'$. The vector $\underline{r}_j$ has rotated by an amount equal to the angular displacement at point Q' due to deformation and translated by an amount equal to the linear displacement of the point Q' due to deformation. In both occasions, the magnitude of the vector $\underline{r}_j$ remains unchanged, since it is part of either the distributed mass rigid payload or the cross section of a beam.

From the above description, and placing a local reference frame at point Q', it can be verified that the integration or summation point M' within each continuous or discrete component relates to the arbitrary point Q' with the following expressions

$$ {}^{I}_{B_j}\underline{v}_j^{M'} = {}^{I}_{B_j}\underline{v}_j^{Q'} - \left({}_{B_j}\underline{r}_j' \right)^{x} {}^{I}_{B_j}\underline{\omega}_j^{Q'} \qquad \text{(V-42)} $$

$$ {}^{I}_{B_j}\underline{v}_{jp}^{M'} = \left({}^{I}_{B_j}\underline{v}_j^{Q'} \right)_p - \left({}_{B_j}\underline{r}_j' \right)^{x} \left({}^{I}_{B_j}\underline{\omega}_j^{Q'} \right)_p \qquad \text{(V-43)} $$

where expression (V-42) relates M' and Q' for the case that M' is an integration point within the elastic domain and expression (V-43) relates M' and Q' for the case that M' is an integration point within the mass distributed rigid payload. In both cases Q' is considered a point within the elastic domain that its motion is known, using expressions (III-15), (III-16). Points Q', M' are shown in Figure V-2.

Equation (V-42) as such will only be used for a beam-modelled structure, meaning that integration of the second term of equation (V-42) in the kinetic energy expression will take place only for a beam structure.

Substituting (III-15), (III-16) into (V-42) and (V-43), with the assumption of small angular displacement, and using the notation established for cluster formation structures, the following expressions are obtained respectively

$$
{}^{I}_{Bj-}v_{j}^{M'} = C_{j}\ {}^{I}_{M-}v_{m}^{J} - \left({}_{Bj-}\rho_{j} + {}_{Bj-}r_{j}\right)^{\times} C_{j}\ {}^{I}_{M-}\omega_{m}^{J} - \left({}_{Bj-}\rho_{j} + {}_{Bj-}r_{j}\right)^{\times} {}_{Bj-}\phi_{j}^{rel}
$$

$$
+ {}_{Bj-}\dot{u}_{j} - \left({}_{Bj-}\dot{u}_{j}\right)_{J} + \left({}_{Bj-}\rho_{j} + {}_{Bj-}r_{j}\right)^{\times} \left({}_{Bj-}\dot{\theta}_{j}\right)_{J} + \left({}_{Bj-}r_{i}\right)^{x} {}_{Bj-}\dot{\theta}_{j} \qquad \text{(V-44)}
$$

$$
{}^{I}_{Bj-}v_{jp}^{M'} = C_{j}\ {}^{I}_{M-}v_{m}^{J} - \left(\left({}_{Bj-}\rho_{j}\right)_{p} + {}_{Bj-}r_{j}\right)^{\times} C_{j}\ {}^{I}_{M-}\omega_{m}^{J} - \left(\left({}_{Bj-}\rho_{j}\right)_{p} + {}_{Bj-}r_{j}\right)^{\times} {}_{Bj-}\phi_{j}^{rel}
$$

$$
+ {}_{Bj-}\dot{u}_{j} - \left({}_{Bj-}\dot{u}_{j}\right)_{J} + \left(\left({}_{Bj-}\rho_{j}\right)_{p} + {}_{Bj-}r_{j}\right)^{\times} \left({}_{Bj-}\dot{\theta}_{j}\right)_{J} + \left({}_{Bj-}r_{i}\right)^{x} {}_{Bj-}\dot{\theta}_{j} \qquad \text{(V-45)}
$$

where

$\left({}_{Bj-}\rho_{j}\right)_{p}$ is the position where the distributed mass payload mounds within component B_j, measured from the origin of the body reference frame B_j

In expression (V-44) the quantity $\underset{Bj\ -\ j}{\dot{\theta}}$ is the rate of the angular deformation at an qrbitrary point within the structure, and if the structure is a beam, then $\underset{Bj\ -\ j}{\dot{\theta}}$ will contain the torsional deformation rate of the beam along with the bending angular displacement rates due to deformation, which in the case of the Timoshenko beam theory will include an extra rotational rate of the cross-section due to shear.

The vector quantity $\underset{-}{r}_j'$ in equations (V-44) and (V-45) has directly been substituted by $\underset{-}{r}_j$, since small linear deformation has been assumed for the elastic domain, therefore the angular displacement of the vector $\underset{-}{r}_j'$ is sufficiently small.

For a beam component equation (V-44) is integrated both over $\underset{Bj\ -}{\rho}_j$ and $\underset{Bj\ -}{r}_j$, whereas for any other structural component only over $\underset{Bj\ -}{\rho}_j$ (locates point Q').

The following expressions can directly be substituted into (V-44) and (V-45):

- Expressions (III-17),(III-18), regarding the deformation approximation of the elastic domain.
- Expressions (V-31),(V-32), which describe the absolute linear and angular velocity of the main platform at the joints to the appendages by using rigid-body modes and component modes.
- Expression (V-33), which describes, using rigid-body modes, the angular velocity of the body reference frame of component B_j, due to articulation, relative to the joint local reference frame within the main platform.

By substitution of the above into (V-44) and (V-45), the following expressions are obtained respectively.

$$ {}^{I}_{Bj}\underline{v}_{j}^{M'} = \left(C_j\left(U_m\right)_j - \left(\underline{\rho}_{Bj\,j} + \underline{r}_{Bj\,j} \right)^{x} C_j \left(\Theta_m\right)_j \right) \dot{\underline{q}}_m + V_j \dot{\underline{q}}_j - \left(\underline{r}_{Bj\,j} \right)^{x} \Omega_j \dot{\underline{q}}_j $$

(V-46)

$$ {}^{I}_{Bj}\underline{v}_{jp}^{M'} = \left(C_j\left(U_m\right)_j - \left(\left(\underline{\rho}_{Bj\,j} \right)_p + \underline{r}_{Bj\,j} \right)^{x} C_j \left(\Theta_m\right)_j \right) \dot{\underline{q}}_m + \left(V_j\right)_p \dot{\underline{q}}_j - \left(\underline{r}_{Bj\,j} \right)^{x} \left(\Omega_j\right)_p \dot{\underline{q}}_j $$

(V-47)

$$ V_j = \left(U_{rj} \,\vdots\, U_{fj} - \left(U_{fj}\right)_j + \left(\underline{\rho}_j\right)^{x} \left(\Theta_{fj}\right)_j \right) \qquad \text{(V-48)} $$

$$ \Omega_j = \left(\Theta_{rj} \,\vdots\, \Theta_{fj} - \left(\Theta_{fj}\right)_j \right) \qquad \text{(V-49)} $$

Substituting (V-46), (V-47) into (V-41) and performing the integrations, the global mass matrix of the cluster structure has the form of (V-36) , where the partitions are

$$ M_{mm} = \int_M \left(U_m\right)^T U_m \, dm + \sum_{j=1}^{k} \left\{ \left(\Theta_m\right)_j^T \; C_j^T \; I^{Bj/J} \; C_j \left(\Theta_m\right)_j + m_j \left(\left(U_m\right)_j^T \left(U_m\right)_j \right) \right\} $$

$$ + \sum_{j=1}^{k} \left\{ m_j \left(- \left(U_m\right)_j^T C_j^T \left(\underline{\rho}_j^{*}\right)^{x} C_j \left(\Theta_m\right)_j + \left(\Theta_m\right)_j^T C_j^T \left(\underline{\rho}_j^{*}\right)^{x} C_j \left(U_m\right)_j \right) \right\} $$

(V-50)

$$M_{mbj}=\underbrace{\left(U_m\right)_j^T C_j^T \int_{Bj,Bjp} V_j dm+\left(\Theta_m\right)_j^T C_j^T \int_{Bj,Bjp}\left(\underset{\sim}{\rho}_j\right)^x V_j dm}_{1}$$

$$+\underbrace{\left(\Theta_m\right)_j^T C_j^T \int_{Bj} i(x)\ \Omega_j dx}_{2}+\underbrace{\left(\Theta_m\right)_j^T C_j^T \left(\sum_{p=1}^{m}\left\{I^{P/P}\left(\Omega_j\right)_p\right\}\right)}_{3}$$

$$\underbrace{+\left(U_m\right)_j^T C_j^T \sum_{p=1}^{m}\left\{\left(\underset{\sim}{r}_j^{\,*}\right)_p^x m_{jp}\left(\Omega_j\right)_p\right\}+\left(\Theta_m\right)_j^T C_j^T\left(\sum_{p=1}^{m}\left\{\left(\underset{\sim}{r}_j^{\,*}\right)_p^x m_{jp}\left(V_j\right)_p\right\}+\sum_{p=1}^{m}\left\{\left(\underset{\sim}{\rho}_j\right)_p^x\left(\underset{\sim}{r}_j^{\,*}\right)_p^x m_{jp}\left(\Omega_j\right)_p\right\}\right)}_{4}$$

(V-51)

$$M_{bj\ bj}=\underbrace{\int_{Bj,Bjp}\left(V_j\right)^T V_j dm}_{5}+\underbrace{\int_{Bj}\left(\Omega_j\right)_p^T\ i(x)\left(\Omega_j\right)_p dx}_{6}+\underbrace{\sum_{p=1}^{m}\left\{\left(\Omega_j\right)_p^T\ I^{P/P}\left(\Omega_j\right)_p\right\}}_{7}$$

$$+\underbrace{\sum_{p=1}^{m}\left\{-\left(V_j\right)_p^T\left(\underset{\sim}{r}_j^{\,*}\right)_p^x m_{jp}\left(\Omega_j\right)_p+\left(\Omega_j\right)_p^T\left(\underset{\sim}{r}_j^{\,*}\right)_p^x m_{jp}\left(V_j\right)_p\right\}}_{8}$$

(V-52)

V-4-2. Comments and Assessment of Method II Based on Mathematical Model C

Mathematical model C is a generic model of a realistic peripheral structure in space. Beam modelled appendages are included in the model. A number of appendages, such as booms, can be accurately modelled as beams. Moreover, the model allows for the inclusion of distributed mass rigid payloads. It is not uncommon in space structures that the appendages may carry rigid distributed mass payloads, such as control hardware units, and in a lot of occasions the centre of mass of the rigid payload is at some distance from the mounting points.

Mathematical model C, is therefore a comprehensive model, which can capture the dynamics of a realistic cluster formation structure in space with the minimum size of formulated differential equations. Nevertheless, it has some drawbacks. Before preceding to those, it may prove helpful to examine closer the terms in the partitioned submatrices of the global mass matrix.

As in mathematical model B, which has been developed with the same method as the current model, the matrix $\mathbf{M}_{mm}$ would be the kinetic energy of the system, if all appended components, loaded with the mass and inertia of the payloads, were rigid and fixed on the main platform. All inertia related terms in $\mathbf{M}_{mm}$ represent the combined inertia of the appendage and the rigid payloads. The term $\mathbf{M}_{b_j b_j}$ would give the kinetic energy of an appendage B_j, loaded with rigid payloads, if the interface constraints on the appendage were real external boundary constraints and the appendage were isolated from the platform. The term $\mathbf{M}_{mb_j}$ is an interaction term between the motion of the main platform and the motion of the appendage B_j.

More specifically, term 1 in (V-51) is the interaction of the main platform with an appended non-beam component B_j, loaded with the mass of the distributed mass rigid payloads concentrated at the mounting points. For facilitating the numerical integration, term 1 integrates directly the mass of the rigid-payloads along with the distributed or discretised mass of the component. Term 2 needs to be calculated only if the appendage has been modelled as a beam structure. Hence, term 1 and 2 would give the interaction of the main platform and a beam appendage carrying concentrated mass. Term 3 gives the contribution in the interaction of the distributed mass payloads. If the rigid payload mounting point is coincident to its centre of mass, then $\mathrm{I}^{p/p}$ is the rotary inertia of the payload around its centre of mass. Terms 4 exist only if the payload is offset, i.e. its centre of mass is on a different location to the mounting point. This distance is described by $\left(\underline{r}_j \right)_p$, and if equals to zero all terms disappear.

Term 5 in (V-52) would give the kinetic energy of a non-beam component, if isolated and with all internal constraints considered as external boundary constraints. If this component has been modelled as a beam then term 6 needs to be included in the mathematical model. In term 6 the matrix quantity Ω_j contains terms for the rotation of the beam appendage as a rigid articulating component, useful mainly for describing the articulation around the beam axis, torsional deformation and bending deformation terms. If the appendage has been modelled as in Timoshenko beam theory the shear and the rotary inertia of the cross-section are directly taken into account by term 6. If static modes have been used to describe the local deformation of the components at the interface with the main platform, Ω_j contains 'correction' terms to re-enforce the interface geometric compatibility. Term 7 exists only if the appendage is loaded with distributed mass rigid payload. If the payload is offset terms 8 complement the rest of the terms.

The drawbacks of the mathematical model C, other than its inherent complexity for programming, are mostly attributed to the essential interference of the analyst with providing specific information to the model. Assuming that the information of the inertia related data is collected from a lumped mass matrix of the component, the following problems can be located. Information about the distributed inertia of a structure is usually not available from the a lumped mass model. Although the inertia of a component can be calculated very accurately by using the nodal lumped mass, the nodal masses of a beam structure cannot provide the inertia of the beam around its longitudinal axis. Moreover, even if the inertia is provided, the distribution of the inertia along the axis needs to be calculated. In theory this may be a simple operation, but in practice, for an arbitrary number of beam appendages of non-uniform cross section, this might be time involving. In addition to these, information needs to be provided to the analyst about the mass and offset of the rigid payload. The mass of the payload cannot be separated easily form the nodal mass of the flexible component in the lumped mass matrix, at least not all the times. The rest of the inertia related information can be retrieved and processed with fair ease to provide the total mass and the inertia of arbitrary non-beam components.

Another drawback of the model is that both a lumped mass finite element model, for extracting nodal masses, and a consistent finite element model of a component, usually necessary for the accurate extraction of the normal modes of the component, need to be derived. Since both models need to be generated, time related disadvantages are expected.

Nevertheless, other than a few disadvantages that occur generally in all computational applications, model C is an excellent tool for design and analysis of realistic cluster formation structures in space.

V-5. Mathematical Model D

V-5-1. Global Mass Matrix Derivation

Mathematical model D has been developed using method III with the intention to model any cluster configuration structure in space by treating all components alike.

The kinetic energy of the multibody system can be expressed as

$$T = \frac{1}{2}\left(\underset{M}{\dot{x}}_m\right)^T M_m^{FEM}\left(\underset{M}{\dot{x}}_m\right) + \frac{1}{2}\sum_{j=1}^{k}\left(\left(\underset{Bj}{\dot{x}}_j\right)^T M_j^{FEM}\left(\underset{Bj}{\dot{x}}_j\right)\right) \qquad \text{(V-53)}$$

where

k is the total number of appended components in the multibody system.

M_m^{FEM} is the consistent mass matrix of the main platform.

$\underset{M}{\dot{x}}_m$ is the $n_t^m \times (6\times 1)$ column matrix containing n_t^m absolute linear and angular velocity vectors (6x1) at the nodal points of the component, and n_t^m the total number of nodes in the main component.

M_j^{FEM} is the consistent mass matrix of the appended component B_j.

$\underset{Bj}{\dot{x}}_j$ is the $n_t^j \times (6\times 1)$ column matrix containing n_t^j absolute linear and angular velocity vectors (6x1) at the nodal points of the component B_j, and n_t^j the total number of nodes in the component B_j.

Kinetic Energy of Main Platform

For the total of nodes in the main platform the following expression can directly be verified

$$\underset{M}{\dot{x}}_m = \Phi_m \dot{q}_m \tag{V-54}$$

where

Φ_m is a $\left(n_t^m \times 6\right) \times \left(n_r^m + n_f^m\right)$ matrix containing n_f^m component modes for approximating the deformation field of the main platform and n_r^m the rigid-body degrees of freedom of the main platform.

Kinetic Energy of Appended Component B_j

The absolute linear and angular velocity of a nodal point on a discrete component can be directly obtained from expressions (III-15) and (III-16) respectively. The following expressions can be substituted into equations (III-15),(III-16).

- Expression (III-17),(III-18) for approximating the deformation field of any component.
- Expression (V-33) for describing the angular velocity of the appended component body reference frame relative to the interface reference frame of the main platform at the joint J.

By substitution, expressions (III-15) and (III-16) obtain the following form

$$\underset{Bj}{{}^{I}v_j^n} = \left(C_j \left(U_m \right)_j - \left(\underset{Bj}{\rho_j} \right)^x C_j \left(\Theta_m \right)_j \right) \dot{q}_m - V_j^n \dot{q}_j \tag{V-55}$$

$$\underset{Bj}{{}^{I}\omega_j^n} = C_j \left(\Theta_m \right)_j \dot{q}_m + \Omega_j^n \dot{q}_j \tag{V-56}$$

where

$$V_j^n = \left(U_{rj}^n \,\middle|\, U_{fj}^n - \left(U_{fj} \right)_j + \left(\underline{\rho}_j \right)^x \left(\Theta_{fj} \right)_j \right) \tag{V-57}$$

$$\Omega_j^n = \left(\Theta_{rj}^n \,\middle|\, \Theta_{fj}^n - \left(\Theta_{fj} \right)_j \right) \tag{V-58}$$

Using (V-55) and (V-56) the absolute linear and angular velocity (6x1) of a nodal point N in the discrete appended component B_j can be expressed in the following compact matrix form

$$\underset{Bj}{\underline{\dot{x}}}{}_j^n = \begin{pmatrix} {}^I\underline{v}_j^n \\ \hline {}^I\underline{\omega}_{Bj}^n \end{pmatrix} = P_j^n \left(\Phi_m \right)_j \dot{\underline{q}}_m + \Psi_j^n \dot{\underline{q}}_j \tag{V-59}$$

where

$$P_j^n = \left(\begin{array}{c|c} C_j & -\left(\underline{\rho}_j \right)^x C_j \\ \hline 0 & C_j \end{array} \right) \tag{V-60}$$

$$\Psi_j^n = \left(\Phi_{rj}^n \,\middle|\, \Phi_{fj}^n + \Pi_j^n \left(\Phi_{fj}^n \right)_j \right) \tag{V-61}$$

$$\Pi_j^n = \left(\begin{array}{c|c} -I & \left(\underline{\rho}_j \right)^x \\ \hline 0 & -I \end{array} \right) \tag{V-62}$$

By stacking the (6x1) vector of (V-59) for all n_t^j nodes of the component B_j, the following form is readily obtained

$$\underset{Bj}{\underline{\dot{x}}}{}_j = P_j \left(\Phi_m \right)_j \dot{\underline{q}}_m + \Psi_j \dot{\underline{q}}_j \tag{V-63}$$

where

$$\Psi_j = \left(\Phi_{rj} \vdots \Phi_{fj} + \Pi_j \left(\Phi_{fj} \right)_j \right) \qquad \text{(V-64)}$$

Ψ_j is a $\left(n_t^j \times 6\right) \times \left(n_r^j + n_f^j\right)$ matrix and

n_t^j is the total number of nodes in the component B_j

n_r^j the rigid-body modes Φ_{rj}

n_f^j the component modes Φ_{fj}

Ψ_j also includes n_f^j number of 'correction' terms $\left(\Phi_{fj} \right)_j$, that re-enforce compatibility between adjacent components if violated by the selected set of component modes Φ_{fj} (Appendix-A).

The matrix Π_j is a (6x6) 'correction' and 'joint' coefficient matrix. By manipulating the entries in Π_j one can control which axis of a joint is locked or free. At the same time 'correction' term coefficients allow only part of the 'correction' terms to be used depending if are essential for a particular direction of a joint or not.

The matrix $\left(\Phi_m \right)_j$ contains the component modes of the main platform at joint J.

Substituting (V-54) and (V-63) into the kinetic energy expression (V-53) the global matrix of the form (V-36) is obtained, where the submatrices are the following

$$M_{mm} = \left(\Phi_m \right)^T M_m^{FEM} \Phi_m + \sum_{j=1}^{k} \left(\Phi_m \right)_j^T \underbrace{\left(P_j \right)^T M_j^{FEM} P_j}_{1} \left(\Phi_m \right)_j \qquad \text{(V-65)}$$

$$M_{m b_j} = \left(\Phi_m \right)_j^T \left(P_j \right)^T \; M_j^{FEM} \; \Psi_j \tag{V-66}$$

$$M_{b_j b_j} = \left(\Psi_j \right)^T M_j^{FEM} \; \Psi_j \tag{V-67}$$

V-5-2. Comments and Assessment of Method III Based on Mathematical Model D

Since method III uses a generalised set of coordinates, the submatrices interpretation is exactly the same as it appears in previous section for the mathematical model B. The use of generalised coordinates, along with the use of the consistent mass matrix of the structure, results in a generic and compact form of differential equations. There is no need to separate the components to beam-modelled or components which may be loaded with distributed mass rigid payloads. All components are treated alike. The result of this is that the complex equations that appear in mathematical model C, along with all the drawbacks detailed in the relevant section can be circumvented. The consistent mass matrix contains all the information regarding concentrated or distributed mass rigid payloads. Utilising the mass matrix explicitly in the equations, all the information is transferred indirectly into the mathematical model.

Moreover, the term designated as 1, in (V-61), is the rigid-body mass matrix (6x6) of component B_j. This is particular useful, since by simple multiplications involving the consistent mass matrix of the component, its inertia characteristics are revealed. The exact form of the matrix is described in chapter II by expression (II-4). Complex computer programs for calculating the rotary inertia and mass of a component, by using information from the lumped mass matrix can be avoided. As importantly, there is no more need to create a lumped mass model of a component, along the consistent one, with obvious computing time related advantages.

The rigid-body mass matrix obtained by expression 1, is extremely accurate, and its accuracy depends on the number of nodes of the component. The rotary inertia of a beam structure around the longitudinal axis can easily be obtained and in actual fact with great accuracy compared to exact hand calculations even for a small number of nodes. It is obvious that the knowledge of the inertia characteristics is not directly needed in model D, but this particular manipulation can be used in conjunction with the loaded-interface method for extracting loaded-interface normal modes for any component in the structure.

The interference of the analyst to provide 'extra' information to the mathematical model, is eliminated. Moreover, the potential accuracy of the system is high since integration schemes have been substituted by multiplication of matrices. In this work, in order to achieve even higher accuracy of results, the consistent finite element matrix of each component, as well as the stiffness matrix, are included in the programming network with precision of 12 decimal places.

Returning to the mathematical model D, it is apparent that the programming of the global mass matrix is straightforward compared to methods I,II. The potential computing time is also reduced since the integration schemes are eliminated both explicitly from the equation and also implicitly from the calculation of the inertia related terms.

The physical significance of each term is clear and especially the interaction dynamics of the platform and the components. The effort to analytically develop the mathematical model D is minimal compared to model C. Programming validation is also easy, since the form of the matrices imported in the model or created within the model is very simple.

V-6. Comparison of the Methods and Conclusions

The assessment of each individual method and indirect comparison to other methods has been performed, based on the mathematical models produced for cluster formation structures in space. In this section, the methods have been compared directly and conclusions drawn. For this purpose a few general criteria have been established out of the experience gained in developing and programming the methods for obtaining efficient mathematical models of multibody structures. A particular pairing of comparisons has been chosen. Method I is compared to method II using the mathematical models A,B respectively. The comparison of the methods I,II is shown in Table V-2. The second pair of comparisons is between methods II and III, using mathematical models C, D. The comparison of the methods II, III is shown in Table V-3.

All methods result in the same order differential equations. Methods I,II are essentially very similar other than the coordinate sets utilised for each. Method I uses a hybrid coordinate set and therefore is akin to nonlinear modelling. Despite its generality in this respect, hybrid coordinate set overcomplicates the resulting set of equations even for the simplest of cluster formation structures. It would be difficult to generalise such a model to include distributed mass payloads and beam-modelled appendages.

The method II, is much more efficient than method I, since it uses a generalised set of coordinates, by describing the rigid body motion using rigid-body modes. Nevertheless, for appended components loaded with distributed mass rigid payloads, the resulting equations are fairly complex which means are difficult to develop, program and validate. Moreover, the interference of the analyst may become laborious.

Method III uses explicitly the consistent mass matrix of the components and a generalised coordinate set. Both these characteristics contribute to the efficient mathematical modelling, and result to a compact form of differential equations. Mathematical model D, obtained by method III, is mostly efficient for modelling cluster formation structures in space. It can incorporate any kind of component modes in the literature, contains 'correction' terms for any possible application, any

gimbal articulation axis can be free, locked or driven, and results in a compact form of equations of low order. Moreover, it has a high potential accuracy of results and the interference of the analyst has been eliminated.

In the form of equations (V-65)-(V-67), method III provides an excellent tool for research, analysis and design of large-scale flexible multibody cluster formation structures in space. For issues involving the dynamical behaviour of category II missions in space, such as main platform attitude control, stringent payload pointing, vibration suppression, control structure interaction, or general control algorithm implementation etc., mathematical model D can definitely be a solid basis for such applications.

As importantly, method III can easily furnish linear low order mathematical modes for virtually any tree-configuration articulated multibody system that belongs in category II missions in space.

Criteria	Method I (Mathematical Model A)	Method II (Mathematical Model B)
	Hybrid Coordinate Set	*Generalised Coordinate Set*
	Discrete or Continuous Components	Discrete or Continuous Components
Model Complexity	High	Low
Analytical Development Effort	Medium	Low
Physical Insight	Difficult	Clear
Programming Effort	High	Low
Potential Numerical Accuracy	Average	Good
Computing Time for Completion of Application	Average	Good
Programming Validation Effort	High	Low
Analyst Interference	Low	Low
Results Verification	Difficult	Easy

Table V-2 Comparative study between method I (model A) and method II (model B)

Criteria	Method II (Mathematical Model C)	Method III (Mathematical Model D)
	Generalised Coordinate Set	*Generalised Coordinate Set*
	Discrete or continuous components	Discrete Components
Model Complexity	High	Low
Analytical Development Effort	High	Low
Physical Insight	Average	Clear
Programming Effort	Very High	Low
Potential Numerical Accuracy	Average	Very High
Computing Time for Completion of Application	High	Low
Programming Validation Effort	Very High	Low
Analyst Interference	Average	None
Results Verification	Very Difficult	Easy
Subject to generalisation	No	Excellent

Table V-3 Comparative study between method II (model C) , method III (model D)

V-7. Generalised Forces

For presentation purposes the generalised forces analysis will be performed assuming a discrete component, ie. a component spatially discretised using the finite element method.

The generalised force vector due to forces and moments applied on a discrete component B_j can be written as

$$\underset{-j}{Q} = \sum_{n=1}^{n_t} \left(\frac{\partial \, {}^{I}\underset{Bj-j}{v}^{n}}{\partial \dot{\underset{-}{q}}} \right)^{T} \cdot \underset{-n}{f} + \sum_{n=1}^{n_t} \left(\frac{\partial \, {}^{I}\underset{Bj-j}{\omega}^{n}}{\partial \dot{\underset{-}{q}}} \right)^{T} \cdot \underset{-n}{q} \qquad \text{(V-68)}$$

where

n_{tj} is the total number of nodes in the component B_j

${}^{I}\underset{Bj-j}{v}^{n}$ is the absolute linear velocity of node n within component B_j

${}^{I}\underset{Bj-j}{\omega}^{n}$ is the absolute angular velocity of node n within component B_j

Equation (V-68) can be written in the following form

$$\underset{-j}{Q} = \sum_{n=1}^{n_t} \left(\frac{\partial \, \dot{\underset{Bj-j}{x}}^{n}}{\partial \dot{\underset{-}{q}}} \right)^{T} \underset{-jn}{F} \qquad \text{(V-69)}$$

where

$$\dot{\underset{Bj-j}{x}}^{n} = \begin{pmatrix} {}^{I}\underset{Bj-j}{v}^{n} \\ {}^{I}\underset{Bj-j}{\omega}^{n} \end{pmatrix} \qquad \text{(V-70)}$$

and

$$\underset{-jn}{F} = \begin{pmatrix} \underset{-n}{f} \\ \underset{-n}{g} \end{pmatrix}$$

is a 6x1 vector of the forces and moments acting at node n of component B_j

Finally the generalised forces acting on the component B_j can be expressed in the compact form

$$\underset{-j}{Q} = \left(\frac{\partial \dot{\underset{Bj-j}{x}}}{\partial \dot{\underset{-}{q}}} \right)^T \cdot \underset{-j}{F} \qquad \text{(V-70)}$$

where

$$\dot{\underset{Bj-j}{x}} = \left(\left(\dot{\underset{Bj-j}{x}}^1 \right)^T \cdots \left(\dot{\underset{Bj-j}{x}}^n \right)^T \right)^T \qquad \text{(V-71)}$$

$$\underset{-}{F_j} = \left(\left(\underset{-j1}{F} \right)^T \cdots \left(\underset{-jn}{F} \right)^T \right)^T \qquad \text{(V-72)}$$

All previous expressions are general enough and can be used to calculate the generalised forces for any component in a multibody chain.

At this point the analysis will be concentrated in a cluster formation structural system. Substituting expression (V-63) into (V-70) for any appended component and (V-54) into (V-70) for the mainbody, the expression for the generalised forces takes the following compact matrix form

$$\underline{Q} = G \ \underline{f} \tag{V-73}$$

where

$$G = \begin{pmatrix} \Phi_m^T & (\Phi_m)_1^T P_1^T & (\Phi_m)_2^T P_2^T & \cdots & (\Phi_m)_n^T P_n^T \\ 0 & \Psi_1^T & 0 & \cdots & 0 \\ 0 & 0 & \Psi_2^T & \cdots & 0 \\ \vdots & \vdots & \vdots & \ddots & \vdots \\ 0 & 0 & 0 & \cdots & \Psi_n^T \end{pmatrix} \tag{V-74}$$

$$\underline{f} = \left(\left(\underline{F}_m \right)^T \left(\underline{F}_1 \right)^T \left(\underline{F}_2 \right)^T \cdots \left(\underline{F}_n \right)^T \right)^T \tag{V-75}$$

and

Φ_m is a $\left(n_t^m \times 6\right) \times \left(n_r^m + n_f^m\right)$ matrix containing n_f^m component modes for approximating the deformation field of the main platform and n_r^m the rigid-body degrees of freedom of the main platform.

Ψ_j is given by (V-64)

P_j is given by (V-60)

V-8. Frequency Response Analysis

Using Lagrange equations it can be shown that the resulting linear equations of motion for a multibody structure have the following form.

$$M_G \ddot{\underline{q}} + B_G \dot{\underline{q}} + K_G \underline{q} = \underline{Q} \tag{V-76}$$

where

M_G is the global mass matrix.

K_G is the global stiffness matrix.

B_G is the global viscous damping matrix.

$\underline{Q}$ is the generalised force vector.

$\underline{q}$ is the hybrid or generalised coordinate set.

Two methods will be exploited for performing a frequency response analysis. The first is a direct method and the second uses a modal substitution. The modal frequency response analysis may be more computationally efficient than direct frequency response analysis if the mathematical model (V-76) still contains a large number of differential equations. This may be the case where the structural system contains a large number of components and a high number of component modes have been used for stringent convergence.

V-8-1. Direct Frequency Response Analysis

Substituting equation (V-73) to (V-76) the following form is obtained

$$M_G \ddot{\underline{q}} + B_G \dot{\underline{q}} + K_G \underline{q} = G \underline{f} \qquad \text{(V-77)}$$

Harmonic excitation is assumed where forces and moments can be applied at any node on the structural system. The harmonic excitation frequency is identical at any forcing point, however forces can have arbitrary magnitude, direction and phase. Using complex notation the harmonic forcing vector can be written as

$$\underline{f} = \underline{f}_o^* e^{j\omega t} \qquad \text{(V-78)}$$

where

ω is the forcing frequency.

$\underline{f}_o^*$ is a complex vector representation where each entry has the form

$$f_{oi}^* = f_{oi} e^{j\varphi_i} \tag{V-79}$$

where

f_{oi} is the magnitude of the force applied at any nodal degree of freedom

φ_i is the phase angle of the force applied at any nodal degree of freedom

The solution should be of the form

$$\underline{q} = \underline{q}_o^* e^{j\omega t} \tag{V-80}$$

where

$$q_{ok}^* = q_{ok} e^{j\psi_k} \tag{V-81}$$

Substituting (V-78) and (V-80) into (V-77) and adding structural damping at component level, the following system of complex algebraic equations is obtained

$$\left(-\omega^2 M_G + j \left(\omega B_G + D_G \right) + K_G \right) \underline{q}_o^* = G \; \underline{f}_o^* \tag{V-82}$$

where D_G is the global structural damping of the system and has the form

$$D_G = \begin{pmatrix} D_{G_1} & & & & \\ & D_{G_2} & & & \\ & & \ddots & & \\ & & & D_{Gj} & \\ & & & & \ddots \end{pmatrix} \tag{V-83}$$

where all other entries not designated are zero and the component B_j generalised structural damping matrix is given by

$$D_{Gj} = j \; g_j \left(\begin{array}{c|c} 0 & \\ \hline & K_{fj} \end{array} \right) \qquad \text{(V-84)}$$

where

0 is a $n_r^j \times n_r^j$ null matrix and n_r^j are the rigid-body degrees of freedom of the component B_i.

K_{fj} is given by (IV-16) for a continuous component B_j and by (IV-20) for a discrete component.

g_j is the structural damping factor for the component B_j.

For the calculation of the structural damping expressions of each individual component it has been assumed that structural damping is uniform within the component. In cases where the damping is not uniform, the calculation of the structural damping dissipation energy may be difficult to obtain for a continuous component. For a discrete component it would be beneficial to obtain the structural damping component matrix directly from a finite element model, where the structural damping can easily be entered at elemental level.

The above equation can be solved for any forcing frequency of interest. The solution can be written as

$$q_{ok}(\omega) \quad \text{and} \quad \psi_k(\omega) \qquad \text{for any k=1,..n} \qquad \text{(V-85)}$$

where n the degrees of freedom of the truncated system.

Finally partitioning (V-85) into the 'modal' responses of the individual components and substituting the appropriate partitions in equations (V-54) or (V-59) the physical displacement - magnitude and phase - can be written as function of the forcing frequency.

V-8-2. Modal Frequency Response Analysis

Modal frequency response analysis can be easily accomplished by the transformation

$$\underline{q}_o^* = P \; \underline{p}_o^* \tag{V-86}$$

where P is the global modal matrix of the structural system obtained by solving the eigenvalue problem related to equation (V-76).

Substituting (V-86) into (V-82) a transformation to the global modal coordinates has been achieved, as opposed to the component modal coordinates of equation (V-82).

$$\left(-\omega^2 P^T M_G P + j \; P^T (\omega B_G + D_G) \; P^T + P^T K_G P \right) \underline{p}_o^* = P^T G \; \underline{f}_o^* \tag{V-87}$$

By retaining only a number of modes in the global modal matrix P, the order of equation (V-87) is reduced. The equation in the form of (V-87) is advantageous over the form (V-82) in cases that the multibody system has been modelled with a large number of component modes.

Although the mass and stiffness related terms in (V-87) are of an uncoupled form the damping terms in general are not. If localised viscous damping is assumed negligible and a uniform structural damping is assumed for all components, the form of (V-87) can be written in a uncoupled -diagonal- form, which is computationally much more efficient to solve. Although this would be ideal, in reality is very rare to come across large multibody structures where such hypothesis would hold true. Nevertheless equations in the form (V-87) may be still beneficial to use since the order of the system can be dramatically reduced. Finally, reconstruction to the physical coordinates can be achieved in two steps using equation (V-86)

VI Computational Implementation

VI-1. Network of Programs

VI-1-1. Network Deliverables

A network of programs has been developed for the computational implementation of mathematical model D. The final deliverables of the network are the eigenvalues of the multibody system and the eigenvectors in modal or physical space. Additionally, physical displacement, velocity and acceleration of any point on the structure can be derived as a function of the forcing frequency using either direct or modal frequency response analysis. Results can be compared to those obtained by direct application of the finite element method for the verification of theoretical integrity of the mathematical model D and as importantly for the assessment of the several component mode sets implemented in the code.

VI-1-2. Network Capabilities

Special care has been exercised so that the network of programs has a simple structure and at the same time be generic enough to model any complex cluster formation multibody structure. Attention has also been paid (within the resources available) in order for the network to perform its tasks in the minimum possible time. The network is easily usable and reliable, since it has been through extensive validation tests.

Components with identical mass, stiffness, damping matrices and interface constraints are only analysed once within the same network run. As it will be demonstrated later in this chapter, this feature has dramatic effect in sparing computing time. Large multibody systems are typical examples of structures with a high number of identical components. Further time reduction is realised since

matrices for identical components are created, stored and retrieved only once. A typical model of cluster formation large flexible multibody structure with a number of identical components has been illustrated in Figure IV-1.

Computing time reduction is also accomplished in extracting static modes using a multiple algebraic solution. Special algorithms have been developed for this operation and have been incorporated along numerical algorithms from the NAG Routines Library.

The modularity of the network structure suggests that for a number of operations only a small part of the network needs to be executed, with obvious computing time related benefits. A few examples would be the addition or removal of components, structural modification on a small number of components, repositioning or reorientation of members, alterations on the interface conditions between adjacent substructures, different component set utilisation and component mode set size reduction.

Other capabilities of the network are of inherent nature, since they are directly linked to the capabilities of the general methodology and the mathematical model derived.

VI-1-3. Implementation of Component Mode Sets

The linear elastic deformation field of each component is approximated using component mode sets. The component modes may be combinations of dynamic and static modes. Several component mode sets have been incorporated in the network of programs. The structure of mathematical model D, being generic and compact, allows the direct implementation of any component mode set possible. 'Correction' terms are included in the mathematical model D so that interface conditions at the boundaries of distinct components are not violated for any component mode sets.

Since structures in space are composed of complex components, within the framework of this network each component has been spatially discretised using the finite element method. The network has been interfaced with the commercial finite

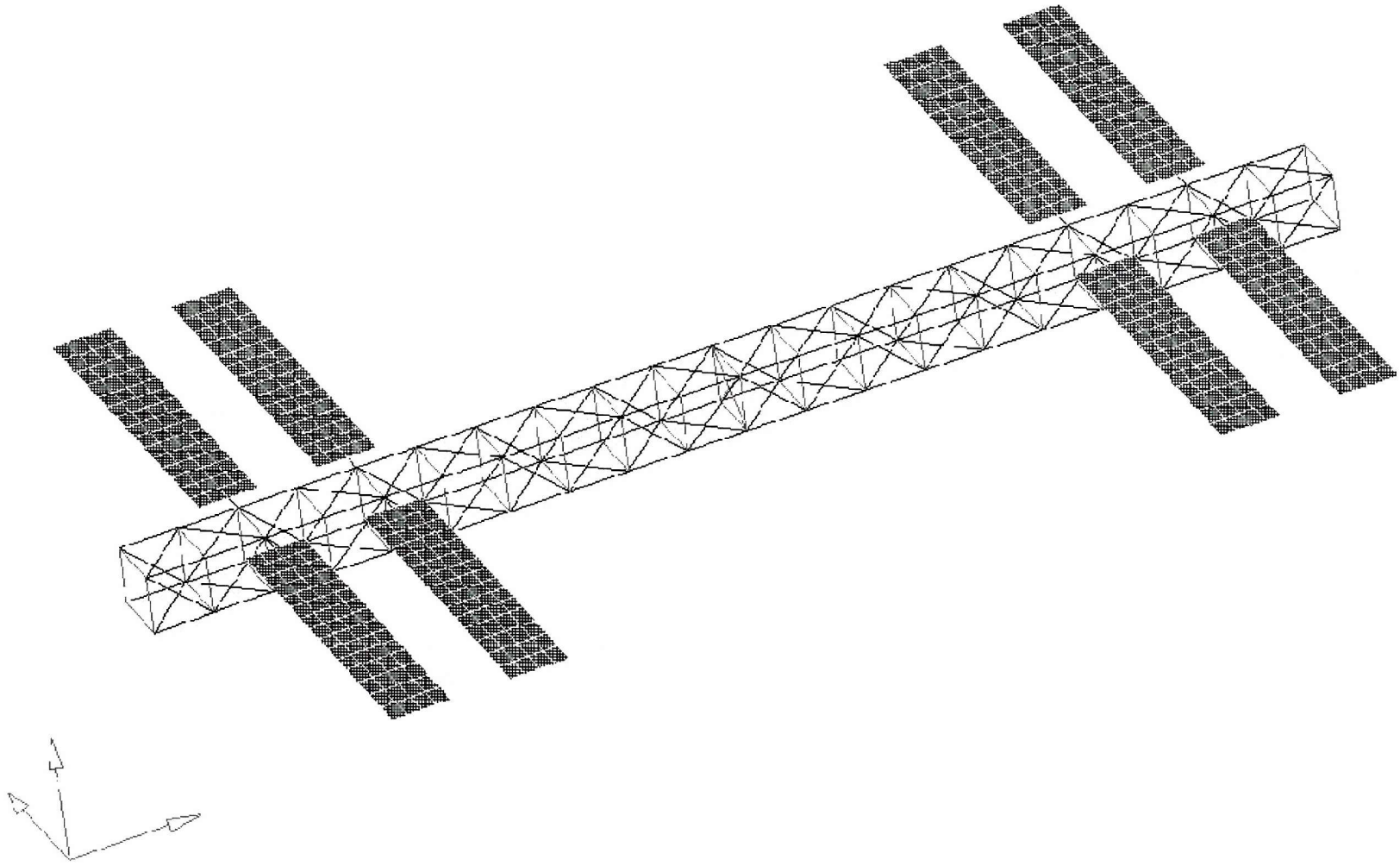

Figure VI-1 Typical Space-Frame Platform Carrying a Number of Solar Panels

element package ANSYS. The finite element model of a component is imported into ANSYS pre-processor and in the solution phase the consistent mass and stiffness matrices of the finite element model are calculated. Using ANSYS post-processor facility the matrices can be output in binary files. Specially adapted programs from ANSYS Programmer's Manual[81] have been employed to output the matrices in 12 decimal places precision, reducing the numerical error. ANSYS solver is also utilised for deriving the rigid-body modes and dynamic normal vibration modes, subject to the interface constraints dictated by the component mode selection.

Within the network of programs the static modes such as redundant constraint and constraint modes, that complement the dynamic modes to form a component mode set, are calculated using specially developed algorithms. In total 5 distinct component mode sets have been implemented, namely the redundant constraint, constraint, loaded-interface, fixed-interface and free-interface component mode sets.

VI-1-4. Network Structure

All data extracted from finite element package ANSYS is processed by several custom developed programs before reaching the final program of the network. Information can also flow into ANSYS and is provided by special programs that output the necessary data in ANSYS language. The final program, which is essentially the programming code for the mathematical model D, calculates the global mass, stiffness, damping matrices and generalised forces acting on the system. Subsequently, using external subroutines form the NAG Routines Library, the natural frequencies and mode shapes of the structural system are obtained. Additionally a direct or modal frequency response analysis can be performed.

The analyst develops the finite element models of the components that need to be analysed in ANSYS language and also provides, using data files, the following information:

i. The kind of flexible component mode set to be used for each component.
ii. The number of component normal modes to be retained in the analysis, thus controlling the size of the formulated problem.

iii. The orientation of the appendages relative to the main platform.
iv. The location points of the appendages on the main platform.
v. The interface constraints between an appendage and the main platform.
vi. The external boundary constraints on the main platform.
vii. The identical components so that they are treated only once.
viii. The forces acting on the system.
ix. The time step for frequency response analysis analysis.

The detailed structure of the network is presented in Table 1. The user's data files, programs developed as well as intermediate and final results data files are presented subsequently.

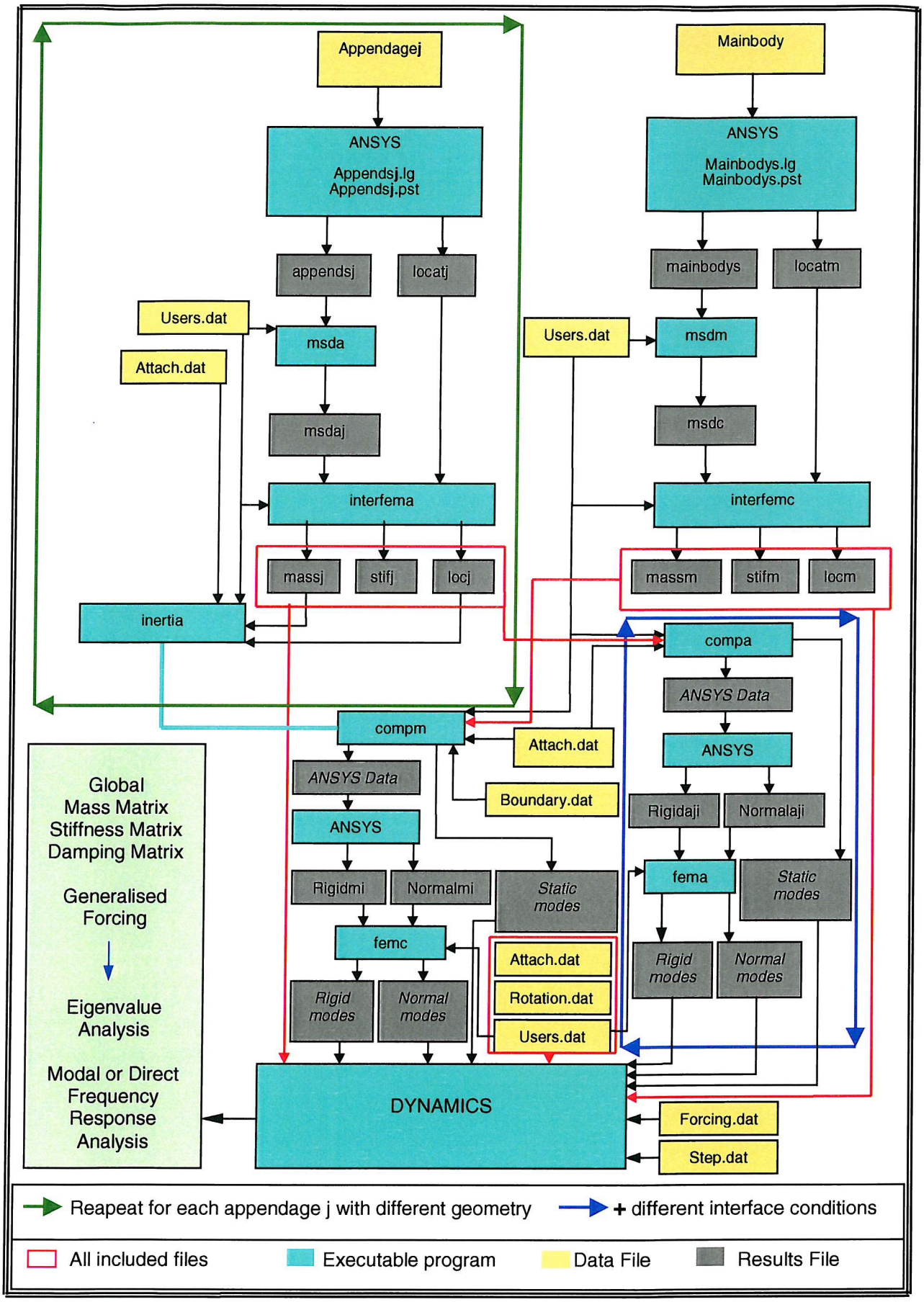

Table VI-1 Network of Programs based on Mathematical Model D

VI-2. Computational Cost

VI-2-1. Background and Assumptions

At this part the concentration is shifted on the computing time related advantages of the proposed method relative to the computer time consumed by the direct application of finite element method for obtaining the eigenvalues and eigenvectors of a structural system. More specifically, it will be demonstrated that it is advantageous to use the proposed method over the more conventional direct finite element approach for formulating and solving the eigenvalue problem. As a direct outcome of the computer time advantage to perform an eigenvalue analysis, it can be easily extrapolated that the proposed method is faster for performing frequency response analysis than the modal, and hence the direct, finite element method.

In general computer time in eigenvalue analysis increases at about the square or cube with an increase in the number of degrees of freedom. Thus, if the structure is divided in a number of components, the separate component mode extraction analyses will consume much less time than the eigenvalue analysis of the whole structure. It is usually the case that the rest of the mathematical operations, ie. substructure assembly to form the reduced order mathematical model and the subsequent eigenvalue analysis of the truncated model, consume only a fraction of the time saved, hence the whole substructuring exercise benefits a large time saving.

Computer time requirements for an eigenvalue analysis depend on a variety of factors. These include amongst others the specific eigenvalue method used, order of the formulated mathematical problem, number of eigenvalues extracted, type of elements and density of the formulated matrices, time spend on each multiply-add loop, time spend to create, store, and read matrices and the memory capabilities of the computer.

Since the purpose is to compare the relative speed of the proposed method to the direct finite element method, not the direct calculation of the CPU time, a few variables can be excluded from the comparative study. In this sense time spend to store and read matrices does not affect the comparison and therefore will be eliminated from the study. Additionally it has been assumed that the computer

capabilities are such as the eigenvalue problem can be solved in core and no spill over effects are present. In fact compromised memory capability is likely to affect only the direct finite element approach, and not the proposed method, since the formulated matrices in the former are of much larger size. Lastly, time spend in generating finite element matrices is linearly proportional to the size of the matrix. Therefore creating a single large matrix or a number of smaller ones should take approximately the same time. The proposed method has a certain advantage over the direct finite element method since matrices of repeated components are not generated a second time. Nevertheless, time spend in creating matrices is not accounted for, although it would be on the benefit of the proposed method. In summary, a number of parameters that would affect the absolute values of computer time estimation are assumed of secondary importance for comparison purposes and therefore eliminated from the analysis.

VI-2-2. Time Estimation of Various Mathematical Operations

VI-2-2-1. Time Estimation for an Eigenvalue Analysis

Eigenvalue extraction has been performed using either the Inverse Power Method or the Givens Method. The former is advantageous to use with large sparse matrices where only a relatively small number of eigenvalues are to be extracted. Matrices derived from finite element method application are indeed large and sparse. The problems associated with the method is poor reliability caused by skipping eigenvalues in cases of high modal density, therefore a Sturm modified version can be used. On the other hand Givens Method is best suited to small order problems and in the cases that the matrices are dense or a large number of eigenvalues needs to be derived. The main problem associated with the method is that it cannot deal with semi-positive definite stiffness matrices, hence it is inappropriate for applications involving articulated multibody structures. This problem can be circumvented with the Modified Givens Method.

The time requirements to perform an eigenvalue analysis using the Inverse Power Method is given by the simplified formula[82] below, leaving aside the secondary variables mentioned in the previous paragraph.

$$\left(T_{eig}\right)_{INV} = k\ E\ \left(\ \tfrac{1}{2}\ N\ C^2 + 20\ N\ C\ \right) \qquad \text{(VI-1)}$$

where

k the time spend for each multiply-add loop

E the number of eigenvalues to be extracted

N the order of the mathematical model

C the number of active columns

The time increases linearly with the number of eigenvalues that need to be extracted, rendering the method expensive if a large number of eigenvalues is expected. Nevertheless, typical finite element matrices are fairly large and sparse, hence N >> C, therefore the method best suited to such problems.

The time required by the Givens method is given by the following simplified formula.[82]

$$\left(T_{eig}\right)_{GIV} = \tfrac{5}{2}\ k\ N^3\left(1+\frac{E}{N}\right) \qquad \text{(VI-2)}$$

The method cannot take advantage of sparse matrices and therefore it is very expensive relative to the Inverse Power Method for dealing with large sparse problems. On the other hand it is ideal for dense matrices such in the cases resulting by application of size truncation methods, and especially so if a large number of eigenvalues are to be extracted. In these cases the number of active columns C is of the same order as the degrees of freedom of the system and the Inverse Power Method looses its advantage over the Givens Method unless only the first few eigenvalues need to be extracted.

Utilising equations (VI-1) and (VI-2) and assuming the number of eigenvalues to be extracted so that E/N is small, the Inverse Power Method is beneficial over the Givens if

$$E < 5\ N^2 / \left(C^2 + 40\ C \right) \qquad \text{(VI-3)}$$

In summary the Inverse Power Method has an advantage over the Givens Method for matrices where N>>C applies, unless a very large number of eigenvalues need to be extracted. For dense matrices, unless a very small number of eigenvalues is needed, Givens is the preferred method. Equation (VI-3) is an excellent way in deciding on the quickest of these methods.

VI-2-2-2. Time Estimation for the Solution of a System of Equations

The time requirement for the solution of a multiple algebraic equation of the form

$$A_{NN} X_{NM} = B_{NM} \qquad \text{(VI-4)}$$

is given by the following simplified equation.[83]

$$T_{alg} = k \left(\tfrac{1}{6}\ C^2\ N + 2\ N\ M\ C \right) \qquad \text{(VI-5)}$$

where the notation is obvious from the previous equations.

The first part of equation (VI-5) is the time required to perform the decomposition of the A_{NM} matrix and the second part is the solution of the multiple algebraic system using a forward and backward substitution.

VI-2-2-3. Time Estimation for Matrix Muitiplication

The time to perform the multiply operation[83]

$$A_{NM} B_{MP} = C_{NP} \qquad \text{(VI-6)}$$

is given by

$$T_{mult} = k\ N\ M\ P\ r \qquad \text{(VI-7)}$$

where

N is the number of rows of the first matrix

M is the number of columns of the first matrix

P is the number of columns of the second matrix

r is a factor accounting for the density of the denser matrix

VI-2-3. Time Requirement for the Global Finite Element Method

The finite element model of a structure is a typical example where is most efficient to utilise the Inverse Power Method. The time required by the direct application of the finite element method is given by

$$\left(T_{eig} \right)_{INV}^{G} = k\ E_g \left(\tfrac{1}{2}\ N_g\ C_g^{\,2} + 20\ N_g\ C_g \right) \qquad \text{(VI-8)}$$

where

k is the time of multiply-add loop

E_g is the number of eigenvalues extracted.

N_g is the order of the global structure mathematical model.

C_g is the number of active columns of the global matrices.

VI-2-4. Time Requirement for the Proposed Method

Although the proposed method (method III) can handle tree configuration multibody systems it has been developed analytically for cluster formation structures. For the purpose of consistence the following analysis refers to a cluster formation multibody structure.

Time Estimation for the Eigenvalue Analysis of Individual Components

The Inverse Power Method has been used to perform eigenvalue analysis on the individual substructures.

$$\left(T_{eigen} \right)_{INV}^{sub} = k \left(E_m \left(0.5\ N_m C_m^2 + 20\ N_m C_m\right) + \sum_{i=1}^{n_{rep}} \left(E_{ai} \left(0.5\ N_{ai} C_{ai}^2 + 20\ N_{ai} C_{ai}\right) \right) \right) \quad \text{(VI-9)}$$

where

E_m is the number of component modes used for the main structure.

N_m is the order of the main structure mathematical model.

C_m is the number of active columns associated to the mainbody

E_{ai} is the number of component modes used for each appended component.

Na_i is the order of the appended component mathematical model.

C_{ai} is the number of active columns associated to each of the appendages.

n_{rep} is the minimum number of appended components that need to be analysed.

Time Estimation for Static Mode Extraction

The time required to extract static modes can be calculated based on equation (VI-5).

$$T_{static} = k \left(\left(0.5\ C_m^2 N_m + 2\ N_m \left(E_{stat}\right)_m C_m\right) + \sum_{i=1}^{n_{rep}} \left(0.5\ C_{ai}^2 N_{ai} + 2\ N_{ai} \left(E_{stat}\right)_{ai} C_{ai}\right) \right) \quad \text{(VI-10)}$$

where the number of static modes for the mainbody and each appe
respectively given as

$$\left(E_{stat}\right)_m = \sum_{i=1}^{n_{app}} \left(dof_{ai}\right) \quad \text{(VI-11)}$$

$$\left(E_{stat}\right)_{ai} = dof_{ai} \qquad \text{(VI-12)}$$

where

n_{app} is the total number of appended substructures.

dof_{ai} is the degree of constraints at each interface.

Time Estimation for the Synthesis of the Global Mass Matrix

The time required to perform all multiplication in order to synthesise the global mass matrix of mathematical model D is based on equation (VI-7), where it has been assumed that the value r equals to unity for all manipulations.

$$\left(T_{mass}\right)_D = T_{mm} + T_{mb} + T_{bb} + T_{\Psi} \qquad \text{(VI-13)}$$

where

$(T_{mass})_D$ is the total time to generate the global mass matrix.

T_{mm} is the time to generate the M_{mm} terms given by equation (V-65).

T_{mb} is the time to generate the M_{mb} terms given by equation (V-66).

T_{bb} is the time to generate the M_{bb} terms given by equation (V-67).

T_{Ψ} is the time to generate the Ψ_j term given by equation (V-64).

The time required for the above operations is as follows

$$T_{mm} = k\left(E_m\ N_m^2 + E_m^2\ N_m + \sum_{l=1}^{n_{rep}}\left(6\ N_m^2 + 6^2 N_m + 6^2 E_{ai} + 6\ E_{ai}^2\right)\right) \qquad \text{(VI-14)}$$

$$T_{bb} = k \left(\sum_{i=1}^{n_{rep}} \left(N_{ai}^2 \; E_{ai} + E_{ai}^2 \; N_{ai} \right) \right) \tag{VI-15}$$

$$T_{mb} = k \left(\sum_{i=1}^{n_{rep}} \left(6 \; N_{ai} \; E_{ai} + 6 \; E_{ai}^2 \right) \right) \tag{VI-16}$$

$$T_{\Psi} = k \left(\sum_{i=1}^{n_{rep}} \left(6 \; N_{ai} \; E_{ai} \right) \right) \tag{VI-17}$$

Time Estimation for the Synthesis of the Stiffness Mass Matrix

The time to generate the global stiffness matrix is given by the next expression and is based on equation (VI-20)

$$\left(T_{stiffness} \right)_D = E_m N_m^2 + E_m^2 N_m + \sum_{i=1}^{n_{rep}} \left(E_{ai} N_{ai}^2 + E_{ai}^2 N_{ai} \right) \tag{VI-18}$$

Time Estimation for the Eigenvalue Analysis of the Reduced Order Global Structural Model

Using equation (VI-3) it can be demonstrated that the eigenvalue analysis is best performed using the Givens Method, unless only the first few eigenvalues are of interest. The time required to perform an eigenvalue analysis on the reduced order mathematical model D can be approximated by the following equation

$$\left(T_{eig} \right)_{GIV}^{Sub} = \frac{5}{2} \; k \; N_r \left(1 + \frac{E_g}{N_r} \right) \tag{VI-19}$$

where

E_g the number of eigenvalues

N_r the order of the reduced mathematical model of the global structure.

The order of the reduced mathematical model is given by the expression

$$N_r = (E_m + E_{ai}) + n_{app} \left(E_{ai} + (E_{stat})_{ai}\right) \quad \text{(VI-20)}$$

For the comparison of the computer time required by the direct finite element approach to perform an eigenvalue analysis relative to the method proposed the Computer Time Ratio parameter **s** is set up and given by the following expression

$$s = (T_{eig})^{G}_{INV} \Big/ \left((T_{eig})^{Sub}_{INV} + (T_{static})_D + (T_{mass})_D + T_{stifness} + (T_{eig})^{Sub}_{GIV} \right) \quad \text{(VI-21)}$$

s>1 implies that the method proposed is faster to the direct element method by as many times as the value of s.

VI-2-5. Case Studies

The time advantage depends on a variety of reasons, but those inherently linked to the structural model are the mathematical size of the entire structure, mathematical size of the individual components, the total number of components, the number of identical components in the system and the number of component modes used for acceptable convergence. It is therefore, the purpose of this section to examine the effects of the above on the computing cost relative to the direct application of the finite element method. For demonstrating clearly the advantages and limitations of the proposed method in terms of computer time a number of case studies have been employed.

VI-2-5-1. Case Study 1

It is the intention to demonstrate the relative computer time required to perform each stage of the proposed method as function of the order of the entire system and compare this to the time consumed by the direct finite element approach for resulting to the eigenvalues of the system.

The structural system modelled, similar to that illustrated in FigureVI-1, is composed of a main platform and eight appended components. The platform carrier is 30 meters long, 1.5 meters high and 1.5 meters wide. It is composed of aluminium hollow beam components positioned appropriately in space in order to create a high stiffness structure. The appendages are may represent solar panels, antennas, booms etc.

In this study case all appendage are considered different to each other. The order of the mathematical model of the main structure is 20% of the degrees of freedom of the structural system and the order of each appendage approximately 10%. The linear elastic deformation of the main structure has been modelled with 30 dynamic modes and for each appendage with 10 dynamic modes. The dynamic modes have been complemented with 6 static modes for each interface node. It has been assumed that static correction modes have been used to model all components. 30 eigenvalues have been obtained from both the finite element model and the reduced size model.

For the number of active columns to the order of the finite element matrices has been assumed that

$$\frac{C_g}{N_g} = \frac{C_m}{N_m} = \frac{C_{ai}}{N_{ai}} = 0.02$$

corresponding to sparse matrices in all cases.

The computing time dependency on the degrees of freedom of the system is illustrated in Figure VI-2. From Figure VI-2 and the formulas developed several conclusions have been drawn.

i. The larger the number of degrees of freedom of the system the higher the time benefits of the proposed method relative to the direct finite element application.

ii. If the total number of the degrees of freedom of the entire structural system is relatively small there may be no advantage in pursuing a substructuring approach. In the particular example this is true if the order of the system is lower than approximately 1400. This limitation has been anticipated for a variety of reasons. Most importantly any substructuring exercise ceases to be beneficial if the generalised modal coordinates tend to be close in number to the physical degrees of freedom of the substructure. In the particular example the physical degrees of freedom have been varied but the number of component modes stayed unchanged.

iii. It is difficult to generalise the findings of this study case for any possible structural configuration for assessing the exact relative time that the various stages of the proposed method require for completion. Relative time depends on various parameters such as the order of the system, number of component modes included, total number of components, number of identical components, density of the formulated matrices, number of eigenmodes extracted etc. In general though, it can be concluded, with parallel examination of the formulas developed, that the most time-consuming stage, within the proposed method, is the process of synthesising the equations of motion and the extraction of the eigenmodes for all the individual components. The extraction of static modes and the eigenvalue analysis of the reduced order global model occupy the least time. This is not to imply that the static modes contribute only minimally to the computer time requirements of the proposed method. At the synthesis stage and the final eigenvalue analysis, each static mode included results to the same time penalty as each dynamic mode.

iv. More specifically, in the particular example the synthesis stage not only is the slowest, but also occupies over 90% of the total time of the substructuring exercise. This can be attributed to a number of reasons:

   a. The number of component modes used is very large, due to the inclusion of static modes for every component. In practice this is not always necessary.
   b. The factor accounting for the density of the matrices in the multiplications involved in the synthesis process has been considered equal to unity. This not always the case and much smaller values can be achieved in reality, accelerating the process by far.
   c. The finite element matrices of the individual components have been assumed sparse and the number of the extracted normal modes fairly low. Increasing the density of the matrices and the number of normal modes extracted the eigenvalue analysis of the individual components may be as computationally time intensive as the synthesis process.

v. This example was purposely designed to offer an advantage to the direct finite element approach. The finite element matrices of the complete structure have been assumed very sparse and a small number of modes have been extracted. Nevertheless, it has been demonstrated that even in the case of a large number of component modes, dissimilar substructures and least favourable matrix multiplications, a substructuring method is in general more computationally efficient to the direct application of the finite element method.

VI-2-5-2. Example Case 2

The purpose of the second example case is to demonstrate the time benefits of the proposed method over the direct finite element method as the number of individual component increases.

In the first case the structure is modelled with eight appended components all assumed to be different to each other. The order of the mathematical model of the

main structure is 20% of the degrees of freedom of the structural system and the order of each appendage approximately 10% of the total.

In the second case the same structure is modelled, with the difference that two of the appendages are included in the mainbody model. The rest six appended components have all been considered different to each other. The order of the mathematical model of the main structure is 40% of the degrees of freedom of the structural system and the order of each of the six appendages approximately 10%.

In the third and fourth cases the same structural models are considered as in first and second case respectively with the difference that the appended components are considered identical.

The last case considers a different structure, where the mainbody occupies 20% of the degrees of freedom of the total system and six dissimilar appendages share the remaining degrees of freedom equally.

For all cases the linear elastic deformation of main structure has been modelled with 30 dynamic modes and for each appendage with 10 dynamic modes. It has been assumed that static correction modes have been used to model all components as in the previous example case. Moreover the ratio of active columns to the order of the components is as detailed in the previous example case.

In Figure VI-3, the Computer Time Ratio s of the proposed method relative to the direct finite element method has been illustrated as function of the total degrees of freedom of the structure. The conclusions of this example case are the listed below.

i. The number of identical component is a crucial factor and the relative speed of the proposed method increases as the number of identical components increase. By examination of the formulas presented it is apparent that the number of identical components affects the time of every stage in the substructuring process other than the final eigenvalue extraction.

ii. The effect of the number of appendages on the computing time of the proposed method is less straightforward. Figure VI-3 demonstrates large

differences in computer speed between two structures with the same number of dissimilar appendages and the same number of total degrees of freedom. The difference between the two cases can be traced in the fact that the distribution of the degrees of freedom between the substructures is much more uniform in the faster of the processes. In fact, uniform distribution results in reduced computer time in all stages of the substructuring analysis other than the final eigenvalue extraction, according to the formulas presented. Moreover, the overall speed performance of this particular case with six appendages is even better than for the case of eight appended components. Since the computer time requirements for the analysis of the mainbody is essentially the same between the two cases, the conclusion is that the uniform distribution of component degrees of freedom can be more important factor for the speed of the substructuring method than the total number of components. This will depend largely on the number of total components, identical components, and component modes. In general though, it is expected that the relative speed of the method should increase as the number of components increase.

iii. In general, the detailed study of the speed of a substructuring method as a function of the number of substructures and the distribution of degrees of freedom can pose an interesting problem. For the structural systems studied in this work such an investigation is surplus since the number and size of the components is predetermined. The particular discussion has been presented only in order to demonstrate that even in the cases that a small number of substructures is present it may still be beneficial to pursue a substructuring method.

iv. For a structure with 'well distributed' degrees of freedom and a large number of appendages a tenfold speed difference between the proposed method and the direct finite element approach may well be a conservative estimate.

VI-2-5-3. Example Case 3

It has been concluded from the first example case that the computer time required for the extraction of normal modes of vibration for the individual components is much higher than for the calculation of static modes. Moreover, the number of dynamic modes can be directly truncated from the component mode set using a cut-off criterion as opposed to the static modes. In any case it is important to assess the benefits of the proposed method relative to the direct application of the finite element method as the number of normal modes increases.

As in the previous cases the structure has been modelled with eight appended components all assumed to be different to each other. The order of the mathematical model of the main structure is 20% of the degrees of freedom of the structural system and the order of each appendage approximately 10%. The ratio of the active columns to the order of the components remains small as in the previous cases.

The normal modes extracted have been varied for both the main structure and each of the appendages. The component mode sets have been complemented with 6 static modes for each interface node. It has been assumed that static correction modes have been used to model all components.

Two cases have been examined. In the first case the total degrees of freedom of the system have been set to 2000 and in the second case to 10000. The speed ratio s for both cases has been illustrated in Figure VI-4. The conclusions of this example case are listed below.

i. Increasing the number of component dynamic modes is crucial to the speed performance of the proposed method relative to the direct finite element method. This implies that serious consideration should be exercised on the number of dynamic modes that need to retained in the analysis.

ii. As anticipated the smaller the order of the system the more important it is to reduce the number of dynamic modes to the bare minimum if the benefits of the proposed method are to be retained.

As discussed previously the speed reduction due to inclusion of static modes is not to be underestimated, since both the synthesis and final eigenvalue analysis are affected by the static mode number as much as by the number of normal modes. It is therefore wise to understand where the inclusion of static modes is necessary and where can be omitted.

VI-2-5-4. Example Case 4

Even in the 'extreme' case that one complete iteration of the proposed method may not be beneficial relative to the direct finite element method for reasons covered in the previous cases, it may still be a gain if only a part of the particular analysis were to be executed for a number of iterations.

Moreover, in a lot of applications a particular component or number of components need to de redesigned whereas the rest remain unchanged. This implies that in the substructuring approach only a part of the process needs to be re-executed. If the particular components are to be redesigned a number of times, the time benefited from one application will be gained multiple times. Perhaps an optimisation loop around only a few components is an example that most has to be benefited.

Other cases may involve an articulated multibody system where a study of the system in a number of configurations is of interest. Reorientation of components in space can be accomplished by executing only the synthesis process of the proposed method and an eigenvalue analysis of the reduced order system. Similar would be the cases of component repositioning relative to the main structure.

To demonstrate the benefits of utilising the proposed method for partial redesigning of the system and for reorientation or general repositioning purposes, a structural system composed of eight appendages has been selected. The mainbody occupies the 60% of the total degrees of freedom and the rest of the degrees of freedom are divided equally between the remaining substructures. As in the previous examples, the linear elastic deformation of main structure has been modelled with 30 dynamic modes and for each appendage with 10 dynamic modes. It has been assumed that

static correction modes have been used to model all components as in the previous example case. Moreover the ratio of active columns to the order of the components is as detailed in the previous example case.

Two cases have been examined. In the first case only two of the appended components have undergone design changes and the relative speed of the proposed method to the direct application of the finite element method has been assessed as a function of the total degrees of freedom of the system. In the second case a reorientation study of all the appended components has been performed. As a control study a complete substructuring exercise has also been performed. The results of the studies have been illustrated in Figure VI-5. The following conclusions have been drawn.

i. As anticipated, the complete application of the proposed method is not faster than the direct application of the finite element method even for a large number of degrees of freedom.

ii. For each redesign process of the two components time has been gained relative to the direct finite element approach. Even if the gains are not enormous repeating the process a large number of times, as in the case of an optimisation routine, a lot has to be profited.

iii. It is obvious that even in this 'extreme' example case a reorientation exercise is quicker using the proposed method. Maybe in the first execution of the proposed method some time is lost relative to the direct finite element approach but the time lost will be made up by the time gained in every reorientation exercise.

VI-2-6. Conclusions on the Computational Cost

It has to be noted that in all comparisons the 'advantage' has been offered to the direct finite element method in order not to bias results in favour the proposed method. These include the inclusion of static modes for all components, a very small active column ratio to the order of the system, a density factor of unity involving all

multiplications performed in the proposed method, a small number of appendages, memory issues etc.

The benefits of the proposed method over the direct finite element application on the computer time requirements are summarised bellow.

i. The speed of the proposed method increases relative to the direct finite element approach as

- The number of degrees of freedom of the structural system increases.
- The distribution of the degrees of freedom is more uniform between the components.
- The number of identical components increases.
- The number of component increases.
- The number of component modes per component decrease.

ii. Even in cases that a single complete application of the proposed method is not beneficial in computational time, it may still be advantageous to utilise the proposed method for a small number of component design iterations, as well as for component reorientation and repositioning studies.

iii. The analyst should exercise judgement on the number of dynamic modes retained in the analysis since these have a pronounced effect on the speed of the proposed method.

iv. In general there is a lot to be gained in computer time terms by the application of the proposed method. In a typical multibody structure, as the ones proposed for future space missions, a tenfold of speed gain seems to be a conservative target to achieve for eigenvalue analysis purposes.

v. If there is a time benefit in eigenvalue analysis, it is straightforward to conclude that the same would apply for a frequency response analysis relative to the direct or modal finite element method frequency response analysis.

VI-3. Conclusions on Computational Implementation

i. The network of programs has been based on mathematical model D therefore any complexity peripheral formation multibody structure can be analysed.

ii. The final deliverables of the network are the eigenvalues of the structural system and the eigenvectors in modal or physical space. Additionally, physical displacement, velocity and acceleration of any point on the structure can be derived as a function of the forcing frequency using either direct or modal frequency response analysis.

iii. The network is interfaced with the commercial finite element package ANSYS. Components of any complexity can be modelled using the finite element method.

iv. Any of the three articulation axes at the interface between the components can be free or locked, thus any non-translating joint configuration can be modelled.

v. Identical components are analysed only once reducing the computational time to a great extend.

vi. Any type of component mode set can be imported. Already 5 component mode sets have been implemented.

vii. Analyst input is minimal since the network is controlled by only 5 user's data files. The analyst can select the kind of component modes to be implemented for each component and the number of normal modes to be retained in the analysis, thus has control over the computer time required and the accuracy of results. Moreover, the analyst can easily specify the orientation and the location of the appendages, the constraints at the interfaces between components and the external boundary constraints on the main platform carrier.

viii. The structure of the network is modular and in many cases only part of the network needs to be executed to obtain solutions, thus reducing computational cost.

ix. The network needs low memory requirements to perform, unlike the direct finite element approach that models the entire structure as a single entity, hence large-scale systems can be analysed with limited computer resources, and computer speed accelerated.

x. The network has been validated over a large range of cases and is therefore reliable.

xi. In general there is a lot to be gained in computer time terms by the application of the proposed method. In a typical multibody structure, as the ones proposed for future missions in space, a tenfold of speed gain seems to be a conservative target to achieve for eigenvalue analysis purposes.

xii. The speed of the method relative to the global finite element method increases as the number of the total degrees of freedom increase, distribution of component degrees of freedom is more uniform, number of components and identical components increase and component mode number decreases.

xiii. If there is a time benefit in eigenvalue analysis, it is straightforward to conclude that the same would apply for a frequency response analysis relative to the direct or modal finite element method frequency response analysis.

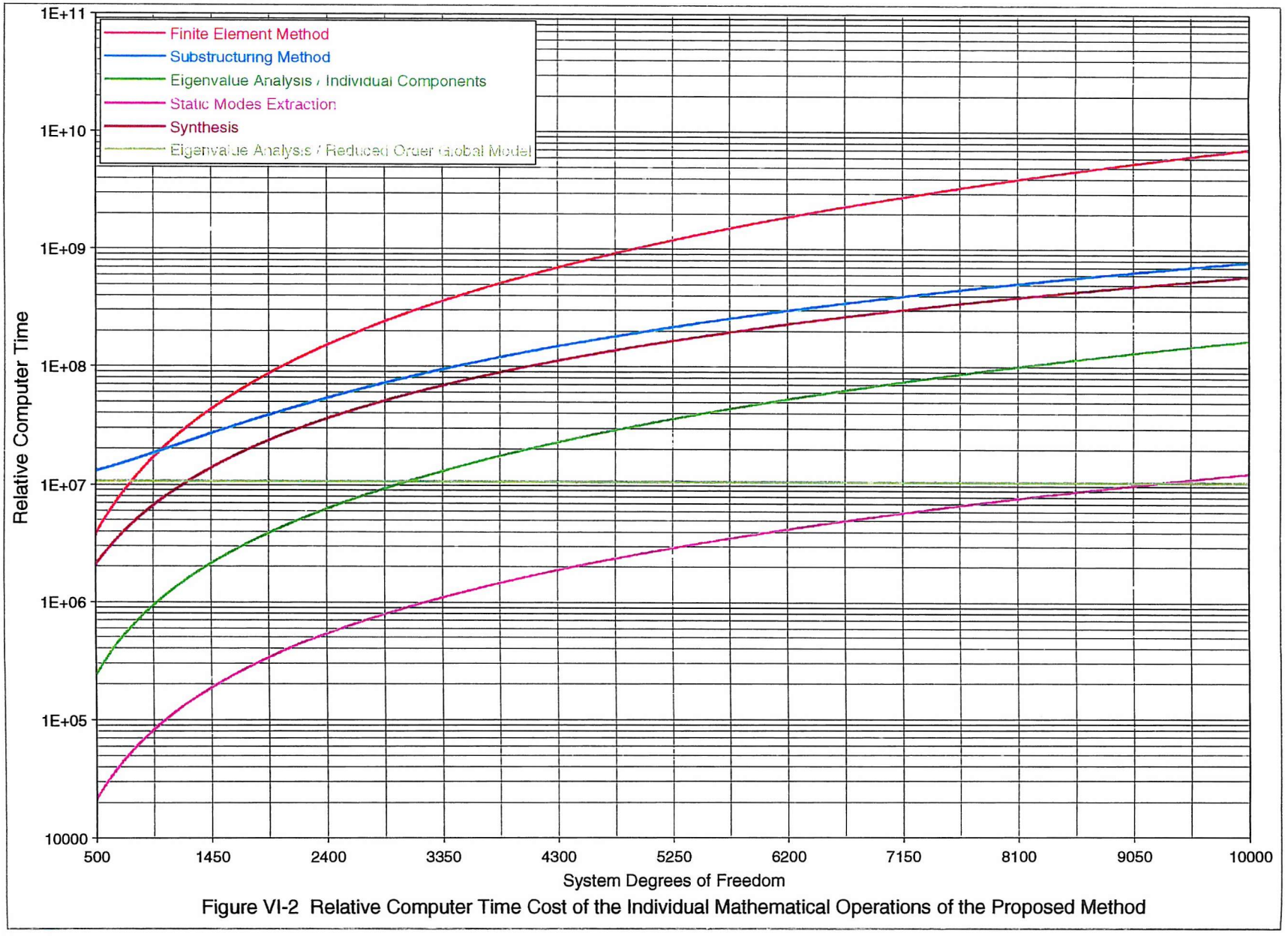

Figure VI-2 Relative Computer Time Cost of the Individual Mathematical Operations of the Proposed Method

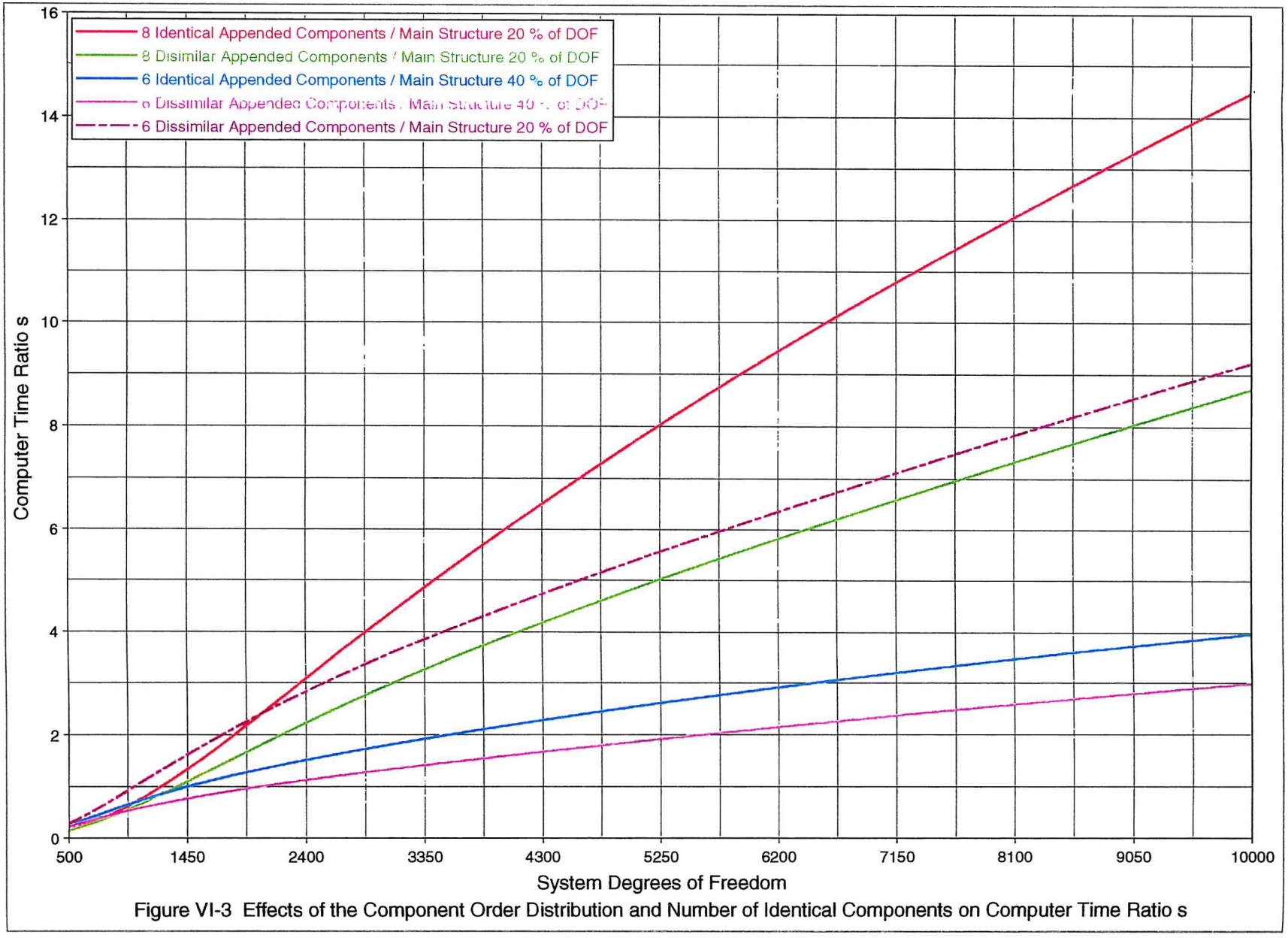

Figure VI-3 Effects of the Component Order Distribution and Number of Identical Components on Computer Time Ratio s

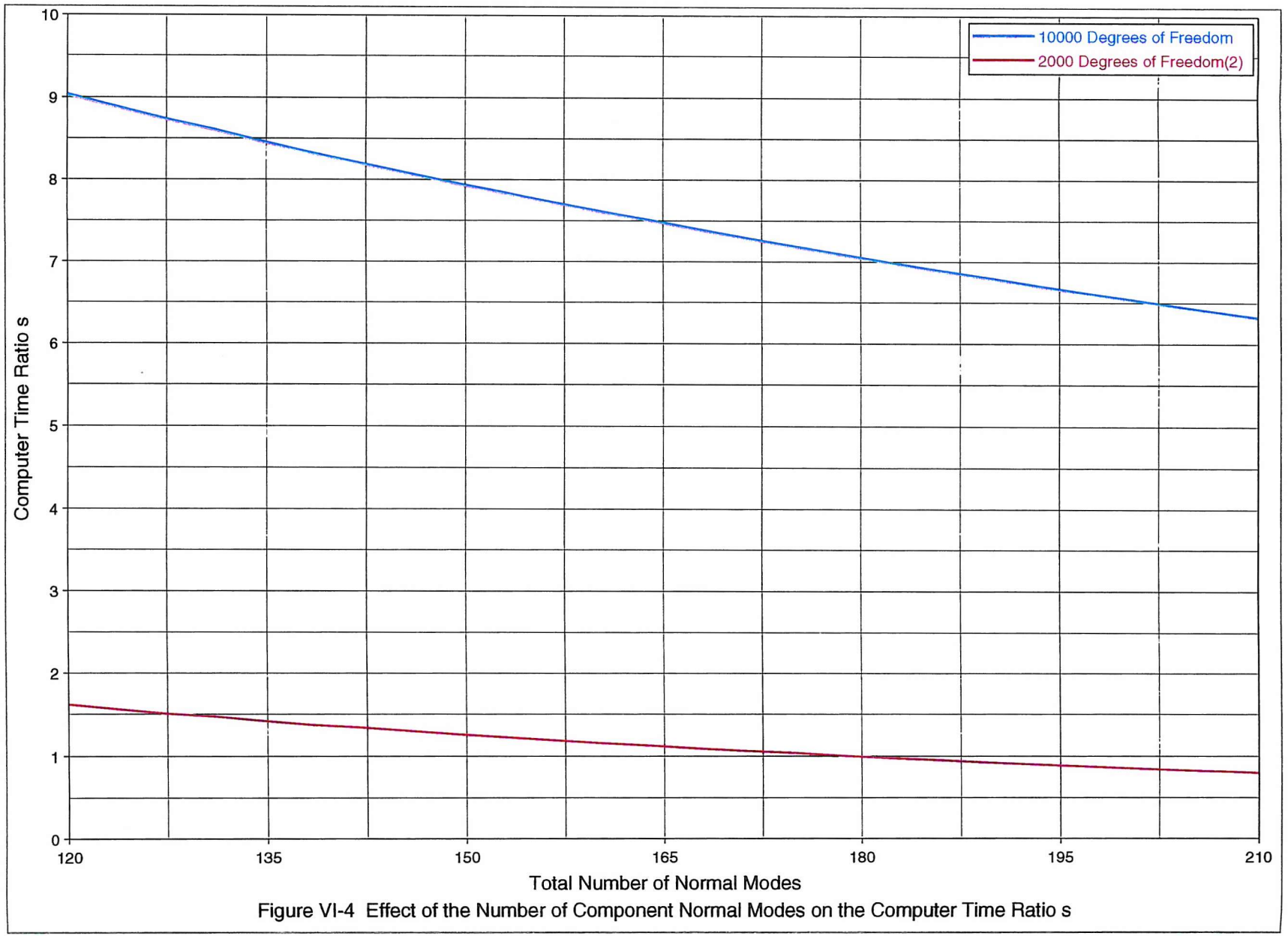

Figure VI-4 Effect of the Number of Component Normal Modes on the Computer Time Ratio s

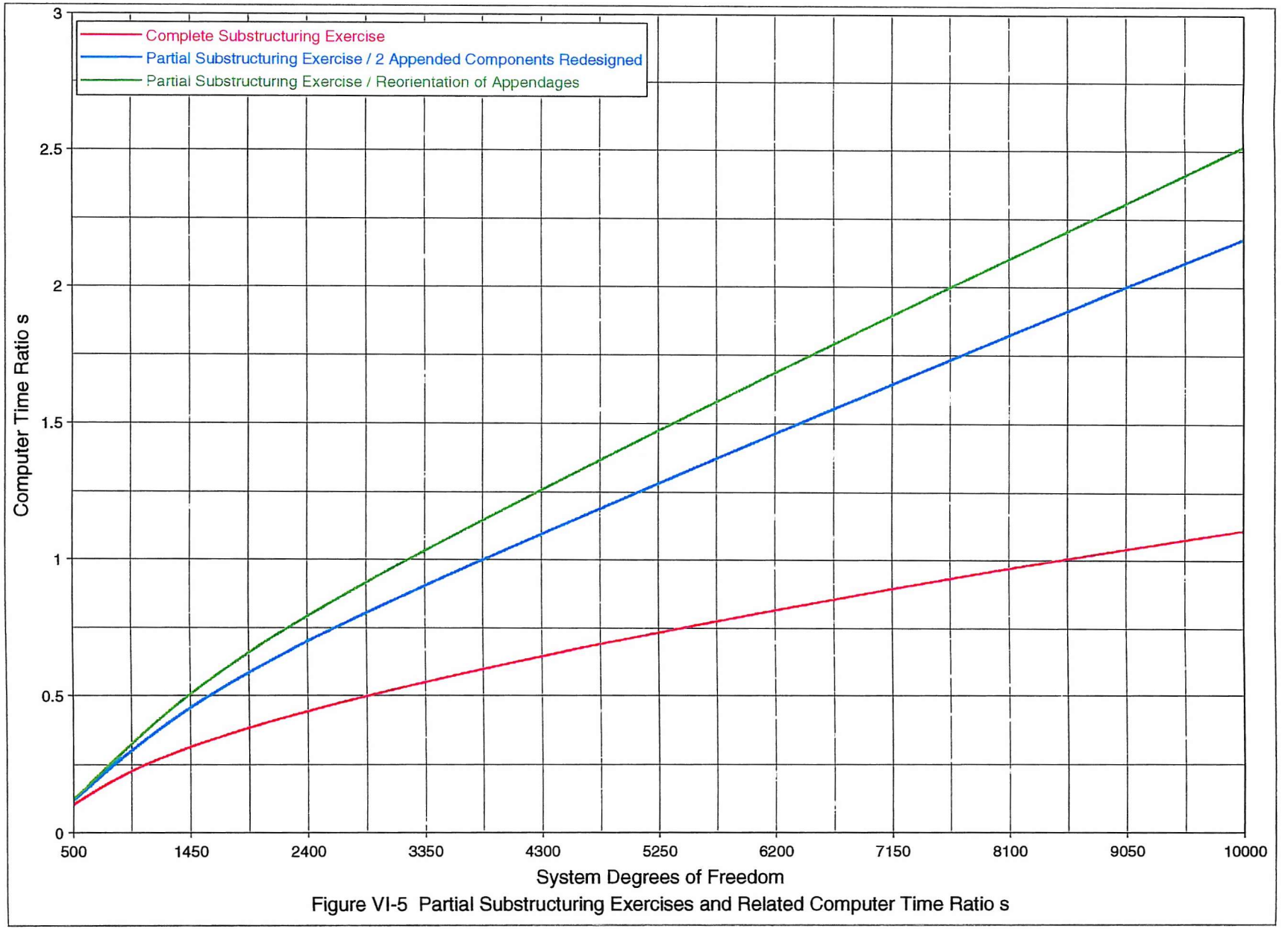

Figure VI-5 Partial Substructuring Exercises and Related Computer Time Ratio s

VII Results

VII-1. Prologue

The natural frequencies of peripheral formation structural configurations have been derived utilising several component mode sets, and results obtained have been compared to those derived by modelling the entire structure using the finite element method. Moreover, frequency response analysis studies have been undertaken. Several conclusions have been reached for both the efficiency of various component mode sets and modelling practices for large flexible structures in space.

The modal frequency response analysis is the most efficient way, within the framework of this work, for demonstrating the accuracy of the global modes derived by using the proposed method. Global finite element frequency response analysis has been used as a benchmark. Cross mode orthogonality methods could also be used for comparing the global modes derived by the proposed method to those derived from direct application of the finite element method. Nevertheless, such an exercise would be difficult to perform due to dimensionality differences between the finite element model and model resulting for the proposed method.

This chapter includes five main case studies. The purpose of the first case study is to demonstrate that large flexible components, such as space-frame platforms, exhibit high modal density and local deformation at the component attachments. In the second case study a structural parametric study is undertaken in order to establish a general criterion which may determine the degree of the local deformation at component interfaces. The third, fourth and fifth case studies compare the effectiveness of several kinds of component mode sets in capturing the deformation of complex components, and thus modelling with accuracy the dynamics of flexible structural systems.

VII-2. Localised Deformation (Case Study I)

A typical example of a platform in space is illustrated in Figure VII-1. This space-frame beam-like lightweight platform is very similar in design to space-frame structures that have been used, amongst others, by NASA for theoretical and experimental research on integrated structure/control optimisation[77,78]. The platform carrier is 30 meters long, 1.5 meters high and 1.5 meters wide. It is composed of aluminium hollow beam components positioned appropriately in space in order to create a high stiffness structure. The total mass of the structure, including the control hardware, does not exceed 300 Kg.

In this case study, the platform is assumed to have docked on a much larger orbiting structure, such as a space station, for servicing purposes. The space-frame platform has been modelled as clamped at the nodal points that belong to the plane where the platform attaches to the docking station (Figure VII-1). A symmetric, uniform Timoshenko beam, clamped at one end and with the first few natural frequencies close to those of the space-frame platform has been devised for comparative studies. The natural frequencies of the space-frame and the equivalent beam structure are shown in Tables VII-1,2 respectively.

Both structures are loaded with mass first and then with mass and rotary inertia at their free ends, at a nodal point at the centre of their respective geometric cross-sections. In order to examine the extent of the localised deformation at the points where the rigid payload attaches to the structure, the deformation field for both the space-frame and the beam equivalent are modelled using free-interface normal modes. Free-interface modes cannot by nature capture the deformation effect of the attached payload on the structure, so they are ideal for this study. A number of free-interface normal modes have been imported into the generic mathematical model and the 30 first eigenfrequencies have been derived for several values of mass and rotary inertia. For each loading case the results have been compared to the eigenfrequencies obtained by modelling both structural systems using the finite element method. For this purpose the first case study has been further divided in several example cases and remarks for each example have been produced. The conclusions of the first case study follow the example cases.

VII-2-1. Example Case 1

Both the space-frame and the beam structure have been loaded with concentrated mass at their free ends. The mass is 16 Kg, which is only a small payload to be carried by the structure and in reality this may represent the mass of a small servo-motor. The first 30 natural frequencies of the loaded beam structure and space-frame have been derived using the finite element method and compared to the natural frequencies obtained using 40 free-interface modes. The results are shown in Tables VII-3,4 respectively. The following remarks can be made:

i. In general, there is a very good agreement in the results between the finite element method and the free-interface method in the case of the beam, as demonstrated in Table VII-3.

ii. The largest differences observed, modes 2,15 etc. (Table VII-3), correspond to axial modes, but these are still small. This is an anticipated result since in the spectrum of the 40 free-interface normal modes employed there is only a very small amount of axial beam modes (Table VII-2), thus convergence is difficult.

iii. The torsional modes of the loaded beam should be the same to the torsional modes of the unloaded beam, since no rotary inertia has been added on the tip of the beam. Extremely small discrepancies between the finite element method and the free-interface results (Table VII-3: modes 3,13 etc.) are mainly due to numerical errors associated with matrix multiplications in mathematical model D and possible rounding errors in the results as presented by the commercial finite element method package ANSYS.

iv. Comparing the frequencies in Tables VII-3,4 to Tables VII-2,1 respectively, another observation would be that the space-frame structure is generally less affected by the inclusion of the mass than the beam structure.

v. For the case of the space-frame, Table VII-4, there is generally a good agreement in the results obtained by the finite element method and the free-interface method.

vi. The highest discrepancy is noted in the case of the axial modes 5, 11 etc, Table VII-4. This discrepancy is fairly considerable for mode 5 (~ 5%), implying at there may be a localised out of plane bending deformation of the cross members supporting the mass. This argument is also supported by the high drop in frequency of the first axial mode in the loaded case compared to the unloaded case (loaded case: mode 5, unloaded case: mode 10). Such high discrepancy is not noted for the bending modes since the cross members supporting the mass are fairly stiff in compression – extension.

VII-2-2. Example Case 2

Exactly the same structural system as previously is presented. In this example case 50 free-interface modes are included. The results are shown in Table VII-5 for the beam and in Table VII-6 for the space-frame. The following remarks can be made:

i. By using a higher number of modes, the difference between the finite element method and the free-interface method is decreased for both structures and for all modes (Tables VII-5,6 versus Tables VII-3,4). This is an anticipated result, since free-interface normal modes belong to a complete set.

ii. Although, by adding 10 extra modes, in the case of the beam structure the difference between the finite element method and the free-interface method has been reduced dramatically for the case of the axial modes, this is not true in the case of the space-frame structure. The improvement on the 1st axial mode (mode 5) in the case of the space-frame is extremely small (Tables VII-6,4), supporting the argument regarding the local bending deformation of the supporting cross-members. The large number of free-interface modes cannot effectively capture the local deformation of the cross-members.

VII-2-3. Example Case 3

This example is similar to the previous one other than that the attached mass has been increased by a fivefold. The mass is 80 Kg, and in reality may represent the mass of a control hardware system. 50 free-interface normal modes have been used and the 30 first natural frequencies obtained have been compared to results from the finite element method. Tables VII-7,8 correspond to the beam and space-frame structures respectively. The following comments can be made:

i. Generally the difference between the finite element method and free-interface method has been increased for both the beam and space-frame (due to extra mass), but are still fairly small, although the mass has been increased by 5 times.

ii. The highest differences are observed in the cases of the axial modes.

iii. The effect of the much larger attached mass causes localised deformation at the attachment points of the space-frame, but the error is not that much more pronounced than in the case of the smaller mass (Tables VII-5,6).

VII-2-4. Example Case 4

In this example the mass is reduced at its initial value of 16 Kg and a small amount of rotary inertia is added at the tip of both the beam and space-frame structures. The rotary inertia has the same value of 100 Kg-m^2 in all three directions. This load may represent in reality a small lightweight solar panel. 50 free-interface normal modes are included to describe the deformation of the beam and space-frame. The first 30 natural frequencies of the beam and space-frame are obtained and compared to those derived by the finite element method, in Tables VII-9,10 respectively. The following comments can be made:

i. Comparing Tables VII-5,7,9 corresponding to the beam structure, we notice that the effect of the small rotary inertia is much stronger than the effect of the large mass attached.

ii. The difference between the finite element method and the free-interface method for the calculation of the mass and rotary inertia loaded beam frequencies is not significant even in the case of inertia attached. This implies that there is no localised deformation as such associated to the beam structure.

iii. Unlike the beam structure, in the case of the space-frame there is a enormous difference between the finite element method and the free-interface method when rotary inertia is added (difference ~ 200%). This strongly suggests that there is high local deformation of the supporting cross-members in torsion and bending in and out of plane.

VII-2-5. Example Case 5

In order to support further the argument for localised deformation at the attachment points of a space-frame structure, in this example the flexible load-supporting cross-members have been substituted by rigid ones. The attached mass is 16 Kg and rotary inertia 100 Kg-m^2 for all three axes, as in the previous example. The natural frequencies of the unloaded space-frame have been calculated using the finite element method and are shown in Table VII-11. 50 free-interface normal modes are used to derive the natural frequencies of the loaded space frame. The 30 first natural frequencies of the system have been compared to the frequencies derived using the finite element method and are shown in Table VII-12. The following remarks can be made:

i. The natural frequencies of the unloaded space-frame with rigid cross-members (Table VII-11) are very close to the natural frequencies of the space-frame with flexible cross-members (Table VII-1). This implies that the rigid cross-members do not stiffen the original structure at any degree.

ii. Using rigid load-supporting cross-members, the difference of the natural frequencies obtained by the finite element method to those resulting form the free-interface method is small, and comparable to the difference observed in the beam case (Table VII-9).

iii. Since the rigid cross-members do not stiffen the unloaded structure, the reduction in the difference of the natural frequencies between the finite element method and the free-interface method (compared to the difference with flexible cross-members) suggests that the previous extreme differences were due to localised deformation at the mass attachment.

iv. Using rigid load-supporting cross-members the localised deformation at the attachments has been diminished.

VII-2-6. Conclusions of Case Study I

i. It was shown that large lightweight structures in space, such as space-frame components, may exhibit high modal density and, in cases, strong local deformation near the attachments of appended payloads.

ii. More conventional structural components such as beams, plates, cylinders etc do not exhibit localised deformation as such at the attachments to appended payload. Using a higher amount of modes, accepted convergence can be easily, however not effectively, accomplished. However, this may not be the case for components that may exhibit localised deformation when loaded, such as the large flexible space-frame structures. For these components even a large number of interface modes may not suffice to offer acceptable convergence.

iii. Modelling a complex geometry lightweight components, such as a space-frame platform, with an equivalent beam, plate, cylinder etc. may be practical for reducing the size of the formulated problem, but erroneous results may be obtained if payloads would be attached on the component.

iv. Approximating the deformation field of structural components that may exhibit local deformation using free-interface normal modes should be avoided, since they may lead to wrong results, even in the lower frequency range. For more conventional components, free-interface normal mode representation of the deformation may be an option, but a large amount of modes may be needed for convergence.

VII-3. Criterion for the Prediction of Local Deformation (Case Study II)

This study case is concerned with the investigation of the parameters which affect the degree of the local deformation of a space-frame component at its attachments to the other components in order to establish a general criterion. For this purpose a structural parametric study has been undertaken. In this case study the space-frame platform of Figure VII-1 has been loaded with two solar panels, as shown in Figure VII-2. The solar panels have been modelled in this case study as beam-like appendages. The structural system is considered free in space.

The obvious structural parameters to be manipulated are the inertia and stiffness characteristics of the appendages and the stiffness of the platform carrier. Both the inertia and stiffness characteristics of any structural component are depended on the geometric characteristics of the component. In order to manipulate the inertia of the components without affecting the stiffness of the components and vice versa, the geometric characteristic of all structural components remain unchanged throughout this case study. The inertia of the appendages will be changed by altering the material density, and the stiffness of the components by altering the material stiffness. The location and orientation of the appendages remain fixed throughout the study.

Free-interface normal modes will be used to indicate the local deformation effects of the space-frame platform. The appendage deformation is approximated by fixed-interface normal modes. For every example case 30 free-interface normal modes for the platform and 12 fixed-interface normal modes for each of the appendages have been included in the mathematical model. The number of modes for both the platform and the appendages are enough for modelling the structural system in the frequency range of interest. The first 30 natural frequencies obtained for each example case have been compared to the results from application of the finite element method. The conclusions of the case study along with the comparative Table VII-18 follow the example cases.

VII-3-1. Example Case 1

For investigating the effect of the appendage stiffness on the local deformation at the attachments of the space-frame platform, 3 values of material stiffness for the appendages are chosen. The material stiffness of the appendages drops by a tenfold in each case, E=7.2E10N/m^2, E=7.2E9N/m^2, E=7.2E8N/m^2. The material density of the appendages is fixed in all three cases at the value of p=270Kg/m^3. The material stiffness and density of the platform are also fixed in all three cases at the values of E=7.2E10N/m^2 and p=2700Kg/m^3 respectively. Using the comparative results in Tables VII-13,14,15 the following remarks can be made:

i. Decreasing the stiffness of the appended payload, the local deformation of the platform at the attachments decreases. A physical explanation to the this observation can be offered; appendages with low stiffness 'give in' more and deform less the space-frame.

ii. For the case of very low appendage stiffness, E=7.2E8N/m^2, the space-frame free-interface normal modes give fairly good results, implying that the local deformation of the platform at the attachments to the appendages is fairly low.

VII-3-2. Example Case 2

If the decrease of the stiffness of the appended payload reduces the deformation of the platform at the attachments, so should the increase of the stiffness of the space-frame. To demonstrate the above, in the current example the material stiffness of the space-frame platform has been increased by a tenfold, whereas its material density has remained unchanged (E=7.2E11N/m^2 and 2700Kg/m^3). The appendages have values of E=7.2E10N/m^2 and 270Kg/m. The results are shown in Table VII-16. The following remarks can be made:

i. Tables VII-13,16 show that by increasing the material stiffness of the platform the local deformation decreases.

ii. Although the natural frequencies of the structural system in Table VII-14 are very different to the frequencies in Table VII-16, the difference between the finite element method and the free-interface method is almost exactly the same in the two cases for every mode. This implies that the local deformation of the space-frame may be related to the relative stiffness of the attached components.

iii. Extending the above observation one may assume that there may be a relationship between the natural frequencies of the platform and the appendages that determines the degree of the local deformation at the attachments.

VII-3-3. Example Case 3

The aim of this example is dual. Firstly to investigate the effect of the increase of the inertia of the appendages on the local deformation of the space-frame at the attachments. Secondly to establish if there is a relationship between the natural frequencies of the platform and the natural frequencies of the appendages that may determine the degree of the local deformation. For this purpose, the material density and material stiffness of the appendage are set at p=2700 Kg/m^3 and E=7.2E10N/m^2 respectively. The material density and material stiffness of the platform are set at p=2700 Kg/m^3 and E=7.2E10N/m^2. If there is a straight relationship between the natural frequencies of the appendages and the platform that determines the local deformation at the attachment of the components, then the difference in the results between the finite element method and the free-interface method for this example should be the same as in Table VII-14. The example case that corresponds to Table VII-14 involves a platform with the same characteristics as the current example case and appendage characteristics of p=270 Kg/m^3 and E=7.2E9N/m^2, thus the same appendage natural frequencies as the current example. The results of the current example are found in Table VII-17. The following comments apply:

i. Comparing the results presented in Tables VII-14,17 we notice that the local deformation is higher in Table VII-17 than in Table VII-14, whereas the natural frequencies of all components are the same in both cases. This

suggests that there is not a straight relationship between the natural frequencies of the appended payload and the natural frequencies of the platform that may determine the degree of the local deformation at the attachments.

ii. The difference between the finite element method and the free-interface method, which determines the degree of the local deformation at the attachments of the main platform, is of the same order as in Table VII-13. The example case that corresponds to Table VII-13 involves a platform with the same characteristics as the current example case and appendage characteristics of p=270 Kg/m^3 and E=7.2E10N/m^2, i.e. appendage with much lower inertia characteristics, and therefore of much higher natural frequencies. This suggests that the effect of increasing the inertia of the appendage is not readily obvious and it seems it may affect only slightly the local deformation of the platform at the attachments. This also suggests that there is not a straight relationship between the natural frequencies of the appended payload and the natural frequencies of the platform that may determine the degree of the local deformation at the attachments.

VII-3-4. Criterion for Local Deformation Prediction

The results regarding the degree of the local deformation of the platform along with the material stiffness and material density of the space-frame and the appendages for the example cases 1,2,3 of the current case study are shown in the collective Table VII-18.

The objective is to establish a general criterion that determines the degree of the local deformation of the carrier platform at the attachments to the appended payload. For this purpose, the natural frequencies of the appendages involved in all previous examples are calculated using the finite element method and shown in Tables VII-19,20,21. The natural frequencies of the platform loaded the inertia of the associated appendages are also calculated and shown in Tables VII-22,23,24. The correspondence of the tables associated to the natural frequencies of the

components for each structural system to the Tables VII-13,14,15,16,17, that determine the degree of the local deformation for each system, is as follows:

Tables VII-19,22 correspond to the structural system associated to Table VII-13; high deformation
Tables VII-20,22 correspond to the structural system associated to Table VII-14; medium deformation
Tables VII-21,22 correspond to the structural system associated to Table VII-15; low deformation
Tables VII-19,23 correspond to the structural system associated to Table VII-16; medium deformation
Tables VII-20,24 correspond to the structural system associated to Table VII-17; high deformation

Comparing for each case the natural frequencies of the platform loaded with the inertia of the appendages to the natural frequencies of the appendages and the associated local deformation of the platform the following remarks can be made:

i. The higher the natural frequencies of the loaded platform relative to the natural frequencies of the appendage, the lower the local deformation of the platform at the attachments. This criterion applies for all example cases.

ii. More specifically, for the particular structural configuration, the higher the fundamental frequency of the loaded platform relative to the fundamental frequency of the appendages, the lower the local deformation of the platform.

iii. For the particular structural system the following quantitative results apply:
   - If the loaded platform's fundamental eigenvalue is twice or more the value of the appendage's fundamental eigenvalue then the local deformation on the platform attachments is low (Tables VII-21,22 and 15).
   - If the loaded platform's fundamental eigenvalue is close to appendage's fundamental eigenvalue then the local deformation on the platform

attachments is of medium degree. (Tables VII-20,22 and 14, Tables VII-19,23 and 15).

- If the loaded platform's fundamental eigenvalue is three times or less the value of the appendage's fundamental eigenvalue then the local deformation on the platform attachments is high (Tables VII-20,24 and 17, Tables VII-19,22 and 13).

iv. The most interesting case concerns the examples that correspond to Tables VII-14,16. In these particular cases, the differences in the results between *the finite element method and the free-interface method are almost identical* for the two structural systems for the whole frequency range. Examining closely the platform natural frequencies in Table VII-22 and comparing those to the natural frequencies of the platform in Table VII-23, we notice that their ratio has identical value throughout the range. The same ratio value have the attached appendages of Tables VII-20 and 19 for all natural frequencies.

v. Utilising the criterion established, one can predict the increase in the local deformation in the example case that corresponds to Table VII-17 relative to the local deformation for the structural system that corresponds to Table VII-14. In both cases the platform has the same mass and stiffness characteristics. In both cases the appendages have the same natural frequencies, but in the case of Table VII-17 the appendages have much higher inertia than in the case of Table VII-14. The higher inertia of the appendages, the lower the loaded natural frequencies of the platform, whereas the natural frequencies of the appendages are the same, thus, as the criterion predicts, the local deformation is higher in the case of Table VII-17.

vi. Comparing the component mass and stiffness characteristics for the cases of Tables VII-13 and 17 it is not obvious in which case the local deformation will be higher (unless one examines the natural frequencies of the components). In both cases the platform has the same mass and stiffness characteristics. The appendages in both cases have the same stiffness characteristics, but the appendages of Table VII-13 are much lighter to the

appendages of Table VII-17. Without the aid of the criterion established, one would expect that the appendages with higher inertia would locally deform the structure more. Based on the criterion though, the appendage with the higher inertia has much lower natural frequencies, but at the same time loads the platform much more and lowers the loaded natural frequencies. In actual fact it proves that in both cases the local deformation is high, but lower in the case of the higher inertia appendages. Apparently by increasing the inertia of the appendages, in the example case of Table VII-17, the natural frequencies of the appendages dropped more, in relative terms to the example of Table VII-13, than the loaded natural frequencies of the platform. Thus, is not essential that increasing the inertia of an appended component the local deformation will definitely increase or decrease. A closer examination of the natural frequencies of the components is essential.

VII-3-5. Conclusions of Case Study II

i. The criterion which determines the extent of the local deformation of the space-frame platform at the attachments with the appended payload has to do with the relationship between the natural frequencies of the platform component, loaded with the inertia of the appendages, and the natural frequencies of the appendages.

ii. The higher the natural frequencies of the platform, loaded with the inertia of the attached payloads, relative to the natural frequencies of the appended payload, the lower is predicted the local deformation of the carrier structure at the attachment.

iii. It is expected that the criterion has limits of application. In the case that the appended component is rigid, it is not anticipated that the local deformation will be infinite. The lower the inertia of the appended component the higher the natural frequencies of the component. Since the loaded natural frequencies of the inboard component have an upper limit the unloaded natural frequencies, it is not expected after a point that by decreasing the inertia of the appended component the local deformation will increase. On

the contrary, after a point the local deformation will start decreasing although the natural frequency of the component will be increasing. Generally for very high appendage natural frequencies relative to the frequencies of the loaded inboard component, caution should be exercised with the interpretation of the criterion.

iv. The criterion can be applied to any inboard component of a multibody structure and not necessarily to the main platform carrier. Inboard component is considered any component that precedes other components.

v. The criterion cannot specify a priori the degree of the local deformation by the natural frequencies of the loaded inboard component and those of the appended payload. The degree of local deformation will depend on the attachment locations and the rigidity of the members that support the payload. But the criterion can definitely predict the possibility of the local deformation being relatively low or high. This is helpful in indicating the number of modes essential for good convergence.

vi. Even in a case that a component does not exhibit local deformation as such, the criterion still suggests that a large amount of component modes need to be used for convergence.

vii. If the local deformation of a component is predicted to be potentially high, special care should be exercised for approximating the deformation field the appropriate component-mode sets that can account for the effect of the local deformation.

VII-4. Component Mode Set Selection (Case Study III)

The aim of this case study is to investigate how different component mode sets compare in the accurate description of the deformation field of the space-frame platform. As explained in the previous case studies, the platform may, under particular conditions, exhibit high local deformation at the interfaces with other

components. The component mode sets which have been examined are shown below and have been assigned with a method number for brevity purposes.

Method I: Free-interface component mode set
Method II: Fixed-interface component mode set
Method III: Loaded-interface component mode set
Method IV: Redundant constraint component mode set
Method V: Constraint component mode set

The structural configuration chosen for this case study is shown in Figure VII-2. The structural system is of exactly the same design as in the previous case studies. For pronouncing the differences between the results obtained for each method, the properties of the components are selected to have such values that the local deformation of the space-frame at the attachments is high. The material properties of both the space-frame platform and the appended components are p=2700 Kg/m^3 and E=7.2E10N/m^2. For the space-frame platform the total number of component modes (static + dynamic modes) is fixed to 30 for all example cases that follow. The appendages are modelled using 12 fixed-interface normal modes in all example cases.

Other than tables which contain natural frequency comparisons, a number of graphs which correspond to frequency response analysis complement the results of this case study. Figure VII-4 corresponds to the frequency response of point 71, at the interface of the main structure with the appendage, where the local deformation is expected to be high. Figure VII-5 corresponds to point 1 away from the interface. The points are shown in Figure VII-2.
For facilitating the presentation of the results shown in tables, Figure VII-6 contains a graphical representation of the natural frequencies obtained using the various component mode sets.

VII-4.1. Example Case 1

A direct finite element frequency response versus a modal finite element frequency response analysis has been undertaken to demonstrate the number of global modes that suffice to model the response of the structural system up to the excitation frequency of 20 Hz. A structural damping factor of 0.02 has been assumed for the entire structure.

Modal response analysis has been performed using 10, 18, 24 and 30 global normal modes of the structure. Table VII-25 shows that the correspondence of the normal mode number to the natural frequencies of the system is as follows

Normal Mode 10 : Frequency 7.68 Hz, 0.38 times the maximum forcing frequency
Normal Mode 18 : Frequency 23.61 Hz, 1.18 times the maximum forcing frequency
Normal Mode 24 : Frequency 26.26 Hz, 1.31 times the maximum forcing frequency
Normal Mode 30 : Frequency 41.96 Hz, 2.09 times the maximum forcing frequency

The frequency response of the structure has been obtained at point 71, located at the interface of the mainbody and the appendage, and has been illustrated in Figure VII-3. The following can be concluded:

i. Modal frequency response analysis using 24 global normal modes gives as good results as using 30 global normal modes for the frequency range of interest. 24 modes correspond to frequency 26.26 Hz which is 1.31 times the forcing frequency. Although it is usually recommended to use modes in the frequency range between 1.5 and 2 times the forcing frequency, in the particular case this would be unnecessary since the extra modes result in virtually no improvement on the frequency response.

ii. Modal response using 24 global modes gives excellent results relative to the direct finite element method frequency response analysis. In actual fact the results are virtually indistinguishable to those obtained for the direct response analysis especially so in the resonance frequencies of the structure.

iii. Using less than 24 modes compromises the results in the higher frequency domain.

In view of the above, an excellent agreement between the direct finite element method frequency response analysis and the methods proposed in this work should give near as good results as those obtained by the modal finite element method frequency response analysis and using as many as 24 global modes.

VII-4-2. Example Case 2

The space-frame platform is modelled using 30 free-interface component modes. The results are shown in Table VII-26 and in figures 4, 5, 6. The following comments apply:

i. The local deformation of the space-frame platform at the attachments is high.

ii. The free-interface component modes are not appropriate for modelling the deformation of the space-frame platform. Free-interface normal modes cannot capture the eigenvalues of the system (Table VII-26) and also fail to predict the frequency response of the structure (Figures VII-4,5).

VII-4-3. Example Case 3

The space-frame platform is modelled using 30 fixed-interface component modes. The results are shown in Table VII-27. The following remarks can be made:

i. The differences in results between the finite element method and the fixed-interface method are high. Comparing Table VII-26 to 25 we notice that the difference in results is of the same order between using fixed-interface components modes and free-interface component modes.

ii. Fixed-interface normal modes should be able to capture the deformation at the attachments due to the loading of the appendages, since by fixing the interface, the deformation near the boundaries is high. In reality though, by

using fixed interface normal modes, there is no coupling between the flexible part of the platform's motion and the rigid and flexible part of the appendages' motion. So in effect the most important part of the interaction dynamics between the components is not modelled.

iii. The fixed-interface component modes may capture the local deformation of the space-frame platform, but are not suitable for modelling the interaction between adjacent components.

iv. Nevertheless, fixed interface mode set would be appropriate for modelling terminal components. In all the examples that follow, the appendages have been modelled using the fixed-interface mode set and the error involved is very low.

VII-4-4. Example Case 4

30 loaded-interface component modes are used in this example case. The results are shown in Table VII-28 and Figure VII-4, 5, 6. The following comments can be made:

i. The difference between the finite element method and the loaded-interface method is very small throughout the frequency range. The largest difference is only 0.3 percent and occurs at mode 26.

ii. The loaded-interface normal modes can capture very accurately the local deformation of the platform.

iii. From Figures VII-4,5 one may observe that the displacement measured at point 71 at the interface as well as at point 1 away from the interface is in extremely good agreement to the direct finite element. It has to be emphasised that for the calculation of the displacements only 24 modes have been retained in the frequency response analysis.

VII-4-5. Example Case 5

The particular structural configuration possesses 6 nonredundant constraints and 6 redundant constraints. Therefore, for keeping the total number of flexible component modes to 30, a combination of 24 fixed-interface normal modes and 6 redundant constraint modes are imported in the mathematical model. The results are shown in Table VII-29 and Figures 4, 5, 6. The following comments apply:

i. The difference between the finite element method and the redundant constraint method is very small thought the frequency range. Largest difference of 0.27 percent occurs at mode 21.

ii. The difference is of comparable order to that of the loaded-interface method. The redundant constraint method generally converges more uniformly than the loaded-interface method.

iii. Referring to Figures VII-4, 5 the redundant interface component modes offer excellent results relative to the finite element direct frequency response. As in the case of modal finite element frequency response analysis, 24 global modes have been retained for the frequency response analysis using the proposed method.

VII-4-6. Example Case 6

The constraint method is a modification of the redundant constraint method. Constraint modes are developed for all the interface constraints, redundant and nonredundant. For keeping the total number of component modes to 30, 12 constraint modes and 18 fixed-interface modes are employed. The results are shown in Table VII-30 and Figures VII-4, 5, 6. The following remarks apply:

i. The difference between the finite element method and the constraint method is very small. The highest difference occurs in mode 21 and is only 0.27%.

ii. Referring to Figures VII-4, 5 the constraint interface component modes offer excellent results relative to the finite element direct frequency response. As

in the case of modal finite element frequency response analysis, 24 global modes have been retained for the frequency response analysis using the proposed method.

VII-4-7. Conclusion of Case Study III

i. The fixed-interface and free-interface component modes are not appropriate, in general, for modelling the dynamics of complex components which may exhibit local deformation.

ii. The loaded-interface component modes give excellent results, but are not appropriate for independent modelling, nonlinear dynamics and may become very involving for the modelling requirements of large chains of components.

iii. The redundant constraint method and the constraint method give as excellent results, or even better, than the loaded-interface method and also circumvent all the associated problems of the latter.

iv. Loaded-interface, redundant constraint and constraint methods give excellent results relative to the finite element method by utilising only a small number of component modes. Moreover, the global modes derived by the method proposed in this work with a combination of any of the above component mode sets have been shown to be extremely close to those obtained by modal analysis of the global finite element model. This has been demonstrated by comparison of the modal finite element frequency response results to those obtained using the proposed method. In both cases the results are indistinguishable to those obtained from the direct finite element response analysis and in both cases only the minimum of 24 global modes have been used for the analysis.

VII-5. Convergence of Component Mode Sets (Case Study IV)

In this section, an investigation of the effect that the number of component modes has on the accuracy of results has been undertaken. The structural configuration is the same as in the previous case study other than that the whole system is assumed to have docked on a much larger structure. The structural system can therefore be modelled as clamped at the free end face. The properties of the components are the same as in the previous case study p=2700 Kg/m^3 and E=7.2E10N/m^2. In this particular case study, the redundant constraint and constraint component mode sets contain the same number of static modes (since the system does not have any rigid body motion), and therefore no distinction between them has been made. The appendages have been modelled using 12 fixed-interface normal modes.

As in the previous case study frequency response graphs have been produced along with tables comparing the natural frequencies obtained using the various component modes. For all frequency response analyses the structural damping factor has been assumed equal to 0.02. 24 global modes have been retained for the frequency response analysis.

For facilitating the presentation of the results in the tables that correspond in this case study, Figure VII-8 contains a graphical representation of the natural frequencies obtained using the various component mode sets.

VII-5-1. Example Case 1

The space-frame platform is modelled using 30 loaded interface component modes. It has been demonstrated in table VII-31 that there is an excellent agreement between the finite element method and the loaded-interface method.

VII-5-2. Example Case 2

In example case 2 the space-frame platform is modelled using 18 loaded interface component modes. The purpose for reducing the number of modes is for comparison

purposes relative to subsequent examples using constraint component mode sets where the number of dynamic normal modes is refrained to 18. In this respect comparison is achieved with the same number of dynamic modes. From Table VII-32 and Figure VII-7 the following can be concluded.

i. 18 loaded interface component modes give almost as good results in the lower frequency range as the case with 30 loaded interface modes. As expected after a cutting off frequency large discrepancies relative to the finite element method are produced (Table VII-32).

ii. Nevertheless for the forcing frequency of interest 18 loaded interface component modes seem to suffice for excellent agreement with the direct finite element response analysis (Figure VII-7).

VII-5-3. Example Case 3

Using the constraint component mode set (or equivalently for this example the redundant constraint component mode set) the space-frame platform is modelled using 30 fixed-interface normal modes and 12 constraint modes. The results are shown in Table VII-33 and Figure VII-7. Generally the constraint method converges better than the loaded-interface method for the same number of dynamic modes in all but a few modes. Relative to the direct finite element frequency response analysis the results obtained in this example case are in excellent agreement.

VII-5-4. Example Case 4

In this example case, 18 fixed-interface normal modes and 6 redundant constraint modes are used. The results are shown in Table VII-34 and Figure VII-7. The following remarks can be made:

i. Comparing Tables VII-34 to 33, there is a very small difference in the eigenvalues obtained by using 12 dynamic modes less for this example. As expected, the difference increases as the mode number increases.

ii. Using only 18 dynamic modes the eigenfrequencies are still better to those obtained by using 30 loaded-interface component modes, other than a few exceptions and definitely much better than those obtained using 18 loaded interface component modes (Tables VII-34, 31,32).

iii. It seems that the constraint component modes give better results than the loaded-interface component modes for the same number of dynamic modes. Although computing time can be saved using less dynamic modes, a penalty is paid for the calculation of static modes which complement the dynamic modes in constraint or redundant constraint component modes. However it has been shown in the previous chapter that the overall time penalty for using static modes is much smaller compared to the total cost for using normal modes of vibration.

iv. As far as frequency response analysis is concerned 18 redundant component modes seem to be adequate for providing excellent results relative to the finite element direct frequency response analysis (Figure VII-7). If the forcing frequency was higher it would definitely be the case that constraint component modes would converge better for the same, minimum number of dynamic modes.

VII-5-4. Example Case 5

In this example case only 6 fixed-interface modes are used in the redundant constraint method. The results are shown in Table VII-35 and comparing them to the results of Tables VII-31,32 the following comments can be made:

i. The eigenfrequencies in this example case have excellent agreement with the finite element method up to the cutting off frequency of mode 12.

ii. Using only 6 fixed-interface modes the difference in results to those using 18 and 30 fixed-interface normal modes is only significant after the cutting off frequency.

iii. If only the low frequency domain is of interest, only a small number of dynamic modes need to be used, thus reducing the size of the formulated problem considerably.

iv. The discrepancy noticed after the cutting off mode is due to the small number of dynamic modes and not due to unmodelled high local deformation of the platform at the attachments.

v. Similar comments apply for the frequency response analysis (Figure VII-7).

VII-5-5. Conclusion of the *Case Study IV*

i. It seems that the constraint component modes give better results than the loaded-interface component modes for the same number of dynamic modes. Considerable computing time can be saved using less dynamic modes whereas the extra time penalty paid for the calculation of static modes which complement the dynamic modes in constraint or redundant constraint component modes is relatively small. This is an extra reason why redundant constraint and constraint modes should be preferred to the loaded interface component modes.

ii. Both the redundant constraint method and the constraint method can accurately model the deformation field of an inboard component with a small number of dynamic modes. If only the low frequency domain is of interest, only a small number of dynamic modes need to be used, thus reducing the size of the formulated problem considerably.

iii. Static modes describe accurately the local deformation at the interfaces whereas dynamic modes the 'global' deformation of the component. If dynamic modes are included in very small numbers then the local deformation at the interfaces will be captured by the static modes and convergence will be excellent up to some frequency, but poor convergence will be noticed suddenly after a cutting off mode.

VII-6. Constraint Versus Redundant Constraint Component Modes (Case Study V)

It is anticipated that the local deformation of the space-frame platform would be very high if the flexible solar panels were substituted by rigid ones. In this case study it has been established that both the redundant constraint and constraint component modes can still model accurately the deformation of the space-frame structure. It has also been intended to demonstrate the most efficient component mode set between the redundant constraint and the constraint sets. For this purpose the bare minimum of 18 dynamic modes has been employed in both component mode sets.

The material density and stiffness of the space-frame are p=2700 Kg/m^3 and E=7.2E10N/m^2 respectively and the material density of the appendages p=2700 Kg/m^3. The structural system is free in space.

VII-6-1. Example Case 1

To demonstrate the degree of the local deformation of the space-frame at the interfaces, the space-frame deformation has been modelled using 30 free-interface component modes. The results have been shown in Table VII-36. The differences between the finite element method and the free-interface method are enormous (~575% for mode 8), suggesting very high local deformation of the platform.

VII-6-2. Example Case 2

The space-frame has been modelled using 24 redundant constraint component modes (18 fixed-interface normal modes and 6 redundant constraint modes). The results have been shown in Table VII-37. The difference between the finite element method and the redundant constraint method are very small throughout the frequency range.

VII-6-3. Example Case 3

The space-frame deformation is modelled using 30 constraint component modes (18 fixed-interface normal modes and 12 constraint modes). The results have been demonstrated in Table VII-38. The difference between the finite element method and the constraint method is very small.

VII-6-4. Conclusions of Case Study V

i. Both the constraint method and the redundant constraint methods have given excellent results even in the case where the local deformation of the space-frame platform at the interface is very high.

ii. For the same number of dynamic modes the redundant constraint component mode set has given as accurate results as the constraint mode set. Since there is only a very small computational time penalty associated with the obtaining a larger set of static modes (if a multiple algebraic solution is performed), it may be beneficial to use the constraint component mode set in order to overcome the problems associated with the redundant constraint component mode set, detailed in chapter II.

VII-7. Collective Conclusions

i. It was shown that large lightweight structural components, such as space-frame platforms, exhibit high modal density and, in cases, high local deformation near the attachments of appended payloads.

ii. A criterion has been established which predicts the possibility of the local deformation being low or high. The higher the natural frequencies of an inboard component, loaded with the inertia of the appended payloads, relative to the natural frequencies of the appended payload, the lower the local deformation of the inboard body at the interfaces is predicted to be. The criterion has boundaries of application. If the natural frequencies of the

appended component are very high compared to the loaded natural frequencies of the inboard component, caution should be exercised with the interpretation of the criterion.

iii. If the local deformation of a component is predicted to be potentially high, special care should be exercised for approximating the deformation field with appropriate component mode sets that can account for the effect of the local deformation at the interfaces. An increased number of component modes may also prove essential.

iv. The right selection of component mode sets is challenging and of foremost importance for large-scale flexible multibody structures In space, since these structures, due to their particular design, large dimensions, lightweight construction, and the large number of components, exhibit high modal density and local deformation at the component interfaces. The consequences of selecting an inappropriate component mode set are listed below in order of increasing impact to the structural dynamics modelling.

- A larger number of component modes will be needed for convergence, therefore the inherently large size of the differential problem will increase further, which is detrimental to computer time involved.
- For components likely to exhibit high local deformation the convergence issue becomes more crucial. Flexible component mode sets that fail to closely resemble the real deformation of the individual components, when attached to each other to form the structure, proved inadequate or even completely inappropriate for efficiently capturing the dynamics of the entire structural system, even in the low frequency range. This implies that even a large number of component modes, employed for convergence, will fail to model the dynamics accurately. Not only the computational cost will increase, but convergence will still be poor.

- Due to high modal density of the particular structural system examined, if component mode sets utilised are not appropriate the chances are that a number of modes will not be captured at all. Unmodelled dynamics is one

of the main causes of destabilisation of structures in space.

v. The fixed-interface and free-interface component modes are not appropriate, in general, for modelling the dynamics of complex components which may exhibit local deformation. Nevertheless, these component mode sets are ideal for simpler components and in particular modelling circumstances can reduce the order and computational cost compared to more sophisticated mode sets.

vi. The loaded-interface component mode set gives excellent results relative to the finite element methods, but is not appropriate for independent modelling, nonlinear dynamics and may become very involving for the modelling requirements of large chains of components.

vii. The redundant constraint and constraint component mode set give as excellent results, or even better, than the loaded interface component mode set and also circumvent all the associated problems of the latter. In actual fact it has been demonstrated that the constraint and redundant constraint component mode sets give better results than the loaded interface component modes for the same number of dynamic modes. Considerable computing time can be saved using a smaller number of dynamic modes, and only a small penalty paid for the calculation of static modes which complement the dynamic modes in constraint or redundant constraint component mode sets. However, regardless of the computational cost involved, the use of redundant constraint or constraint component modes should be preferred due to the aforementioned problems encountered with the loaded interface component modes.

viii. It was shown that both the redundant constraint and constraint component mode set can accurately model the deformation field of an inboard component with a small number of dynamic modes. If only the low frequency domain is of interest, a very small number of dynamic modes need to be used, thus reducing the size of the formulated problem considerably. In fact if dynamic modes are included in very small numbers then the local

deformation at the interfaces will still be captured by the static modes and convergence will be excellent up to some frequency, but poor convergence will be noticed suddenly after a cutting off mode. On the other hand, if static modes are not accounted for in a component that may exhibit high local deformation at the interfaces, then the deformation at the interface will be poorly approximated and convergence will be extremely difficult even if a large number of dynamic modes are included. If static modes are included even for a component that is not likely to exhibit local deformation at the interfaces, then the convergence will be accelerated.

ix. A redundant component mode set cannot be defined or obtained in the cases of statically determinate and underdeterminate components, unlike the constraint mode set. This leads to the conclusion that the constraint component mode set is better suited than the redundant constraint component mode set for the dynamics modelling of large-scale articulated multibody systems.

x. The global modes derived by the method proposed in this work with a combination of any of the loaded, redundant constraint and constraint component mode sets have been shown to be extremely close to those obtained by modal analysis of the global finite element model. This has been demonstrated by comparison of the modal finite element frequency response results to those obtained using the proposed method. In both cases the results are indistinguishable to those obtained from the direct application of the finite element response analysis and in both cases only the minimum of 24 global modes have been used for the analysis.

xi. Lastly, the theoretical integrity of the mathematical model D has been verified, since it can give results with extreme accuracy to the finite element method, even with a low number of degrees of freedom. This model can definitely be used for studies related to structures that belong in category II missions in space.

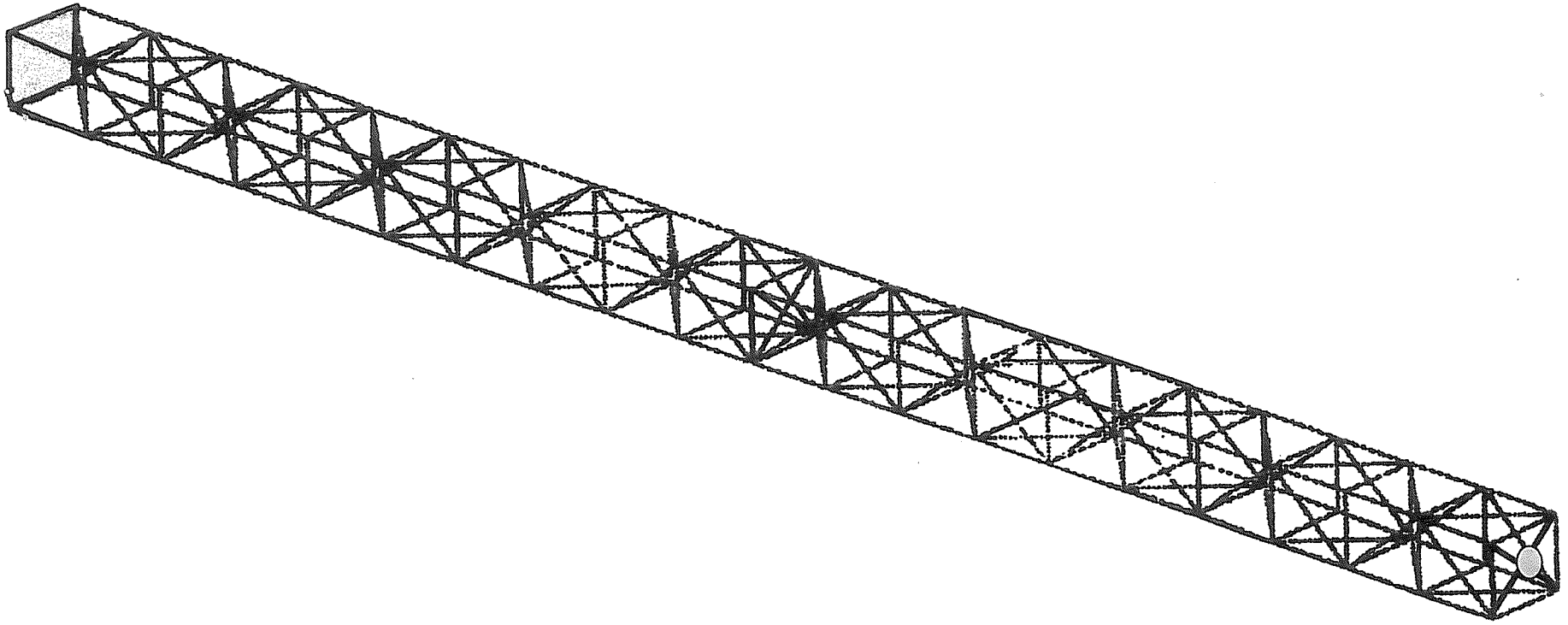

Figure VII-1 Typical Space-Frame Platform

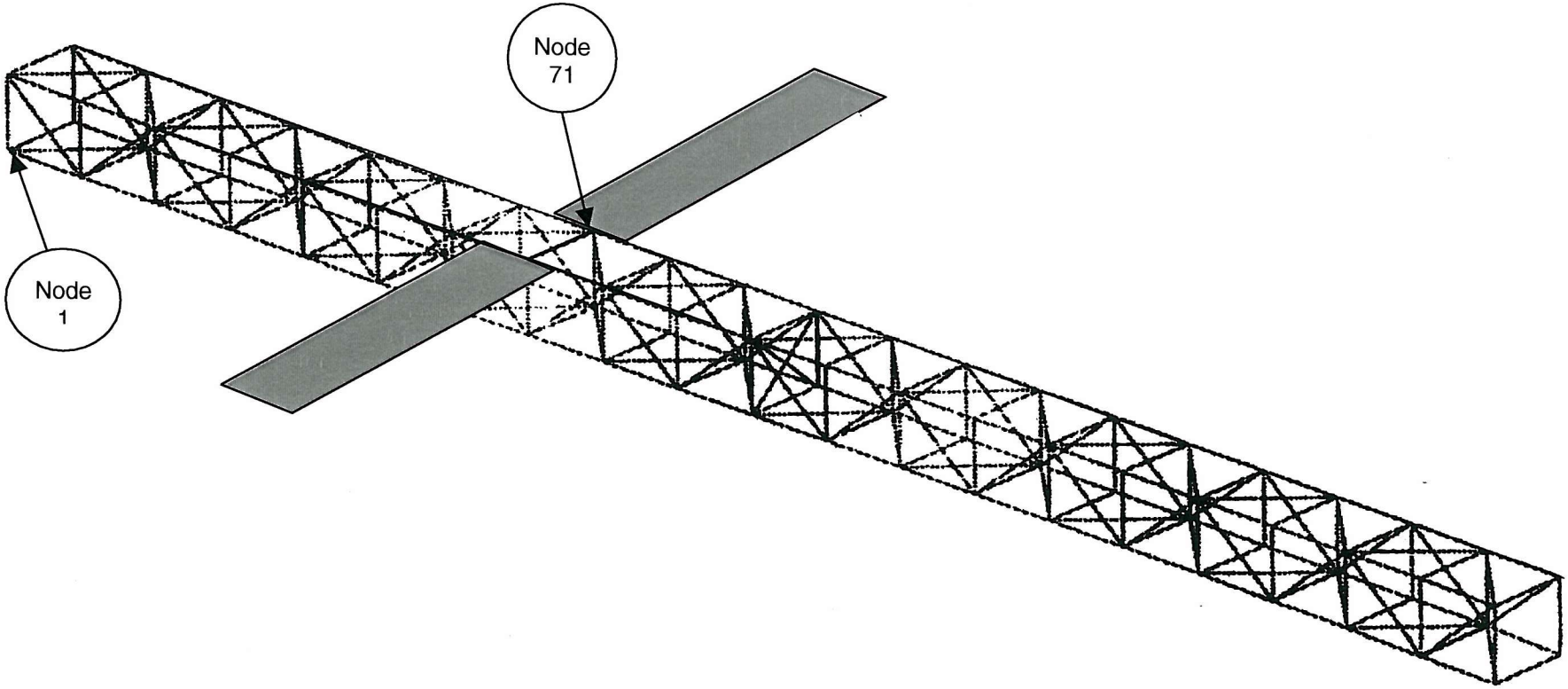

Figure VII-2 Space-Frame Platform and Solar Panels

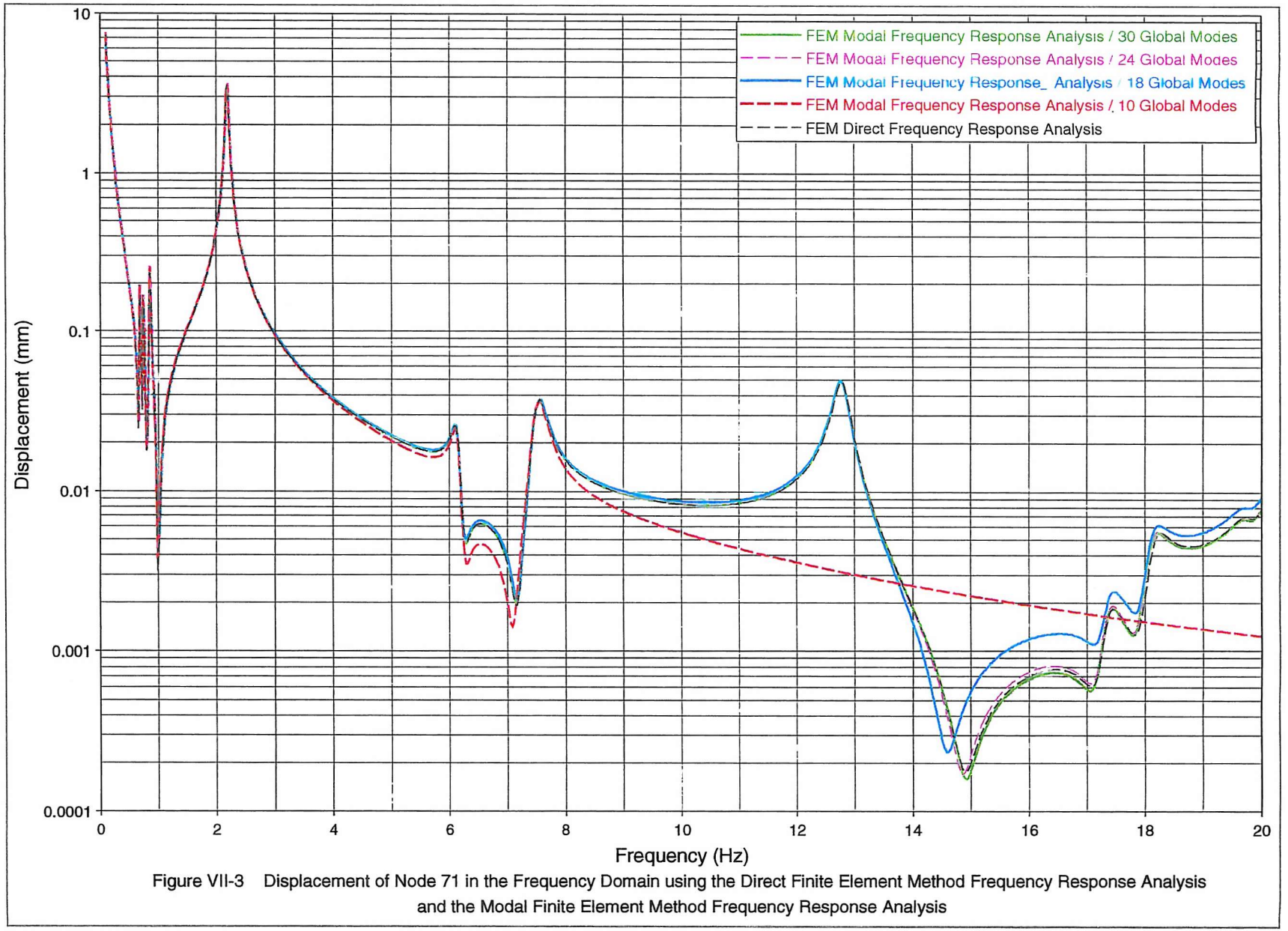

Figure VII-3 Displacement of Node 71 in the Frequency Domain using the Direct Finite Element Method Frequency Response Analysis and the Modal Finite Element Method Frequency Response Analysis

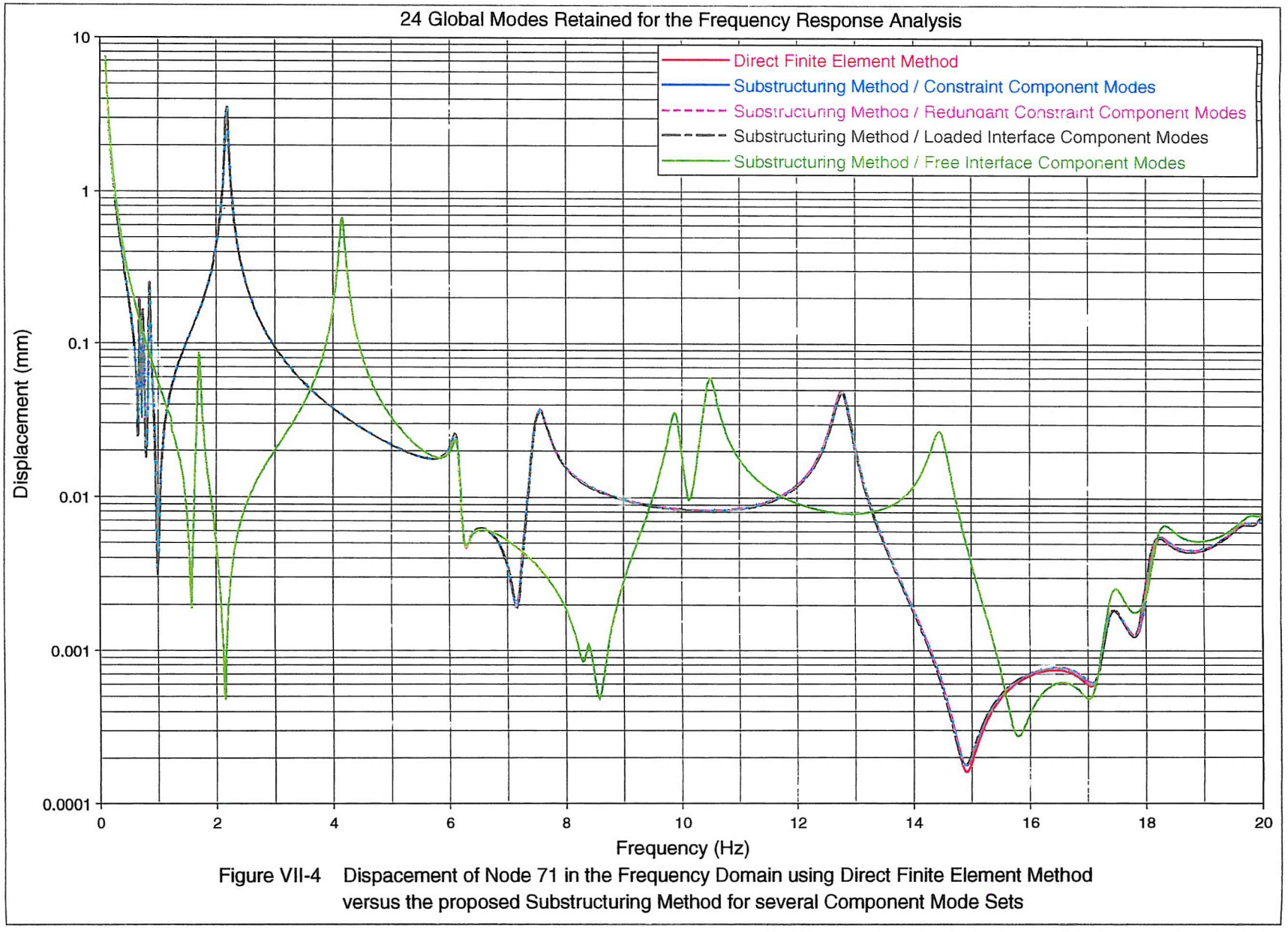

Figure VII-4 Dispacement of Node 71 in the Frequency Domain using Direct Finite Element Method versus the proposed Substructuring Method for several Component Mode Sets

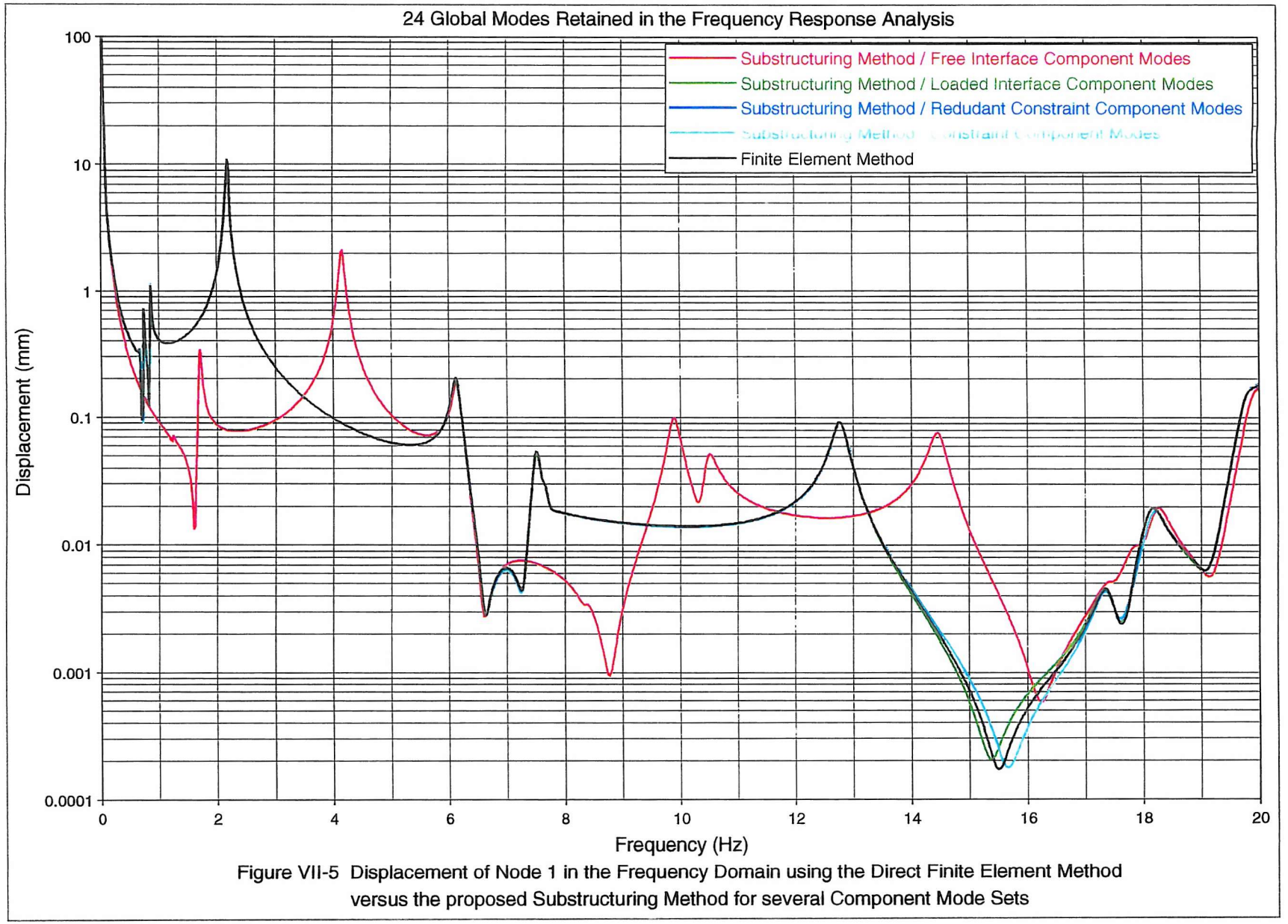

Figure VII-5 Displacement of Node 1 in the Frequency Domain using the Direct Finite Element Method versus the proposed Substructuring Method for several Component Mode Sets

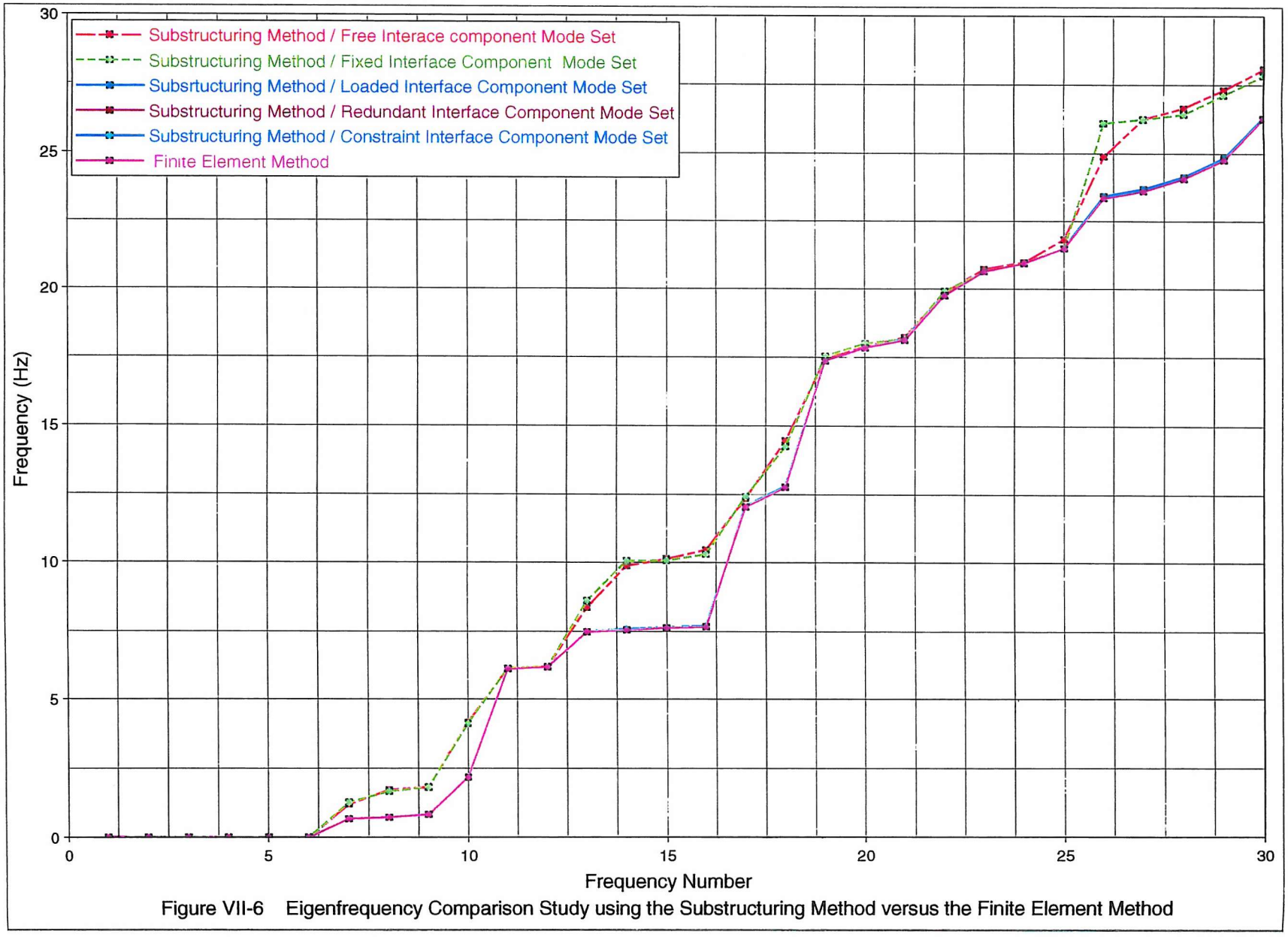

Figure VII-6 Eigenfrequency Comparison Study using the Substructuring Method versus the Finite Element Method

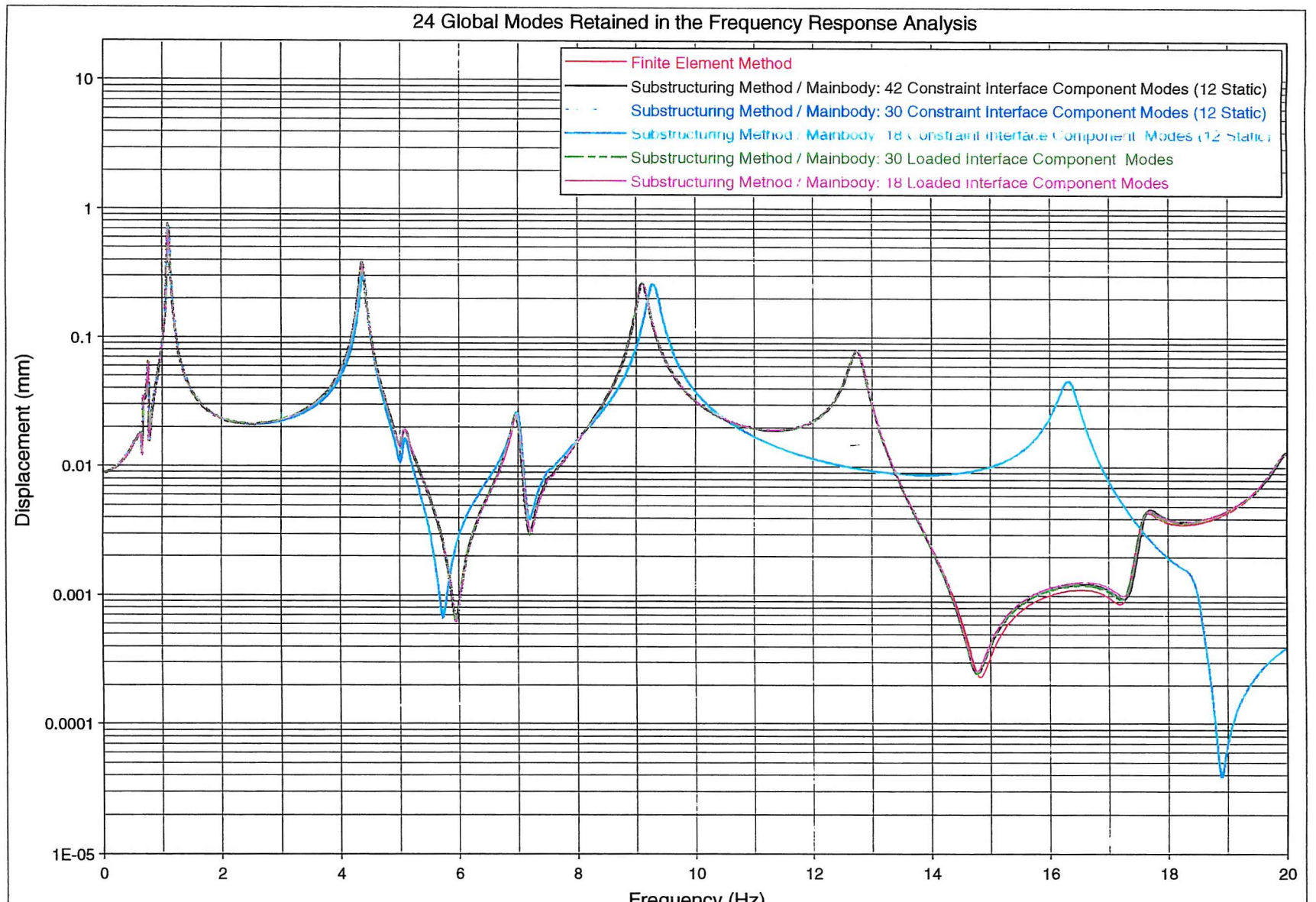

Figure VII-7 Effect of Order Truncation at Component Level on the Accuracy of the Frequency Response Analysis

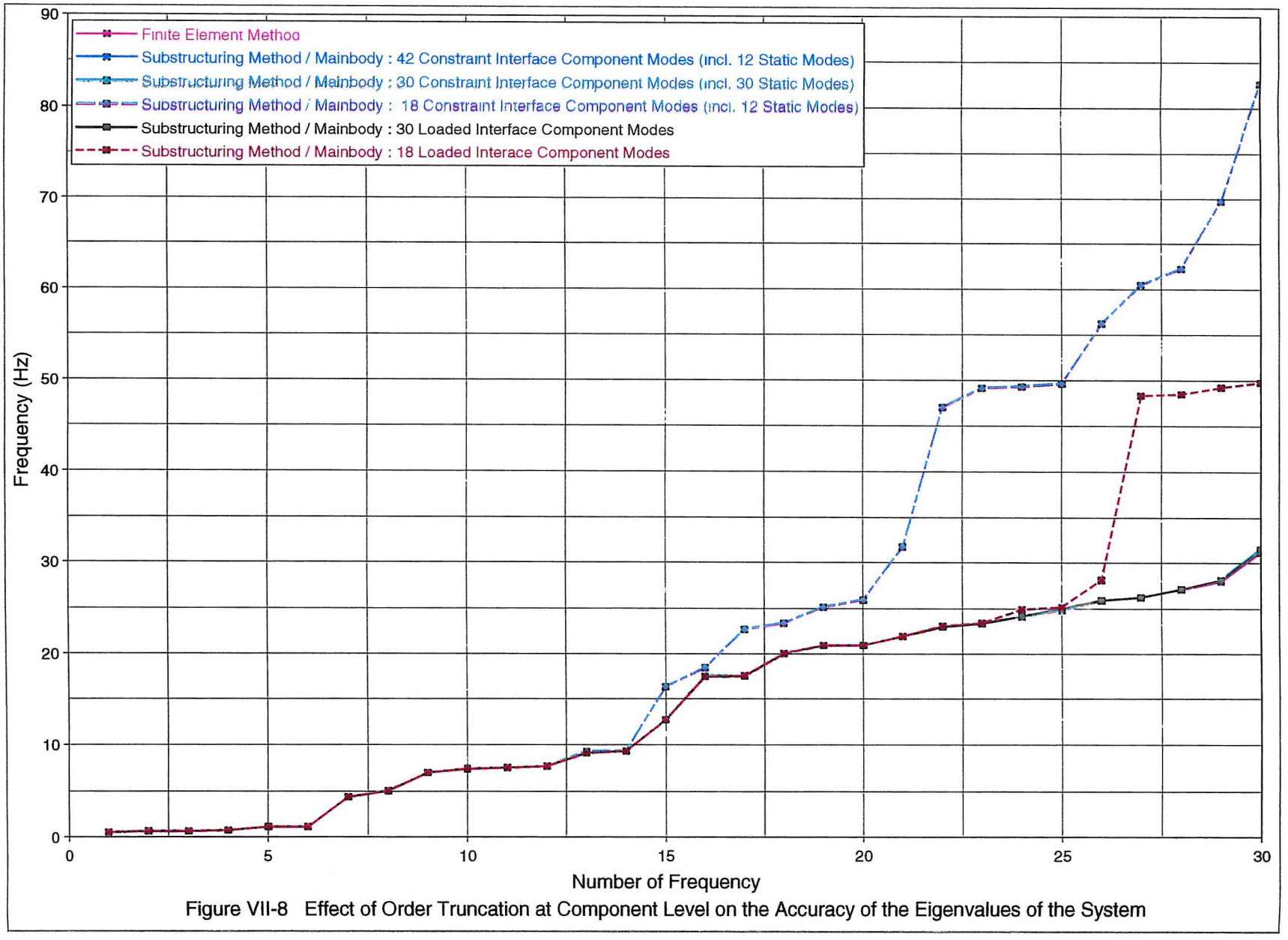

Figure VII-8 Effect of Order Truncation at Component Level on the Accuracy of the Eigenvalues of the System

Mode	Freqency(Hz)	Mode Type
1	1.2465	1st Bending Plane A
2	1.2497	1st Bending Plane B
3	7.3501	2nd Bending Plane A
4	7.4500	2nd Bending Plane B
5	10.2370	1st Torsional
6	17.2440	2nd Torsional
7	18.8180	3rd Bending Plane A
8	19.2660	3rd Bending Plane B
9	21.5230	3rd Torsional
10	22.3100	1st Axial
11	30.5180	—
12	31.5840	—
13	32.7500	—
14	33.5260	—
15	40.3290	—
16	44.2480	—
17	44.4670	—
18	44.8340	—
19	45.3520	—
20	45.9430	—
21	46.0130	—
22	46.5340	—
23	46.5590	—
24	46.8240	—
25	47.7460	—
26	48.7680	—
27	48.9900	—
28	49.8530	—
29	50.1840	—
30	50.9840	—
31	51.2200	—
32	51.8420	—
33	51.9980	—
34	52.0740	—
35	52.7900	—
36	53.0650	—
37	53.6040	—
38	53.9230	—
39	53.9830	—
40	54.5680	—
41	54.6760	—
42	54.6850	—
43	54.8150	—
44	54.8570	—
45	54.9620	—
46	55.0190	—
47	55.0710	—
48	55.1120	—
49	55.1810	—
50	55.2380	—

Table VII-1 Natural Frequencies (Hz) of the cantilever beam-like space-frame platform shown in Figure VII-1

Mode	Frequency(Hz)	Mode Type
1	1.2573	1st Bending Plane A
2	1.2573	1st Bending Plane B
3	7.8610	2nd Bending Plane A
4	7.8610	2nd Bending Plane B
5	21.9280	3rd Bending Plane A
6	21.9280	3rd Bending Plane B
7	26.2560	1st Torsional
8	42.7350	4th Bending Plane A
9	42.7350	4th Bending Plane B
10	43.0360	1st Axial
11	70.1480	5th Bending Plane A
12	70.1480	5th Bending Plane B
13	78.8120	2nd Torsional
14	103.9000	6th Bending Plane A
15	103.9000	6th Bending Plane B
16	129.1800	2nd Axial
17	131.4900	3rd Torsional
18	143.6800	7th Bending Plane A
19	143.6800	7th Bending Plane B
20	184.3900	4th Torsional
21	189.1500	—
22	189.1500	—
23	215.5300	—
24	237.5900	—
25	239.9400	—
26	239.9400	—
27	291.1700	—
28	295.6800	—
29	295.6800	—
30	302.2300	—
31	345.2200	—
32	355.9700	—
33	355.9700	—
34	389.4200	—
35	399.8300	—
36	420.4300	—
37	420.4300	—
38	455.0900	—
39	477.2500	—
40	488.7000	—
41	488.7000	—
42	511.0800	—
43	560.4200	—
44	560.4200	—
45	565.8400	—
46	567.8900	—
47	625.6100	—
48	635.2600	—
49	635.2600	—
50	655.3500	—

Table VII-2 Natural Frequencies (Hz) of a cantilever symmetric and uniform Timoshenko beam

Mode	FEM	Method I	Difference(%)
1	0.77358	0.77374	0.02056
2	0.77358	0.77374	0.02058
3	6.13270	6.13320	0.00813
4	6.13270	6.13328	0.00946
5	18.54500	18.54881	0.02057
6	18.54500	18.54977	0.02572
7	26.25600	26.25706	0.00404
8	31.23200	31.36784	0.43495
9	37.76200	37.77613	0.03742
10	37.76200	37.78049	0.04897
11	63.66800	63.70815	0.06306
12	63.66800	63.72113	0.08345
13	78.81200	78.81378	0.00226
14	96.03300	96.12325	0.09398
15	96.03300	96.15351	0.12548
16	102.18000	104.24335	2.01933
17	131.49000	131.49836	0.00636
18	134.57000	134.74786	0.13217
19	134.57000	134.80849	0.17722
20	178.96000	179.26776	0.17197
21	178.96000	179.37814	0.23365
22	182.13000	184.39629	1.24432
23	184.39000	187.15773	1.50102
24	228.83000	229.34314	0.22425
25	228.83000	229.53283	0.30714
26	237.59000	237.59332	0.00140
27	265.72000	274.04489	3.13296
28	283.82000	284.61845	0.28132
29	283.82000	284.93734	0.39368
30	291.17000	291.17563	0.00193

Table VII-3 Natural frequency(Hz) comparative study between the Finite Element Method and Method I* for the loaded beam structure**

* 40 free-interface normal modes

** load mass: m=16 Kg

Mode	FEM	Method I	Difference(%)
1	1.09440	1.09443	0.00318
2	1.09680	1.09690	0.00936
3	6.72420	6.72784	0.05411
4	6.81100	6.81487	0.05682
5	9.75730	10.22958	4.84029
6	10.23600	10.23610	0.00096
7	17.24400	17.24443	0.00251
8	17.64900	17.68942	0.22905
9	18.06500	18.10899	0.24353
10	21.52300	21.52408	0.00502
11	23.09700	23.17848	0.35279
12	30.48400	30.49068	0.02190
13	31.24500	31.36996	0.39993
14	31.63500	31.65869	0.07490
15	32.11500	32.26888	0.47915
16	44.24800	44.24892	0.00208
17	44.46700	44.46838	0.00310
18	44.83400	44.83570	0.00379
19	45.13000	45.35251	0.49305
20	45.34900	45.41361	0.14248
21	45.41000	45.68870	0.61374
22	45.98900	45.99930	0.02239
23	46.01600	46.01943	0.00744
24	46.81800	46.81970	0.00362
25	47.74300	47.74490	0.00398
26	48.76700	48.76864	0.00337
27	48.79400	48.82225	0.05789
28	49.84800	49.85107	0.00617
29	50.17000	50.17534	0.01065
30	50.98400	50.98540	0.00274

Table VII-4 Natural frequency(Hz) comparative study between the Finite Element Method and Method I* for the loaded space-frame platform**

* 40 free-interface normal modes

** load mass: m=16 Kg

Mode	FEM	Method I	Difference(%)
1	0.77358	0.77374	0.02047
2	0.77358	0.77374	0.02047
3	6.13270	6.13310	0.00652
4	6.13270	6.13310	0.00652
5	18.54500	18.54765	0.01427
6	18.54500	18.54765	0.01427
7	26.25600	26.25706	0.00404
8	31.23200	31.33271	0.32246
9	37.76200	37.77074	0.02315
10	37.76200	37.77074	0.02316
11	63.66800	63.69215	0.03794
12	63.66800	63.69216	0.03795
13	78.81200	78.81378	0.00226
14	96.03300	96.08626	0.05546
15	96.03300	96.08630	0.05550
16	102.18000	103.70705	1.49447
17	131.49000	131.49836	0.00636
18	134.57000	134.67418	0.07742
19	134.57000	134.67422	0.07745
20	178.96000	179.13573	0.09820
21	178.96000	179.13582	0.09824
22	182.13000	184.39629	1.24432
23	184.39000	185.82855	0.78017
24	228.83000	229.12168	0.12747
25	228.83000	229.12205	0.12763
26	237.59000	237.59332	0.00140
27	265.72000	271.74865	2.26880
28	283.82000	284.26261	0.15595
29	283.82000	284.26268	0.15597
30	291.17000	291.17563	0.00193

Table VII-5 Natural frequency(Hz) comparative study between the Finite Element Method and Method I* for the loaded beam structure**

* 50 free-interface normal modes

** load mass: m=16 Kg

Mode	FEM	Method I	Difference(%)
1	1.09440	1.09443	0.00309
2	1.09680	1.09690	0.00925
3	6.72420	6.72772	0.05239
4	6.81100	6.81471	0.05440
5	9.75730	10.22442	4.78734
6	10.23600	10.23610	0.00095
7	17.24400	17.24443	0.00250
8	17.64900	17.68804	0.22120
9	18.06500	18.10696	0.23229
10	21.52300	21.52408	0.00502
11	23.09700	23.17748	0.34846
12	30.48400	30.49041	0.02103
13	31.24500	31.36531	0.38506
14	31.63500	31.65742	0.07087
15	32.11500	32.26067	0.45360
16	44.24800	44.24892	0.00208
17	44.46700	44.46838	0.00309
18	44.83400	44.83570	0.00379
19	45.13000	45.35249	0.49299
20	45.34900	45.39630	0.10431
21	45.41000	45.66688	0.56569
22	45.98900	45.99842	0.02048
23	46.01600	46.01920	0.00696
24	46.81800	46.81964	0.00351
25	47.74300	47.74485	0.00387
26	48.76700	48.76860	0.00329
27	48.79400	48.82116	0.05567
28	49.84800	49.85093	0.00588
29	50.17000	50.17487	0.00971
30	50.98400	50.98539	0.00272

Table VII-6 Natural frequency(Hz) comparative study between the Finite Element Method and Method I* for the loaded space-frame platform**

* 50 free-interface normal modes

** load mass: m=16 Kg

Mode	FEM	Method I	Difference(%)
1	0.41288	0.41297	0.02068
2	0.41288	0.41297	0.02068
3	5.66690	5.66735	0.00796
4	5.66690	5.66735	0.00796
5	17.83800	17.98155	0.80475
6	17.97900	17.98155	0.01420
7	17.97900	17.99831	0.10741
8	26.25600	26.25706	0.00404
9	37.16700	37.17712	0.02723
10	37.16700	37.17712	0.02724
11	63.06400	63.09070	0.04233
12	63.06400	63.09070	0.04235
13	78.81200	78.81378	0.00226
14	90.19000	92.28997	2.32838
15	95.43000	95.48892	0.06174
16	95.43000	95.48896	0.06178
17	131.49000	131.49836	0.00636
18	133.98000	134.08909	0.08142
19	133.98000	134.08913	0.08145
20	174.45000	178.56916	2.36123
21	178.37000	178.56926	0.11171
22	178.37000	178.76970	0.22409
23	184.39000	184.39629	0.00341
24	228.26000	228.57888	0.13970
25	228.26000	228.57927	0.13987
26	237.59000	237.59332	0.00140
27	260.26000	266.91751	2.55802
28	283.27000	283.74814	0.16879
29	283.27000	283.74822	0.16882
30	291.17000	291.17563	0.00193

Table VII-7 Natural frequency(Hz) comparative study between the Finite Element Method and Method I* for the loaded beam structure**

* 50 free-interface normal modes

** load mass: m=80 Kg

Mode	FEM	Method I	Difference(%)
1	0.78793	0.78808	0.01933
2	0.78939	0.78954	0.01942
3	4.48520	4.72572	5.36256
4	5.96480	5.97751	0.21307
5	6.03850	6.05178	0.21987
6	10.23400	10.23474	0.00727
7	16.56200	16.68050	0.71548
8	16.95400	17.08139	0.75141
9	17.24500	17.24543	0.00249
10	21.52300	21.52404	0.00484
11	23.00500	23.06830	0.27517
12	30.11200	30.42730	1.04708
13	30.35300	30.49125	0.45548
14	31.07800	31.41502	1.08442
15	31.60500	31.60948	0.01416
16	44.10100	44.24892	0.33540
17	44.24800	44.46837	0.49804
18	44.44500	44.80858	0.81804
19	44.46700	44.83560	0.82894
20	44.83500	45.13632	0.67207
21	45.35200	45.35367	0.00368
22	45.97900	45.98530	0.01370
23	46.01500	46.01726	0.00492
24	46.81700	46.81907	0.00442
25	47.74200	47.74407	0.00433
26	48.76600	48.76810	0.00431
27	48.76800	48.80624	0.07842
28	49.84500	49.84930	0.00862
29	50.15900	50.17001	0.02195
30	50.98400	50.98529	0.00254

Table VII-8 Natural frequency(Hz) comparative study between the Finite Element Method and Method I* for the loaded space-frame platform**

* 50 free-interface normal modes

** load mass: m=80 Kg

Mode	FEM	Method I	Difference(%)
1	0.77003	0.77020	0.02157
2	0.77003	0.77020	0.02158
3	5.71530	5.72339	0.14151
4	5.71530	5.72339	0.14153
5	5.71800	5.75951	0.72602
6	15.17300	15.49281	2.10779
7	15.17300	15.49284	2.10797
8	27.48100	29.02983	5.63599
9	27.48100	29.02996	5.63649
10	31.23200	31.33271	0.32246
11	46.52300	49.38645	6.15490
12	46.52300	49.38671	6.15548
13	53.16300	53.99408	1.56326
14	73.23800	77.49976	5.81905
15	73.23800	77.50019	5.81965
16	102.18000	103.70705	1.49447
17	105.46000	107.12987	1.58342
18	106.82000	112.81307	5.61043
19	106.82000	112.81361	5.61094
20	146.70000	154.82028	5.53530
21	146.70000	154.82112	5.53587
22	158.13000	160.67321	1.60831
23	182.13000	185.82855	2.03072
24	192.46000	203.10171	5.52931
25	192.46000	203.10301	5.52999
26	211.11000	214.56845	1.63822
27	243.70000	257.26626	5.56679
28	243.70000	257.26732	5.56722
29	264.45000	268.89151	1.67953
30	265.72000	271.74865	2.26880

Table VII-9 Natural frequency(Hz) comparative study between the Finite Element Method and Method I* for the loaded beam structure**

* 50 free-interface normal modes

** load: m=16 Kg, Ix,Iy,Iz=100 Kg.m^2

Mode	FEM	Method I	Difference(%)
1	1.09210	1.09273	0.05727
2	1.09460	1.09516	0.05128
3	2.22640	6.60554	196.69171
4	2.22700	6.62680	197.56615
5	2.76700	6.75211	144.02270
6	6.73850	10.20975	51.51369
7	6.82610	15.99929	134.38399
8	9.75880	16.81528	72.30889
9	10.74300	17.24554	60.52812
10	17.24400	21.52383	24.81925
11	17.66100	21.81117	23.49904
12	18.07800	22.96068	27.00895
13	21.52300	23.15009	7.55976
14	23.09800	28.33511	22.67342
15	30.67500	31.59475	2.99836
16	31.25500	33.81395	8.18733
17	31.63700	40.49112	27.98658
18	32.13700	41.98755	30.65175
19	44.24800	44.25367	0.01281
20	44.46800	44.48513	0.03851
21	44.83600	44.87034	0.07659
22	45.14200	45.39238	0.55466
23	45.35000	45.96616	1.35867
24	45.43000	45.98158	1.21413
25	45.98900	46.53610	1.18963
26	46.02300	47.21560	2.59130
27	46.82600	48.14033	2.80684
28	47.75300	48.76595	2.12122
29	48.77800	49.16839	0.80035
30	48.79400	50.27580	3.03685

Table VII-10 Natural frequency(Hz) comparative study between the Finite Element Method and Method I* for the loaded space-frame platform**

* 50 free-interface normal modes

** load: m=16 Kg, Ix,Iy,Iz=100 Kg.m^2

Mode	Frequency(Hz)
1	1.2465
2	1.2497
3	7.3518
4	7.4519
5	10.2390
6	17.7750
7	18.8410
8	19.2940
9	22.4560
10	23.1900
11	30.5700
12	32.8340
13	33.6450
14	34.0970
15	44.2520
16	44.4840
17	44.8730
18	45.4190
19	46.1170
20	46.7740
21	46.8660
22	46.9610
23	47.9290
24	48.6550
25	48.8770
26	48.9980
27	50.1320
28	50.4790
29	51.2330
30	51.2930
31	51.9200
32	52.0990
33	52.3960
34	52.9770
35	53.3940
36	53.7440
37	54.1800
38	54.3870
39	54.6670
40	54.6810
41	54.7770
42	54.8610
43	54.8730
44	55.0610
45	55.0810
46	55.1050
47	55.2680
48	55.4220
49	55.4870
50	56.1540

Table VII-11 Natural Frequencies (Hz) of the cantilever beam-like space-frame platform with rigid load-supporting cross-members, shown in Figure VII-1

Mode	FEM	Method I	Difference(%)
1	1.09270	1.09272	0.00202
2	1.09510	1.09626	0.10635
3	6.61330	6.61925	0.09004
4	6.65240	6.67414	0.32682
5	6.80410	6.86145	0.84291
6	17.03300	17.16009	0.74612
7	17.38900	17.53125	0.81806
8	17.77500	17.77611	0.00623
9	20.94400	20.98543	0.19780
10	23.18700	23.18858	0.00680
11	23.53800	24.54421	4.27483
12	29.59400	30.37675	2.64495
13	30.22000	31.07875	2.84167
14	34.07200	34.07890	0.02026
15	42.12300	44.25327	5.05727
16	42.57400	44.40317	4.29646
17	42.61300	44.42943	4.26263
18	44.25200	44.48672	0.53042
19	44.48500	44.87483	0.87632
20	44.87300	45.34003	1.04079
21	45.41900	45.42027	0.00279
22	46.11700	46.11880	0.00390
23	46.95900	46.96068	0.00357
24	47.92800	47.92955	0.00324
25	48.36100	48.47292	0.23143
26	48.58600	48.62640	0.08316
27	48.99700	48.99890	0.00388
28	50.13100	50.13315	0.00428
29	51.23000	51.23185	0.00362
30	51.29200	51.29347	0.00286

Table VII-12 Natural frequency(Hz) comparative study between the Finite Element Method and Method I* for the loaded space-frame platform** with rigid load-supporting cross-members

* 50 free-interface normal modes

** load: m=16 Kg, Ix,Iy,Iz=100 Kg.m^2

Mode	FEM	Method I	Difference(%)
1	0.00000	0.00004	-
2	0.00000	0.00005	-
3	0.00000	0.00017	-
4	0.00000	0.00033	-
5	0.00000	0.00035	-
6	0.00001	0.00066	-
7	1.81740	3.31977	82.66589
8	2.09470	5.00522	138.94680
9	2.47850	5.18888	109.35557
10	3.24190	6.29948	94.31429
11	6.27390	6.40071	2.02124
12	6.32010	7.29478	15.42194
13	12.04500	12.04631	0.01090
14	16.83600	16.87912	0.25611
15	17.74200	17.75169	0.05461
16	18.49600	18.56660	0.38169
17	19.03700	19.14161	0.54950
18	20.08500	20.09752	0.06232
19	20.98700	21.00715	0.09600
20	21.04100	21.08251	0.19728
21	22.21700	22.90720	3.10664
22	23.45000	25.05482	6.84358
23	23.51500	26.63992	13.28907
24	23.75700	26.93608	13.38168
25	24.70500	27.56352	11.57062
26	26.65400	28.33958	6.32394
27	27.27700	31.76815	16.46497
28	27.69300	32.32499	16.72621
29	28.38900	33.26585	17.17865
30	40.69500	41.02809	0.81851

Table VII-13 Natural Frequency (Hz) Comparative Studies between the Finite Element Method and Method I* for the structure** shown in Figure VII-2

* Space-frame: 30 free-interface normal modes
Beam appendage: 12 fixed-interface normal modes

** Properties: Space-frame E=7.2E10 N/m^2 p=2700 Kg/m^3
Beam appendage E=7.2E10 N/m^2 p=270 Kg/m^3

Mode	FEM	Method I	Difference(%)
1	0.00000	0.00004	-
2	0.00000	0.00005	-
3	0.00000	0.00017	-
4	0.00000	0.00033	-
5	0.00000	0.00035	-
6	0.00001	0.00066	-
7	1.26380	1.54706	22.41324
8	1.33850	1.63117	21.86520
9	1.41960	1.64617	15.96023
10	2.00190	2.39003	19.38807
11	6.26310	6.26391	0.01295
12	6.30970	6.31080	0.01750
13	8.48330	9.59981	13.16128
14	8.75500	10.15410	15.98056
15	8.92290	10.15988	13.86296
16	9.06440	10.33413	14.00787
17	12.09500	12.12107	0.21554
18	16.90800	16.94915	0.24339
19	17.75000	17.75944	0.05316
20	18.50600	18.57644	0.38061
21	19.35100	19.36260	0.05993
22	20.19800	20.20770	0.04803
23	21.02100	21.03105	0.04779
24	21.13000	21.13793	0.03754
25	23.02300	23.17991	0.68154
26	24.68900	26.46277	7.18446
27	25.16700	26.65639	5.91804
28	25.56200	27.00346	5.63908
29	25.64100	27.55289	7.45637
30	26.65600	28.22944	5.90275

Table VII-14 Natural Frequency (Hz) Comparative Studies between the Finite Element Method and Method I* for the structure** shown in Figure VII-2

* Space-frame: 30 free-interface normal modes
Beam appendage: 12 fixed-interface normal modes

** Properties: Space-frame E=7.2E10 N/m^2 p=2700 Kg/m^3
Beam appendage E=7.2E9 N/m^2 p=270 Kg/m^3

Mode	FEM	Method I	Difference(%)
1	0.00000	0.00004	-
2	0.00000	0.00005	-
3	0.00000	0.00017	-
4	0.00000	0.00033	-
5	0.00000	0.00035	-
6	0.00000	0.00066	-
7	0.50587	0.51674	2.14966
8	0.50651	0.51966	2.59596
9	0.51034	0.52093	2.07578
10	0.74304	0.75869	2.10650
11	3.12760	3.21053	2.65141
12	3.14750	3.21345	2.09530
13	3.16840	3.22823	1.88842
14	3.23070	3.30723	2.36884
15	6.26670	6.26714	0.00705
16	6.31550	6.31579	0.00467
17	8.72170	8.94921	2.60851
18	8.79500	8.99578	2.28292
19	8.83410	9.00230	1.90400
20	8.85810	9.02892	1.92841
21	12.07900	12.08011	0.00918
22	16.71600	16.82869	0.67416
23	17.00000	17.40932	2.40777
24	17.24000	17.61095	2.15170
25	17.31700	17.61638	1.72884
26	17.37400	17.65051	1.59152
27	17.76400	17.83212	0.38349
28	18.46800	18.58455	0.63107
29	19.50600	19.52073	0.07551
30	20.24800	20.26956	0.10650

Table VII-15 Natural Frequency(Hz)Comparative Studies between the Finite Element Method and Method I* for the structure** shown in Figure VII-2

* Space-frame: 30 free-interface normal modes
Beam appendage: 12 fixed-interface normal modes

** Properties: Space-frame $E=7.2E10\ N/m^2$ $p=2700\ Kg/m^3$
Beam appendage $E=7.2E8\ N/m^2$ $p=270\ Kg/m^3$

Mode	FEM	Method I	Difference(%)
1	0.00000	0.00027	-
2	0.00000	0.00054	-
3	0.00000	0.00084	-
4	0.00000	0.00127	-
5	0.00001	0.00174	-
6	0.00001	0.00308	-
7	3.99650	4.89221	22.41245
8	4.23260	5.15818	21.86783
9	4.48910	5.20561	15.96115
10	6.33060	7.55787	19.38633
11	19.80600	19.80819	0.01107
12	19.95300	19.95650	0.01754
13	26.82700	30.35741	13.15991
14	27.68600	32.11011	15.97960
15	28.21700	32.12831	13.86155
16	28.66400	32.67927	14.00808
17	38.24900	38.33014	0.21214
18	53.46700	53.59136	0.23260
19	56.13000	56.15861	0.05097
20	58.52100	58.73022	0.35751
21	61.19300	61.22895	0.05875
22	63.87300	63.90081	0.04354
23	66.47500	66.50432	0.04410
24	66.81800	66.84367	0.03842
25	72.80400	73.29001	0.66755
26	78.07400	83.68291	7.18410
27	79.58600	84.29298	5.91433
28	80.83400	85.38301	5.62759
29	81.08300	87.12901	7.45657
30	84.29400	89.26891	5.90185

Table VII-16 Natural Frequency (Hz) Comparative Studies between the Finite Element Method and Method I* for the structure** shown in Figure VII-2

* Space-frame: 30 free-interface normal modes
Beam appendage: 12 fixed-interface normal modes

** Properties: Space-frame $E=7.2E11\ N/m^2$ $p=2700\ Kg/m^3$
Beam appendage $E=7.2E10\ N/m^2$ $p=270\ Kg/m^3$

Mode	FEM	Method I	Difference(%)
1	0.00000	0.00001	-
2	0.00000	0.00003	-
3	0.00000	0.00013	-
4	0.00000	0.00022	-
5	0.00000	0.00032	-
6	0.00000	0.00047	-
7	0.67496	1.21965	80.69921
8	0.73492	1.69795	131.03904
9	0.85123	1.81744	113.50749
10	2.18110	4.15299	90.40816
11	6.12260	6.13471	0.19774
12	6.19700	6.21413	0.27640
13	7.47970	8.38139	12.05514
14	7.55270	9.88725	30.91016
15	7.63120	10.14852	32.98722
16	7.68150	10.46960	36.29630
17	12.02600	12.34272	2.63360
18	12.76600	14.46281	13.29161
19	17.36400	17.41714	0.30602
20	17.83000	17.85553	0.14319
21	18.12300	18.22758	0.57706
22	19.74100	19.85850	0.59520
23	20.63100	20.72985	0.47914
24	20.93400	20.95958	0.12221
25	21.48400	21.82548	1.58947
26	23.36300	24.88031	6.49450
27	23.60700	26.23831	11.14633
28	24.06900	26.64211	10.69056
29	24.76900	27.30266	10.22916
30	26.26400	28.05617	6.82369

Table VII-17 Natural Frequency Comparative (Hz) Studies between the Finite Element Method and Method I* for the structure** shown in Figure VII-2

* Space-frame: 30 free-interface normal modes
Beam appendage: 12 fixed-interface normal modes

** Properties: Space-frame $E=7.2E10\ N/m^2$ $p=2700\ Kg/m^3$
Beam appendage $E=7.2E10\ N/m^2$ $p=2700\ Kg/m^3$

Table Number	Platform Properties	Appendage Properties	Degree of Local Deformation
13	E=7.2e10 N/m^2 P=2700 Kg/m^3	E=7.2e10 N/m^2 P=270 Kg/m^3	High
14	E=7.2e10 N/m^2 P=2700 Kg/m^3	E=7.2e9 N/m^2 P=270 Kg/m^3	Medium
15	E=7.2e10 N/m^2 P=2700 Kg/m^3	E=7.2e8 N/m^2 P=270 Kg/m^3	Low
16	E=7.2e11 N/m^2 P=2700 Kg/m^3	E=7.2e10 N/m^2 P=270 Kg/m^3	Medium
17	E=7.2e10 N/m^2 P=2700 Kg/m^3	E=7.2e10 N/m^2 P=2700 Kg/m^3	High

Table VII-18 Collective table for example cases in case study 2

Mode	Frequency(Hz)
1	5.1281
2	5.1281
3	32.132
4	32.132
5	89.952
6	89.952
7	176.22
8	176.22
9	291.25
10	291.25
11	415.29
12	435.03
13	435.03
14	607.67
15	607.67

Table VII-19 Natural frequencies of a cantilever beam appendage*

* Properties: E=7.2E10 N/m^2 p=270 Kg/m^3

Mode	Frequency(Hz)
1	1.6217
2	1.6217
3	10.161
4	10.161
5	28.445
6	28.445
7	55.727
8	55.727
9	92.100
10	92.100
11	131.33
12	137.57
13	137.57
14	192.16
15	192.16

Table VII-20 Natural frequencies of a cantilever beam appendage*

* Properties: E=7.2E9 N/m^2 p=270 Kg/m^3 or
E=7.2E10 N/m^2 p=2700 Kg/m^3

Mode	Frequency(Hz)
1	0.51281
2	0.51281
3	3.2132
4	3.2132
5	8.9952
6	8.9952
7	17.622
8	17.622
9	29.125
10	29.125
11	41.529
12	43.503
13	43.503
14	60.767
15	60.767

Table VII-21 Natural frequencies of a cantilever beam appendage*

* Properties: E=7.2E8 N/m^2 p=270 Kg/m^3

Mode	Frequency(Hz)
1	0.
2	0.
3	0.
4	0.
5	0.
6	0.
7	1.9333
8	2.2832
9	2.8124
10	3.5679
11	6.2767
12	12.056
13	16.896
14	17.750
15	18.509
16	19.288
17	20.262
18	21.032
19	21.127
20	23.218
21	26.648
22	27.154
23	27.413
24	28.237
25	40.583
26	40.723
27	44.180
28	44.232
29	44.806
30	44.975

Table VII-22 Natural Frequencies (Hz) of space-frame platform* loaded with the inertia of the appendages**

* Properties: E=7.2E10 N/m^2 p=2700 Kg/m^3

** Properties: p=270 Kg/m^3

Mode	Frequency(Hz)
1	0.
2	0.
3	0.42796E-05
4	0.69442E-05
5	0.72302E-05
6	0.79422E-05
7	6.1137
8	7.2200
9	8.8934
10	11.283
11	19.849
12	19.996
13	38.124
14	53.429
15	56.132
16	58.530
17	60.993
18	64.073
19	66.509
20	66.811
21	73.421
22	84.267
23	85.870
24	86.688
25	89.294
26	128.34
27	128.78
28	139.71
29	139.87
30	141.69

Table VII-23 Natural Frequencies (Hz) of space-frame platform* loaded with the inertia of the appendages**

* Properties: E=7.2E11 N/m^2 p=2700 Kg/m^3

** Properties: p=270 Kg/m^3

Mode	Frequency(Hz)
1	0.
2	0.
3	0.
4	0.
5	0.
6	0.37609E-06
7	0.72148
8	0.80417
9	0.96729
10	2.4590
11	6.1676
12	6.2594
13	11.759
14	12.324
15	17.197
16	17.439
17	17.794
18	19.675
19	20.634
20	20.942
21	21.572
22	26.239
23	26.594
24	26.714
25	27.651
26	35.779
27	39.802
28	40.719
29	43.154
30	44.179

Table VII-24 Natural Frequencies (Hz) of space-frame platform*

loaded with the inertia of the appendages**

* Properties: E=7.2E10 N/m^2 p=2700 Kg/m^3

** Properties: p=2700 Kg/m^3

Mode	Frequency (Hz)
1	0.0
2	0.0
3	0.0
4	0.0
5	0.0
6	0.0
7	0.67496
8	0.73492
9	0.85123
10	2.1811
11	6.1226
12	6.1970
13	7.4797
14	7.5527
15	7.6312
16	7.6815
17	12.026
18	12.766
19	17.364
20	17.830
21	18.123
22	19.741
23	20.631
24	20.934
25	21.484
26	23.363
27	23.607
28	24.069
29	24.769
30	26.264
31	26.792
32	27.670
33	28.346
34	36.806
35	40.421
36	41.955
37	44.180
38	44.231
39	44.374
40	44.811

Table VII-25 Natural Frequency obtained by direct Finite Element Method for the structure* in case study 3

* Properties: Space-frame E=7.2E10 N/m^2 p=2700 Kg/m^3
Beam appendage E=7.2E10 N/m^2 p=2700 Kg/m^3

Mode	FEM	Method I	Difference(%)
1	0.00000	0.00001	-
2	0.00000	0.00003	-
3	0.00000	0.00013	-
4	0.00000	0.00022	-
5	0.00000	0.00032	-
6	0.00000	0.00047	-
7	0.67496	1.21965	80.69921
8	0.73492	1.69795	131.03904
9	0.85123	1.81744	113.50749
10	2.18110	4.15299	90.40816
11	6.12260	6.13471	0.19774
12	6.19700	6.21413	0.27640
13	7.47970	8.38139	12.05514
14	7.55270	9.88725	30.91016
15	7.63120	10.14852	32.98722
16	7.68150	10.46960	36.29630
17	12.02600	12.34272	2.63360
18	12.76600	14.46281	13.29161
19	17.36400	17.41714	0.30602
20	17.83000	17.85553	0.14319
21	18.12300	18.22758	0.57706
22	19.74100	19.85850	0.59520
23	20.63100	20.72985	0.47914
24	20.93400	20.95958	0.12221
25	21.48400	21.82548	1.58947
26	23.36300	24.88031	6.49450
27	23.60700	26.23831	11.14633
28	24.06900	26.64211	10.69056
29	24.76900	27.30266	10.22916
30	26.26400	28.05617	6.82369

Table VII-26 Natural Frequency Comparative (Hz) Studies between the Finite Element Method and Method I* for the structure** in case study 3

* Space-frame: 30 free-interface normal modes
Beam appendage: 12 fixed-interface normal modes

** Properties: Space-frame $E=7.2E10\ N/m^2$ $p=2700\ Kg/m^3$
Beam appendage $E=7.2E10\ N/m^2$ $p=2700\ Kg/m^3$

Mode	FEM	Method II	Difference(%)
1	0.00000	0.00046	-
2	0.00000	0.00087	-
3	0.00000	0.00181	-
4	0.00000	0.00236	-
5	0.00000	0.00284	-
6	0.00000	0.00344	-
7	0.67496	1.26756	87.79724
8	0.73492	1.67777	128.29230
9	0.85123	1.81160	112.82107
10	2.18110	4.15323	90.41899
11	6.12260	6.13664	0.22935
12	6.19700	6.21677	0.31902
13	7.47970	8.47861	13.35495
14	7.55270	9.83764	30.25322
15	7.63120	10.11636	32.56583
16	7.68150	10.45278	36.07737
17	12.02600	12.33336	2.55580
18	12.76600	14.46565	13.31386
19	17.36400	17.42141	0.33064
20	17.83000	17.89120	0.34326
21	18.12300	18.25241	0.71405
22	19.74100	19.86517	0.62901
23	20.63100	20.75593	0.60555
24	20.93400	20.96335	0.14020
25	21.48400	21.94355	2.13902
26	23.36300	24.95248	6.80341
27	23.60700	26.24642	11.18068
28	24.06900	26.66969	10.80515
29	24.76900	27.29772	10.20921
30	26.26400	27.84476	6.01875

Table VII-27 Natural Frequency Comparative (Hz) Studies between the Finite Element Method and Method II* for the structure** in case study 3

* Space-frame: 30 fixed-interface normal modes
Beam appendage: 12 fixed-interface normal modes

** Properties: Space-frame E=7.2E10 N/m^2 p=2700 Kg/m^3
Beam appendage E=7.2E10 N/m^2 p=2700 Kg/m^3

Mode	FEM	Method III	Difference(%)
1	0.00000	0.00046	-
2	0.00000	0.00087	-
3	0.00000	0.00181	-
4	0.00000	0.00235	-
5	0.00000	0.00284	-
6	0.00000	0.00344	-
7	0.67496	0.67498	0.00297
8	0.73492	0.73495	0.00407
9	0.85123	0.85125	0.00290
10	2.18110	2.18123	0.00590
11	6.12260	6.12290	0.00492
12	6.19700	6.19730	0.00491
13	7.47970	7.48596	0.08370
14	7.55270	7.55917	0.08567
15	7.63120	7.63805	0.08982
16	7.68150	7.68795	0.08397
17	12.02600	12.02907	0.02555
18	12.76600	12.77325	0.05676
19	17.36400	17.36568	0.00969
20	17.83000	17.83104	0.00586
21	18.12300	18.12925	0.03450
22	19.74100	19.74317	0.01097
23	20.63100	20.63204	0.00503
24	20.93400	20.93442	0.00201
25	21.48400	21.48551	0.00705
26	23.36300	23.43257	0.29777
27	23.60700	23.70678	0.42268
28	24.06900	24.13692	0.28221
29	24.76900	24.83856	0.28084
30	26.26400	26.26793	0.01495

Table VII-28 Natural Frequency Comparative (Hz) Studies between the Finite Element Method and Method III* for the structure** in case study 3

* Space-frame: 30 loaded-interface normal modes
Beam appendage: 12 fixed-interface normal modes

** Properties: Space-frame E=7.2E10 N/m^2 p=2700 Kg/m^3
Beam appendage E=7.2E10 N/m^2 p=2700 Kg/m^3

Mode	FEM	Method IV	Difference(%)
1	0.00000	0.00045	-
2	0.00000	0.00087	-
3	0.00000	0.00181	-
4	0.00000	0.00236	-
5	0.00000	0.00284	-
6	0.00000	0.00344	-
7	0.67496	0.67499	0.00381
8	0.73492	0.73512	0.02690
9	0.85123	0.85125	0.00293
10	2.18110	2.18127	0.00787
11	6.12260	6.12286	0.00433
12	6.19700	6.19731	0.00504
13	7.47970	7.48023	0.00702
14	7.55270	7.55322	0.00688
15	7.63120	7.63174	0.00710
16	7.68150	7.68201	0.00660
17	12.02600	12.05462	0.23795
18	12.76600	12.77676	0.08431
19	17.36400	17.37182	0.04504
20	17.83000	17.83579	0.03250
21	18.12300	18.17311	0.27648
22	19.74100	19.76561	0.12465
23	20.63100	20.63895	0.03852
24	20.93400	20.93724	0.01547
25	21.48400	21.49376	0.04543
26	23.36300	23.36671	0.01589
27	23.60700	23.61768	0.04526
28	24.06900	24.08495	0.06627
29	24.76900	24.79578	0.10810
30	26.26400	26.26866	0.01773

Table VII-29 Natural Frequency Comparative (Hz) Studies between the Finite Element Method and Method IV * for the structure** in case study 3

* Space-frame: 6 redundant constraint modes
24 fixed-interface normal modes
Beam appendage: 12 fixed-interface normal modes

** Properties: Space-frame $E=7.2E10\ N/m^2$ $p=2700\ Kg/m^3$
Beam appendage $E=7.2E10\ N/m^2$ $p=2700\ Kg/m^3$

Mode	FEM	Method V	Difference(%)
1	0.00000	0.00035	-
2	0.00000	0.00068	-
3	0.00000	0.00074	-
4	0.00000	0.00090	-
5	0.00000	0.00098	-
6	0.00000	0.00201	-
7	0.67496	0.67498	0.00282
8	0.73492	0.73495	0.00398
9	0.85123	0.85125	0.00290
10	2.18110	2.18127	0.00779
11	6.12260	6.12286	0.00431
12	6.19700	6.19731	0.00501
13	7.47970	7.48014	0.00587
14	7.55270	7.55314	0.00588
15	7.63120	7.63173	0.00699
16	7.68150	7.68200	0.00647
17	12.02600	12.05456	0.23749
18	12.76600	12.77674	0.08413
19	17.36400	17.37181	0.04497
20	17.83000	17.83578	0.03244
21	18.12300	18.17293	0.27551
22	19.74100	19.76556	0.12442
23	20.63100	20.63893	0.03846
24	20.93400	20.93723	0.01542
25	21.48400	21.49374	0.04535
26	23.36300	23.36656	0.01523
27	23.60700	23.61759	0.04488
28	24.06900	24.08492	0.06613
29	24.76900	24.79573	0.10790
30	26.26400	26.26865	0.01770

Table VII-30 Natural Frequency Comparative (Hz) Studies between the Finite Element Method and Method V * for the structure** in case study 3

* Space-frame: 12 constraint modes
18 fixed-interface normal modes
Beam appendage: 12 fixed-interface normal modes

** Properties: Space-frame $E=7.2E10\ N/m^2$ $p=2700\ Kg/m^3$
Beam appendage $E=7.2E10\ N/m^2$ $p=2700\ Kg/m^3$

Mode	FEM	Method III	Difference(%)
1	0.54570	0.54572	0.00346
2	0.65064	0.65066	0.00326
3	0.66780	0.66783	0.00377
4	0.76607	0.76610	0.00362
5	1.10740	1.10746	0.00549
6	1.13800	1.13806	0.00488
7	4.36180	4.36220	0.00922
8	5.04950	5.04972	0.00445
9	6.96820	6.97159	0.04867
10	7.36950	7.38230	0.17368
11	7.53070	7.53832	0.10122
12	7.67510	7.68043	0.06946
13	9.09480	9.09734	0.02793
14	9.30120	9.30178	0.00620
15	12.73600	12.74233	0.04973
16	17.46400	17.46881	0.02756
17	17.55700	17.56191	0.02796
18	20.01600	20.01978	0.01888
19	20.90800	20.90932	0.00631
20	20.92000	20.92047	0.00222
21	21.96400	21.98206	0.08221
22	23.00400	23.02072	0.07268
23	23.35700	23.42315	0.28319
24	24.07000	24.13828	0.28368
25	24.81600	25.02215	0.83070
26	25.89300	25.92073	0.10708
27	26.27400	26.28191	0.03011
28	27.11400	27.15130	0.13757
29	28.03800	28.11203	0.26405
30	31.19300	31.38107	0.60291

Table VII-31 Natural Frequency Comparative (Hz) Studies between the Finite Element Method and Method III * for the structure** in case study 4

* Space-frame: 30 loaded-interface normal modes
Beam appendage: 12 fixed-interface normal modes

** Properties: Space-frame E=7.2E10 N/m^2 p=2700 Kg/m^3
Beam appendage E=7.2E10 N/m^2 p=2700 Kg/m^3

Mode	ANSYS	Method III	Difference (%)
1	0.54570	0.54572	0.00353
2	0.65064	0.65066	0.00336
3	0.66780	0.66783	0.00388
4	0.76607	0.76610	0.00376
5	1.10740	1.10746	0.00550
6	1.13800	1.13806	0.00488
7	4.36180	4.36220	0.00925
8	5.04950	5.04999	0.00975
9	6.96820	6.98281	0.20972
10	7.36950	7.38292	0.18210
11	7.53070	7.54021	0.12622
12	7.67510	7.69862	0.30638
13	9.09480	9.10143	0.07287
14	9.30120	9.30187	0.00722
15	12.73600	12.74971	0.10765
16	17.46400	17.47853	0.08318
17	17.55700	17.57667	0.11201
18	20.01600	20.02141	0.02704
19	20.90800	20.90995	0.00932
20	20.92000	20.92057	0.00274
21	21.96400	21.98409	0.09146
22	23.00400	23.13224	0.55746
23	23.35700	23.46586	0.46607
24	24.07000	24.88774	3.39734
25	24.81600	25.19612	1.53174
26	25.89300	28.12669	8.62662
27	26.27400	48.34568	84.00580
28	27.11400	48.51600	78.93339
29	28.03800	49.20957	75.51029
30	31.19300	49.77220	59.56207

Table VII-32 Natural Frequency Comparative (Hz) Studies between the Finite Element Method and Method III * for the structure** in case study 4

* Space-frame: 18 loaded-interface normal modes
Beam appendage: 12 fixed-interface normal modes

** Properties: Space-frame E=7.2E10 N/m^2 p=2700 Kg/m^3
Beam appendage E=7.2E10 N/m^2 p=2700 Kg/m^3

Mode	FEM	Method IV	Difference(%)
1	0.54570	0.54572	0.00347
2	0.65064	0.65066	0.00326
3	0.66780	0.66783	0.00377
4	0.76607	0.76610	0.00345
5	1.10740	1.10745	0.00474
6	1.13800	1.13806	0.00493
7	4.36180	4.36235	0.01269
8	5.04950	5.05005	0.01088
9	6.96820	6.96864	0.00626
10	7.36950	7.36976	0.00357
11	7.53070	7.53103	0.00434
12	7.67510	7.67556	0.00603
13	9.09480	9.09743	0.02896
14	9.30120	9.30162	0.00446
15	12.73600	12.74435	0.06555
16	17.46400	17.48309	0.10933
17	17.55700	17.58738	0.17306
18	20.01600	20.05210	0.18037
19	20.90800	20.91620	0.03920
20	20.92000	20.92333	0.01591
21	21.96400	22.00168	0.17155
22	23.00400	23.00890	0.02131
23	23.35700	23.36064	0.01558
24	24.07000	24.08313	0.05453
25	24.81600	24.86468	0.19615
26	25.89300	25.91174	0.07236
27	26.27400	26.27969	0.02166
28	27.11400	27.15608	0.15520
29	28.03800	28.11790	0.28495
30	31.19300	31.52193	1.05451

Table VII-33 Natural Frequency Comparative (Hz) Studies between the Finite Element Method and Method IV/ V * for the structure** in case study 4

* Space-frame: 12 redundant constraint modes
30 fixed-interface normal modes
Beam appendage: 12 fixed-interface normal modes

** Properties: Space-frame $E=7.2E10\ N/m^2$ $p=2700\ Kg/m^3$
Beam appendage $E=7.2E10\ N/m^2$ $p=2700\ Kg/m^3$

Mode	FEM	Method IV	Difference(%)
1	0.54570	0.54572	0.00347
2	0.65064	0.65066	0.00326
3	0.66780	0.66783	0.00377
4	0.76607	0.76610	0.00345
5	1.10740	1.10745	0.00475
6	1.13800	1.13806	0.00494
7	4.36180	4.36238	0.01330
8	5.04950	5.05010	0.01188
9	6.96820	6.96865	0.00652
10	7.36950	7.36976	0.00357
11	7.53070	7.53103	0.00434
12	7.67510	7.67558	0.00631
13	9.09480	9.09764	0.03122
14	9.30120	9.30162	0.00453
15	12.73600	12.74447	0.06647
16	17.46400	17.48430	0.11625
17	17.55700	17.59165	0.19734
18	20.01600	20.05516	0.19567
19	20.90800	20.91709	0.04346
20	20.92000	20.92365	0.01744
21	21.96400	22.00233	0.17451
22	23.00400	23.00920	0.02261
23	23.35700	23.36068	0.01574
24	24.07000	24.08477	0.06135
25	24.81600	24.86540	0.19907
26	25.89300	25.91377	0.08022
27	26.27400	26.27976	0.02192
28	27.11400	27.15922	0.16679
29	28.03800	28.12992	0.32786
30	31.19300	31.57207	1.21524

Table VII-34 Natural Frequency Comparative (Hz) Studies between the Finite Element Method and Method IV/ V * for the structure** in case study 4

* Space-frame: 12 redundant constraint modes
18 fixed-interface normal modes
Beam appendage: 12 fixed-interface normal modes

** Properties: Space-frame $E=7.2E10\ N/m^2$ $\rho=2700\ Kg/m^3$
Beam appendage $E=7.2E10\ N/m^2$ $\rho=2700\ Kg/m^3$

Mode	FEM	Method IV	Difference(%)
1	0.54570	0.54572	0.00347
2	0.65064	0.65066	0.00327
3	0.66780	0.66783	0.00378
4	0.76607	0.76610	0.00354
5	1.10740	1.10752	0.01078
6	1.13800	1.13807	0.00622
7	4.36180	4.37704	0.34937
8	5.04950	5.05552	0.11921
9	6.96820	6.98867	0.29380
10	7.36950	7.36992	0.00566
11	7.53070	7.53111	0.00550
12	7.67510	7.67873	0.04736
13	9.09480	9.26299	1.84929
14	9.30120	9.31632	0.16252
15	12.73600	16.31712	28.11806
16	17.46400	18.46661	5.74100
17	17.55700	22.68856	29.22798
18	20.01600	23.34225	16.61796
19	20.90800	25.16080	20.34055
20	20.92000	25.95071	24.04735
21	21.96400	31.78053	44.69372
22	23.00400	46.99796	104.30341
23	23.35700	49.14400	110.40375
24	24.07000	49.30519	104.84085
25	24.81600	49.59712	99.85945
26	25.89300	56.19048	117.01032
27	26.27400	60.44980	130.07461
28	27.11400	62.21302	129.44979
29	28.03800	69.73042	148.69970
30	31.19300	82.65286	164.97246

Table VII-35 Natural Frequency Comparative (Hz) Studies between the Finite Element Method and Method IV/ V * for the structure** in case study 4

* Space-frame: 12 redundant constraint modes
6 fixed-interface normal modes
Beam appendage: 12 fixed-interface normal modes

** Properties: Space-frame $E=7.2E10\ N/m^2$ $p=2700\ Kg/m^3$
Beam appendage $E=7.2E10\ N/m^2$ $p=2700\ Kg/m^3$

Mode	FEM	Method I	Difference(%)
1	0.00000	0.00046	-
2	0.00000	0.00087	-
3	0.00000	0.00181	-
4	0.00007	0.00235	-
5	0.00011	0.00283	-
6	0.00017	0.00344	-
7	0.72154	1.59081	120.47360
8	0.80420	5.42372	574.42451
9	0.96731	6.24239	545.33493
10	2.45910	9.82287	299.44966
11	6.16760	11.36533	84.27482
12	6.25940	13.45489	114.95490
13	11.75900	17.01452	44.69361
14	12.32500	17.43194	41.43562
15	17.19700	17.62541	2.49117
16	17.44000	18.23226	4.54278
17	17.79400	20.68957	16.27274
18	19.67500	20.95511	6.50627
19	20.63400	21.69468	5.14044
20	20.94200	25.49247	21.72892
21	21.57200	26.53678	23.01492
22	26.23900	26.78879	2.09533
23	26.59400	27.51230	3.45302
24	26.71400	32.19353	20.51182
25	27.65100	32.66011	18.11547
26	35.77900	40.75704	13.91329
27	39.80100	43.43987	9.14265
28	40.71700	44.18175	8.50935
29	43.15100	44.35021	2.77909
30	44.17900	44.81438	1.43820

Table VII-36 Natural Frequency Comparative (Hz) Studies between the Finite Element Method and Method I* for the structure** in case study 5

* Space-frame: 30 free-interface normal modes

** Properties: Space-frame $E=7.2E10\ N/m^2$ $p=2700\ Kg/m^3$
Beam appendage $E\rightarrow\infty$ $p=2700\ Kg/m^3$

Mode	FEM	Method IV	Difference(%)
1	0.00000	0.00045	-
2	0.00000	0.00087	-
3	0.00000	0.00181	-
4	0.00007	0.00235	-
5	0.00011	0.00284	-
6	0.00017	0.00344	-
7	0.72154	0.72157	0.00443
8	0.80420	0.80445	0.03134
9	0.96731	0.96735	0.00418
10	2.45910	2.45929	0.00754
11	6.16760	6.16789	0.00464
12	6.25940	6.25979	0.00617
13	11.75900	11.76686	0.06687
14	12.32500	12.33038	0.04361
15	17.19700	17.21049	0.07845
16	17.44000	17.47005	0.17230
17	17.79400	17.79774	0.02103
18	19.67500	19.69200	0.08638
19	20.63400	20.64018	0.02994
20	20.94200	20.94483	0.01352
21	21.57200	21.58363	0.05391
22	26.23900	26.24153	0.00964
23	26.59400	26.61124	0.06483
24	26.71400	26.73016	0.06050
25	27.65100	27.67703	0.09415
26	35.77900	35.92830	0.41730
27	39.80100	40.27763	1.19753
28	40.71700	41.01338	0.72790
29	43.15100	44.15899	2.33597
30	44.17900	44.18945	0.02366

Table VII-37 Natural Frequency Comparative (Hz) Studies between the Finite Element Method and Method IV * for the structure** in case study 5

* Space-frame: 6 redundant constraint modes
18 fixed-interface normal modes

** Properties: Space-frame $E=7.2E10\ N/m^2$ $p=2700\ Kg/m^3$
Beam appendage $E\rightarrow\infty$ $p=2700\ Kg/m^3$

Mode	FEM	Method V	Difference(%)
1	0.00000	0.00041	-
2	0.00000	0.00085	-
3	0.00000	0.00145	-
4	0.00007	0.00186	-
5	0.00011	0.00234	-
6	0.00017	0.00265	-
7	0.72154	0.72157	0.00364
8	0.80420	0.80423	0.00351
9	0.96731	0.96735	0.00418
10	2.45910	2.45928	0.00747
11	6.16760	6.16788	0.00462
12	6.25940	6.25978	0.00615
13	11.75900	11.76685	0.06678
14	12.32500	12.33037	0.04354
15	17.19700	17.21048	0.07839
16	17.44000	17.47001	0.17208
17	17.79400	17.79774	0.02100
18	19.67500	19.69198	0.08628
19	20.63400	20.64017	0.02991
20	20.94200	20.94483	0.01351
21	21.57200	21.58362	0.05386
22	26.23900	26.24153	0.00963
23	26.59400	26.61122	0.06476
24	26.71400	26.73015	0.06045
25	27.65100	27.67701	0.09406
26	35.77900	35.92822	0.41706
27	39.80100	40.27719	1.19644
28	40.71700	41.01329	0.72768
29	43.15100	44.15827	2.33430
30	44.17900	44.18916	0.02300

Table VII-38 Natural Frequency Comparative (Hz) Studies between the Finite Element Method and Method V * for the structure** in case study 5

* Space-frame: 12 constraint modes
18 fixed-interface normal modes

** Properties: Space-frame E=7.2E10 N/m^2 p=2700 Kg/m^3
Beam appendage E→∞ p=2700 Kg/m^3

VIII Synopsis and Conclusions

It has been demonstrated that a nonlinear recursive Lagrangian approach of generalised coordinates is a well suited methodology for the dynamics modelling of complex articulated open-loop structures in space. Within this approach, and as opposed to global modelling practices, such as the direct application of the finite element method, structural systems can be modelled as collections of distinct flexible and rigid components. System order truncation techniques can be performed at component level reducing the computational cost and memory requirements associated with solution of large differential problems. Moreover, independent component modelling by different contractors, experimental data inclusion and decentralised control algorithm designs can also be implemented.

The main characteristic of this formulation is its recursive nature which permits a great deal of physical insight in the nonlinear system kinematics and results in a minimal set of differential equations of motion. At the same time, the articulated component kinematical expressions are formed relative to the inboard components, particularly useful for control applications. Admittedly, recursive methods are more elaborate in deriving the absolute kinematical expressions of components, accounting for the motion of the preceding components and at the same time for the interface constraints. The procedure may be complex in terms of kinematical descriptions, but on the other hand does not involve intensive computational implementation and can be subjected to systematic treatment for the kinematics modelling of large chains of interconnected components.

The geometrically nonlinear kinematics were formulated using the floating reference frame concept. Interface constraints were systematically introduced to describe the relative kinematics between adjacent flexible components, allowing any articulation axis to be locked, free or driven. 'Correction terms' introduced in the kinematical expressions

of the outboard components are particularly attractive for the incorporation of component modes by enforcing geometric interface compatibility.

The nonlinear expressions describing the kinematics of a component as part of a muitibody chain were symbolically reduced to linear expressions. Three distinct linear kinematical expressions were produced from this transition, and formulated using either hybrid or generalised coordinate sets. Using these expressions, three linear methods were established, all capable of modelling the dynamics of large-scale structural systems that belong to category II missions in space.

The first of the methods uses a hybrid set of coordinates where for each component the rigid-body part of the motion is described by physical displacement coordinates and the linear elastic deformation by generalised coordinates. In the second method, the hybrid set is substituted by a generalised coordinate set, since the rigid-body motion of each component has been described using rigid-body modes, modelling allowed only with the assumption of small rotational displacement. In both methods the structural system can be composed of either continuous or discrete components. In the third method all components are necessarily considered discrete. The consistent mass matrix of each component in the structure appears explicitly in the equations of motion of the multibody system. The third method also utilises a generalised coordinate set.

For assessment and comparison, it was decided that the methods should be examined on their suitability in modelling peripheral multibody structures. Mathematical models of peripheral structural systems can be developed analytically, as opposed to generic tree-configurations models which are best developed computationally. Analytical formulations would definitely facilitate comparison at a theoretical and also computational level. The general criteria for method comparison were set as the mathematical model development effort and complexity, physical insight capability, programming effort, potential numerical accuracy, potential computing time for application completion, programming validation effort, analyst interference with the data input, and generalisation to modelling generic tree-configuration multibody systems.

Based on the criteria set, it was demonstrated that method III, which uses a generalised coordinate set and explicitly the consistent mass matrices of the components, is most efficient of all the methods developed. The mathematical model D, derived by direct application of this method, is a generic mathematical model of a peripheral structure in space. The explicit appearance of the consistent mass matrix of each component in the equations of motion, distinguishes this model from the rest and makes it particularly attractive. The resulting equations of motion can be presented in a compact form, thus facilitating the programming. Avoiding integration/summation schemes, unlike the other models, the potential numerical accuracy of mathematical model D is very high. Additionally the potential computing time for the completion of an application is lower. Lastly, the analyst interference to provide data to the mathematical model, which cannot be obtained in a systematic manner, is eliminated.

Within any of the methods developed, the issue of distributed flexibility modelling would be much simplified if at the same time the size of the formulated problem was not a concern. For modelling component deformation efficiently, several component mode sets have been utilised in this work and may be combinations of dynamic and static modes. Imaginary constraints, that belong to the set of internal physical coordinates, have been proposed for defining static modes in the cases of statically determinate and underdeterminate components.

For both the computational implementation of mathematical model D and for demonstrating the efficiency of the various components mode set, a network of programs has been developed. The final deliverables of the network are the eigenvalues of the multibody system and the eigenvectors in modal or physical space. Additionally, physical displacement, velocity and acceleration of any point on the structure can be derived as a function of the forcing frequency using either direct or modal frequency response analysis. Since structures in space are composed of complex components, within the framework of this network each component has been spatially discretised using the finite element method. For this purpose, the network has been interfaced with the commercial finite element package ANSYS.

It has been demonstrated that, in general, the computational speed of the proposed method relative to the direct application of the finite element method increases as the total degrees of freedom increase, the distribution of component degrees of freedom is more uniform, total number of components and identical components increase and component mode number decreases. This translated to a typical peripheral multibody structure means that for an eigenvalue analysis a tenfold of speed gain over the finite element method may be a conservative target to expect. Furthermore, if there is a time benefit in eigenvalue analysis, it is straightforward to conclude that the same would apply for a frequency response analysis relative to the direct or modal finite element method frequency response analysis.

Utilising the network, several study cases have been undertaken and the natural frequencies obtained using mathematical model D were directly compared to the natural frequencies resulting by modelling the entire structural system using the finite element method. In addition, modal frequency response studies have performed for further validation of the method relative to the global finite element analysis, and for verifying that the structural system eigenvectors obtained are accurate.

Large-scale flexible multibody structures in space, due to there particular design, large dimensions, lightweight construction, and the large number of components, exhibit high modal density and local deformation at the component interfaces. It was demonstrated that the kind of flexible component modes employed in a mathematical model is of foremost importance for the accurate modelling of the dynamics of these structures. Combination of component modes that fail to closely resemble the real deformation of the individual components, when attached to each other to form the structure, proved inadequate or completely inappropriate for efficiently capturing the dynamics of the entire structural system, even in the low frequency range. If component mode selection is not appropriate the chances are that a number of modes will not be predicted, due to the high modal density of the particular structural systems. Unmodelled dynamics can be a main cause of destabilisation for structures in space, due to structure-control interaction. Moreover, the inherently large differential problem will increase further if the flexible component modes employed cannot model efficiently the linear elastic deformation of

the components. Finally, a qualitative criterion has been developed that predicts the possibility of local deformation at the interfaces being low or high. The criterion can be used as a guidance to the number and type of component modes best utilised.

More precisely, the fixed-interface and free-interface component mode sets are not appropriate, in general, for modelling of complex components which can exhibit local deformation at their interfaces to other components. Nevertheless, these component mode sets are ideal for simpler components, reducing the order and computational cost of problem compared to more sophisticated mode sets. The proposed loaded-interface component mode set gives excellent results, but is not appropriate for independent modelling, and may become very involving for the modelling requirements of large chains of components. The redundant constraint and constraint component mode set provide as excellent results, or even better, than the loaded interface method and also circumvent all the associated problems of the later. Moreover, both use a smaller amount of dynamic modes to offer the same accuracy of results as the loaded-interface component modes, thus reducing computational cost. Nevertheless, redundant component modes cannot be defined or obtained in the cases of statically determinate and underdeterminate components. On the other hand, constraint modes can be used in such cases with the introduction of imaginary constraints. This leads to the conclusion that constraint component modes are better suited than redundant constraint modes for the dynamics modelling of large-scale articulated multibody systems.

In summary, the theoretical integrity of the mathematical model D has been demonstrated, since it can provide results with extreme accuracy relative to the finite element method, even with a low number of degrees of freedom, subject to the component modes used. It has also been demonstrated that method III, that explicitly utilises the consistent mass and stiffness matrices of the individual components, is mostly suitable for the linear dynamics modelling of articulated multibody structures in space. Most importantly, employing the right type and number of component modes, the method can deliver extremely accurate results compared to the finite element method, with a low number of differential equations. Additionally, it has been shown that this method is more computationally efficient to the direct finite element approach.

For issues involving the dynamical behaviour of category II missions in space, such as main platform attitude control, stringent payload pointing, vibration suppression, control-structure interaction, sequential or integrated control-structure optimisation or general robust control algorithm investigation, mathematical model D can definitely be a solid basis for such applications. In this respect, the network of programs that supports mathematical model D can be employed for realistic research studies in the dynamics and control area of large-scale flexible structures in space. Moreover, method III, can easily furnish linear low order mathematical models for any tree-configuration structural system in category II missions in space.

Appendix-A

Recursive Kinematics of Articulated Components

A-1. Prologue

The aim of this appendix is to derive general expressions for the kinematics of a component in a multibody system with non-translating joints. Such is the case where components are connected via spherical, universal, revolute, clamped or torsionally elastic joints. The components are considered articulated, in the sense that any gimbal articulation axis can be free or locked. This part of the nonlinear kinematical analysis is recursive. The particular kinematical procedure followed in this work is only possible for multibody systems where no closed-loops and multi-point interfaces are formed between the articulated components. Structures in space are typical examples of open-loop multibody systems with operational components joint at single-point interfaces.

Initially the interface constraints between the two adjacent components are considered as either rotationally free (spatially articulating component) or fixed (locked component). The resulting mathematical expressions are general enough to employ any component mode set without violating the interface conditions. This is accomplished with the introduction of 'correction terms' into the joint component kinematical expressions. The physical significance of these terms is analysed by the use of rotating observers positioned appropriately in the adjacent components. From this nonlinear analysis a great deal of insight has been profited for the kinematics of a component in a multibody chain, and the suitable mathematical expressions accounting for the geometric interface conditions between adjacent elastic bodies have been derived. Since any joint configuration can be considered as a combination of locked (fixed) and articulating (free) axes, the component interface kinematics can

be generalised for any possible joint. The final expressions of the component kinematics as a part of a multibody system for arbitrary interface constraints have been presented.

Equations (III-11), (III-13), and repeated here as (A-1), (A-2), give the angular and linear velocity respectively of a frame travelling with an arbitrary point Q' on a flexible component B_i. These equations refer to the component B_i being disjoint to the multibody system; in other words the effect of the motion of other components in the multibody system on the motion of the component B_i has not been accounted for. The objective is to express the angular and linear velocity of the frame travelling with the arbitrary point Q' in the component B_i considering the influence of the motion of the inboard component B_{i-1}. In essence a kinematical relationship needs to be established for expressing the angular and linear velocity of the frame travelling with point Q' using the kinematical parameters that determine the motion of the preceding component at the interface. If such a kinematical expression is defined for two adjacent bodies, then by utilising it repeatedly for all components in the structure, the motion of any component can be expressed in terms of the motion of all components in the same multibody chain.

The kinematical formulation in this chapter, like in chapter III, is geometrically nonlinear. More specifically, nonlinear component kinematics involve the overall motion of each component in the multibody system to be perceived as a rigid-body motion relative to which elastic deformation can be observed. In this sense, one can assign to each component a suitably positioned floating reference frame that moves with the rigid part of the motion and relative to which the deformation can be measured. Therefore, the overall motion of each component can be described in terms of the motion of a floating reference frame, and deformation relative to it. A schematic presentation of the aforementioned is illustrated in Figure A-1.

The following equations (A-1), (A-2) have been proved in chapter III (equations (III-11), (III-13)) and are

$$\underset{\sim}{{}^{I}\omega_i^{Q'}} = \underset{\sim}{{}^{I}\omega_i^{Bi}} + \underset{\sim}{\dot{\theta}_i} \tag{A-1}$$

$$\underset{\sim}{{}^{I}v_i^{Q'}} = \underset{\sim}{{}^{I}v_i^{Ji}} + \underset{\sim}{{}^{I}\omega_i^{Bi}} \times \underset{\sim}{\rho_i} + \underset{\sim}{\dot{u}_i} \tag{A-2}$$

where

$\underset{\sim}{{}^{I}\omega_i^{Q'}}$ is the absolute angular velocity of a frame travelling with an arbitrary point Q' in the component B_i

$\underset{\sim}{{}^{I}\omega_i^{Bi}}$ is the absolute angular velocity of the body reference frame (floating reference frame) of the component B_i .

$\underset{\sim}{\dot{\theta}_i}$ is the rate of change of the angular displacement at an arbitrary point Q due component deformation

$\underset{\sim}{{}^{I}v_i^{Q'}}$ is the absolute linear velocity of an arbitrary point Q' in the component B_i.

$\underset{\sim}{{}^{I}v_i^{Ji}}$ is the absolute linear velocity of point J_i , the origin of the body reference frame of the component B_i .

$\underset{\sim}{\rho_i}$ is the position of an arbitrary point Q' before the deformation, measured from the origin J_i of the body reference frame B_i.

$\underset{\sim}{\dot{u}_i}$ the rate of change of the linear displacement of point Q' due to deformation as perceived by an observer travelling with the body reference frame B_i.

A-2. Kinematics of a Component Joint at a Non-Translating Interface

Three reference frames have been assigned that rotate and translate with points J_i^-, J_i^+, J_i, which are shown in Figure A-1. J_i is the origin of the body reference frame B_i, J_i^+ the position of J_i after the deformation of the component B_i, and J_i^- the interface point located at the inboard component B_{i-1}. Components B_i and B_{i-1} are joint at the interface points J_i^+ and J_i^-.

For a non-translating joint, the geometric compatibility between the adjacent components B_i and B_{i-1} can be expressed as

$$\underset{\sim}{r}_i^{J_i^+} = \underset{\sim}{r}_{i-1}^{J_i^-} \tag{A-3}$$

where the above notation is obvious from Figure 1. Equation (A-3) implies that points J_i^+, J_i^- are coincident at any instant.

Differentiating equation (A-3) with time and relative to the inertial reference frame I, the absolute linear velocity compatibility equation at the interface is obtained as

$$\underset{\sim}{v}_i^{J_i^+} = \underset{\sim}{v}_{i-1}^{J_i^-} \tag{A-4}$$

Utilising equation (A-2), which gives the absolute linear velocity of an arbitrary point Q' on the disjoint component B_i, we can express the absolute linear velocity of point J_i^+ as

$$\underset{\sim}{v}_i^{J_i^+} = \underset{\sim}{v}_i^{J_i} + \left(\underset{\sim}{u}_i^{+} \right)_{J_i} \tag{A-5}$$

where $\underset{\sim}{\rho}_i = 0$, since $\underset{\sim}{\rho}_i$ is the position of J_i^+ from the origin J_i of body frame B_i prior to the deformation.

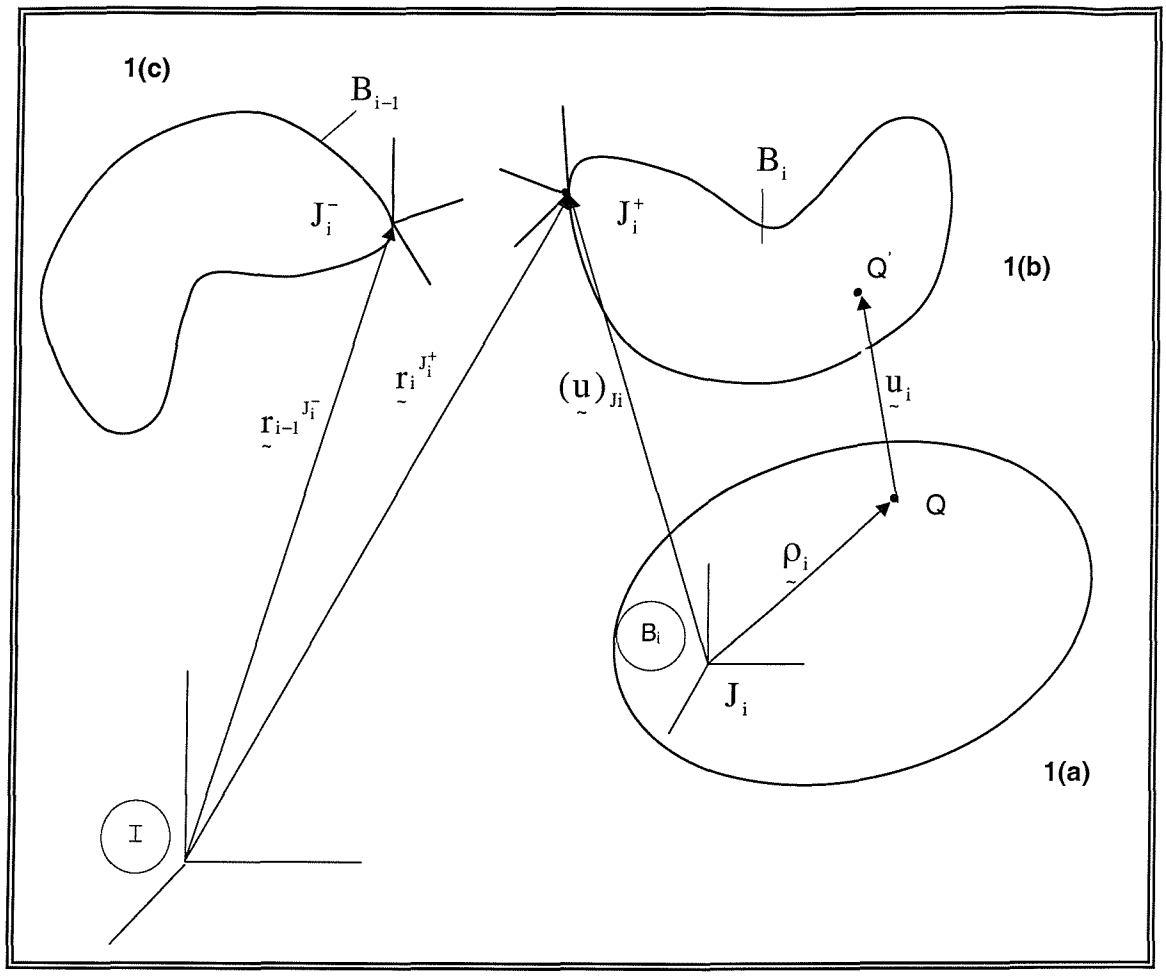

Figure A-1 General displacement component kinematics

(a) Rigid-body motion of component B_i

(b) Combined rigid-body motion and deformation of component B_i

(c) Component B_{i-1} arbitrarily displaced and deformed

Substituting the compatibility equation (A-4) into equation (A-5) the following expression is obtained

$$ {}^{I}\underset{\sim}{v}_i^{J_i} = {}^{I}\underset{\sim}{v}_{i-1}^{J_i^-} - \left(\overset{+}{\underset{\sim}{u}}_i\right)_{J_i} \qquad \text{(A-6)} $$

Equation (A-6) connects the absolute linear velocity of the origin J_i of the body frame B_i to the absolute linear velocity of the interface point J_i^- in the inboard component

B_{i-1}. Equation (A-6) is valid for any interface condition between two adjacent components as long as there is no relative translation between them.

Substituting (A-6) to (A-2), the absolute velocity of an arbitrary point Q' within the component B_i can be expressed as

$$\underset{\sim}{{}^{I}v_i}^{Q'} = \underset{\sim}{{}^{I}v_{i-1}}^{J_i^-} + \underset{\sim}{{}^{I}\omega_i}^{Bi} \times \underset{\sim}{\rho_i} + \overset{+}{\underset{\sim}{u}}_i - \left(\overset{+}{\underset{\sim}{u}}_i \right)_{J_i} \qquad \text{(A-7)}$$

Equation (A-7) relates the absolute velocity of an arbitrary point on an articulated component to the absolute velocity of the inboard component at the interface, and is valid for any non-translating interface.

The term $\left(\overset{+}{\underset{\sim}{u}} \right)_{J_i}$ in (A-7) can be considered a 'correction term'. Its existence ensures that whatever the pattern of the deformation of the component B_i at the interface, the compatibility equation (A-4) would hold. Indeed, substituting J_i^+ for Q' equation (A-7) becomes

$$\underset{\sim}{{}^{I}v_i}^{J_i^+,} = \underset{\sim}{{}^{I}v_{i-1}}^{J_i^-}$$

regardless the value of $\underset{\sim}{u}$ at the interface. If the 'correction term' did not appear in the (A-7), then by substituting J_i^+ for Q' in equation (A-7) the following expression would be obtained

$$\underset{\sim}{{}^{I}v_i}^{J_i^+,} = \underset{\sim}{{}^{I}v_{i-1}}^{J_i^-} + \left(\overset{+}{\underset{\sim}{u}} \right)_{J_i} \qquad \text{(A-8)}$$

From (A-8), it is obvious that if the 'correction term' did not exist, then the compatibility equation would not hold unless the linear displacement of the deformation pattern were zero at the interface.

There are cases that the analyst would use deformation patterns that have linear displacement value different to zero at a non-translating interface. In these cases it is obvious from (A-8) that the compatibility equation (A-4) would be violated. On the other hand, with the appearance of the 'correction term' in equation (A-7), compatibility equation (A-4) would be maintained for any deformation pattern. The 'correction term' acts by displacing the deformation pattern $\underset{\sim}{u}_i$ by $\left(\underset{\sim}{u}_i\right)_{J_i}$.

All component mode sets that include static modes will have value different to zero at the interface. If the linear deformation of a component is described by a set of component modes that their linear combination would give a non-zero value in the displacement coordinates at the interface of an articulated component with the inboard component, equation (A-7) responds by 'displacing' each mode by an amount $\left(\overset{+}{\underset{\sim}{u}}\right)_{Ji}$ so that geometrical compatibility is accomplished. If a particular mode k in the set has zero displacement value at the interface, then for this mode $\left(\overset{+}{\underset{\sim}{u}}\right)^k_{Ji}$ will be zero and will not affect the equation (A-7). In this respect any component mode set can be used without violating the geometrical compatibility between components.

Similarly as for equation (A-6), for Q' equal to J_i^+ equation (A-1) is expressed as

$$ {}^{I}\underset{\sim}{\omega}_i{}^{J_i^+} = {}^{I}\underset{\sim}{\omega}_i{}^{Bi} + \left(\overset{+}{\underset{\sim}{\theta}}_i\right)_{Ji} \qquad \text{(A-9)} $$

where no assumption has yet been made for geometric compatibility of angular velocities between adjacent components.

Using the addition theorem for angular velocities[23], the following general expression connects the angular velocities of the coincident reference frames J_i^+, J_i^-

$$\underset{\sim}{{}^{I}\omega_i}^{J_i^+} = \underset{\sim}{{}^{I}\omega_{i-1}}^{J_i^-} + \underset{\sim}{{}^{J_i^-}\omega_i}^{J_i} + \underset{\sim}{{}^{J_i}\omega_i}^{J_i^+} \tag{A-10}$$

A-3. Kinematics of a Component Connected at a Fixed or Torsionally Elastic Joint

The interface conditions for defining a fixed interface between adjacent components can be expressed as

$$\underset{\sim}{{}^{I}\omega_i}^{J_i^+} = \underset{\sim}{{}^{I}\omega_{i-1}}^{J_i^-} \tag{A-11}$$

Equation (A-11) implies that the reference frames J_i^+, J_i^- are co-rotational.

Substituting (A-11) into (A-9) the following expression can be written

$$\underset{\sim}{{}^{I}\omega_i}^{Bi} \overset{def}{=} \underset{\sim}{{}^{I}\omega_i}^{Ji} = \underset{\sim}{{}^{I}\omega_{i-1}}^{J_i^-} - \left(\underset{\sim}{\dot{\theta}}^{+}\right)_{Ji} \tag{A-12}$$

Equation (A-12) expresses the absolute angular velocity of the fixed component B_i relative to the angular velocity of the previous component at the interface point J_i^-.

Substituting (A-12) into (A-1) and (A-7), the following expressions are obtained respectively

$$\underset{\sim}{{}^{I}\omega_i}^{Q'} = \underset{\sim}{{}^{I}\omega_{i-1}}^{J_i^-} + \underset{\sim}{\dot{\theta}_i}^{+} - \left(\underset{\sim}{\dot{\theta}}^{+}\right)_{Ji} \tag{A-13}$$

$$ {}^{I}\underset{\sim}{v}_i^{Q'} = {}^{I}\underset{\sim}{v}_{i-1}^{J_i^-} + {}^{I}\underset{\sim}{\omega}_{i-1}^{J_i^-} \times \underset{\sim}{\rho}_i + \overset{+}{\underset{\sim}{u}}_i - \left(\left(\overset{+}{\underset{\sim}{\theta}} \right)_{Ji} \times \underset{\sim}{\rho}_i + \left(\overset{+}{\underset{\sim}{u}}_i \right)_{J_i} \right) \qquad \text{(A-14)} $$

Equations (A-13) and (A-14) express the absolute angular and linear velocity of a frame travelling with an arbitrary point Q' within the component B_i that is rigidly attached to the inboard component B_{i-1}.

The terms $\left(\overset{+}{\underset{\sim}{\theta}} \right)_{Ji}$, $\left(\overset{+}{\underset{\sim}{\theta}} \right)_{Ji} \times \underset{\sim}{\rho}_i$ can be considered 'correction terms'. It can be verified that the component mode sets are allowed to have different to zero angular displacement at the interface of the component B_i, without violating the compatibility condition (A-11).

Equation (A-13) and (A-14) can be interpreted using different reference frame descriptions. Considering the reference frame J_i^-, that travels (rotates and translates) with point J_i^-, the following interpretation can be given to (A-13) and (A-14):

The component B_i, attached rigidly to component B_{i-1}, has an absolute angular velocity ${}^{I}\underset{\sim}{\omega}_{i-1}^{J_i^-}$ and an absolute linear velocity ${}^{I}\underset{\sim}{v}_{i-1}^{J_i^-}$, and the observer travelling with J_i^- can measure at any instant an angular deformation and a linear displacement

$$ {}^{J_i^-}\underset{\sim}{\vartheta}_i = \left(\underset{\sim}{\theta}_i - \left(\underset{\sim}{\theta} \right)_{Ji} \right) $$

$$ {}^{J_i^-}\underset{\sim}{\upsilon}_i = \underset{\sim}{u}_i - \left(\left(\underset{\sim}{\theta} \right)_{Ji} \times \underset{\sim}{\rho}_i + \left(\underset{\sim}{u}_i \right)_{J_i} \right) $$

respectively, so that $\left(\underset{\sim}{\vartheta}_i\right)_{J_i^+} = 0$ and $\left(\underset{\sim}{\upsilon}_i\right)_{J_i^+} = 0$, and the compatibility equation (A-4) and (A-11) can be maintained.

Exactly the same interpretation can be given using reference J_i^+ , since due to geometric compatibility considerations (A-4), (A-11) is coincident and co-rotational to reference frame J_i^-.

For interpreting equations (A-13) and (A-14) using the reference frame J_i or equivalently reference body frame B_i, equations (A-13) and (A-14) are best rewritten as

$$ {}^{I}\underset{\sim}{\omega}_i{}^{Q'} = \left({}^{I}\underset{\sim}{\omega}_{i-1}{}^{J_i^-} - \left(\underset{\sim}{\dot{\theta}}^{+}\right)_{Ji} \right) + \underset{\sim}{\dot{\theta}}_i^{+} \qquad \text{(A-13b)} $$

$$ {}^{I}\underset{\sim}{v}_i{}^{Q'} = \left({}^{I}\underset{\sim}{v}_{i-1}{}^{J_i^-} - \left(\underset{\sim}{\dot{u}}_i^{+}\right)_{J_i} \right) + \left({}^{I}\underset{\sim}{\omega}_{i-1}{}^{J_i^-} - \left(\underset{\sim}{\dot{\theta}}^{+}\right)_{Ji} \right) \times \underset{\sim}{\rho}_i + \underset{\sim}{\dot{u}}_i^{+} \qquad \text{(A-14b)} $$

where the term in the parenthesis of (A-13b) is the ${}^{I}\underset{\sim}{\omega}_i{}^{J_i}$ as verified by equation (A-12), and the additional term in equation (A-14b) is the ${}^{I}\underset{\sim}{v}_i{}^{J_i}$ as verified by equation (A-6). Using the forms (A-13b) and (A-14b) the following interpretation can be offered.

An observer located at the reference frame J_i can measure the time-varying angular and linear displacement of a frame due to component deformation equal to $\underset{\sim}{\theta}_i$, $\underset{\sim}{u}_i$ at any instant. The reference frame that the observer travels on, has an absolute angular and linear velocity of

$$ {}^{I}\underset{\sim}{v}_i{}^{J_i} \overset{(A-12)}{=} {}^{I}\underset{\sim}{v}_{i-1}{}^{J_i^-} - \left(\underset{\sim}{\dot{u}}_i^{+}\right)_{J_i} $$

$$ {}^{I}\underset{\sim}{\omega}_{i}^{J_i} \overset{(A-6)}{=} {}^{I}\underset{\sim}{\omega}_{i-1}^{J_i^-} - \left(\overset{+}{\underset{\sim}{\theta}}\right)_{Ji} $$

respectively, which are regulated by the rate of the angular and linear deformation at the interface point, so that the compatibility equations (A-4), (A-11) can be conserved. The observer at J_i always maintains a time-varying distance and angular displacement from the interface of the components, which equals to $-\left(\underset{\sim}{u}_i\right)_{J_i}$ and $-\left(\underset{\sim}{\theta}\right)_{Ji}$ respectively. The aforementioned description is schematically presented in Figure A-2.

If the angular and linear displacement $\left(\underset{\sim}{u}_i\right)_{J_i}$ and $\left(\underset{\sim}{\theta}\right)_{Ji}$ were zero at the interface, then J_i^-, J_i reference frames would be coincident and co-rotational at all times. If only the angular displacement due to deformation is zero, then the frames would be co-rotational but not coincident. Lastly if only the linear displacement due to deformation were zero, then the frames would be coincident but not co-rotational.

Conclusively, the kinematics of the fixed joint demand that angular and linear displacement due to deformation at the interface to be zero. Even if the values of deformation are not chosen to be zero, the 'correction terms' accomplish this, by displacing the deformation pattern translationally and rotationally. The frame J_i is not necessarily coincident and co-rotational to the interface reference frames, and therefore it would be erroneous to consider compatibility equations in order that ${}^{I}\underset{\sim}{\omega}_{i}^{B_i} = {}^{I}\underset{\sim}{\omega}_{i}^{J_i^-}$ and ${}^{I}\underset{\sim}{u}_{i}^{J_i} = {}^{I}\underset{\sim}{u}_{i}^{J_i^-}$, unless the deformation pattern that approximates the deformation of the disjoint component was selected to assume zero value angular and linear displacement at the potential interface point.

Equation (A-13) and (A-14) would also be appropriate for modelling the case of two components that are connected at a torsionally elastic joint. That is straightforward to be verified by assuming that a torsional spring is part of either the inboard component B_{i-1} or the outboard component B_i. In the former case the torsional spring would connect to component B_i at point J_i^+ and in the later to the component B_{i-1} at point J_i^-. In either case the torsional spring can be considered as an integrated part of the flexible component.

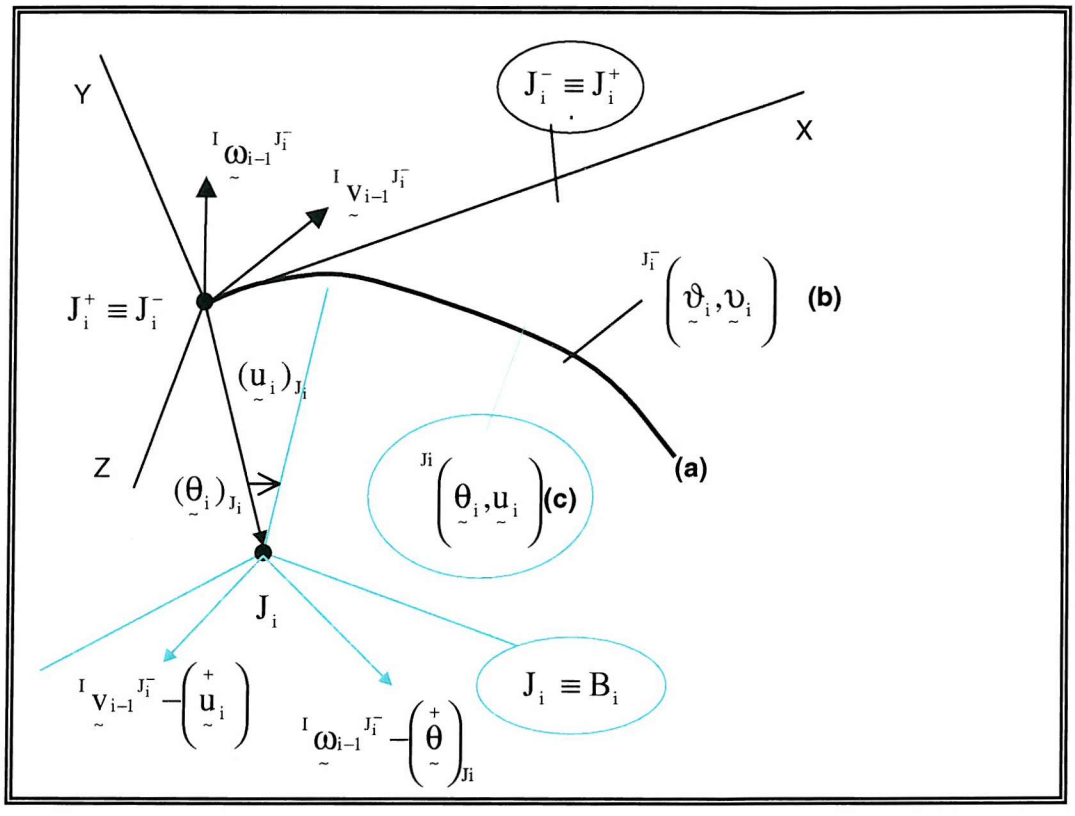

Figure A-2 (a) Position of the component B_i in the deformed and displaced position and rigidly attached to the inboard component at interface J_i^-, J_i^+

(b) Angular and linear deformation as observed from reference frames $J_i^- \equiv J_i^+$

(c) Angular and linear deformation as observed from reference frames $J_i \equiv B_i$

A-4. Kinematics for a Spatially Articulating Component

A spherical joint allows 3 rotational displacements in space and restricts the translational displacements. An articulating component that connects to the preceding one via a spherical joint can perform a three-dimensional rotation due to interface or external forces and torques applied on it or be free to rotate in space as an floating object due to initial conditions.

Unlike in the cases of a fixed joint or torsionally elastic joint, the spherical joint interface conditions can be defined by

$$ {}^{J_i^-}\underset{\sim}{\omega}_i{}^{J_i} \neq 0 \qquad \text{(A-15)} $$

The quantity ${}^{J_i^-}\underset{\sim}{\omega}_i{}^{J_i}$ is the cornerstone of free or driven articulation kinematics and is the angular velocity of the body frame of component B_i , measured relative to an observer located at the interface J_i^- , within component B_{i-1} , and it will be symbolised as

$$ {}^{J_i^-}\underset{\sim}{\omega}_i{}^{J_i} \overset{def}{=} {}^{J_i^-}\underset{\sim}{\omega}_i{}^{B_i} \overset{def}{=} \underset{\sim}{\omega}_i{}^{rel} \qquad \text{(A-16)} $$

Substituting (A-15) into (A-10) the following expression can be obtained

$$ {}^{I}\underset{\sim}{\omega}_i{}^{J_i^+} \neq {}^{I}\underset{\sim}{\omega}_i{}^{J_i^-} \qquad \text{(A-17)} $$

which implies that the reference frames J_i^+ and J_i^- have different angular velocities and thus cannot be co-rotational. Equation (A-17) can be considered the interface condition for two adjacent components connected with a spherical joint. If (A-17) is violated to an equality, then the spherical joint becomes a fixed joint, equation (A-11).

Utilising the addition theorem for angular velocities, (A-17) can also be written as

$$ {}^{J_i^-}\underset{\sim}{\omega}{}^{J_i^+} \neq 0 \qquad \text{(A-18)} $$

which means that an observer translating and rotating with the reference frame J_i^- at the interface of the component B_{i-1}, can observe the reference frame J_i^+ to be rotating with angular velocity ${}^{J_i^-}\underset{\sim}{\omega}^{J_i^+}$. More specifically this angular velocity consists of the rigid-body motion of the component B_i and the angular displacement rate due to deformation of the component at the interface, measured relative to the body reference frame of component B_i. This can be shown by rewriting (A-18) with the use of the addition theorem as

$$ {}^{J_i^-}\underset{\sim}{\omega}^{J_i^+} = {}^{J_i^-}\underset{\sim}{\omega}_i^{J_i} + {}^{J_i}\underset{\sim}{\omega}^{J_i^+} \tag{A-19} $$

and verifying that

$$ {}^{J_i}\underset{\sim}{\omega}_i^{J_i^+} \overset{def}{=} \left(\overset{+}{\underset{\sim}{\theta}}\right)_{J_i} \tag{A-20} $$

Substituting equation (A-13) into (A-12) and using the definitions (A-16), (A-20), the following expression is obtained

$$ {}^{I}\underset{\sim}{\omega}_i^{B_i} = {}^{I}\underset{\sim}{\omega}_i^{J_i^-} + \underset{\sim}{\omega}_i^{rel} \tag{A-21} $$

Equation (A-21) connects the absolute angular velocity of the body frame B_i to the absolute angular velocity of the interface point J_i^- within component B_{i-1}. Substituting equation (A-21) into (A-1) and (A-7) the following expressions are derived

$$ {}^{I}\underset{\sim}{\omega}_i^{Q'} = {}^{I}\underset{\sim}{\omega}_{i-1}^{J_i^-} + \underset{\sim}{\omega}_i^{rel} + \overset{+}{\underset{\sim}{\theta}} \tag{A-22} $$

$$ {}^{I}\underset{\sim}{v}_i^{Q'} = {}^{I}\underset{\sim}{v}_{i-1}^{J_i^-} + \left({}^{I}\underset{\sim}{\omega}_i^{J_i^-} + \underset{\sim}{\omega}_i^{rel} \right) \times \underset{\sim}{\rho}_i + \overset{+}{\underset{\sim}{u}}_i - \left(\overset{+}{\underset{\sim}{u}}_i\right)_{J_i} \tag{A-23} $$

Expressions (A-22) and (A-23) give the absolute angular and linear velocity of a frame relative to an arbitrary point on a component B_i in relation to the absolute angular and linear velocities of the interface frame within the inboard component.

As for equations (A-13) and (A-14), a similar physical interpretation for equations (A-22) and (A-23) can offered. The interpretation has been demonstrated schematically in Figure A-3.

For a spherical joint, the angular diplacement at the interface, as measured by an observer travelling with reference frame $\bar{J}_i$, can be zero or non-zero. This is suggested by the fact that no rotational 'correction terms' exist in the equations (A-22) and (A-23) for the angular deformation. This is so, because whatever the value of the angular displacement, the interface condition (A-17) cannot be violated, so there is no need for 'correction terms'. In Figure A-3 the angular displacement is depicted as non-zero relative to the body reference frame B_i, but this is not suggestive that it should necessarily be non-zero. On the other hand, the linear displacement has been 'corrected' to zero since the spherical joint cannot allow translation between the adjacent components.

Nevertheless, from the kinematics of the spherical articulation there is no physical mechanism to restraint the value of the angular displacement to zero. Considering that rigid-body angular displacement is allowed by the spherical joint kinematics, so should angular displacement due to deformation. In this sense, it may be beneficial to use deformation patterns which have non-zero angular displacement value at the interface with the inboard component. Maybe a zero angular displacement pattern can affect the accuracy of the results, since the physical mechanism of the articulation is not dealt with properly, but whatever the case the interface condition (A-17) will still hold.

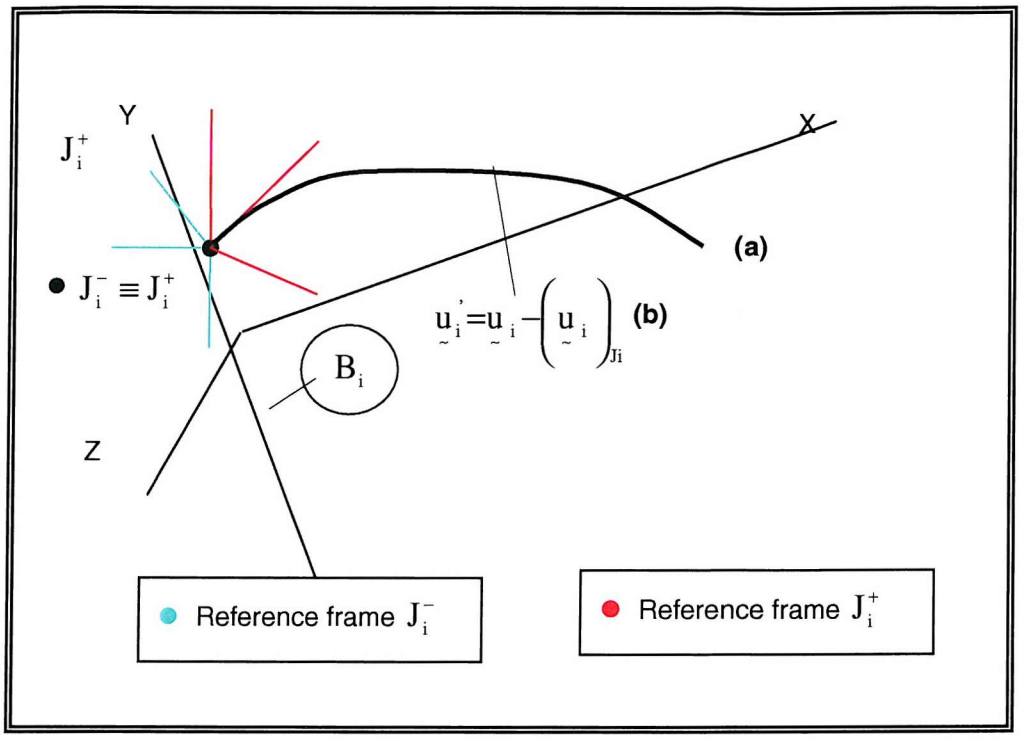

Figure A-3. (a) Position of the component B_i in the deformed and displaced and articulating relative to the inboard component B_{i-1}

(b) Linear displacement due to deformation of component B_i as observed from reference frames J_i^+, J_i^-

A-5. Kinematics of a Free or Driven Component for Arbitrary Articulation Axes

Equations (A-13), (A-14) correspond to a component connected at a fixed or torsionally elastic joint, and equations (A-22), (A-23) to a spatially articulating component. Combining the two sets of equations (A-13) with (A-22) and (A-14) with (A-23), the following expression can be accomplished

$$\underset{\sim}{{}^{I}\omega_i}^{Q'} = \underset{\sim}{{}^{I}\omega_{i-1}}^{J_i^-} + \underset{\sim}{\omega_i}^{rel} + \underset{\sim}{\dot{\theta}}^{+} - \left(\underset{\sim}{\dot{\theta}}^{+}\right)_{J_i} \qquad \text{(A-24)}$$

$$ {}^{I}\underset{\sim}{v}_i^{Q'} = {}^{I}\underset{\sim}{v}_{i-1}^{J_i^-} + \left({}^{I}\underset{\sim}{\omega}_i^{J_i^-} + \underset{\sim}{\omega}_i^{rel} \right) \times \underset{\sim}{\rho}_i + \overset{+}{\underset{\sim}{u}}_i - \left(\left(\overset{+}{\underset{\sim}{u}}_i \right)_{J_i} + \left(\overset{+}{\underset{\sim}{\theta}} \right)_{J_i} \times \underset{\sim}{\rho}_i \right) \qquad \text{(A-25)} $$

Equations (A-24) and (A-25) combine all the terms that are contained in their counterpart sets. Equations (A-24), (A-25) can therefore be used to describe the component kinematics of an outboard component for any non-translating joint. By removing term ω_i^{rel} from (A-24) and (A-25), equations (A-13) and (A-14) are obtained respectively. By removing the 'correction term' $(\Theta)_j$, equation (A-22) and (A-23) are obtained respectively.

Revolute and universal joints can be considered as consisting of combinations of locked and free articulation axes. The equations (A-24) and (A-25) can be written as two sets of three equations each. Each equation can correspond to a different axis of a joint and each axis can be treated separately. Therefore, (A-24), (A-25) can be used to model any non-translating joint configuration. The following Table A-1 sums up the different cases for an arbitrary axis k.

It has been shown that if component mode sets have more angular displacement freedom than required in any direction due to deformation, then the correction terms that correspond to the particular direction will zero the angular displacement, so that the interface conditions are not violated. If a flexible component mode set has less angular freedom than the joint requires in a particular direction, the interface conditions are not violated, but the kinematical description may be not so accurate. In any case, the component mode sets incorporated in this work have been selected so that they may have more angular deformation freedom, and not less.

By applying equations (A-24) and (A-25) repeatedly for all components in a multibody chain, the absolute angular and linear velocities of an arbitrary point on any component B_i can be expressed in terms of independent kinematical parameters that specify the motion of the components preceding and including B_i in the chain. In this way the motion of any component in a multibody system can be coupled to the motion of all other components in the system.

Joint Axis k	Articulating Driven or Free	Locked or Elastic
${}^{k}\omega_i^{rel}$	Yes	No
${}^{k}\left(\overset{+}{\theta}\right)_{J_i}$	No	Yes

Table A-1. 'Correction term' ${}^{k}\left(\overset{+}{\theta}_i\right)_{J_i}$ and articulation term ${}^{k}\omega_i^{rel}$ can be omitted or included in the equations (A-24), (A-25) for component B_i depending on the articulation of axis k.

Appendix - B

Mechanisms of Geometric Noniinearity in Multibody Systems

In the dynamics of multibody structural systems geometric nonlinearity is introduced for two reasons; component large angle arbitrary rotational displacement and / or time-varying configuration.

B-1. Large Angle Arbitrary Rotational Displacement

According to Euler's theorem[28] an arbitrary rotational displacement of a rigid body is equivalent to a rotation around a fixed axis. In other words, if a rigid body is rotationally displaced form an initial orientation in space to another, the new orientation of the body can be described by specifying an appropriate axis and an angle of rotation around the axis. This description of the body's arbitrary rotational displacement is performed in a single step by defining an axis in space and a rotation angle around this axis. The rotational displacement around a single axis will be considered in the context of this section as a simple rotation.

A rotation matrix, and more specifically a direction cosine rotation matrix, can be directly defined using the projections of the unit vectors along the orthogonal axes of a reference frame B to the axes of an arbitrary oriented reference frame A. In this sense, a rotation matrix is a measure of the relative orientation of two reference frames. If the orientation between two reference frames can be described using a rotation matrix, so should the orientation of a body relative to a reference frame. Equivalently, the rigid body simple rotational displacement, which gives a new orientation of a body relative to a reference frame, can be described by the use of a single rotation matrix. Rotation matrices have a string of useful properties, and amongst them, most importantly, the orthonormality property; the inverse of a rotation matrix equals its transpose.

Returning to the Euler's theorem, a rotation matrix can be derived, to describe the orientation, i.e. the rotational displacement, of a body, as a function of a vector defining the orientation of an axis and an angle of rotation around this axis. Without presenting the exact form of the particular rotation matrix, it is

$$C = C\left(\underline{\lambda}, \phi \right) \tag{B-1}$$

where the vector λ is a vector coincident to the axis of rotation and ϕ is the angle of rotation around the axis. The vector quantity λ and ϕ are considered the parameters of the rotational displacement or else the parameter set of the rotation matrix C. Other parametric expressions of the rotation matrices will be presented latter in this appendix.

If a rigid body is rotationally displaced in a sequence of simple rotations, through specific axes in space and angles of rotation, and acquires a final orientation, the angular displacement can still be described, according to Euler's theorem, by defining a single axis in space and an angle of rotation around this axis. It can be proved using the mathematical expression of Euler's theorem, that if the sequence of rotations changes, whereas the axis of each rotation and the angle of the rotations remain unaltered, the final orientation of the body will be different. The above statement can also be proved true without the use of a particular parametric expression of a rotation matrix. If a rotational displacement can be described by a rotation matrix, then a sequence of rotations can be shown to be the multiplication product of the rotation matrices corresponding to each rotation. Since, in general, matrices do not commute in multiplication, the final orientation of the body is dependant on the sequence of the rotations.

The implication of the above is that rotational displacement, in general, is not a vector quantity, and the commutative rule of addition of vectors cannot be applied. If a body is displaced in a sequence of simple rotations, the sequence of rotations along with the rotational displacement parameters - axis of rotation and angle of rotation in the case of Euler's theorem - need to be defined in order to determine the final position of the body. Using an example of two consecutive rotations, the following applies,

$$\underline{\underline{\theta}}_1+\underline{\underline{\theta}}_2 \neq \underline{\underline{\theta}}_2+\underline{\underline{\theta}}_1 \tag{B-2}$$

where $\underline{\underline{\theta}}$ is the rotational displacement and is symbolised with a double underline to indicate a pseudo-vector quantity.

Defining an orthogonal reference system the quantity $\underline{\underline{\theta}}$ can be expressed as

$$\underline{\underline{\theta}}=\begin{pmatrix}\theta_x\\ \theta_y\\ \theta_z\end{pmatrix}$$

where θ_i, for i=x,y,z are the projections of the quantity $\underline{\underline{\theta}}$ to the axis of the orthogonal reference frame x,y,z respectively. At a first glance, one may assume that the values θ_i, which define the orientation and the magnitude of $\underline{\underline{\theta}}$, would also define the axis of rotation and the angle of rotation, thus, according to Euler's theorem, $\underline{\underline{\theta}}$ would be a valid description of the orientation of the body in space. One can write $\underline{\underline{\theta}}$ as

$$\underline{\underline{\theta}}=\begin{pmatrix}\theta_x\\ \theta_y\\ \theta_z\end{pmatrix}=\begin{pmatrix}\theta_x\\ 0\\ 0\end{pmatrix}+\begin{pmatrix}0\\ \theta_y\\ 0\end{pmatrix}+\begin{pmatrix}0\\ 0\\ \theta_z\end{pmatrix} \tag{B-3}$$

The above form implies that if rotational displacement were a vector quantity it would equivalently be written as the sums of the rotational displacements around the reference system axes with no concern on the priority of summation. But the form (B-3) fails to give the sequence pattern of the rotations, thus does not specify uniquely the final position of the body. It is evident that $\underline{\underline{\theta}}$ cannot qualify as the description of rotational displacement, since it misses information about the sequence of rotation and therefore θ_i cannot define the orientation of the body. The assumption that the

values of θ_i can specify the axis of rotation and the magnitude of the rotational displacement is not true. Defining the orientation of a body using $\underline{\underline{\theta}}$ is insufficient.

The conclusion that rotational displacement is not a vector quantity is in general true for an arbitrary rotational displacement of a rigid body. In specific cases, it can be shown that rotational displacement is a vector quantity. If a body is rotationally displaced in a sequence of large angle rotations around parallel axes, then the final position of the body can be reached regardless the sequence. This exception is typically found in the case in plane kinematics. Another exception regards the small arbitrary rotational displacement, which can be viewed as a vector quantity. The sequence of displacing a rigid body through a series of small rotations does not affect the final position of the body. Both statements can be verified using the mathematical expression of Euler's theorem and any other parametric description of a rotational matrix or can be shown geometrically. These exceptions do not mean that the Euler's theorem, or more generally a rotation matrix description of the orientation, is not applicable in the case of planar or small rotational displacement, but that the sequencing of rotations is redundant in large planar and small rotational displacement analysis.

Up to this stage, it was shown that large arbitrary rotational displacement is not a vector quantity, and for its description the use of rotation matrices is essential. Based on Euler's theorem, the Euler rotation matrix expression presented in (B-1) utilises the orientation of an axis of rotation and an angle of rotation as rotational displacement parameters. Several other descriptions of a rotation matrix are possible using different sets of rotational parameters. In other words there are various ways to describe arbitrary large angular displacement, i.e. the orientation of a body in space, by the use of different angular displacement parameter sets.

The most relevant to this work rotational parameter set is the Euler angles set or else orientation, attitude angle set.[26] This set uses a sequence of 3 simple linear independent rotations around either the orthogonal axes of the body frame (body sequence) or around the axes of a suitable reference frame (space sequence) in

order to define a rotation matrix and therefore the orientation of the body in space. More specifically the Euler angles rotation matrix is given by

$$C = C_i(\theta_1)\, C_j(\theta_2)\, C_k(\theta_3) \qquad \text{for } i,j,k = 1,2,3 \text{ and } i \neq j,\ j \neq k \qquad \text{(B-4)}$$

$C_i(\theta_1)$ is a direction cosine rotation matrix corresponding to the first rotation around axis i

$C_j(\theta_2)$ is a direction cosine rotation matrix corresponding to the second rotation around axis j

$C_k(\theta_3)$ is a direction cosine rotation matrix corresponding to the third rotation around axis k

In total there are 24 independent combinations of space and body sequences that can be used to define Euler angles rotation matrices. The $\theta_1, \theta_2, \theta_3$ rotation angles are the Euler angles or else orientation, attitude angles. C_i , C_j, C_k are considered principal rotation matrices, since simple linearly independent rotations are performed around the orthogonal axes of the body reference frame or an independent reference frame for acquiring the Euler angles rotation matrix.

Another useful parametric rotational set is the Euler parameter set, which uses a 4 parametric description of the rotational displacement[24]. The redundant rotational parameter description may have particular advantages relative the 3 parameter description, but also implies that the 4 parameters are not independent.

B-2. Rotational Kinematics

This far the general characteristics of the rotational displacement have been examined and the means to represent it parametrically with the use of rotation matrices has been explored. The properties of the large arbitrary rotational displacement affect the kinematical expressions of a body undergoing arbitrary

rotational motion. The kinematics of the rotation is involved with the arbitrary angular displacement evolving with time. The rotation matrix associated with the orientation of a body, or else with the angular displacement of a body, is time dependent.

By definition[27] the skew-symmetric matrix ω^x, called an angular velocity matrix of a reference frame B relative to a reference frame A and expressed at the reference frame B is given by

$$\omega^x = C^T \dot{C} \tag{B-5}$$

where C is a generic rotation matrix specifying the orientation of B in A and the overdot implies time differentiation. The rotation matrix C is considered generic, and (B-5) applies regardless to the particular parameter set utilised.

C is an orthonormal matrix, hence equation (B-5) can also be written as

$$\dot{C} - C\,\omega^x = 0 \tag{B-6}$$

Equation (B-6) is the cornerstone of rotational kinematics. Equation (B-6) is a matrix differential equation, has time varying angular velocity coefficients, and in general cannot be solved in closed-form. The equation implies that if the history of the angular velocity is known, then by integration, the orientation of a body (or frame) can be specified at any instant. Such is the case when the history of the angular velocity has been obtained by the solution of Euler's attitude equations of motion. Generally, Euler's equations are coupled to Netwon's equations, for the combined rotational and translational motion of the body, and, in general, the nonlinear coupled differential set is solved numerically, along with the equation (B-6) to obtain the attitude history of a body moving in space.

As analysed before the mathematical expression of the generic rotation matrix C depends on the parametric set employed. Equation (B-6) can also be written in the form

$$\underline{\omega} = f\left(E\left(\underline{p}\right), \dot{\underline{p}}\right) \tag{B-7}$$

The above form is symbolic, where E is a matrix which depends on the rotational displacement parameter set $\underline{p}$, and $\dot{\underline{p}}$ is the rate of change of the parameter set. It should be noted that E is not a rotation matrix. Expression (B-7) states that the angular velocity of a body (or a reference frame) depends on the rate of angular displacement parameters, but also on the particular orientation of the body at any instant. The expression that relates the angular velocity to the rate of angular displacement parameters is, in general, nonlinear. This is due to the nonlinear form of E as function of the angular displacement set.

The fact that there should be, in general, a nonlinear relationship between the angular velocity and the rates of the angular displacement parameters introduced indirectly by the nonlinear form of matrix E can be shown without mathematical means. Since the rotational displacement depends on the sequence of rotations, angular velocity should depend on the orientation of the body at any instant. The orientation of a body, described by a time-varying rotation matrix, is a nonlinear function of the rotational displacement parameter set (which is evident from geometric considerations). Since angular displacement depends on orientation and orientation is a nonlinear function of the rotational displacement parameter set, so should the angular velocity. The above consideration correlates the angular displacement characteristic of sequencing to the nonlinear nature of rotational kinematics.

In this sense, in planar or small arbitrary rotational displacement, where the sequence of rotations does not affect the orientation of the body, angular velocity should be independent to the orientation of the body and a linear relationship between the angular velocity and the rates of rotational displacement parameters should exist. In mathematical terms it is

$$\underline{\omega} = \dot{\underline{\theta}}$$

All above considerations can be proved mathematically using any form of a rotation matrix expression.

For the case of the Euler angles rotational parameter set it can be shown that equation (B-7) has the particular form

$$\underline{\omega} = E(\theta)\ \dot{\underline{\theta}} \tag{B-8}$$

where $E(\theta)$ is the Euler angle matrix and $\underline{\theta}$ the vector of the rate of change of the Euler angles, or else attitude angles. E is a trigonometric function of the orientation angles.

In a Lagrangian formulation the orientation angles and their rates can be used as generalised coordinates (in the general Lagragian context). Therefore, in the Lagrange equations partial derivatives of the expressions involving the angular velocity of a body (as a nonlinear function of the orientation angles) relative to the orientation angles and their rates, introduce nonlinear terms in the equations of motion.

For a single body performing planar rotation or for a body performing arbitrary small angle rotations the Euler angle matrix does not have any physical significance since the sequence of rotations is not restrictive. Mathematically it can be proved that

$$E(\theta_1, \theta_2, \theta_3) = \mathbf{1} \tag{B-9}$$

As explained earlier in these two cases the rotational displacement becomes a vector quantity. One can express vector rotational displacement as a linear combination of rigid-body modes. Rigid-body modes can be perceived as simple, small rotational displacements, and since the sequence of rotational displacements in not restrictive in these cases, a linear combination of simple rotational displacements is acceptable. The time-dependant coefficients of the linear combination of rigid-body modes are considered the generalised coordinates of the rotation, or more generally the rotational displacement parameter set. At the same time the angular velocity can be

expressed as a linear combination of rigid-body modes with time dependent coefficients the rates of the generalised coordinates.

B-3. Time-varying Configuration

Time-varying configuration of a multibody structural system is another cause of nonlinearity. Although in essence time-varying configuration is caused by large angular displacement, the mechanism of introducing the nonlinearity into the equations of motion is distinct. For example, a multibody system with articulating components that all perform large planar rotations is described by a set of nonlinear differential equations, although E_i (θ_1, θ_2, θ_3)=1, for i=1,2,..,k, where k is the total number of components in the multibody system.

The mechanism of nonlinearity can be traced directly in the rotation matrices. Rotation matrices are used in this case for expressing a vector quantity form a particular reference frame to another. The components of a vector quantity may have different values in different reference frames, with the constraint that the magnitude of the vector is constant. The time-varying rotation matrix C_i between two reference frames, that in the case of a multibody system may represent the body frames of two adjacent and relatively rotating components, is at any instant a nonlinear function of the set of the rotational displacement parameters that describe the relative orientation of the two components.

Even in the case of large planar rotation the rotation matrix does not reduce to unity, unlike the Euler angle rotation matrix. In the case, though, of small arbitrary rotations the rotation matrix reduces to unity, and in essence the system is not considered of time-varying configuration. Of course, for time-varying configuration of components that perform large arbitrary rotations both the rotation matrix C_i and E_i matrix are nonlinear functions of the rotational displacement parameter set. Vectorial expressions transformed from one reference frame to another, where the orientation of the frames is a nonlinear function of the rotational displacement parameter set (i.e in the case of large angle orientation), introduce nonlinear terms in the equations of motion. For reference purposes the several cases are presented in Table B-1.

System	Kinematics	Time-Varying Rotation Matrix C	Matrix E	Equations of Motion
Single Body	Large Angle Arbitrary Rotation	C nonlinear or omitted (C =1)*	E nonlinear	nonlinear
Single Body	Large Angle Planar Rotation	C =1	E=1	linear
Single Body	Small Angle Arbitrary Rotation	C =1	E=1	linear
Articulating Structure	Large Angle Arbitrary Relative Rotations	C_i nonlinear	E_i nonlinear	nonlinear
Articulating Structure	Large Angle Planar Relative Rotations	C_i nonlinear	E_i =1	Nonlinear
Articulating Structure	Small Angle Arbitrary Relative Rotations	C_i =1	E_i =1	Linear

Table B-1 Reference table for the dynamics description of several systems

* This depends on the expression of the vector quantities on the body reference frame or an inertial reference frame.

References

1. Graves, P.C., Joshi, S.M, " *Modelling and Control of Flexible Space Platforms with Articulated Payloads* ", Third Annual NASA/DoD Conference on Control Structure Interaction Technology, San Diego, Ca., Jan. 29 – Feb. 2, 1989, pp. 181-210.
2. Meirovitch, L., Hale, A.L., " *On the Substructure Synthesis Method* ", AIAA Journal, Vol. 19, 1981, pp. 940-947.
3. Meirovitch, L., Hale, A.L., " *A General Dynamic Synthesis for Structures with Discrete Substructures* ", AIAA Paper 80-0798, 1980, pp. 790-800.
4. Meirovitch, L., " *A Stationarity Principle for the Eigenvalue Problem for Rotating Structures* ", AIAA Journal, Vol. 14, 1976, pp.1387-1394.
5. Engels, R.C., " *The Assumed Modes Method with Static Constraint Modes* ", AIAA Paper 90-1038-CP, 1990, pp. 1922-1931.
6. Meirovitch, L., Hale, A.L., " *A Rayleigh-Ritz Approach to the Synthesis of Large Structures with Rotating Flexible Components* ", NASA CP-2001, 1976, pp. 531-542.
7. Petyt, M, " *Introduction to Finite Element Vibration Analysis* ", Cambridge University Press, 1990.
8. MacNeal, R.H., " *A Hybrid Method of Component Mode Synthesis* ", Computers & Structures, Vol. 1, 1971, pp. 581-601.
9. Graig, R.R., Chang, C., " *A Review of Substructure Coupling Methods for Dynamic Analysis* ", NASA CP-2001, 1976, pp.393-408.
10. Graig, R.R.," *Methods of Component Mode Synthesis* ", Shock and Vibration Digest, Vol.9, 1977, pp.3-10.
11. Hurty, W.C., " *Dynamic Analysis of Structural Systems Using Component Modes* ", AIAA Journal, Vol.3, 1965, pp. 678-685.
12. Hintz, R.M., " *Analytical Methods in Component Modal Synthesis* ", AIAA Journal, Vol.13, 1975, pp.1007-1016.

13. Rubin, S., " *Improved Component-Mode Representation for Structural Dynamic Analysis* ", AIAA Journal, Vol. 13, 1975, pp. 995-1006.
14. Craig, R.R., " *A Review of Time-Domain and Frequency-Domain Component-Mode Synthesis Methods* ", The International Journal of Analytical and Experimental Modal Analysis, Vol.2, No.2, 1987, pp. 59-72.
15. Graig, R.R., Chang, C., " *On the Use of Attachment Mode in Substructure Coupling for Dynamic Analysis* ", AIAA Paper 77-405, 1977, pp. 89-99.
16. Yoo, W.S., Haug, E.J., " *Dynamics of Articulated Structures. Part I, Theory* ", Journal of Structures & Mechanisms, Vol. 14, No. 1, 1986, pp. 105-126.
17. Yoo, W.S., Haug, E.J., " *Dynamics of Articulated Structures. Part II, Computer Implementation and Applications* ", Journal of Structures & Mechanisms, Vol. 14, No. 2, 1986, pp. 177-189.
18. Smith, M.J., Hutton, S.G., " *A General Substructure Synthesis Formulation for a Free-Interface Component Mode Representation* ", The International Journal of Analytical and Experimental Modal Analysis, Vol.9, No.3, 1994, pp. 175-189.
19. Spanos, J.T., Tsuha, W.S., " *Selection of Component Modes for Flexible Multibody Simulation* ", AIAA Journal of Guidance, Control and Dynamics, Vol.14, No.2, 1990, pp. 278-286.
20. Lee, A.Y., Tsuha, W.S., " *Component Model Reduction Methodology for Articulated Multiflexible Body Structures* ", AIAA Journal of Guidance, Control and Dynamics, Vol. 17, No.4, 1993, pp. 864-867.
21. Craig, R.R., Hale, A.L., " *Block-Krylov Component Synthesis Method for Structural Model Reduction* ", AIAA Journal of Guidance, Control and Dynamics, Vol. 11, No. 6, 1987, pp. 562-570.
22. Meirovitch, L., " *Computational Methods in Structural Dynamics* ", Sljthoff & Noordhoff, 1980.
23. Kane, T.R., Levinson, D.A., " *Dynamics: Theory and Applications* ", McGraw-Hill, 1985.
24. Shabana, A.A., " *Dynamics of Multibody Systems* ", John Wiley & Sons, 1989.
25. Meirovitch, L., " *Elements of Vibration Analysis* ", McGraw-Hill, 1986.

26. Junkins, J.L., Turner, J.D., " *Optimal Spacecraft Rotational Maneuvers* ", Elsevier, 1986.

27. Kane, T.R., Likins P.W., Levinson, D.A., " *Spacecraft Dynamics* ", McGraw-Hill, 1983.

28. Hughes, P.C., " *Spacecraft Attitude Dynamics* ", John Wiley & Sons, 1986.

29. Kortum, W., Sharp, R.S., (editors), " *Multibody Computer Codes in Vechicle System Dynamics* ", Supplement to Vehicle System Dynamics, Vol.22, 1993.

30. Graig, R.R., " *Structural Dynamics* ", John Wiley & Sons, 1981.

31. Junkins, J.L., Kim, Y., " *Introduction to Dynamics and Control of Flexible Structures* ", AIAA Education Series, 1993.

32. Graig, R.R., T-J. Su, " *A Review of Model Reduction Methods for Structural Control Design* ", Proceedings of the First International Conference on " *Dynamics of Flexible Structures in Space*", Cranfield, UK, May, 1990, pp. 121-134.

33. Mantikas, N., " *Dynamics of the COFS-II Space Shuttle Based System for a Manoeuvre of the Antenna* ", Mphil Thesis, College of Aeronautics, Cranfield University, Oct. 1993.

34. Meirovitch, L., " *Analytical Methods in Vibrations* ", The MacMillan Company, 1967.

35. Joshi, S.M., " *Control of Large Flexible Space Structures* ", Lecture Notes in Control and Information Sciences, Vol.131, Springer-Verlag, NY, 1989.

36. Jefferson, J.W., et al, " *Computational Methods for Structural Mechanics and Dynamics* ", NASA, CP-3034, Part 2, 1989.

37. Hurty, W.C., Rubinstein, M.F., " *Dynamics of Structures* ", Prentice Hall, Inc.

38. Fletcher, H.J., Rongved,L., Yu, E.Y., " *Dynamics Analysis of a Two-Body Gravitationally Oriented Satelite*", The Bell System Technical Journal, September, 1963, pp. 2239-2258.

39. Hooker, W.W., Margulies, G., " *The Dynamical Attitude Equations for an n-Body Satellite* ", The Journal of the Astronautical Sciences, Vol. XII, No. 4, 1965, pp. 123-128.

40. Roberson, R.E., Wittenburg, J., " *A Dynamical Formalism for an Arbitrary Number of Interconnected Rigid-Bodies, with Reference to the Problem of*

Satellite Attitude Control ", Systems Dynamics, Session 46, Paper 46.D, 1966, pp. 46D.1-46D9.

41. Hooker, W.W., " *A Set of r Dynamical Attitude Equations for an Arbitrary n-Body Satellite Having r Rotational Degrees of Freedom* ", AIAA Journal, Vol. 8, No. 7, 1970, 1205-1207.
42. Likins, P.W., " *Dynamics and Control of Flexible Space Vehicles* ", Technical Report 32-1329, Jet Propulsion Laboratory, 1970.
43. Likins, P.W., " Analytical Dynamics and Nonrigid Spacecraft Simulation", Technical Report 32-1593, Jet Propulsion Laboratory, 1974.
44. Likins, P.W., " *Point-Connected Rigid Bodies in a Topological Tree* ", Celestial Mechanics 11, 1975, pp. 301-317.
45. Hooker, W.W.," *Equations of Motion for Interconnected Rigid and Elastic Bodies: A Derivation Independent of Angular Momentum* ", Celestial Mechanics 11, 1975, pp. 337-359.
46. Likins, P.W.," *A Study of Attitude Control Concepts for Precision-Pointing Nonrigid Spacecraft* ", NASA CR-2619, 1975.
47. Ho, J.Y.L., " *Direct Path Method for Flexible Mulibody Spacecraft Dynamics* ", Journal of Spacecraft, Vol.14, No.2, 1974, pp. 102-110.
48. Paul, B., " *Analytical Dynamics of Mechanisms-A Computer Oriented Overview* ", Mechanism and Machine Theory, Vol.10, 1975, pp. 481-507.
49. Jerkovsky, W., " *The Structure of Multibody Dynamics Equations* ", AIAA Journal of Guidance and Control, Vol.1, No. 3, 1978, pp. 173-182.
50. Hughes, P.C., " *Dynamics of a Chain of Flexible Bodies* ", The Journal of the Astronautical Sciences, Vol. XXVII, No.4, 1979, pp. 359-380.
51. Bodley, C.S., Devers, D.A., Park, C.A., Frisch H.P., " *A Digital Computer Program for the Dynamic Interaction Simulation of Controls and Structure (DISCOS)* " Vol. I, NASA Technical Paper 1219, 1978.
52. Singh, R.P., VanderVoort R.J., Likins, P.W., " *Dynamics of Flexible Bodies in Tree Topology – A Computer-Oriented Approach* ", AIAA Journal of Guidance, Control and Dynamics", Vol.8, No. 5, 1985, pp. 584-590.

53. Tadikonda, S.S.K., Mordfin, T.G., Hu, T.G., " *Assumed Modes Method and Articulated Flexible Multibody Dynamics* ", AIAA Journal of Guidance, Control and Dynamics, Vol.18, No. 3, 1995, pp. 404-410.

54. Craig, R.R., Antnhoy, T.C., " *On the Use of Component Modes in Multibody Dynamics*", AIAA/ ASME/ ASCE/ AHS Structures, Structural Dynamics & Materials Conference, Vol.3, 1996, pp. 1522-1529.

55. Lim, S.P., Liu, A.Q., Liew, K.M., " *Dynamics of Flexible Multibody Systems Using Loaded-Interface Substructure Synthesis Approach* ", Computational Mechanics 15, 1994, pp. 270- 283.

56. Meirovitch L., Kwak, M.K., " *Dynamics and Control of Spacecraft with Retargeting Flexible Antennas* ", AIAA Journal of Guidance, Control and Dynamics, Vol.13, No. 2, 1990, pp. 241-248.

57. Lee, S., Junkins, J.L., " *Explicit Generalization of Lagrange"s Equations for Hybrid Coordinate Dynamical Equations* ", AIAA Journal of Guidance, Control and Dynamics, Vol. 15, No. 6, 1992, pp. 1443-1452.

58. Meirovitch L., Stemple, T., " *Hybrid Equations of Motion for Flexible Multibody Systems Using Quasicoordinates* ", AIAA Journal of Guidance, Control and Dynamics, Vol. 18, No.4, 1995, pp. 678-688.

59. Cyril, X., Angeles, J., Misra, A., " *Dynamics of Flexible Mechanical Systems* ", Transactions of the Canadian Society for Mechanical Engineers, Vol. 15, No. 3, 1991, pp. 235-256.

60. Pradham, S., Modi, V.J., Misra, A.K., " *Order N Formulation for Flexible Multibody Systems in Tree Topology: Lagrangian Approach* ", AIAA Journal of Guidance, Control and Dynamics, Vol. 20, No. 4, 1997, pp. 665-672.

61. Shabana, A.A., " *Flexible Multibody Dynamics: Review of Past and Recent Developments* ", Multibody System Dynamics, Vol. 1, 1997, pp. 189-222.

62. Shiehlen, W., " *Multibody System Dynamics: Roots and Perspectives* ", Multibody System Dynamics, Vol. 1, 1997, pp. 149-188.

63. Tadikonda, S., " *Articulated, Flexible Multibody Dynamics Modelling: Geostationary Operational Environmental Satellite-8 Case Study* ", AIAA Journal of Guidance, Control and Dynamics, Vol. 20, No.2 , 1997, pp. 276-283.

64. Seshu, P., " *Substructuring and Component Mode Synthesis* ", Shock and Vibration, Vol.4, No. 3, 1997, pp. 199-210.

65. Williams, T., Mostarshedi, M., " *Model Reduction Results for Flexible Space Structures*", Fifth Annual NASA / DOD Conference on Control Structure Interaction Technology, 1992, pp. 79-96.

66. Kurdila, A., Papastavridis, J.G., Kamat, M.P., " *Role of Maggi"s Equations in Computational Methods for Constrained Multibody Systems* ", AIAA Journal of Guidance, Control and Dynamics, Vol. 13, No. 1, 1990, pp. 113-120.

67. Wehage, R.A., Haug, E.J., " *Generalised Coordinate Partitioning for Dimension Reduction in Analysis of Constraints Dynamic Systems* ", Journal of Mechanical Design, Vol.104, 1982, pp. 247-255.

68. Craig, R.R., Bampton, M.C.C., " *Coupling of Substructures for Dynamic Analysis* ", AIAA Journal, Vol.6, No. 7, 1968, pp. 1313-1319.

69. Kirk, C.L., inman, D., (editors) " *Dynamics of Flexible Structures in Space* ", The Second International Conference, Cranfield, UK, September, 1993.

70. Bianchi, G., Schiehlen, W., (editors), " *Dynamics of Multibody Systems* ", Springer-Verlag, Berlin, 1986.

71. Carroll, K.A., Hughes, P.C., " *Controller Order Reduction for Flexible Spacecraft Using Closed-Loop Balancing Methods* ", Proceedings of the First International Conference on " *Dynamics of Flexible Structures in Space* ", Cranfield, UK, May 1990, pp. 105-120.

72. Song, J.O., Haug, E.J., " *Dynamic Analysis of Planar Flexible Mechanisms* ", Computational Methods in Applied Mechanics and Engineering, Vol. 24, 1980, pp. 359-381.

73. Sudana, W., Dubowsky, S., " *The Application of Finite Element Methods to the Dynamic Analysis of Flexible Spatial and Co-Planar Linkage Systems* ", Journal of Mechanical Design, Vol.103, 1981, pp. 643-651.

74. Lowen, G.G., Chassapis, C., " *The Elastic Behaviour of Linkages: An Update* ", Mechanism and Machine Theory, Vol. 21, No. 1, 1986, pp. 33-42.

75. Kane, T.R., Wang, C.F., " *On the Derivation of Equations of Motion* ", SIAM Journal of Applied Mathematics, Vol.13, No.2, June 1965.

76. Williams, C.J.H., Crellin E.B., Gotts, S.A., " *Mathematical Methods in Flexible Spacecraft Dynamics* ", Final Report, ESTEC Contract No. 2405/75 AK, 1976.
77. Belvin, W.K., et al., " *The LaRC CSI Phase-0 Evolutionary Model Testbed: Design and Experimental Results* ", Fourth Annual NASA/DoD Conference on Control Structure Interaction Technology, 1990, pp. 594-613.
78. Maghami, P.G., et al, " *An Optimisation-Based Integrated Controls-Structures Design Methodology for Flexible Space Structures* ", NASA Technical Paper 3283, 1993.
79. Cook, R.D, " *Concepts and Applications of Finite Element Analysis* ", Willey, NY, 1981.
80. Russel, W.J., " *On the Formulation of Equations of the Rotational Motion of a N-Body Spacecraft* ", TR-0200 (4133)-2, Aerospace Corporation, El Secundo, Ca., 1969.
81. ANSYS Programmer's Manual for Revision 5.0, Swanson Analysis Systems, Inc., 1993.
82. MSC/NASTRAN Handbook for Dynamic Analysis, MSC/NASTRAN Version 63.
83. MSC/NASTRAN Applications Manual Vol II, MSC/NASTRAN Version 65.